

UC Berkeley

Planning & Evaluation

Title

Tool Development For Peak Electrical Demand Limiting Using Building Thermal Mass

Permalink

<https://escholarship.org/uc/item/96d4v93b>

Authors

Braun, James E.
Lee, Kyung-Ho

Publication Date

2004

FINAL REPORT

**TOOL DEVELOPMENT FOR PEAK ELECTRICAL
DEMAND LIMITING USING BUILDING THERMAL MASS**

JANUARY 2004

Ray W. Herrick Laboratories
School of Mechanical Engineering
Purdue University

Sponsored by
California Institute for Energy and Efficiency

Submitted by
James E. Braun, Principal Investigator
Kyoung-Ho Lee, Graduate Research Assistant

Table of Contents

1.	INTRODUCTION	1
1.1.	BACKGROUND AND GOALS	1
1.2.	ACCOMPLISHMENTS	1
2.	LITERATURE REVIEW	4
2.1.	DETAILED BUILDING MODELS FOR ERS.....	4
2.2.	PRECOOLING TEST AT ERS BUILDING	6
2.3.	SIMPLIFIED BUILDING MODEL.....	7
3.	DEVELOPMENT OF ERS BUILDING MODEL: TRNSYS MODEL	10
3.1.	ERS BUILDING DESCRIPTIONS	10
3.2.	TRNSYS BUILDING MODEL	12
3.2.1.	TRNSYS [Klein et al., 1994] Modeling.....	12
3.2.2.	Results	14
4.	DEVELOPMENT OF ERS BUILDING MODEL: INVERSE MODEL	20
4.1.	INVERSE BUILDING MODEL.....	20
4.1.1.	Building Thermal Network.....	20
4.1.2.	Building Model Training Algorithm	23
4.2.	VALIDATION OF INVERSE MODEL	26
4.2.1.	Data Set Description.....	26
4.2.2.	Validation Using Simulated Data.....	26
4.2.3.	Validation Using Field Data.....	34
5.	PEAK DEMAND-LIMITING CONTROL STRATEGY	47
5.1.	DEMAND-LIMITING STRATEGY	47
5.2.	SIMULATION STUDIES	48
5.2.1.	Methods of study	48
5.2.2.	Results	50
6.	CONCLUSIONS.....	60
7.	REFERENCES	61
APPENDICES		
A.	Information on ERS Building Construction	A-1
B.	Building Parameters for the ERS whole combined zones	B-1
C.	All Results for Demand-Limiting Simulations	C-1

List of Figures

Figure 2.1 Comparison of simulated and measured cooling load for the ERS building, (a) CAV case and (b) VAV case.	5
Figure 3.1 Schematic diagram of floor plan for the ERS.	11
Figure 3.2 Configuration of west test rooms (not scaled).	11
Figure 3.3 Schedule of cooling setpoint for Night-setup(Phase 1) and Precooling(Phase 2).	13
Figure 3.4 Calculated ground temperature according to heat flux through floor.	14
Figure 3.5 Erms for TRNSYS model for each test rooms.	15
Figure 3.6 Measured and simulated results of TRNSYS model for east test rooms in Phase 1. ...	16
Figure 3.7 Measured and simulated results of TRNSYS model for south test rooms in Phase 1. 16	
Figure 3.8 Measured and simulated results of TRNSYS model for west test rooms in Phase 1. ...	17
Figure 3.9 Measured and simulated results of TRNSYS model for interior test rooms in Phase 1.	17
Figure 3.10 Measured and simulated results of TRNSYS model for east test rooms in Phase 2. ...	18
Figure 3.11 Measured and simulated results of TRNSYS model for south test rooms in Phase 2.	18
Figure 3.12 Measured and simulated results of TRNSYS model for west test rooms in Phase 2. 19	
Figure 3.13 Measured and simulated results of TRNSYS model for interior test rooms in Phase 2.	19
Figure 4.1 Thermal network for test rooms of the ERS building.	21
Figure 4.2 Training and testing process and building model.	23
Figure 4.3 E_{rms} of inverse model using simulated data set in case of training with NS and testing with NS according to training duration from 1 week to 4 weeks.	30
Figure 4.4 E_{rms} of inverse model using simulated data set in case of training with PC and testing with PC according to training duration from 1 week to 4 weeks.	30
Figure 4.5 E_{rms} of inverse model using simulated data set in case of training with NS and testing with PC according to training duration from 1 week to 4 weeks.	30
Figure 4.6 E_{rms} of inverse model using simulated data set in case of training with PC and testing with NS according to training duration from 1 week to 4 weeks.	30
Figure 4.7 Measured and calculated results of inverse model using simulated data set for testing duration of 4 weeks with training duration of 3 weeks (training with NS and training with NS).	31

Figure 4.8 Measured and calculated results of inverse model using simulated data set for testing duration of 4 weeks with training duration of 2 weeks (training with PC and training with PC).....	31
Figure 4.9 Measured and calculated results of inverse model using simulated data set for testing duration of 4 weeks with training duration of 4 weeks (training with NS and training with PC).....	32
Figure 4.10 Measured and calculated results of inverse model using simulated data set for testing duration of 4 weeks with training duration of 2 weeks (training with PC and training with NS).....	32
Figure 4.11 E_{rms} of inverse model using simulated data set according to control strategies in training in case of 1 week training data set.	33
Figure 4.12 E_{rms} of inverse model using simulated data set according to control strategies in training in case of 2 week training data set.	33
Figure 4.13 E_{rms} of inverse model using simulated data set according to control strategies in training in case of 3 week training data set.	33
Figure 4.14 E_{rms} of inverse model using simulated data set according to control strategies in training in case of 4 week training data set.	34
Figure 4.15 Testing E_{rms} of inverse model using field data with training data types.	35
Figure 4.16 Measured and calculated results of inverse model using field data (case:11, training with Phase 1 and testing with Phase 1).	36
Figure 4.17 Measured and calculated results of inverse model using field data (case: 22, training with Phase 2 and testing with Phase 2).	36
Figure 4.18 Measured and calculated results of inverse model using field data (case:33, training with both Phase 1 and Phase 2 and testing with both Phase 1 and Phase 2).	37
Figure 4.19 Prediction E_{rms} of inverse model for east test rooms with training & testing control type.	38
Figure 4.20 Prediction E_{rms} of inverse model for south test rooms with training & testing control type.	38
Figure 4.21 Prediction E_{rms} of inverse model for west test rooms with training & testing control type.	38
Figure 4.22 Prediction E_{rms} of inverse model for interior test rooms with training & testing control type.	39
Figure 4.23 Prediction E_{rms} of inverse model for combined test rooms with training & testing control type.	39

Figure 4.24 Measured and calculated results of inverse model for east test rooms (case:12, Training with Phase 1 and testing with Phase 2).	40
Figure 4.25 Measured and calculated results of inverse model for east test rooms (case:21, Training with Phase 2 and testing with Phase 1).	40
Figure 4.26 Measured and calculated results of inverse model for south test rooms (case:12, Training with Phase 1 and testing with Phase 2).	41
Figure 4.27 Measured and calculated results of inverse model for south test rooms (case:21, Training with Phase 2 and testing with Phase 1).	41
Figure 4.28 Measured and calculated results of inverse model for west test rooms (case:12, Training with Phase 1 and testing with Phase 2).	42
Figure 4.29 Measured and calculated results of inverse model for west test rooms (case:21, Training with Phase 2 and testing with Phase 1).	42
Figure 4.30 Measured and calculated results of inverse model for interior test rooms (case:12, Training with Phase 1 and testing with Phase 2).	43
Figure 4.31 Measured and calculated results of inverse model for interior test rooms (case:21, Training with Phase 2 and testing with Phase 1).	43
Figure 4.32 Measured and calculated results of inverse model for combined test rooms (case:12, Training with Phase 1 and testing with Phase 2).	44
Figure 4.33 Measured and calculated results of inverse model for combined test rooms (case:21, Training with Phase 2 and testing with Phase 1).	44
Figure 4.34 Measured and calculated results of inverse model for combined test rooms(case:3'1', Training with Phase 3' and testing with Phase 1').	45
Figure 4.35 Measured and calculated results of inverse model for combined test rooms(case:3"2', Training with Phase 3" and testing with Phase 2').	45
Figure 4.36 Comparison of measured and calculated cooling loads of inverse model for night- setup and precooling on August 10 to 11 in Phase 1 and August 19 to 20 in Phase 2.	46
Figure 5.1 Setpoint temperatures for night-setup and demand-limiting strategies.	47
Figure 5.2 Measured and calculated results of inverse model for night-setup operation of east test rooms on August 11 test in Phase 1.	49
Figure 5.3 Measured and calculated results of inverse model for night-setup operation of west test rooms on August 11 test in Phase 1.	49
Figure 5.4 Measured and calculated results of inverse model for night-setup operation of whole combined test rooms on August 11 test in Phase 1.	50
Figure 5.5 Peak load ratio for east test rooms	51

Figure 5.6 Peak load ratio for west test rooms	52
Figure 5.7 Peak load ratio for combined test rooms	52
Figure 5.8 Simulated night-setup and demand-limiting control for east test rooms (PC start-time of midnight and DL start-time of 7 am).	54
Figure 5.9 Simulated night-setup and demand-limiting control for east test rooms (PC start-time of midnight and DL start-time of 1 pm).	54
Figure 5.10 Simulated night-setup and demand-limiting control for east test rooms (PC start-time of 7 am and DL start-time of 1 pm).	55
Figure 5.11 Simulated night-setup and demand-limiting control for west test rooms (PC start-time of midnight and DL start-time of 7 am).	56
Figure 5.12 Simulated night-setup and demand-limiting control for west test rooms (PC start-time of midnight and DL start-time of 1 pm).	56
Figure 5.13 Simulated night-setup and demand-limiting control for west test rooms (PC start-time of 7 am and DL start-time of 1 pm).	57
Figure 5.14 Simulated night-setup and demand-limiting control for combined test rooms (PC start-time of midnight and DL start-time of 7 am).	58
Figure 5.15 Simulated night-setup and demand-limiting control for combined test rooms (PC start-time of midnight and DL start-time of 1 pm).	58
Figure 5.16 Simulated night-setup and demand-limiting control for combined test rooms (PC start-time of 7 am and DL start-time of 1 pm).	59

List of Tables

Table 4.1 Training with night-setup data set and testing with night-setup data set.	27
Table 4.2 Training with precooling data set and testing with precooling data set.	27
Table 4.3 Training with night-setup data set and testing with precooling data set.	27
Table 4.4 Training with precooling data set and testing with night-setup data set.	27
Table 4.5 Material property bounds used in building training algorithm.	28
Table 4.6 Physical properties bound used in building training algorithm.	28
Table 4.7 Cases for training performance evaluation.	34
Table 4.8 Cases for testing performance evaluation.	35

Nomenclature

A	:	area
\mathbf{A}	:	coefficient matrix in the state space representation
\mathbf{B}	:	coefficient matrix in the state space representation
C	:	capacitance
\mathbf{C}	:	coefficient matrix in the state space representation
DL	:	demand-limiting control strategy
DST	:	daylight saving time
\mathbf{D}	:	coefficient matrix in the state space representation
E_{rms}	:	normalized RMS error (%) for the test period
e	:	transfer function coefficients for past history of heat flows
$J_{b,p}$:	building regression cost function at point p
N	:	number of hours in the test data set
NS	:	night-setup control strategy
N_{test}	:	number of hours in the test data set
N_{train}	:	training duration in hours
PC	:	precooling control strategy
\dot{Q}	:	heat transfer rate
\dot{Q}''	:	heat transfer flux
\dot{Q}_b	:	rate of instantaneous heat gain to the building air
$\dot{Q}_{c,k}$:	calculated cooling load at time step k
$\dot{Q}_{d,k}$:	baseline cooling loads at time step k
$\dot{Q}_{d,m}$:	maximum detailed model load during the testing period.
$\dot{Q}_{m,k}$:	measured cooling load at time step k
$\dot{Q}_{m,max}$:	maximum measured load during the testing period
PLR	:	peak load ratio, defined as $PLR = \frac{\dot{Q}_{max,NS,on-peak}}{\dot{Q}_{max,DL,on-peak}}$
R	:	thermal resistance
\mathbf{S}	:	series of row vectors containing transfer function coefficients for inputs
T	:	temperature

t	:	time
U	:	heat transfer coefficient
\mathbf{u}	:	vector of input variables
\mathbf{x}	:	vector of state variables
\mathbf{Y}	:	vector of output variables

Greeks

τ_{eff}	:	effective solar transmittance into building
--------------	---	---

Subscripts

a	:	ambient
avg	:	averaged
b	:	building
e	:	external wall
f	:	floor
g	:	ground
g,rad	:	radiative heat gain
g,conv	:	convective heat gain
i	:	internal
on-peak:		during on-peak period which demand-limiting is considered
r	:	roof
sol	:	solar irradiative absorption
z	:	zone

1. INTRODUCTION

1.1. BACKGROUND AND GOALS

Most commercial buildings have been dedicated HVAC systems to meet their comfort needs. In larger commercial buildings, the control of this equipment is achieved through use of computerized control systems, which allow the flexibility of running the building under different control strategies. Most control systems vary the building temperatures using a strategy called night-setup control. Under night-setup control, the air temperatures are in the middle of the comfort range and the cooling equipment is usually active during daytime hours. During the night and weekends, a high temperature setpoint is sent out by the control system and the cooling system is typically inactive during these periods. However, recently there has been an increased emphasis on developing dynamic building control strategies, which attempt to minimize the total cooling costs of a building and reduce peak cooling demand.

Accurate building modeling tools are needed for predicting the building thermal loads under different control strategies. The work described in this report involved development and evaluation of models using data from the Energy Resource Station (ERS) at the Iowa Energy Center (IEC). Models trained with data from the ERS were used to estimate peak cooling load reduction associated with different demand-limiting and precooling strategies. The IEC is a relatively lightweight structure that is representative of small commercial buildings. Demand reduction results for this building would be smaller than those possible for larger commercial buildings. The specific work tasks that provided the basis for the results described in this report are summarized as follows:

- A. Develop forward simulation model for the ERS building
- B. Develop inverse simulation model for the ERS building
- C. Evaluate demand-limiting control strategies

1.2. ACCOMPLISHMENTS

A TRNSYS model for test zones at the ERS was developed. Each of the eight test zones in the building were divided into conditioned and plenum spaces. Data necessary for TRNSYS simulation input were averaged over 30-minute periods and simulations were conducted with a time step of 30 minutes. Detailed building material property information is found in Appendix A.

Calculated cooling loads were compared with measured cooling loads for test results associated with both night-setup and precooling. In general, errors in cooling load estimates were larger for data obtained with precooling than with night-setup. Normalized RMS errors (%) were 5% to 12% for night-setup and 15 to 18% for precooling operation. The primary purpose in developing the TRNSYS building model was to allow of generation of data over a wide range of conditions in order to evaluate an inverse model for the ERS building.

An inverse model for the ERS building was developed and validated using measured and simulated data for the building. The building thermal network was modified for the ERS building from the network model which was developed by Braun and Chaturverdi (2000). Parameters of the model were determined through a training process involving global and local searches. The study performed using simulated data showed that the model predicted cooling loads very well having normalized RMS error of less than 3%, trained with two or three weeks of precooling data and tested with night-setup data. Nine days of measured data were available for night setup control and eight days were available with a precooling strategy in place. For application to the measured data, the normalized RMS error was about 4.8% for the case of training with 14 days that included a mixture precooling and night-setup control where the model was tested for the night-setup data. In the case of training with the 14 days of mixed data and testing with precooling data, the normalized RMS error was about 7.7%. The best parameters for the model were obtained by training using all 17 days of data. This inverse model was used for the evaluation of demand-limiting control strategies for this building.

The aim of the demand-limiting control strategies investigated in this study was to reduce peak cooling load compared to night setup control. The strategies involve adjusting zone temperature setpoints within the comfort region during the on-peak, occupied period to achieve a certain target cooling load, precooling the building with a 67 °F setpoint during some portion of the off-peak, unoccupied period, and maintaining the zone temperature at the lower end of the comfort region during the off-peak, occupied period. The upper comfort limit for the zone setpoints during the on-peak period was 76°F. The estimated on-peak peak cooling load reductions were very significant. For all the test zones combined, a 25% peak load reduction was estimated for precooling beginning at midnight and ending at 7 am with an on-peak period from 7 am to 6 pm. As the start of the on-peak period moves later in the day, the potential for peak load reduction is increased, but the influence of precooling is diminished. If the on-peak period began at 3 pm, then the peak load reduction for the on-peak period increased to about 45%. In this case, the primary peak load reduction results from keeping a low zone temperature during the off-peak, occupied period and allowing full utilization of the comfort region during the on-peak, occupied

period. The increased potential occurs because the energy storage of the building becomes a larger fraction of the on-peak cooling requirements for shorter on-peak periods.

2. LITERATURE REVIEW

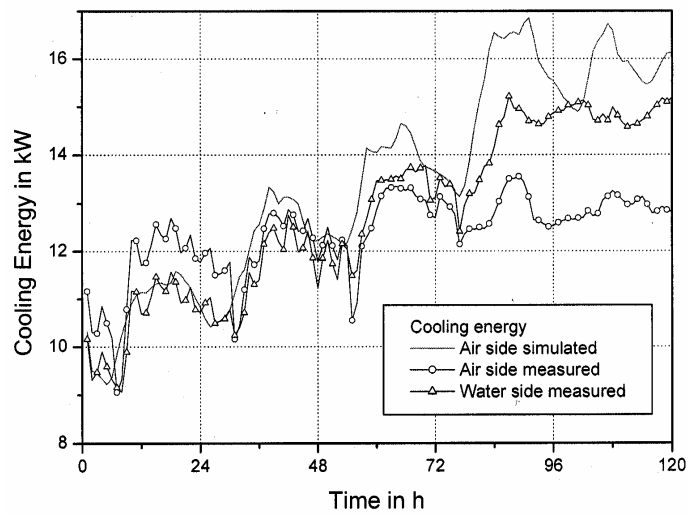
2.1. DETAILED BUILDING MODELS FOR ERS

The IEA [Travesi et al., 2001] reported an empirical validation of building models for the Iowa Energy Center ERS. The International Energy Agency (IEA) has initiated more than 30 tasks for its solar heating and cooling program since 1977. One of them is task 22 that establishes a technical basis for analyzing solar, low-energy buildings with available and emerging building energy analysis tools. The report for this task represents the results of empirical validation of TRNSYS, PROMETHEUS, DOE, and IDA-ICE. Three tests were conducted at the ERS as an integrated simulation exercise. The first exercise was an unrealistic theoretical case, where dynamic variations in the load behavior were caused only by the weather conditions. This test utilized a constant air volume setup with low internal loads. The test was conducted over a five-day period from June 18 to 22, 1999. The thermostats in the test rooms were programmed with constant set-points for heating and cooling in the test rooms without night setback/setup. The thermostats in the rest of the ERS were also programmed for a constant set-point schedule. The second exercise was a partially dynamic case, where the internal loads and control strategies were more realistic. This second exercise utilized a variable air volume setup with scheduled internal loads. The test was conducted over a four day period from February 5 to 8, 1999. The test rooms were operated utilizing variable-air-volume reheat. Another feature was the use of thermostat schedules as well as scheduled internal sensible loads for the test rooms. The thermostats in the test rooms were programmed for night setback/setup control. The third exercise was a very dynamic case with a variable air volume setup, variable internal loads and scheduled system operation. Test rooms were operated using variable air volume reheat and also a thermostat schedule and scheduled internal loads were used. The test was conducted over a five day period from June 12 to 16, 1999.

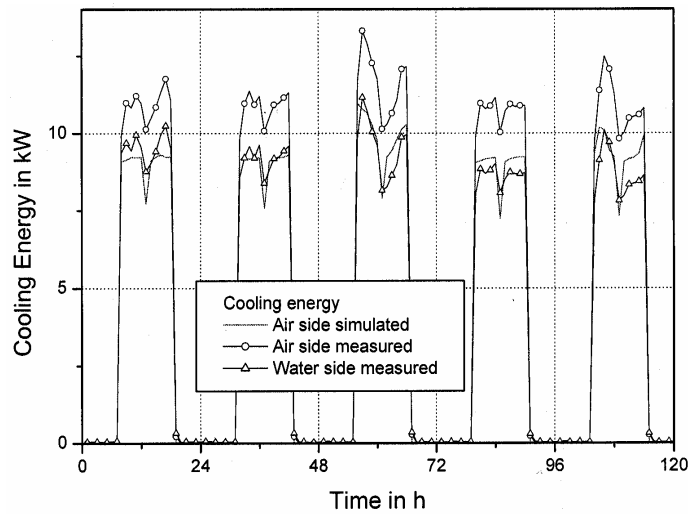
TRNSYS was used as one of the tools for ERS building model comparisons. The basis for the building model were a set of architecture drawings of the real building in combination with a manual containing information about the properties of wall layers and windows. The model had eight zones for the ERS building, A and B test zones for the East, South, West and Interior test rooms. Plenum zones above each test rooms were not included in the model. The model utilized many measured data for inputs to calculate cooling and heating loads of building model. The inputs included: ground temperature for the floor wall condition of the test rooms, adjacent spaces temperature for the adjacent wall conditions of each test rooms, ceiling

temperature for the ceiling boundary conditions, ventilation flow rate, temperature and relative humidity for each test rooms, base board heater watts and lighting watts for internal gains, wind information for calculation of convective heat transfer coefficients of the walls, and data for incident radiation.

The model had a mean error of 11% for cooling energy supplied to the test rooms by the AHU system A during the first exercise. More accurate results were obtained for the second and third exercises with mean errors of 4% and 2%, respectively.



(a)



(b)

Figure 2.1 Comparison of simulated and measured cooling load for the ERS building, (a) CAV case and (b) VAV case.

Figure 2.1 (a) and (b) give the calculated and measured cooling energy for the first and third tests, respectively. There are some fairly significant differences between the air and water-side measurements. Presumably the water-side measurements were more accurate. The model agrees fairly well with the water-side measurements for the VAV setup, but tends to overestimate the loads for the CAV setup. The reasons for these differences are not obvious.

This particular model representation requires a lot of measured input data for the calculation of cooling loads for the test rooms. Therefore, it was not suitable for the purpose of our project based on the requirement that the model needs to generate load data for the training of inverse models.

2.2. PRECOOLING TEST AT ERS BUILDING

As part of an ASHRAE project, Purdue University used the Iowa Energy Center ERS to demonstrate the potential for load shifting associated with a simple building thermal mass precooling strategy [Braun et al. (2002a) and Braun and Lawrence (2002b)]. Uniform control strategies were applied to the entire facility and two different tests were carried out. In the first phase of testing (Phase 1), the specified strategy for the entire building was night setup control. A setpoint of 74°F was specified during the occupied period (7 am to 6 pm) and a setpoint of 80°F was to be used for the unoccupied period (6 pm to 7 am). The first test began at midnight on August 3, 2001. During the first few days of testing, the zone temperature in the west zones exceeded 80 °F in the early evening due to solar loads between 6 pm and sundown causing the air-handling system to initiate cooling to maintain the 80 °F setpoint. Due to a minimum flow requirement for the VAV box and no internal gains at night, the other zones were precooled significantly during these periods resulting in an undesirable representation of night setup control. Raising the unoccupied temperature setpoint to 90 °F eliminated this condition and five more days of testing were performed from midnight on August 9 through 12, 2001.

For the second test (Phase 2), the entire building was run with a simple precooling strategy. The daytime cooling setpoint was 74 °F from 6 am to 6 pm. Then, the temperature was setup to 90 °F from 6 pm to midnight. The midnight precooling temperature setpoint was 68 °F from midnight to 6 am. The precooling test started at midnight on August 14 and ended at the end of the day on August 20, 2001. Internal gains within each zone were simulated using baseboard heat and lights. Both the baseboard heat and lighting have two stages of control. The maximum output of the heaters is 1800W (900W per stage) for each test zones. During the testing, both

stages of lights were turned on in the test rooms. No blind was used in the test rooms. Additional internal gains are simulated in the test rooms. Baseboard heating was to be run from 7 am to 6pm daily. There is an on-site weather station with measurements of outdoor dry bulb, relative humidity, wind speed and direction, total normal solar flux, and global horizontal solar flux. Measurements for each zone include air flow rate, supply air temperature, return air temperature, and reheat power input. Zone sensible cooling requirements were estimated from these measurements.

2.3. SIMPLIFIED BUILDING MODEL

A simulation tool was created to develop and analyze dynamic building control [Braun and Chaturvedi (2000) and Chaturvedi and Braun (2002)]. This tool was used to study alternative control strategies at a field site near Chicago as well as to view the impact of location and utility rates on the savings potential of control strategies.

The tool inputs include user specified utility rates, weather data, control strategy and operating characteristics of the cooling equipment (e.g. maximum chiller load). The components of the tool are the building model, the cooling plant model and the air handler model. A comfort monitor was incorporated to evaluate comfort violations.

The basis for the simulation tool was presented by Montgomery (1998) However, the inverse building model previously developed required large, rich training data sets and exhibited numerical oscillations. To minimize the training required and to create a more robust and stable building model, a physical building model was developed by using a thermal network of resistors and capacitors [Braun and Chaturvedi (2000) and Chaturvedi and Braun (2002)]. The model uses transfer functions to predict the cooling loads where the coefficients are constrained to obey energy balances in the network. The number of parameters used in the model was determined by studying simplified wall models and comparing the predicted heat flow from the inside surface of the wall to the results of a finite difference wall model (baseline case). Two-node representations of the wall were found to give a good trade off between accuracy and complexity. The two-node wall models had RMS errors of about 0.5%.

The building model uses two-node representations of the lumped external walls, lumped internal walls, the roof and the floor. The internal building mass (furnishings etc) was included as a zone thermal capacitance. The model training algorithm requires only a rough building description (approximate wall areas, thicknesses and basic construction materials used). The resistors and capacitors are bounded based on typical material properties (e.g. thermal

conductivity, density and specific heat) and estimates of dimensions. The training algorithm uses a combination of a local and global optimization method to determine the ‘best’ parameter estimates within the bounded region. The global phase identifies the region within the bounded space for the optimum, using a systematic search algorithm. The local phase uses derivative information to obtain better estimates of the optimal parameters.

The simplified building model predictions were compared with cooling load data from detailed simulated building models and from a field site. For simulated data, two building types (thermally heavy and thermally light), five different climatic conditions (spanning cooler to moderate to hot climates), six combinations of training and testing strategies and four training durations (one week to one month) were investigated. The results for a month of testing showed high accuracy with the testing RMS errors varying from 0.2% to 4% irrespective of the testing conditions chosen. In general, the model extrapolated very well to new conditions and was robust and accurate. However, the results were sensitive to the training conditions chosen. Buildings with high thermal resistance to the ambient (thermally heavy) were found to have smaller testing errors. Cities with more extreme ambient conditions (e.g. Phoenix) displayed larger testing errors. Training strategies which incorporated the greatest variations in temperature setpoints resulted in the lowest testing errors. One such strategy was the Maximum Discharge strategy, in which the building is pre-cooled at a setpoint of 67°F for six hours prior to occupancy. The off-peak occupied setpoint is at the lower limit of the comfort range (69°F) and the on-peak occupied setpoint is at the upper limit of the comfort range (77°F). The unoccupied setpoint is 80°F. One week of training with the Maximum Discharge strategy resulted in testing errors less than 1%. Night Setup, on the other hand, proved to be the poorest training strategy. Even with Night Setup as the training strategy, the testing errors with 14 days of training were small (2-3%). With one month of training data, the model accuracy was found to be insensitive to the training strategy used. It is recommended that the model be trained with strategies like Maximum Discharge for 7 days.

The simplified building model was also tested using field site data from the Ameritech facility. The building and cooling plant data used was collected during previous work on the facility but needed to be sorted and aligned in a consistent format. Solar data were approximated using measured data from a nearby weather station. The building was modeled as a single zone and an average of eight scattered temperature values was used to estimate the building temperature. Approximate building dimensions were used in the building training algorithm. The internal gains profile was approximated using fixed gains during three distinct periods (weekday occupied, weekday unoccupied and weekend occupied). The specific values for the internal gains

were learned during training. The model RMS testing errors were less than 10%. Greater inaccuracy of the results as compared to the simulation studies can be attributed to a number of factors. The internal gains schedule was not exact. Due to frequent after hours requests, multiple chillers were active on weekends and during unoccupied periods. These effects could not be captured in the tool. In addition, modeling the building as a single zone and using only eight temperatures to calculate an average building temperature, contribute to the deviation.

3. DEVELOPMENT OF ERS BUILDING MODEL: TRNSYS MODEL

3.1. ERS BUILDING DESCRIPTIONS

The ERS (Energy Resource Station) is part of the Iowa Energy Center, a non-profit research and education organization funded through and by utilities operating in Iowa. The ERS is a demonstration and test facility built to compare different energy-efficient measures (EEMs), to record energy consumption, and to disseminate information concerning energy efficient design and operation of buildings. The ERS is located in Andeney, Iowa. Its latitude is 41.71 degrees North and longitude is 93.61 degrees West. A schematic diagram of the floor plan for the ERS is shown in Figure 3.1 [Price and Smith, 2000]. The ERS is divided into three major area, the general area and two sets of test rooms, designated A and B. Each set of test rooms is comprised of an east, south, west, and interior room. The general area consists of office space, a display room, a computer center, two classrooms, service rooms, a media center, a reception space, and a mechanical room. Figure 3.2 shows structure of west test rooms in not scaled dimension.

The ERS is equipped with three variable-air-volume air handling units (AHUs). Two of the AHUs are identical, with each AHU serving four test rooms. The AHUs and test rooms are referred to as the ERS test systems with the systems distinguished as the A and B systems. Each test room is a mirror image of its matching pair with identical construction. The pairs of test rooms have identical exposures yielding identical external thermal loads and may have identical internal thermal loads. The third AHU serves the general areas of the facility including offices, reception space, two class rooms, a computer center, a display room, service spaces, and the media center. It is referred to as the general area system. Detailed information on building construction can be found in Appendix A.

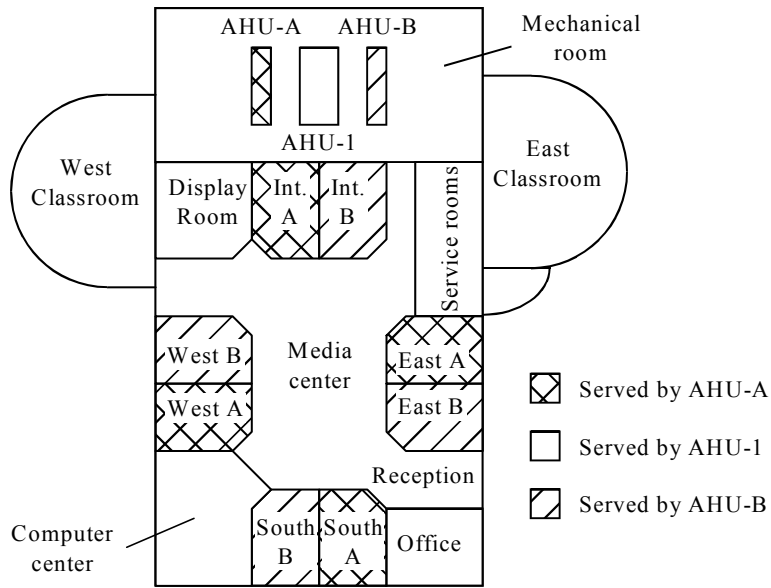


Figure 3.1 Schematic diagram of floor plan for the ERS.

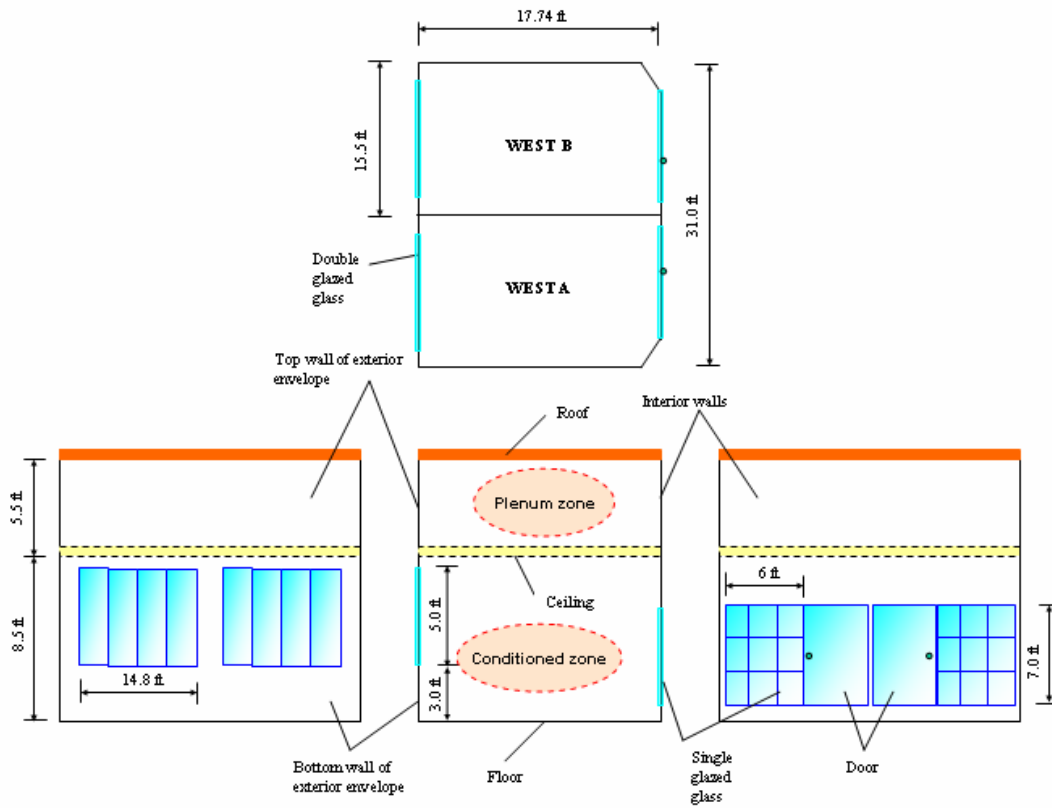


Figure 3.2 Configuration of west test rooms (not scaled).

3.2. TRNSYS BUILDING MODEL

3.2.1. TRNSYS [Klein et al., 1994] Modeling

The Type-56 multi-zone model in TRNSYS was used in this study. Sixteen thermal zones were considered with eight zones for the conditioned zones in test rooms East A, East B, South A, South B, West A, West B, Interior A and Interior B and the other eight zones for the plenum spaces associated with each of the test rooms. Configurations and properties for the wall layers and windows are provided by Price and Smith (2000) and Travesi et al. (2001). Both sets of information on the ERS building construction were used to see which information evaluate which provided more realistic simulation results. Results showed the information referred to properties provided by Travesi et al. resulted in better results for the TRNSYS model in this work at least, compared to measured data.

Infiltration and latent gains were neglected for all zones and the model was used to determine the sensible cooling requirements assuming that the zone setpoints could be maintained at all times. Inputs for the Type-56 multi-zone building model are ambient temperature, relative ambient humidity, sky temperature, incident radiation for orientations of north, south, east, and west, incident beam radiation for orientation of north, south, east, and west, angle of incidence for orientation of north, south, east, and west, and supply volume air flow rate for each test rooms. The measured input data was ambient temperature, humidity, and solar radiation, supply airflow rate into each test rooms. The Type-16 radiation processor, Type-69 calculation of sky temperature and Type-33 psychrometrics routines were used to calculate other inputs for the Type-56. Cooling schedules for the both Phase 1 and Phase 2 tests are shown in Figure 3.3.

Since every zone was air-conditioned at the same cooling set point, internal boundary walls between each zone were assumed to be adiabatic.

Ground temperatures for the floors were set at a constant temperature. Initially the ground condition was modeled with an adiabatic wall boundary condition on the underside. However, it was found that the overall cooling loads for the ERS building are sensitive to this assumption and that ground heat loss can be significant. As a result, a constant temperature boundary condition was assumed at the bottom of floor wall contacting with the ground surface. No soil effect was included in this study. The ground surface temperature was estimated from a steady-state analysis of the floor and measurements from the literature. Steady-state heat loss through the floor is expressed as

$$\dot{Q}_f = U_f A_f (T_z - T_g) \quad (3.1)$$

Arranging for the ground temperature gives

$$T_g = T_f - \frac{\dot{Q}_f}{U_f A_f} \quad (3.2)$$

And heat loss through floor also can be written as

$$\dot{Q}_f = \dot{Q}_f'' A_f \quad (3.3)$$

For the ERS building, $U_f = 0.866 \text{ W/m}^2\text{K}$ was estimated and the floor area is $A_f = 66.2 \text{ m}^2$. The calculated ground temperature for the interior test rooms as a function of heat flux through the floor is shown in Figure 3.4. The average ground temperature was estimated using experimental results from Thomas and Rees (1999) and Zhou et al. (2002) that gave an estimated steady-state floor surface heat flux of $5 \text{ W/m}^2\text{K}$. With this estimate, the estimated ground temperature was determined as 17.5°C .

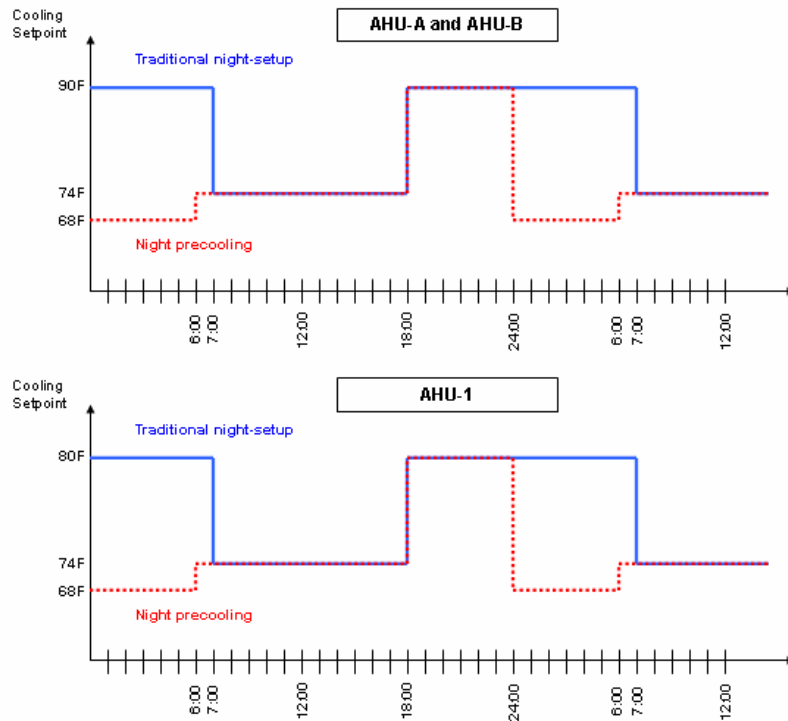


Figure 3.3 Schedule of cooling setpoint for Night-setup(Phase 1) and Precooling(Phase 2).

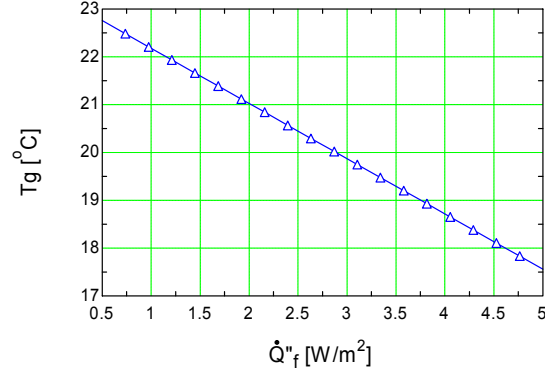


Figure 3.4 Calculated ground temperature according to heat flux through floor.

Return airflow rates from the conditioned zone to the plenum zone were considered to be the same as the supply airflow rates and available from the measurements.

One stage of the baseboard heater was set ON and two stages of lighting were set ON in the modeling. It was assumed that 90% of the lighting energy was radiation and 10% was convection. For the heaters, 5% was assumed to be radiation and 95% convection. Measured power input for the lighting and heat radiator data were used. Furthermore, the thermal efficiency of the baseboard heater was assumed to be 95% by assuming that 5% of heat is lost by heat conduction through the walls and floors going out of the zones.

During the Phase 1 and 2 tests, Daylight Saving Time (DST) was in place and it was necessary to consider DST in calculating the solar time for the Type-16 radiation processor.

Air temperature and sensible cooling load for each zone were set as the outputs of the Type-56 multi-zone building model.

3.2.2. Results

In this study, the integrated root mean square errors evaluated at the end of the testing period and expressed as a percentage of the maximum baseline load were used as a criterion for determining model accuracy. This error reflects the total error in sensible energy requirement over the given period and is defined as:

$$E_{rms} = \frac{100}{\dot{Q}_{m,max}} \sqrt{\frac{\sum_{k=1}^N (\dot{Q}_{c,k} - \dot{Q}_{m,k})^2}{N-1}} \quad (3.6)$$

where E_{rms} = normalized RMS error (%) for the test period, N = number of hours in the test data set, $\dot{Q}_{m,max}$ = maximum measured load during the testing period, $\dot{Q}_{c,k}$ = calculated load at a time stage k, and $\dot{Q}_{m,k}$ = measured load at a time stage k.

Figure 3.5 shows E_{rms} (%) for the test rooms considered in this work for the last three days of each test phase. The ERS building model results were first compared with test data for Phase 1. Some parameters of the model were adjusted and then the model was applied to the Phase 2 test conditions. Calibration involves adjusting parameters to reduce errors between calculated and measured cooling loads. However, it was not possible to find calibrated parameters to reduce errors for both Phase 1 and Phase 2 tests. The cooling load results from the TRNSYS model agree more closely with the Phase 1 than Phase 2 measurements. The model did not provide a great representation of the thermal mass effect even though the building material properties and geometry specifications were considered in detail.

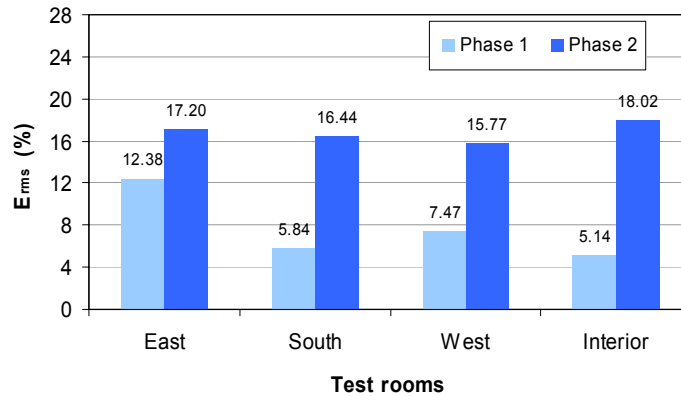
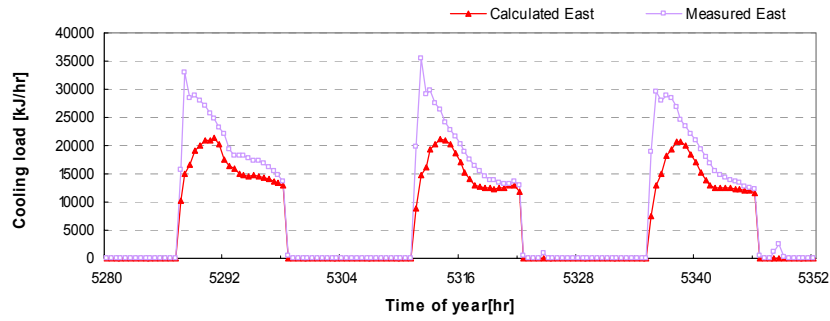
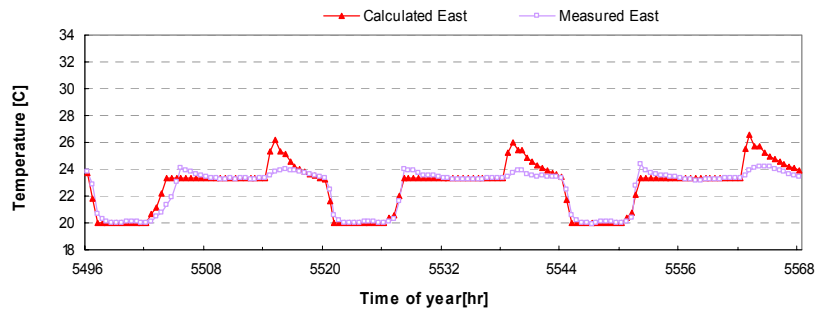


Figure 3.5 Erms for TRNSYS model for each test rooms.

Figure 3.6 through Figure 3.13 show comparisons of calculated and measured cooling loads and zone temperatures for the night setup and precooling test periods, respectively. The TRNYS model does a pretty good job of estimating cooling loads, except for the east rooms under night setup operation. For the precooling period, calculated cooling loads during nighttime and early morning are lower than measured loads.

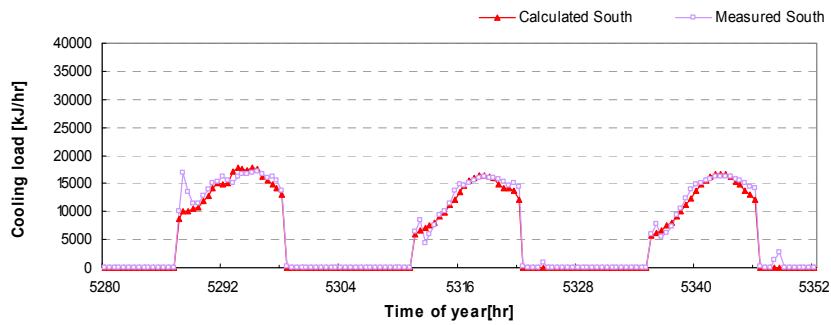


(a) Cooling loads for east test rooms

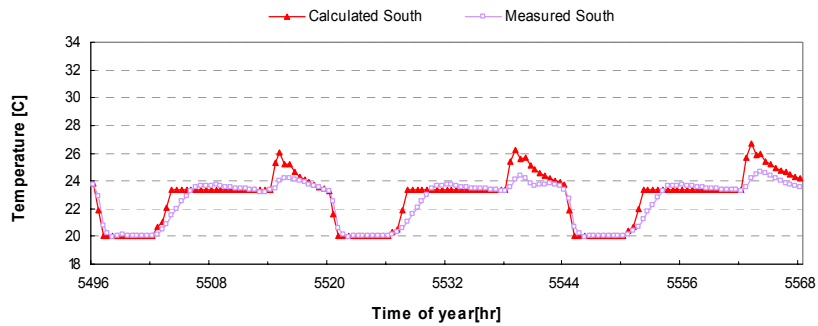


(b) Room temperature for east test rooms

Figure 3.6 Measured and simulated results of TRNSYS model for east test rooms in Phase 1.

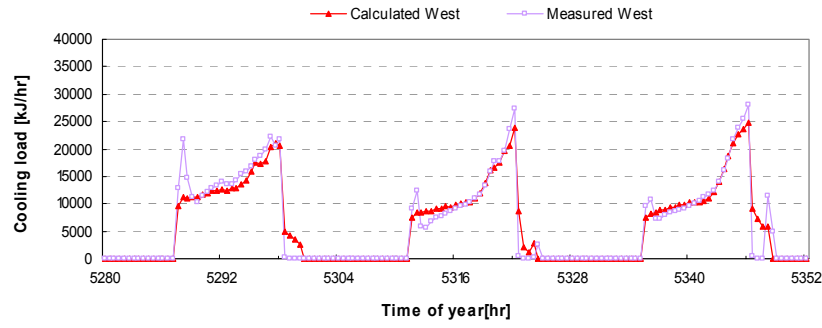


(a) Cooling loads for south test rooms

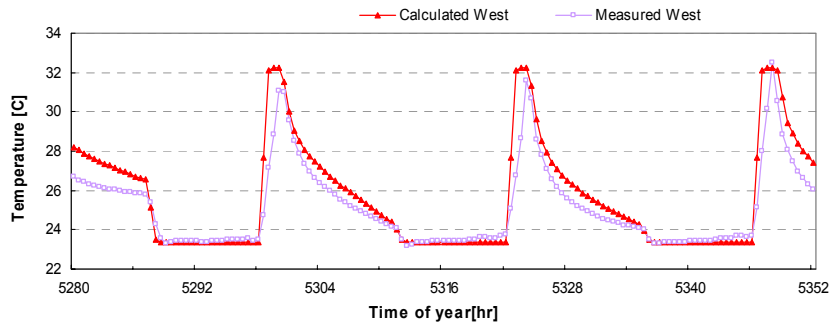


(b) Room temperature for south test rooms

Figure 3.7 Measured and simulated results of TRNSYS model for south test rooms in Phase 1.

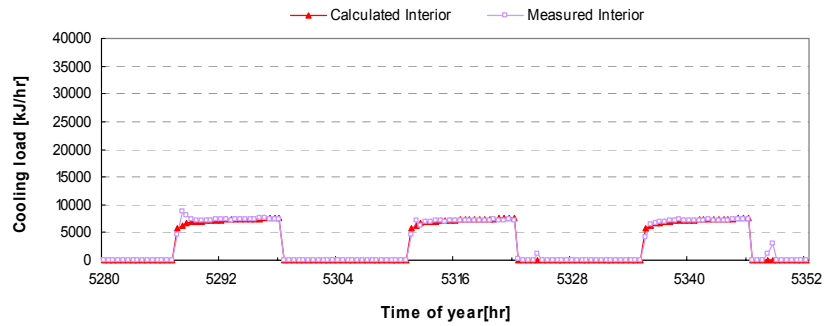


(a) Cooling loads for west test rooms

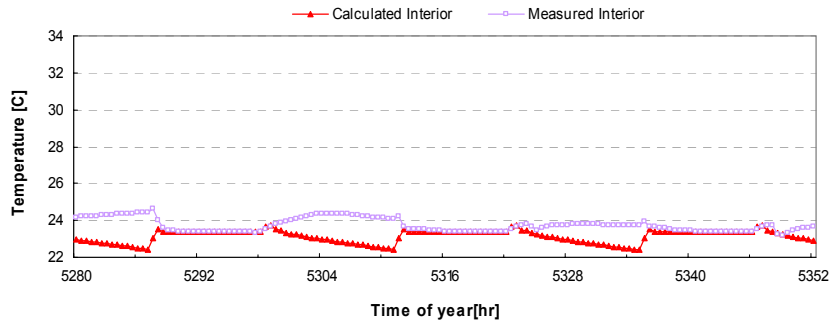


(b) Room temperature for west test rooms

Figure 3.8 Measured and simulated results of TRNSYS model for west test rooms in Phase 1.

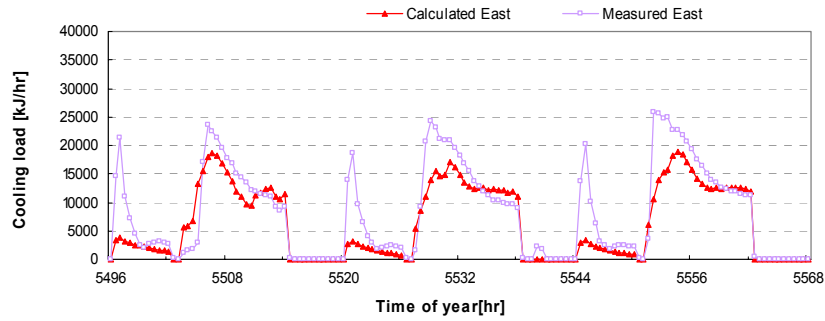


(a) Cooling loads for interior test rooms

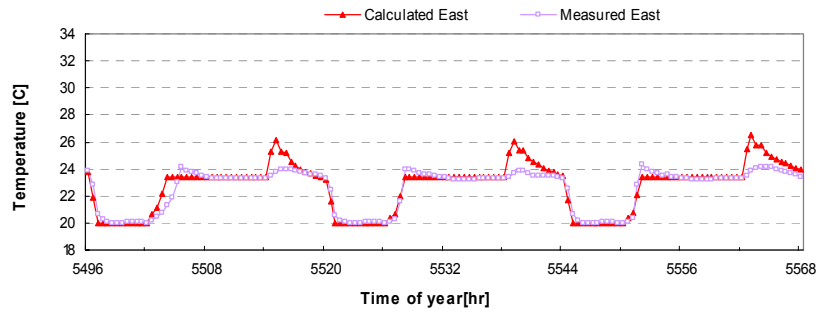


(b) Room temperature for interior test rooms

Figure 3.9 Measured and simulated results of TRNSYS model for interior test rooms in Phase 1.

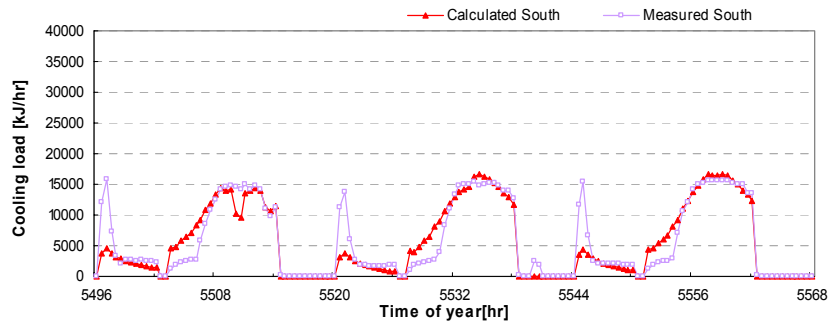


(a) Cooling loads for east test rooms

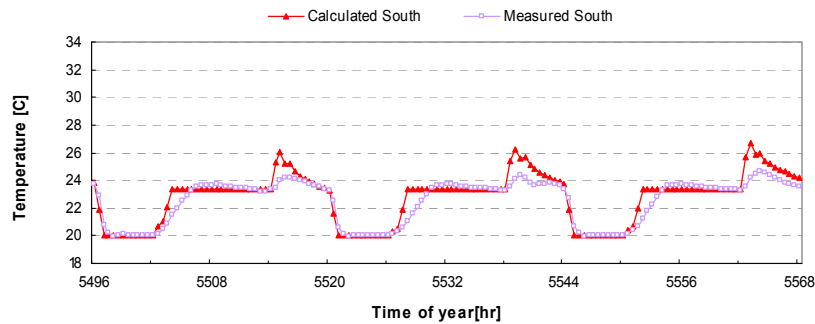


(b) Room temperature for east test rooms

Figure 3.10 Measured and simulated results of TRNSYS model for east test rooms in Phase 2.

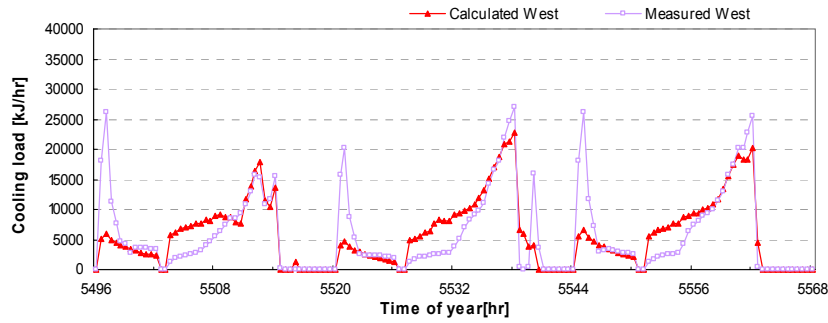


(a) Cooling loads for south test rooms

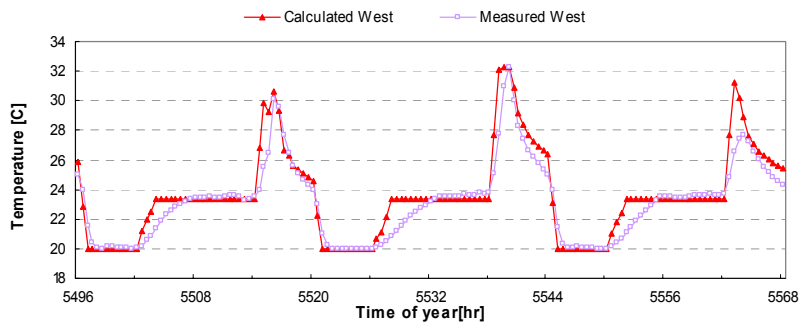


(b) South test rooms south test rooms

Figure 3.11 Measured and simulated results of TRNSYS model for south test rooms in Phase 2.

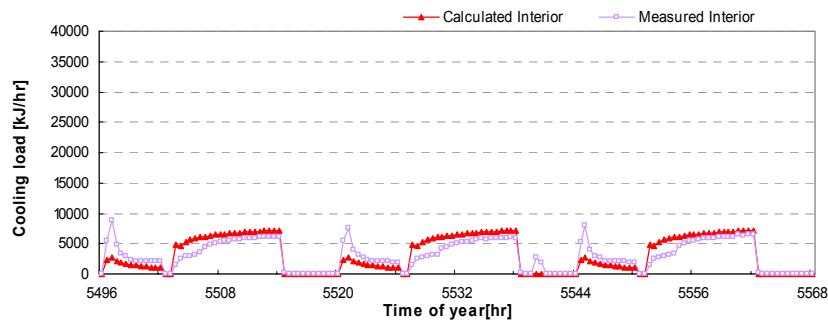


(a) Cooling loads for west test rooms

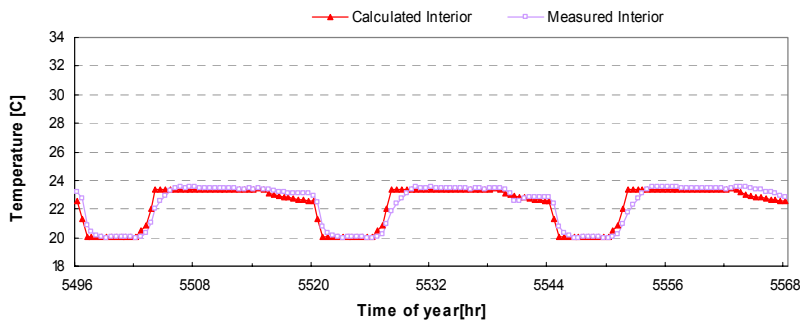


(b) Room temperature for west test rooms

Figure 3.12 Measured and simulated results of TRNSYS model for west test rooms in Phase 2.



(a) Cooling loads for interior test rooms



(b) Room temperature for interior test rooms

Figure 3.13 Measured and simulated results of TRNSYS model for interior test rooms in Phase 2.

4. DEVELOPMENT OF ERS BUILDING MODEL: INVERSE MODEL

4.1. INVERSE BUILDING MODEL

4.1.1. Building Thermal Network

Figure 4.1 shows thermal networks for external and internal test rooms of the ERS building respectively. Each of the test rooms is modeled as a single zone enclosed by external walls, internal walls, the roof and the floor with multiple walls being lumped together as a single wall.

Each of the walls uses two capacitors to represent the mass of the walls and three resistors to represent the wall coupling to the ambient, the conduction within the wall and the wall coupling to the zone. It was assumed that the solar radiation through the window irradiated only on the floor. Since internal radiation is due to lights located on the ceiling, there was no internal radiation on the ceiling.

Using an energy balance at each node, a state-space formulation was set up for the building model [Braun and Chaturvedi (2000) and Chaturvedi and Braun (2002)].

$$\frac{d\mathbf{x}_b}{dt} = \mathbf{A}_b \mathbf{x}_b + \mathbf{B}_b \mathbf{u}_b \quad (4.1)$$

$$\mathbf{Y}_b = \dot{Q}_b = \mathbf{C}_b \mathbf{x}_b + \mathbf{D}_b \mathbf{u}_b \quad (4.2)$$

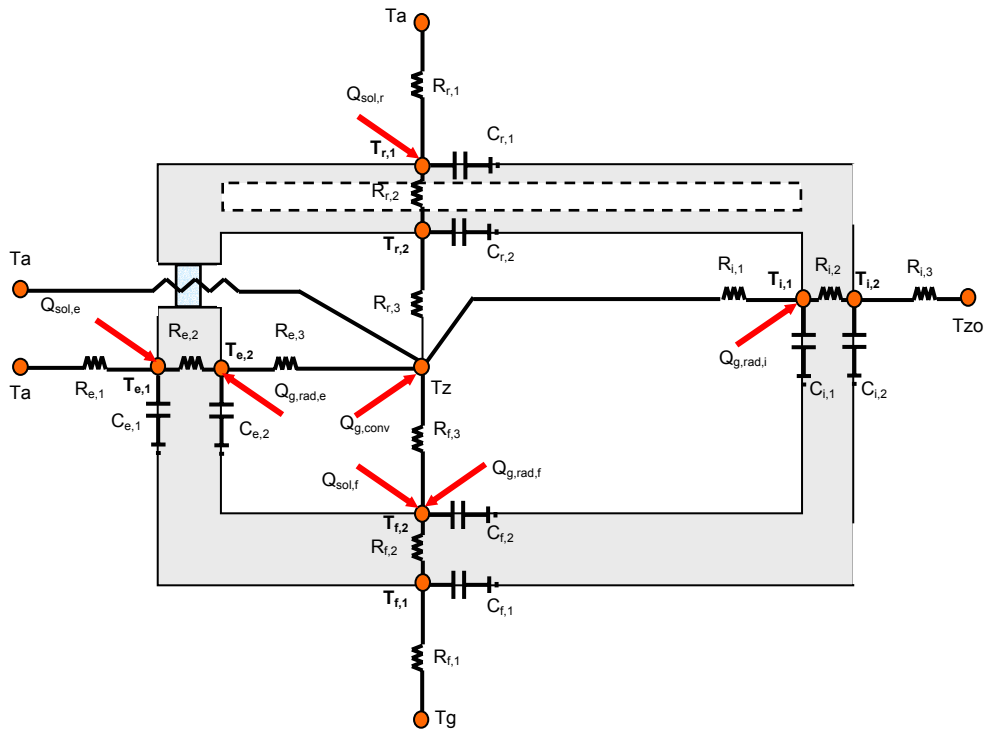
where \dot{Q}_b = rate of instantaneous heat gain to the building air.

The state and input vectors in the above representation are

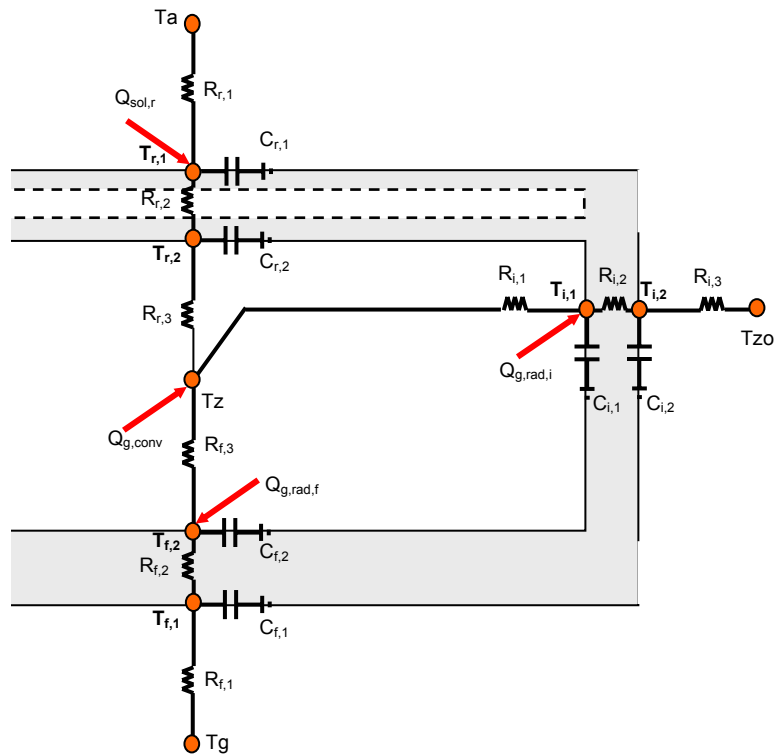
$$\mathbf{x}_b^T = [T_{r1}, T_{r2}, T_{e1}, T_{e2}, T_{f1}, T_{f2}, T_{i1}, T_{i2}] \quad (4.3)$$

$$\mathbf{u}_b^T = [T_z, T_a, T_g, Q_{sol,r}, Q_{sol,e}, Q_{g,rad,f}, Q_{g,rad,e}, Q_{g,rad,i}, Q_{sol,f}, Q_{g,conv}] \quad (4.4)$$

There are 8 state variables (two nodal temperatures in each of the four walls) and 10 input variables in the model. The elements of the coefficient matrices in the state space representation are in terms of the resistors and capacitors used in the different walls. The non-zero elements of the coefficient matrices in the state space representation are given below in equations 4.5 to 4.8.



(a) Network for external test rooms of east, south and west test rooms



(b) Network for interior test room

Figure 4.1 Thermal network for test rooms of the ERS building.

$$\mathbf{A}_b =$$

$$\begin{bmatrix} \frac{-1}{R_{r1}C_{r1}} + \frac{-1}{R_{r2}C_{r1}} & \frac{1}{R_{r2}C_{r1}} & 0 & 0 & 0 & 0 & 0 & 0 & 0 \\ \frac{1}{R_{r2}C_{r2}} & \frac{-1}{R_{r2}C_{r2}} + \frac{-1}{R_{r3}C_{r2}} & 0 & 0 & 0 & 0 & 0 & 0 & 0 \\ 0 & 0 & \frac{-1}{R_{e1}C_{e1}} + \frac{-1}{R_{e2}C_{e1}} & \frac{1}{R_{e2}C_{e1}} & 0 & 0 & 0 & 0 & 0 \\ 0 & 0 & \frac{1}{R_{e2}C_{e2}} & \frac{-1}{R_{e2}C_{e2}} + \frac{-1}{R_{e3}C_{e2}} & 0 & 0 & 0 & 0 & 0 \\ 0 & 0 & 0 & 0 & \frac{-1}{R_{f1}C_{f1}} + \frac{-1}{R_{f2}C_{f1}} & \frac{1}{R_{f2}C_{f1}} & 0 & 0 & 0 \\ 0 & 0 & 0 & 0 & \frac{1}{R_{f2}C_{f2}} & \frac{-1}{R_{f2}C_{f2}} + \frac{-1}{R_{f3}C_{f2}} & 0 & 0 & 0 \\ 0 & 0 & 0 & 0 & 0 & 0 & \frac{-1}{R_{i1}C_{i1}} + \frac{-1}{R_{i2}C_{i1}} & \frac{1}{R_{i2}C_{i1}} & 0 \\ 0 & 0 & 0 & 0 & 0 & 0 & \frac{1}{R_{i2}C_{i2}} & \frac{-1}{R_{i2}C_{i2}} + \frac{-1}{R_{i3}C_{i2}} & 0 \end{bmatrix} \quad (4.5)$$

$$\mathbf{B}_b =$$

$$\begin{bmatrix} 0 & \frac{1}{R_{r1}C_{r1}} & 0 & \frac{1}{C_{r1}} & 0 & 0 & 0 & 0 & 0 & 0 \\ \frac{1}{R_{r3}C_{r2}} & 0 & 0 & 0 & 0 & 0 & 0 & 0 & 0 & 0 \\ 0 & \frac{1}{R_{e1}C_{e1}} & 0 & 0 & \frac{1}{C_{e1}} & 0 & 0 & 0 & 0 & 0 \\ \frac{1}{R_{e3}C_{e2}} & 0 & 0 & 0 & 0 & 0 & \frac{1}{C_{e2}} & 0 & 0 & 0 \\ 0 & 0 & \frac{1}{R_{f1}C_{f1}} & 0 & 0 & 0 & 0 & 0 & 0 & 0 \\ \frac{1}{R_{f3}C_{f2}} & 0 & 0 & 0 & 0 & \frac{1}{C_{f2}} & 0 & 0 & \frac{\tau_{eff}}{C_{f2}} & 0 \\ \frac{1}{R_{i1}C_{i1}} & 0 & 0 & 0 & 0 & 0 & 0 & \frac{1}{C_{i1}} & 0 & 0 \\ \frac{1}{R_{i3}C_{i2}} & 0 & 0 & 0 & 0 & 0 & 0 & 0 & 0 & 0 \end{bmatrix} \quad (4.6)$$

$$\mathbf{C}_b^T = \left[0, \frac{1}{R_{r3}}, 0, \frac{1}{R_{e3}}, 0, \frac{1}{R_{f3}}, \frac{1}{R_{i1}}, \frac{1}{R_{i3}} \right] \quad (4.7)$$

$$\mathbf{D}_b^T = \left[\frac{-1}{R_{r3}} + \frac{-1}{R_{e3}} + \frac{-1}{R_{f3}} + \frac{-1}{R_{i1}} + \frac{-1}{R_{wi}} + \frac{1}{R_{wi}}, 0, 0, 0, 0, 0, 0, 0, 1 \right] \quad (4.8)$$

The methodology for determining the values of these resistors and capacitors is outlined in the next section.

4.1.2. Building Model Training Algorithm

The training algorithm is divided into two phases, a global search and a local search [Braun and Chaturvedi (2000) and Chaturvedi and Braun (2002)]. The global search uses a global systematic search to determine reasonable values of the building resistors and capacitors. It uses initial parameter estimates obtained from a crude building description to appropriately bound the parameters and searches within the bounded region. The local search uses a local regression method to further improve the R and C estimates. The combination of a local and a global phase provides a robust algorithm for determining an accurate model and only requires minimum preliminary building information. Figure 4.2 represents the concept of training and testing process.

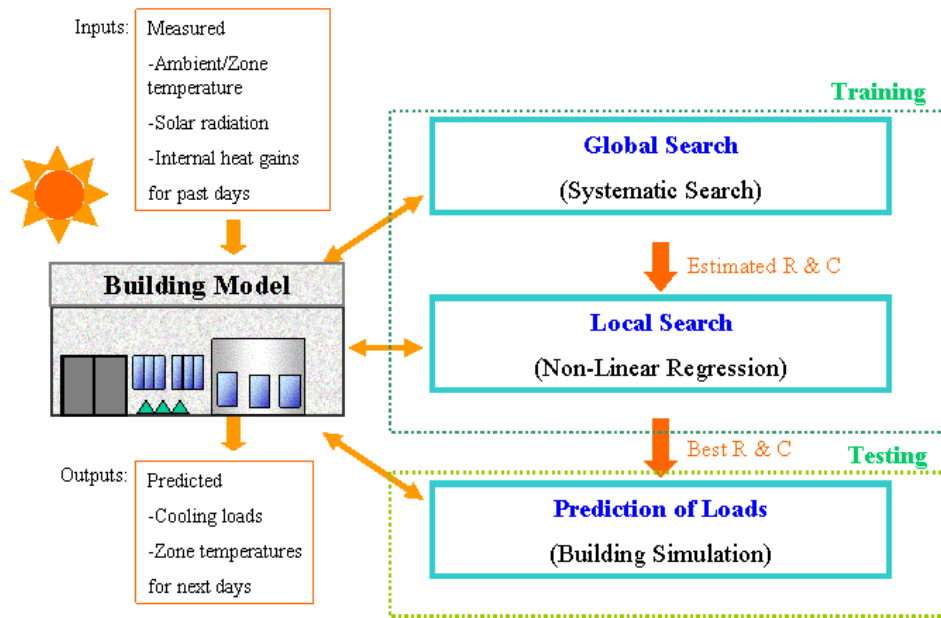


Figure 4.2 Training and testing process and building model.

Once the required region in which the parameters lie is identified, then the training algorithm generates a user specified number of points (m) within the bounded space using the global systematic point generation algorithm. At each generated point p, the magnitudes of each of the R's and C's are calculated. The state-space representation is then solved using the methodology of Seem et al. (1989) to predict the transient heat flow to the building as a transfer function of the input and state variables. The transfer function time step is assumed to be one hour. The heat flow to the building is given as:

$$\dot{Q}_{b,k} = \left(\sum_{j=0}^8 \mathbf{S}_{b,j} \mathbf{u}_{b,k-j} \right) - \left(\sum_{j=1}^8 e_{b,j} \dot{Q}_{b,k-j} \right) \quad (4.9)$$

where $\dot{Q}_{b,k}$ = rate of instantaneous heat transfer to the building air, $\mathbf{S}_{b,j}$ = series of row vectors containing transfer function coefficients for the input matrix in the building state space representation, and $e_{b,j}$ = scalar transfer function coefficients for past histories of heat flow to the building. The coefficients $\mathbf{S}_{b,j}$ and $e_{b,j}$ are calculated from the coefficient matrices \mathbf{A}_b , \mathbf{B}_b , \mathbf{C}_b , \mathbf{D}_b as outlined by Seem et al. (1989). The combined heat gain to the zone air at a given hour is removed by the cooling system to maintain temperature setpoints within the building. The instantaneous zone cooling load $\dot{Q}_{zs,k}$ can be calculated using an instantaneous energy balance on the zone given as:

$$C_z \cdot \frac{dT_{z,k}}{dt} = \dot{Q}_{b,k} - \dot{Q}_{zs,k} \quad (4.10)$$

where $T_{z,k}$ is the instantaneous zone temperature at time step k and C_z represents the effective zone capacitance which accounts for the air and any furnishings not included in the internal wall structure.

From equation 4.9, $\dot{Q}_{b,k}$ can be expressed as function of the instantaneous zone temperature. Hence, given the instantaneous temperature setpoint at the beginning and the end of the hour (one of the model inputs), equation 4.10 can be integrated to solve for instantaneous zone cooling load. However, for computational simplicity, it is assumed that the average heat gains and average cooling rate are constant over the hour and are evaluated at the average temperature over the hour and that the variation in setpoint is linear over the hour. The average temperature is then approximated as:

$$T_{avg,k} = \frac{1}{2}(T_{z,k} + T_{z,k-1}) \quad (4.11)$$

where $T_{avg,k}$ = average air temperature at hour k.

Since the zone temperature is assumed to vary linearly, the left hand side of equation 4.10 is:

$$\frac{dT_{z,k}}{dt} = \frac{T_{z,k} - T_{z,k-1}}{\Delta t} \quad (4.12)$$

where $\Delta t = 1$ hour.

Using these approximations and given the hourly inputs, the instantaneous zone cooling load necessary to maintain a fixed or linearly varying temperature setpoint can be calculated using equations 4.10-4.12. In the current model, only cooling loads were modeled i.e. in cases where the zone cooling load is negative (i.e. a heating load is required), the zone temperature is assumed to be floating. The current model can easily be extended to model situations where a heating setpoint, cooling setpoint and a dead zone (temperature range in which temperature is allowed to float) are specified. In such situations, if the cooling load is negative, the floating temperature is calculated. If it falls outside the dead zone, then the heating load required to maintain the heating setpoint is calculated using equations 4.9 and 4.10. In the current approach, the cooling load is set to zero if it is negative and the average floating temperature over the hour is determined from equations 4.9-4.12 as:

$$T_{avg,k} = \frac{\sum_{l=2}^9 \mathbf{S}_0(l) \mathbf{u}_{b,k}(l) + (\sum_{j=1}^8 \mathbf{S}_j \mathbf{u}_{b,k-j}) - (\sum_{j=1}^8 e_j \dot{Q}_{b,k-j}) + 2 \cdot C_z \cdot T_{z,k-1}}{(2 \cdot C_z - \mathbf{S}_0(1))} \quad (4.13)$$

where $\mathbf{S}_0(1)$ is the first element of the \mathbf{S}_0 vector (coefficient of $T_{z,k}$), l denotes the l^{th} element of the vectors.

Using the average floating temperature, the instantaneous floating zone temperature is calculated from equation 4.11 and the past histories of the zone heat flow are updated.

At each generated point, cooling loads (and temperatures) are determined for the entire training period. Cooling load predictions for the entire training duration are then compared with the baseline values (detailed model predictions or field measurements). The criterion used for comparison is the integrated root mean square errors for the training duration, which can be represented as:

$$J_{b,p} = \sqrt{\frac{\sum_{k=1}^{N_{train}} (\dot{Q}_{d,k} - \dot{Q}_{zs,k})^2}{N_{train} - 1}} \quad (4.14)$$

where $J_{b,p}$ = building regression cost function at point p, $\dot{Q}_{d,k}$ = baseline cooling loads at time step k, and N_{train} = training duration in hours.

The algorithm outputs the R and C values corresponding to the point with the minimum errors. These estimates are taken as the starting point for the local phase. In the local phase, the algorithm uses a local regression method and generates improved estimates for the R's and C's. The regression cost function for the building is given in equation 4.14, with the point p corresponding to a set of values of R's and C's. Since both $\dot{Q}_{d,k}$ and $\dot{Q}_{zs,k}$ are dependent on past histories, the regression cost function is non-linear. The local regression algorithm used is the Levenberg Marquardt method. The routine uses a finite difference Jacobian to determine a local minimum. A minimum is chosen to correspond to the point where either the parameter estimates do not differ significantly (according to a specified tolerance) in successive iterations or the reduction in cost function falls below the specified tolerance criteria.

4.2. VALIDATION OF INVERSE MODEL

4.2.1. Data Set Description

Two types of data sets were used in this study to validate the simplified building model:

- A. Simulated data: Cooling load and zone temperature data were generated for the ERS building using the TRNSYS model. Weather data involving ambient temperature and solar radiation used for generation of simulated data set was averaged yearly data for the ERS site, provided by the IEC. The simulated data were used to investigate the effect of training duration requirement and training control strategy requirement on the accuracy of the simplified model. Simulated data for the training of the inverse model were generated for a period starting on July 2 and data for the testing of prediction performance of the model for a period beginning on August 6. Four kinds of durations for training data were considered from 1 week to 4 weeks and two testing data sets were produced for 1 week and 1 month.
- B. Measured data: The building model predictions were compared with measured cooling load data for Phase 1 and 2 test periods.

4.2.2. Validation Using Simulated Data

Application Model to TRNSYS Data

For the simulated data modeling studies, two strategies were used for training and testing: Night-setup (NS) and Precooling (PC). The temperature setpoints for each of these strategies were shown in Figure 3.3. The resultant data sets from the TRNSYS ERS building model were used as inputs to the simplified building model. A part of the resultant data set was used for

training and the remainder was used for testing the models. Using the TRNSYS generated data sets, the simplified building model training algorithm was used to obtain the best resistor and capacitor estimates for all the different simulation conditions. Table 4.1 to Table 4.4 show all cases studied using simulated data set.

Table 4.1 Training with night-setup data set and testing with night-setup data set.

Training period	Control in training	Testing with 1 & 4 weeks
1 week	Night-setup	Night-setup
2 weeks	Night-setup	Night-setup
3 weeks	Night-setup	Night-setup
4 weeks	Night-setup	Night-setup

Table 4.2 Training with precooling data set and testing with precooling data set.

Training period	Control in training	Testing with 1 & 4 weeks
1 week	Precooling	Precooling
2 weeks	Precooling	Precooling
3 weeks	Precooling	Precooling
4 weeks	Precooling	Precooling

Table 4.3 Training with night-setup data set and testing with precooling data set.

Training period	Control in training	Testing with 1 & 4 weeks
1 week	Night-setup	Precooling
2 weeks	Night-setup	Precooling
3 weeks	Night-setup	Precooling
4 weeks	Night-setup	Precooling

Table 4.4 Training with precooling data set and testing with night-setup data set.

Training period	Control in training	Testing with 1 & 4 weeks
1 week	Precooling	Night-setup
2 weeks	Precooling	Night-setup
3 weeks	Precooling	Night-setup
4 weeks	Precooling	Night-setup

Table 4.5 and Table 4.6 give the bounds used for the global search phase of model training corresponding to the ERS building.

Table 4.5 Material property bounds used in building training algorithm.

Property	Bounds	External wall	Internal wall	Roof wall	Floor Wall
Conductivity (Btu/hr-F-ft)	Minimum	1E-3	1E-3	1E-5	1E-3
	Maximum	1.1	1.1	5E3	1.1
Specific heat * density (Btu/F-ft ³)	Minimum	0.1	0.1	0.1	0.1
	Maximum	30	10	50	30

Table 4.6 Physical properties bound used in building training algorithm.

Bounds	Effective transmittance	Internal convective coefficient	External convective coefficient	Effective zone capacitance
Minimum	0.1	0.1	2.0	0
Maximum	0.9	1.0	6.0	150 (for each zone) 800 (for whole zones)

The trained simplified building model was tested using a separate set of test data. An extensive simulation study was conducted to analyze the impact of training duration as well as dependency of the model on the control strategy used for training.

The model training data set was varied from a one-week to a one-month period chosen in July and the testing data set was chosen to be from one week to one month in August as described in the previous section.

The integrated root mean square errors evaluated at the end of the testing period and expressed as a percentage of the maximum baseline load were used as a criterion for determining the model accuracy.

Results

The impact of training duration on the prediction of cooling loads was investigated varying the training duration from 1 week to 4 weeks. Figures 4.3 to 4.6 show the E_{rms} of the prediction of cooling loads trained with simulated data and tested with other simulated data. Results of training with NS and testing with NS are shown in Figure 4.3. Training with more than 3 weeks of data resulted in errors of less than 4% for both testing of 1 week and 4 weeks. Results

of training with PC and testing with PC are represented in Figure 4.4. Errors for the case of training with 2 and 3 weeks of data also gave errors of less than 4%. In the case of training with NS and testing with PC as shown in Figure 4.5, training durations of 3 and 4 weeks resulted in significantly errors. However, training with PC and testing with NS as shown in Figure 4.6, gave errors less than 3% for 2 or 3 week training durations. From these results it is found that at least 2 weeks data is necessary for the training of the inverse model and it is preferable to have training data obtained with some degree of precooling strategy in place.

Hourly simulated cooling loads and zone temperatures from the TRNSYS and inverse models are given in Figures 4.7 to 4.10 for the testing period. Cooling loads and average zone temperatures are for all of the test zones combined. The inverse model does a very good job of capturing the dynamics of the simulated building.

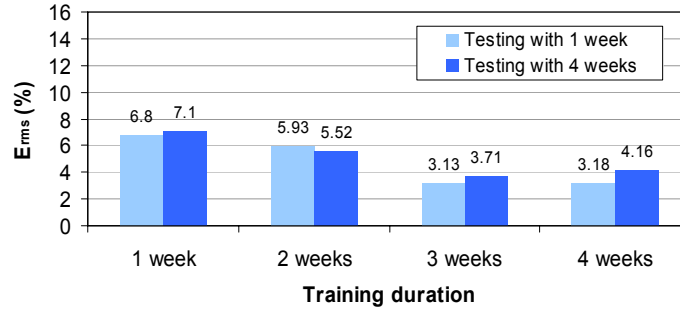


Figure 4.3 E_{rms} of inverse model using simulated data set in case of training with NS and testing with NS according to training duration from 1 week to 4 weeks.

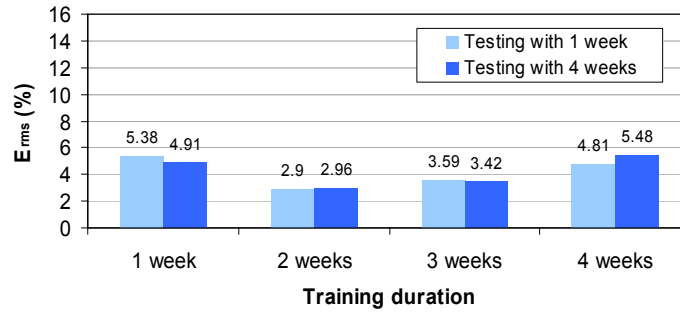


Figure 4.4 E_{rms} of inverse model using simulated data set in case of training with PC and testing with PC according to training duration from 1 week to 4 weeks.

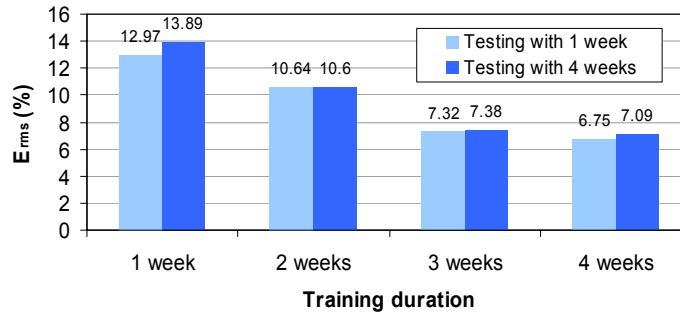


Figure 4.5 E_{rms} of inverse model using simulated data set in case of training with NS and testing with PC according to training duration from 1 week to 4 weeks.

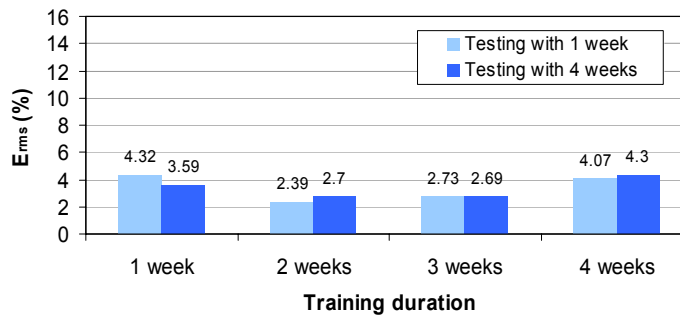
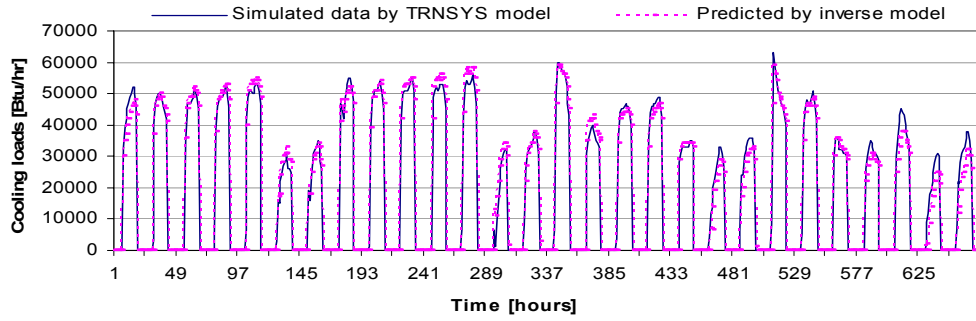
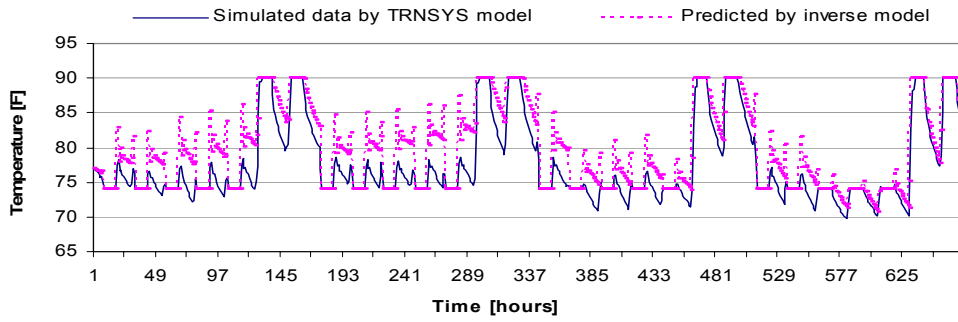


Figure 4.6 E_{rms} of inverse model using simulated data set in case of training with PC and testing with NS according to training duration from 1 week to 4 weeks.

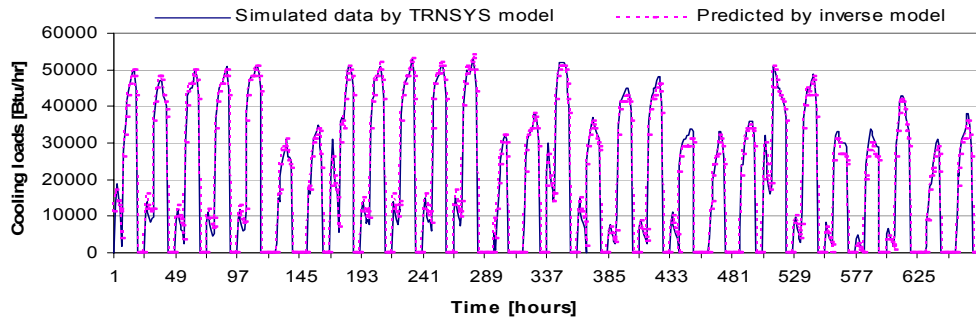


(a) Cooling loads

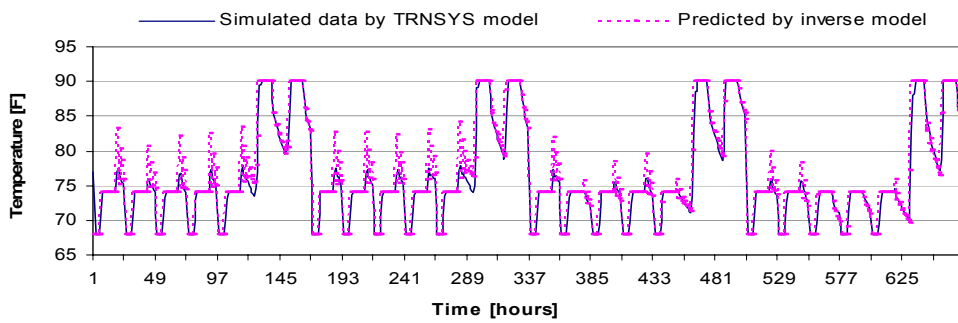


(b) Zone temperature

Figure 4.7 Measured and calculated results of inverse model using simulated data set for testing duration of 4 weeks with training duration of 3 weeks (training with NS and training with NS).

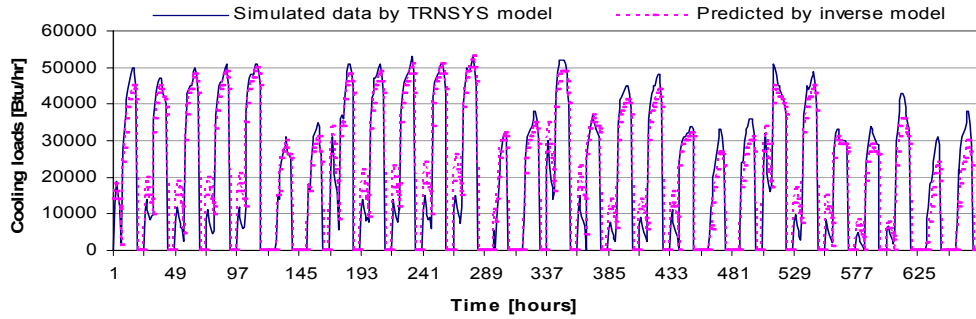


(a) Cooling loads

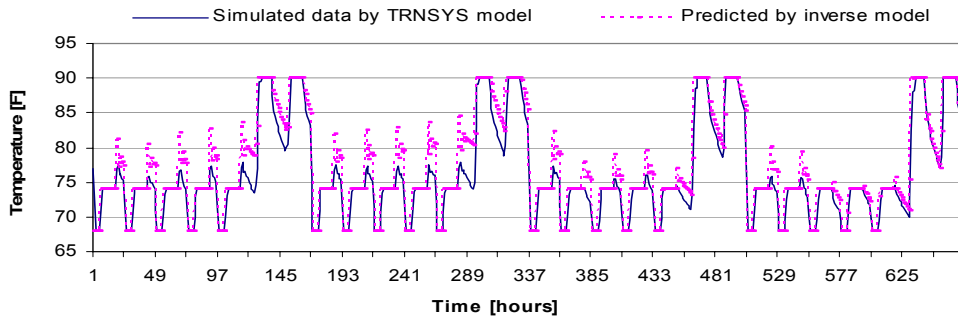


(b) Zone temperatures

Figure 4.8 Measured and calculated results of inverse model using simulated data set for testing duration of 4 weeks with training duration of 2 weeks (training with PC and training with PC).

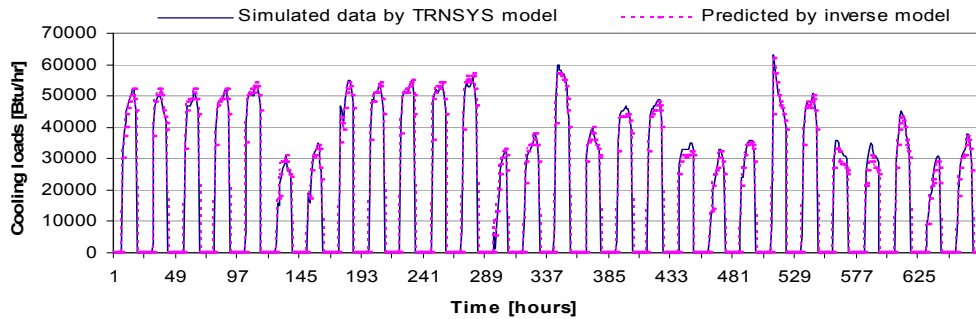


(a) Cooling loads

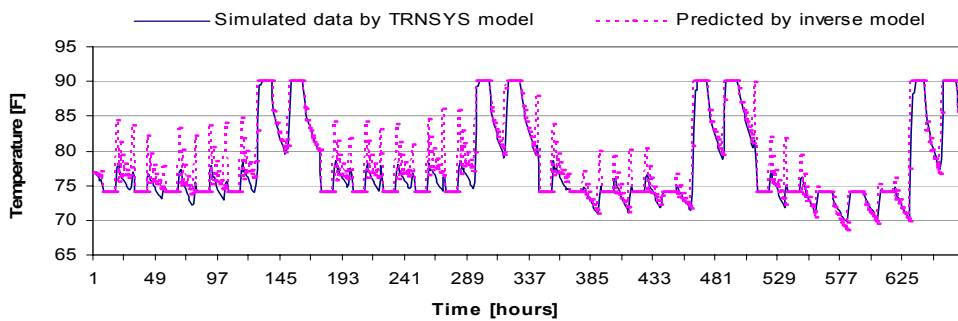


(b) Zone temperatures

Figure 4.9 Measured and calculated results of inverse model using simulated data set for testing duration of 4 weeks with training duration of 4 weeks (training with NS and training with PC).



(a) Cooling loads



(b) Zone temperatures

Figure 4.10 Measured and calculated results of inverse model using simulated data set for testing duration of 4 weeks with training duration of 2 weeks (training with PC and training with NS).

The impact of the control strategy used in training and testing is illustrated in the results of Figures 4.11 to 4.14. In general, training with NS showed higher errors than training with PC. As the training data duration increases, the difference in errors associated with the use of different training controls strategies tends to be reduced. However, the testing duration doesn't have significant effect on the results.

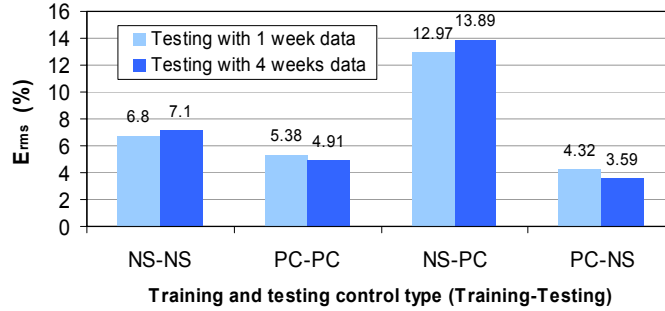


Figure 4.11 E_{rms} of inverse model using simulated data set according to control strategies in training in case of 1 week training data set.

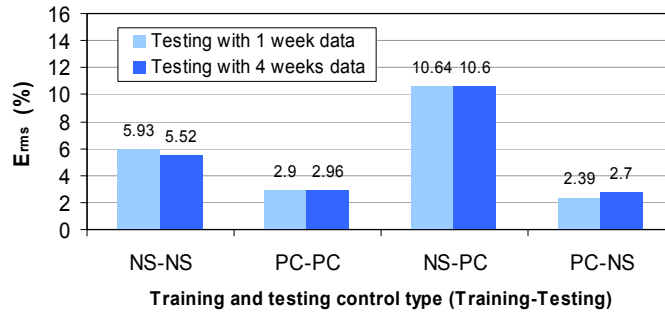


Figure 4.12 E_{rms} of inverse model using simulated data set according to control strategies in training in case of 2 week training data set.

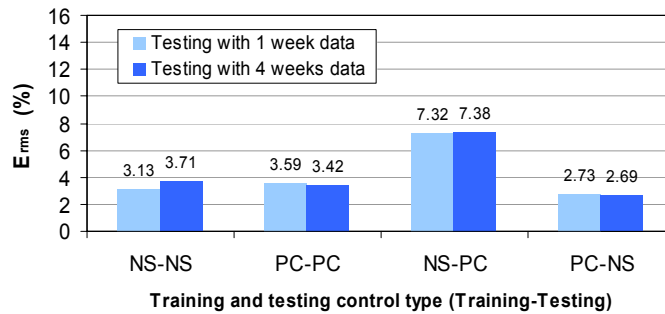


Figure 4.13 E_{rms} of inverse model using simulated data set according to control strategies in training in case of 3 week training data set.

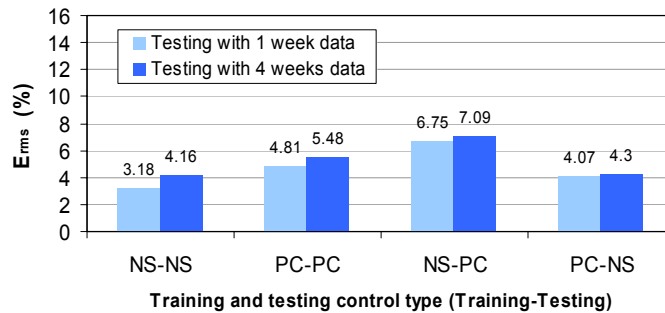


Figure 4.14 E_{rms} of inverse model using simulated data set according to control strategies in training in case of 4 week training data set.

4.2.3. Validation Using Field Data

Application Model to ERS Field Data

For the studies using field data, both night setup and precooling control were considered. The temperature setpoints for each of these strategies were shown in Figure 3.3. The measured data sets for the Phase 1 and Phase 2 tests at the ERS building were used as inputs to the simplified building model. A part of the resultant data set was used for training the models and the remainder was used for testing the models. Using the measured data sets, the simplified building model training algorithm was used to obtain the best resistor capacitor and estimates. The bounds given in Table 4.5 and 4.6 were also used for the global phase of model training. The trained simplified building model was tested using a separate set of test data.

The inverse model was evaluated using both training and testing performance. Table 4.7 shows all cases for evaluation of training performance and Table 4.8 represents all cases for evaluation of testing performance. In the cases for testing performance evaluation, the third and fourth cases were designed to investigate the impact of training duration. And since three days for testing is not enough to compensate for the initial conditions of model, the testing data set was extended to nine days by using the three days of data three times in sequence.

Table 4.7 Cases for training performance evaluation.

Name of case	Training	Testing	Data duration
11	Phase 1	Phase 1	9 days
22	Phase 2	Phase 2	8 days
33	Phase 1 + Phase 2	Phase 1 + Phase 2	17 days

Table 4.8 Cases for testing performance evaluation.

Name of case	Training	Testing	Zones
12	Phase 1	Phase 2	Each test zones and combined zones
21	Phase 2	Phase 1	Each test zones and combined zones
3'1'	6 days of Phase 1 + Phase 2 (Phase 3')	Rest 3 days of Phase 1 (Phase 1')	Combined zones
3''2'	Phase 1 + 5 days of Phase 2 (Phase 3'')	Rest 3 days of Phase 2 (Phase 2')	Combined zones

Results

The training performances of the inverse model were first investigated by training and testing using the same data sets for the cases summarized in Table 4.7. Figure 4.15 shows prediction error according to training data type for all zones combined. Errors were calculated using both the entire data period and using the last three days in order to consider initial state effects. Results show that training performance improves with a greater training duration or the use of the precooling control strategy. Figures 4.16 to 4.18 give cooling loads and zone temperatures for these cases over the last three days of training data. The inverse model does a much better job of representing the building dynamics than the TRNSYS model.

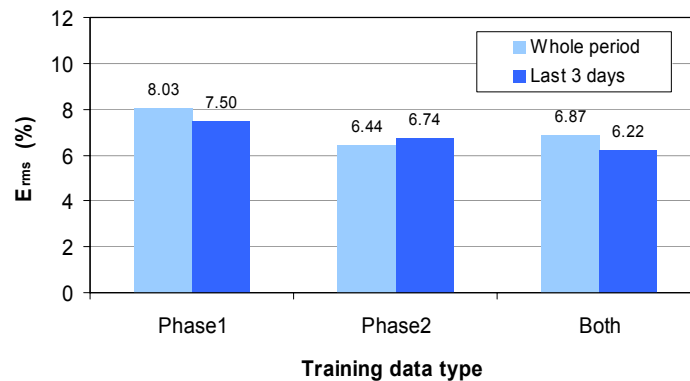
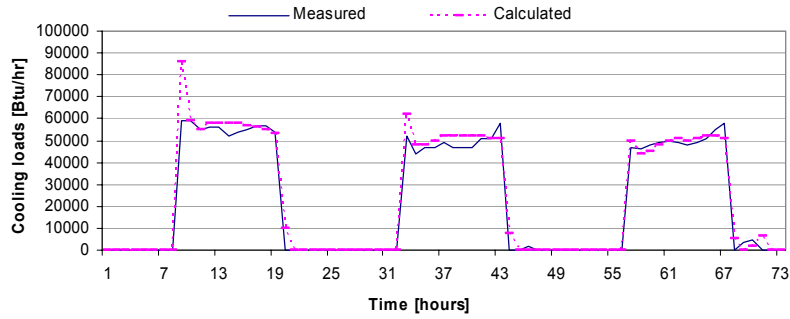
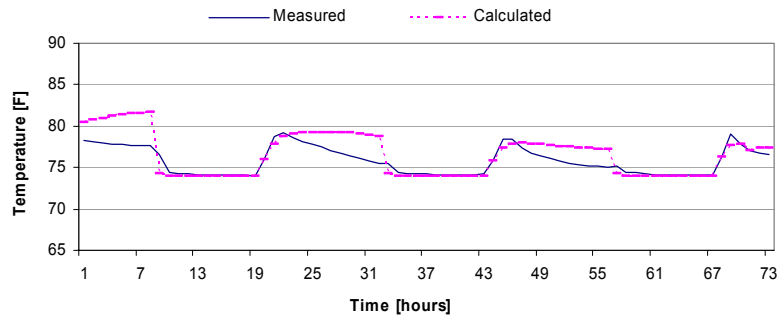


Figure 4.15 Testing E_{rms} of inverse model using field data with training data types.

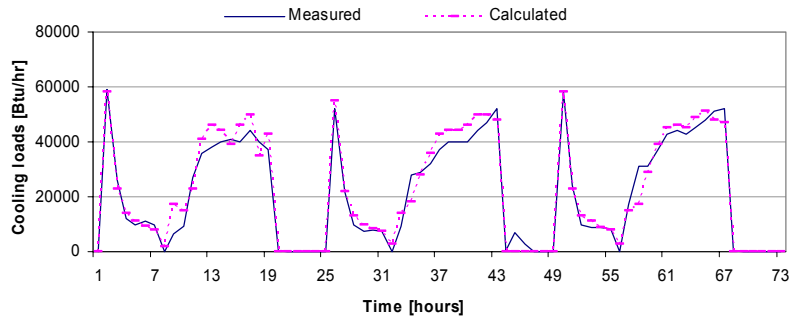


(a) Cooling loads

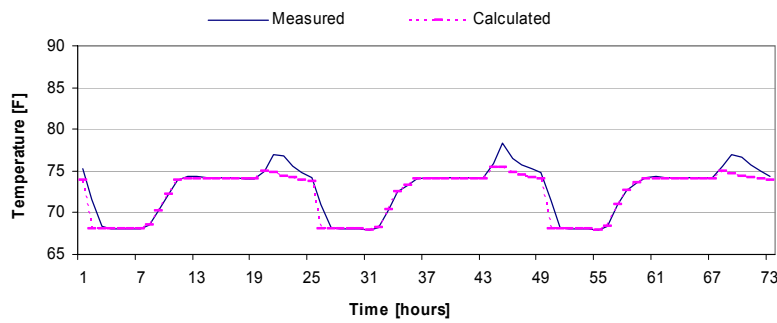


(b) Zone temperatures

Figure 4.16 Measured and calculated results of inverse model using field data (case:11, training with Phase 1 and testing with Phase 1).

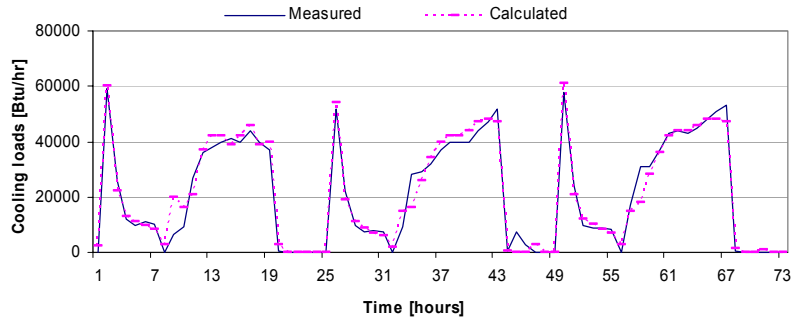


(a) Cooling loads

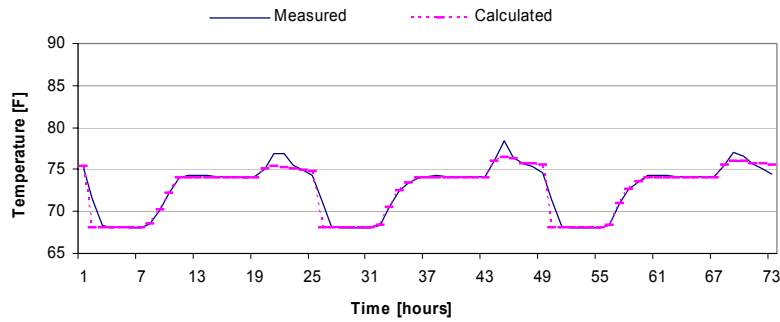


(b) Zone temperatures

Figure 4.17 Measured and calculated results of inverse model using field data (case: 22, training with Phase 2 and testing with Phase 2).



(a) Cooling loads



(b) Zone temperatures

Figure 4.18 Measured and calculated results of inverse model using field data (case:33, training with both Phase 1 and Phase 2 and testing with both Phase 1 and Phase 2).

Results for testing performing are presented for the different training and testing scenarios summarized in Table 4.8. Testing performance of the inverse model was investigated for east, south, west, interior and combined test rooms and prediction errors for these cases are shown in Figures 4.19 to 4.23. Generally the model predicts cooling loads well compared with measured cooling loads. For the combined zones, prediction errors were within 8% except the case of training with phase 2 and testing with phase 1, which had about a 12% prediction error. A better model could be obtained if more data were available at a wider range of conditions. Figures 4.24 to 4.35 show cooling loads and zone temperature for each case. The inverse model does a very good job of capturing the dynamics of the different zone loads. However, training with precooling data leads to overpredictions of load for night setup, whereas training with night setup leads to underpredictions of load for the precooling period.

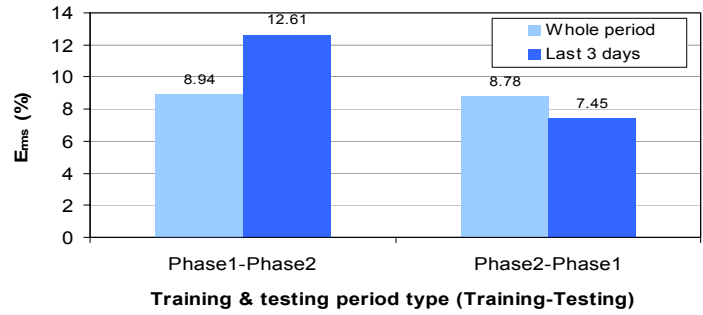


Figure 4.19 Prediction E_{rms} of inverse model for east test rooms with training & testing control type.

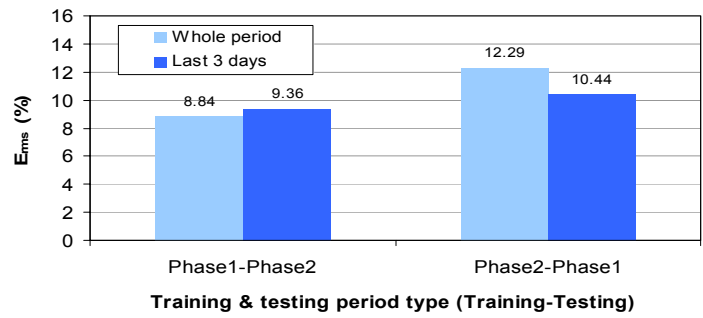


Figure 4.20 Prediction E_{rms} of inverse model for south test rooms with training & testing control type.

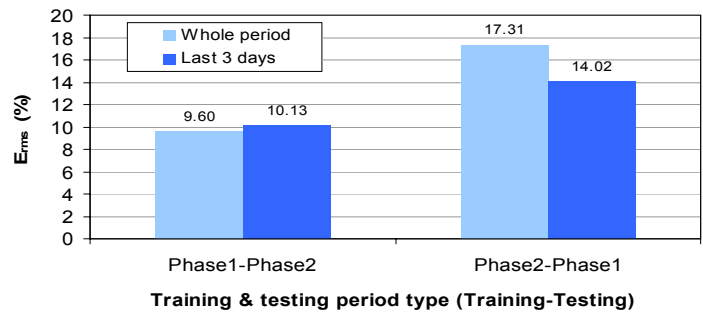


Figure 4.21 Prediction E_{rms} of inverse model for west test rooms with training & testing control type.

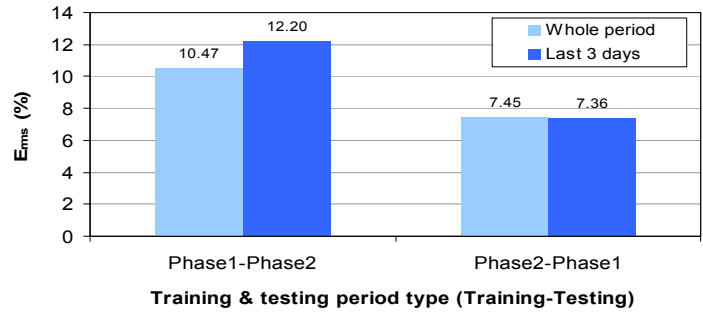


Figure 4.22 Prediction E_{rms} of inverse model for interior test rooms with training & testing control type.

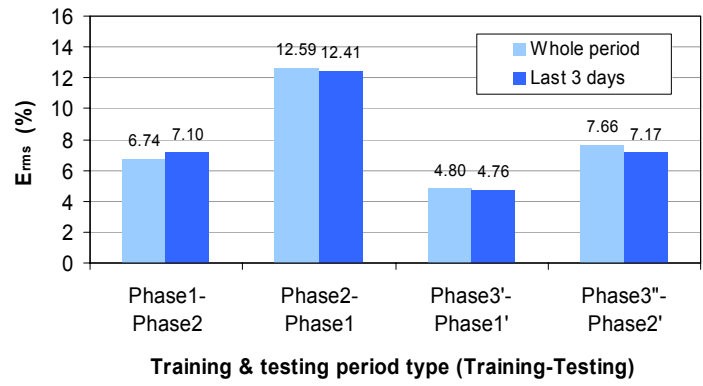
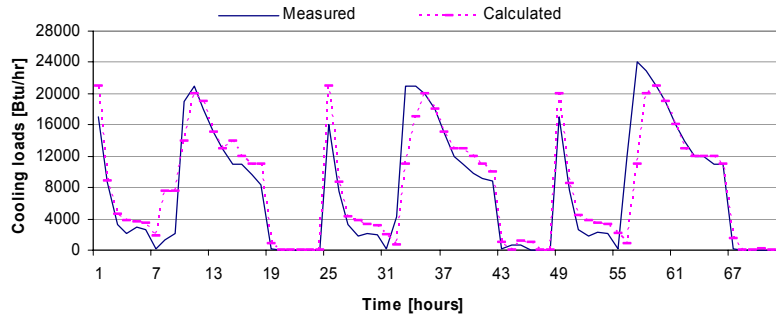
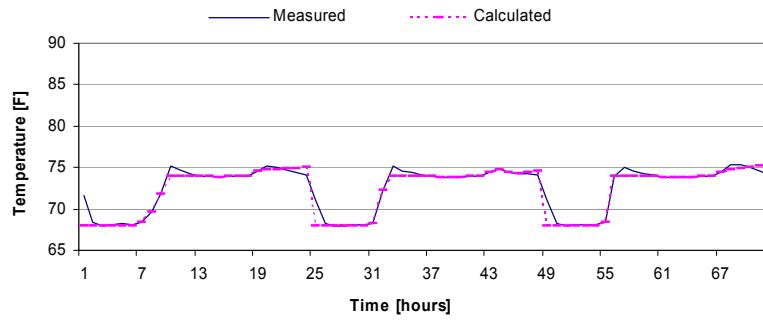


Figure 4.23 Prediction E_{rms} of inverse model for combined test rooms with training & testing control type.

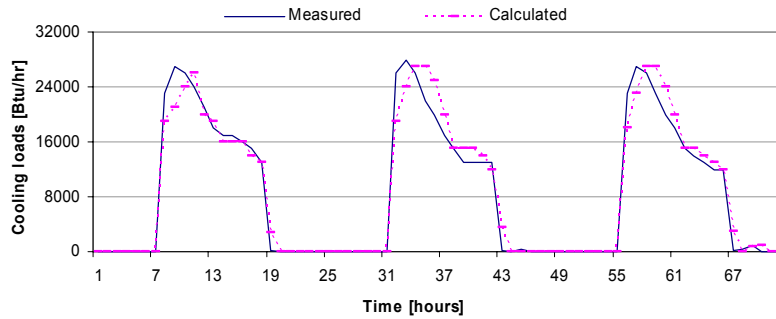


(a) Cooling loads

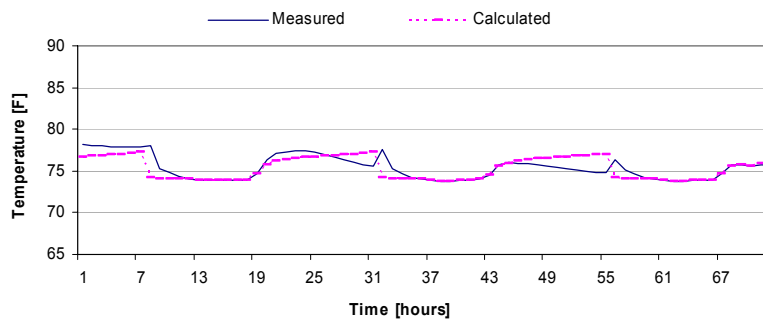


(b) Zone temperatures

Figure 4.24 Measured and calculated results of inverse model for east test rooms (case:12, Training with Phase 1 and testing with Phase 2).

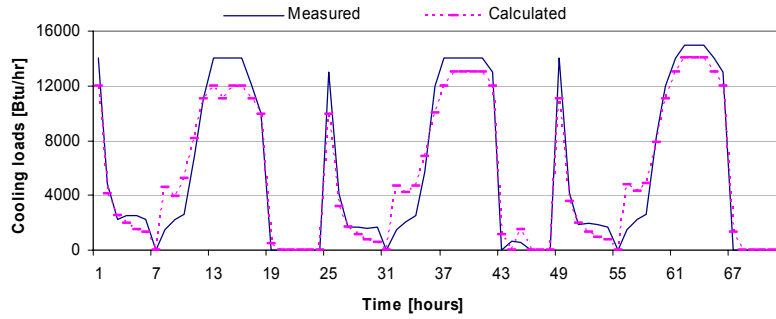


(a) Cooling loads

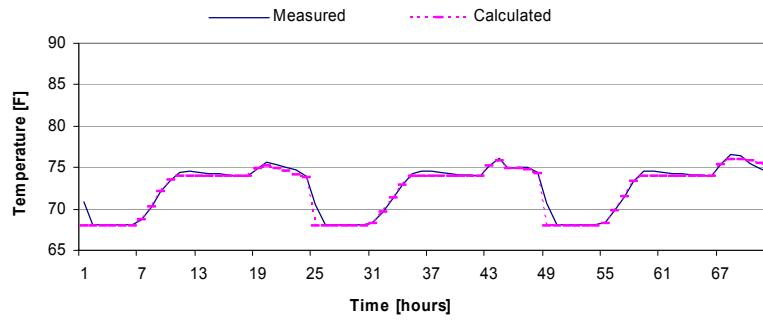


(b) Zone temperatures

Figure 4.25 Measured and calculated results of inverse model for east test rooms (case:21, Training with Phase 2 and testing with Phase 1).

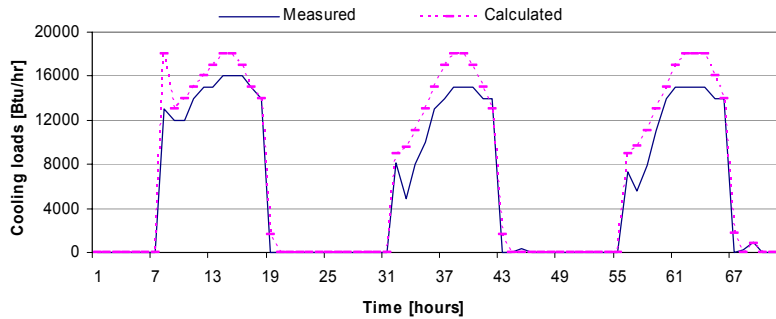


(a) Cooling loads

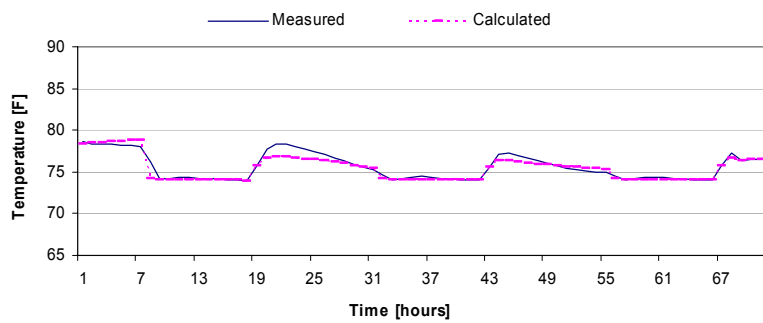


(b) Zone temperatures

Figure 4.26 Measured and calculated results of inverse model for south test rooms (case:12, Training with Phase 1 and testing with Phase 2).

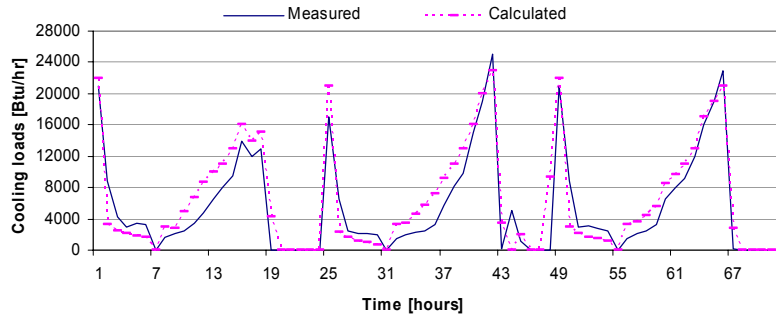


(a) Cooling loads

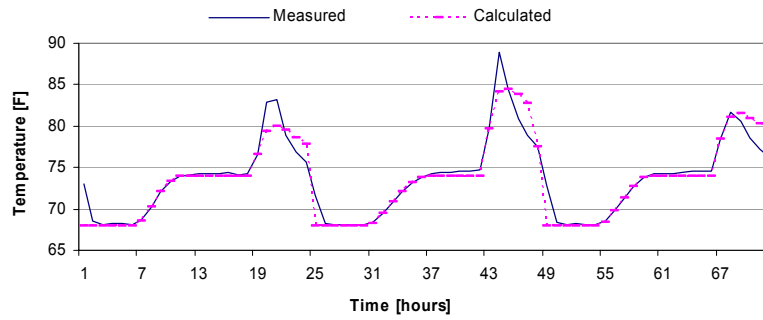


(b) Zone temperatures

Figure 4.27 Measured and calculated results of inverse model for south test rooms (case:21, Training with Phase 2 and testing with Phase 1).

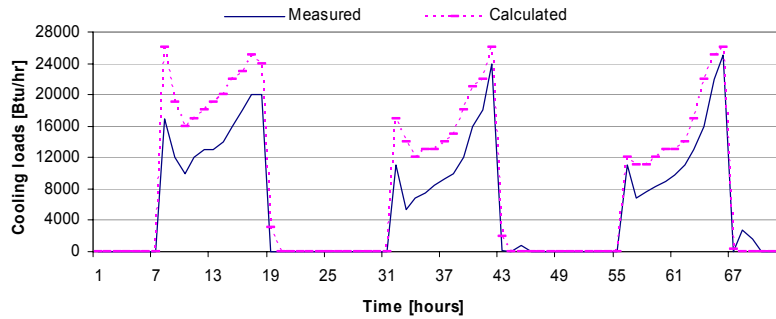


(a) Cooling loads

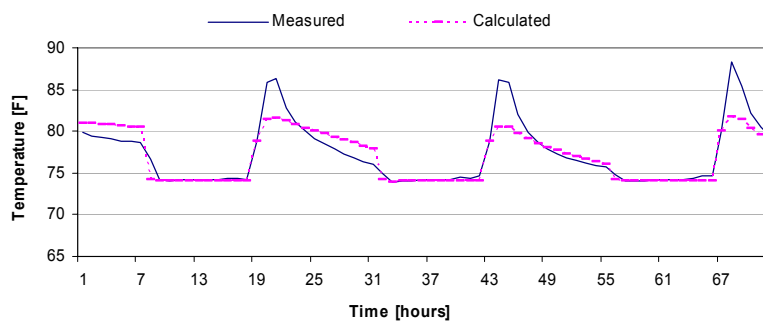


(b) Zone temperatures

Figure 4.28 Measured and calculated results of inverse model for west test rooms (case:12, Training with Phase 1 and testing with Phase 2).

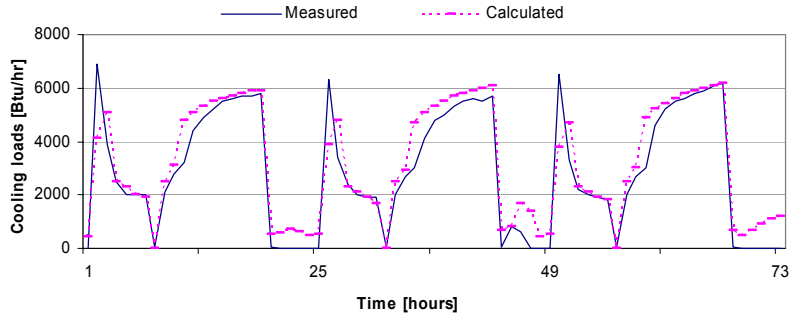


(a) Cooling loads

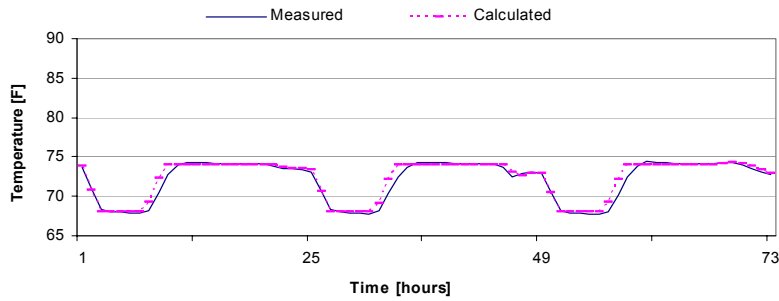


(b) Zone temperatures

Figure 4.29 Measured and calculated results of inverse model for west test rooms (case:21, Training with Phase 2 and testing with Phase 1).

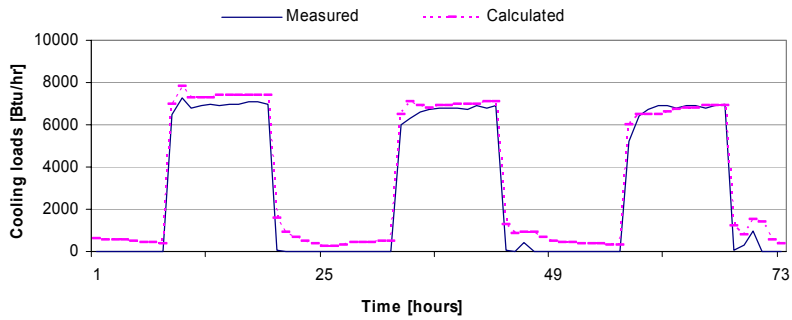


(a) Cooling loads

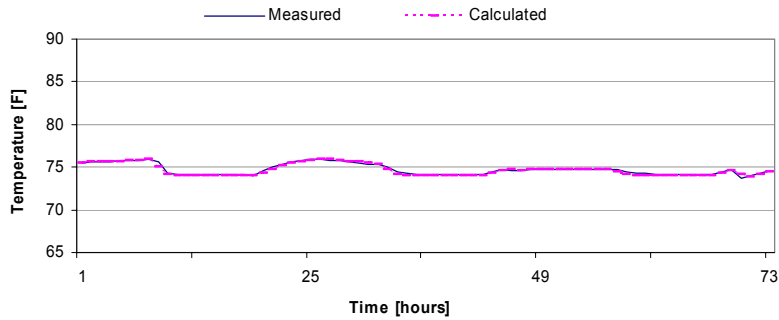


(b) Zone temperatures

Figure 4.30 Measured and calculated results of inverse model for interior test rooms (case:12, Training with Phase 1 and testing with Phase 2).

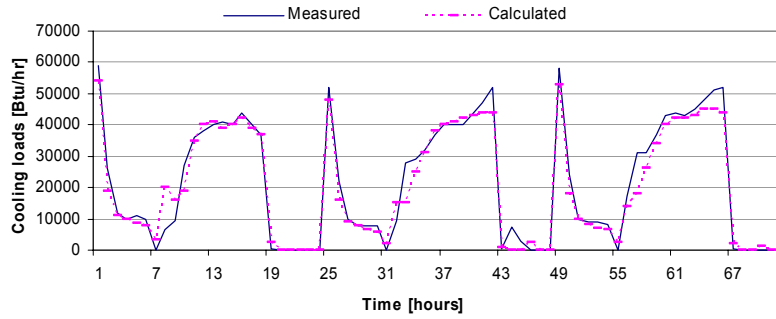


(a) Cooling loads

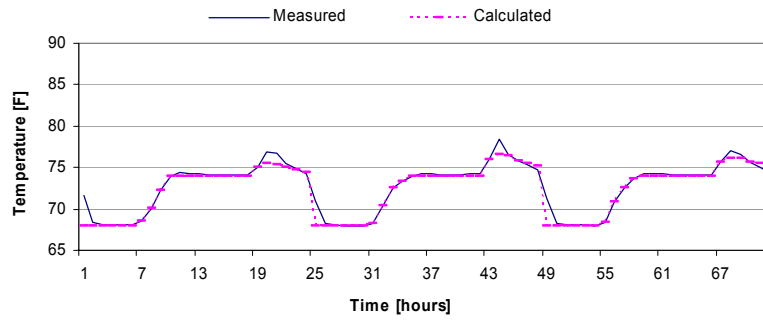


(b) Zone temperatures

Figure 4.31 Measured and calculated results of inverse model for interior test rooms (case:21, Training with Phase 2 and testing with Phase 1).

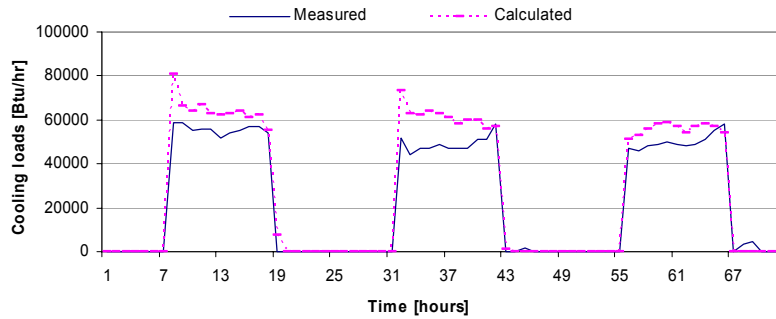


(a) Cooling loads

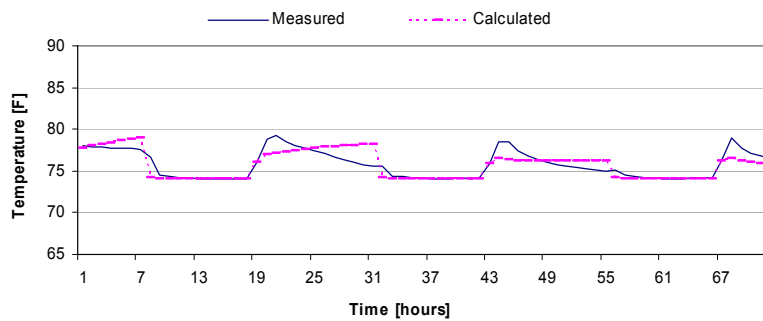


(b) Zone temperatures

Figure 4.32 Measured and calculated results of inverse model for combined test rooms (case:12, Training with Phase 1 and testing with Phase 2).

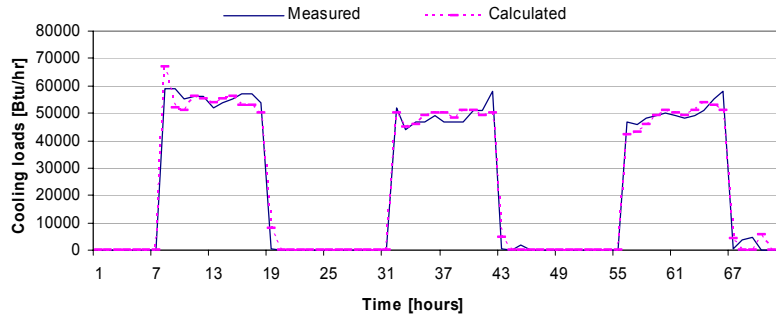


(a) Cooling loads

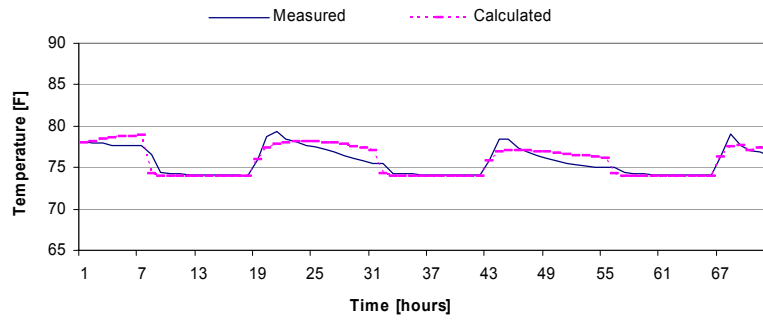


(b) Zone temperatures

Figure 4.33 Measured and calculated results of inverse model for combined test rooms (case:21, Training with Phase 2 and testing with Phase 1).

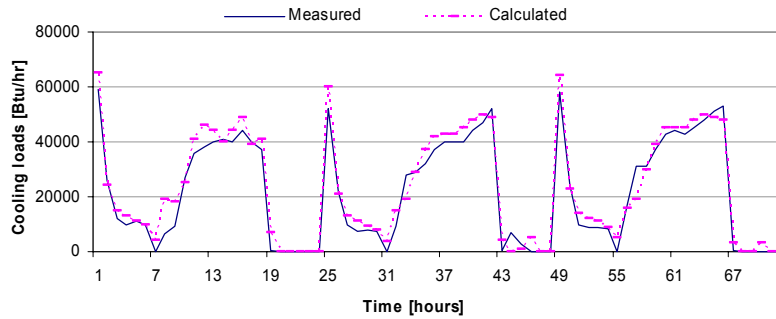


(a) Cooling loads

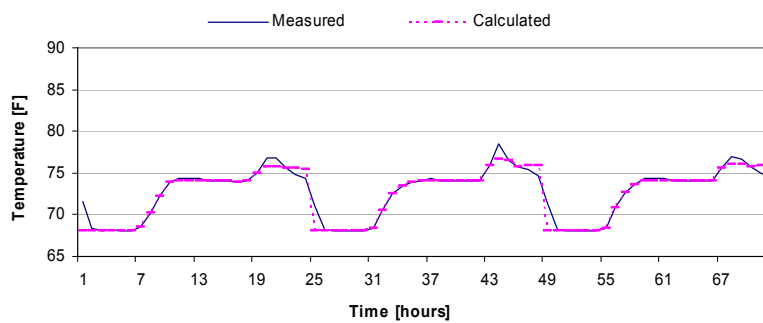


(b) Zone temperatures

Figure 4.34 Measured and calculated results of inverse model for combined test rooms(case:3'1', Training with Phase 3' and testing with Phase 1').



(a) Cooling loads



(b) Zone temperatures

Figure 4.35 Measured and calculated results of inverse model for combined test rooms(case:3'2', Training with Phase 3' and testing with Phase 2').

Figure 4.36 compares the calculated and measured cooling loads for two days of the Phase 1 and Phase 2 test periods. Because the two data sets from Aug.10 to 11 and Aug.19 to 20 have similar solar radiation and ambient temperature conditions, these cooling loads are useful for evaluating the impact of precooling on load shifting. The simulated cooling load matches the actual cooling loads very well. For both simulated and measured results, the occupied period load was about 23% less for the precooling tests. The peak load was reduced by about 9%. However, the control strategy was not designed to maximize peak load reduction. Much greater peak load reductions would be possible if the zone temperatures were varied within the comfort region rather than being held constant. Such a strategy would keep the zone temperatures low at the beginning of occupancy and raise them later in the day. This would have the effect of increasing the early occupancy loads and decreasing the late occupancy loads. The next step was to evaluate the impact of such a demand-limiting strategy on peak loads using the inverse model develop in this project for the Iowa Energy Center. This is considered in the next section.

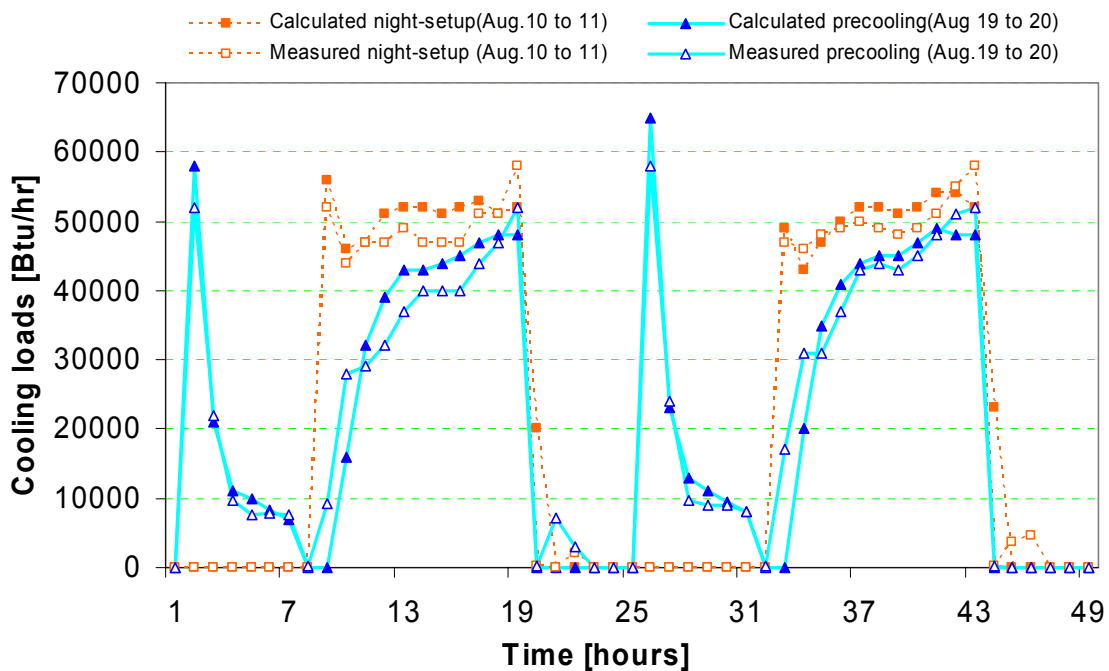


Figure 4.36 Comparison of measured and calculated cooling loads of inverse model for night-setup and precooling on August 10 to 11 in Phase 1 and August 19 to 20 in Phase 2.

5. PEAK DEMAND-LIMITING CONTROL STRATEGY

5.1. DEMAND-LIMITING STRATEGY

A demand-limiting control strategy in this work is defined as a strategy that aims to “limit” the peak cooling load under a specified target cooling load during the on-peak period by adjusting room setpoint temperature within the comfort range. Figure 5.1 represents setpoint temperatures for both night-setup(NS) and demand-limiting(DL) control strategies. In the demand-limiting strategy, the building is pre-cooled by lowering the setpoint to 67°F. In this study, the duration of the precooling period was varied. During the occupied period, the setpoint is set at the lower end of the comfort limit at 69°F until the cooling load would exceed a certain target demand-limiting cooling load. When the building cooling load would exceed the target load, the setpoint temperature increases in order to limit the building cooling load to the target load. In this study, the target load was adjusted each day through iteration so as to utilize the entire comfort range. A secant method was used to determine the target load that would yield a zone temperature at the end of occupied period of 76°F. After the occupied period, the setpoints were set at 80°F until the start of the precooling period.

In order to evaluate the potential for a demand-limiting control strategy, the last day of Phase 1 (Aug. 11) operation was chosen for comparison with a base case of night setup control. Every simulation was conducted for an identical set of ten days in a row to erase the initial condition effects and reach a steady-periodic condition.

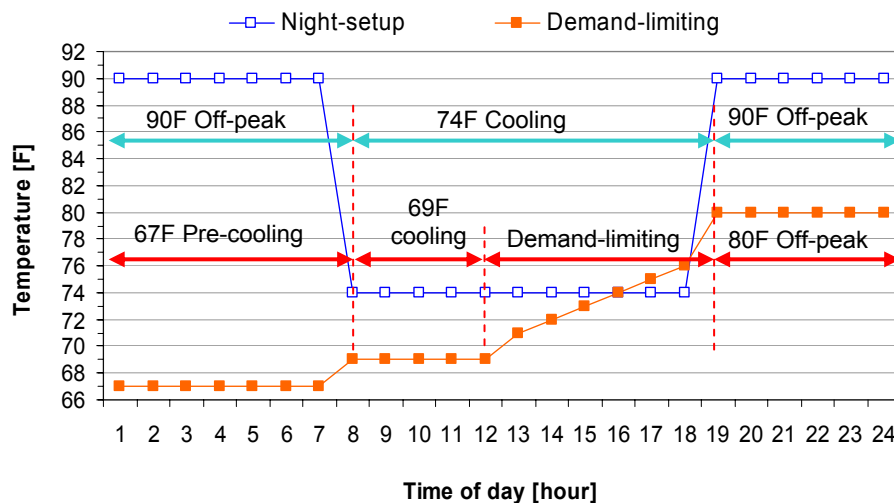


Figure 5.1 Setpoint temperatures for night-setup and demand-limiting strategies.

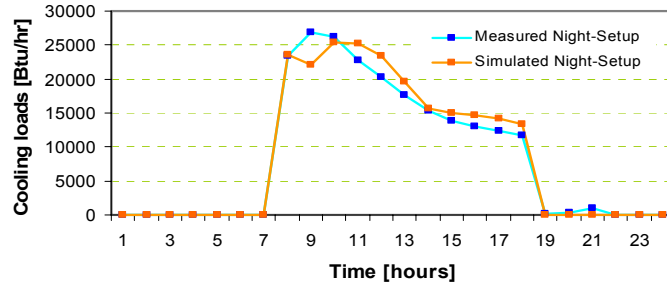
5.2. SIMULATION STUDIES

5.2.1. Methods of study

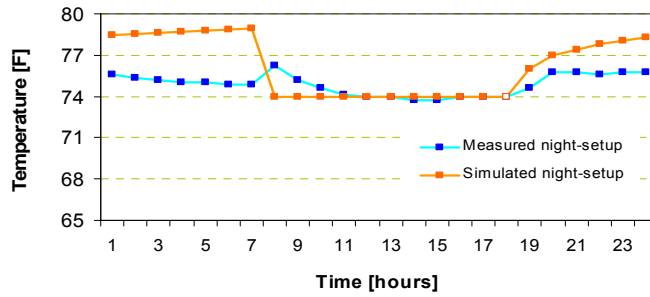
In this study, the east, west and combined test rooms were considered for evaluation of the demand-limiting control strategy because these three test zones cover the range of diversity in cooling load profiles for the ERS building. Cooling loads for the east rooms have a peak in the morning and the west rooms have a peak in the afternoon. The load profile for the combined test rooms is relatively flat compared to the east and west zones, but is representative of a small commercial building.

The demand-limiting period or on-peak period, where the demand-limiting strategy is applied, was varied by changing the start-time from 7 am to 3 pm. The precooling period was also changed by varying the start-time from 10 pm to 7am. A start-time of 7 am for precooling represents no precooling during the off-peak period and represents a limiting case.

In order to evaluate the demand-limiting control strategy, the inverse model was trained using all of the available data from Phase 1 and 2 testing. The parameters are given in Appendix B. The model was then used to compare night setup and demand-limiting strategies for the last day of the Phase 1 test period (August 11). Figures 5.2 to 5.4 show comparisons of measured and predicted cooling loads and zone temperatures for this single day for the east, west and combined test rooms, respectively. The times are measured from midnight. Cooling loads occurred from 7 am to 6 pm. The model did a good job of predicting the cooling loads under night-setup control for all three cases.

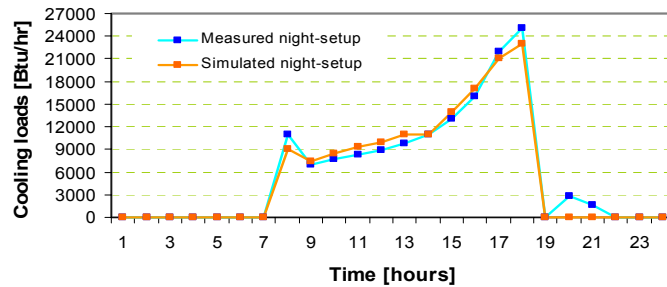


(a) Cooling loads

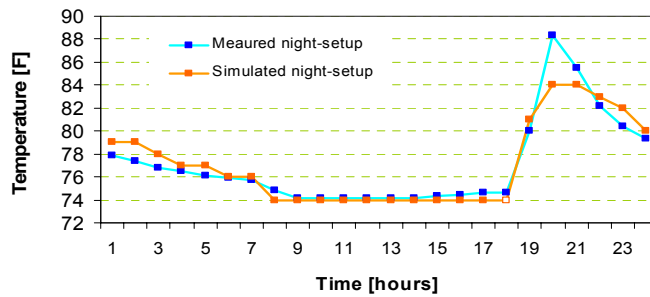


(b) Zone temperatures

Figure 5.2 Measured and calculated results of inverse model for night-setup operation of east test rooms on August 11 test in Phase 1.

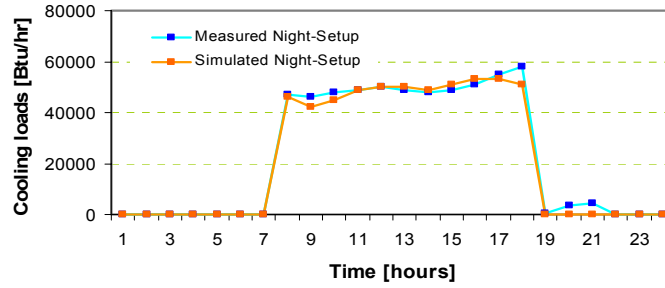


(a) Cooling loads

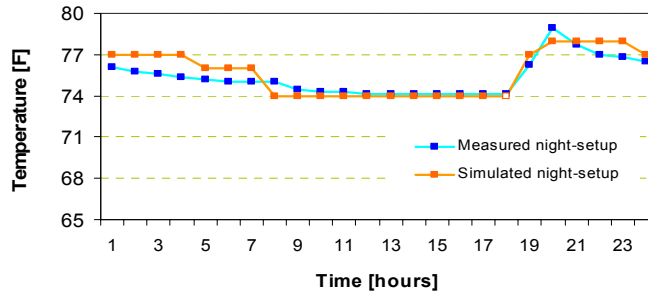


(b) Zone temperatures

Figure 5.3 Measured and calculated results of inverse model for night-setup operation of west test rooms on August 11 test in Phase 1.



(a) Cooling loads



(b) Zone temperatures

Figure 5.4 Measured and calculated results of inverse model for night-setup operation of whole combined test rooms on August 11 test in Phase 1.

5.2.2. Results

The performance of the demand-limiting control strategy was characterized in terms of a peak load ratio (PLR) defined as the ratio of the peak load during the on-peak period under demand-limiting(DL) control strategy to the peak cooling load during the on-peak period under night-setup(NS) control strategy.

$$PLR = \frac{\dot{Q}_{\max,DL,on-peak}}{\dot{Q}_{\max,NS,on-peak}} \quad (5.1)$$

Figures 5.5 to 5.7 show PLR for the east, west and combined zones, respectively, as a function of the start time for demand limiting (or on-peak period) for different precooling start times. For the east test rooms, PLR decreases dramatically as the start time of the demand-limiting period is delayed. The precooling start time has a smaller effect, but its effect is greater when the demand period begins earlier in the day. For this east-facing zone, the potential for demand reduction is tremendous when the demand period begins in the afternoon. For an

afternoon on-peak period, the peak on-peak load can be reduced to about 30% of the peak load for night setup even without any precooling.

For the west test rooms, PLR is nearly independent of the start of the demand period until a start-time of 3 pm. Furthermore, PLR has a small dependence on the precooling duration. Without any precooling, the peak on-peak cooling demand can be reduced to about 65% of the peak load associated with night setup control.

For the combined zones, the trend is somewhat similar to the west zone results but the impact is reduced. Precooling becomes more important as the start of the on-peak period moves earlier in the day. For an on-peak period beginning at 7 am, the maximum peak load reduction was about 23% compared to night setup control. For an afternoon start to the on-peak period, the peak load reduction for the on-peak period was about 45% without any precooling. The ERS is representative of a small commercial building. The potential for peak load reduction through use of building thermal mass is tremendous for this building. Even greater potential exists for large commercial buildings.

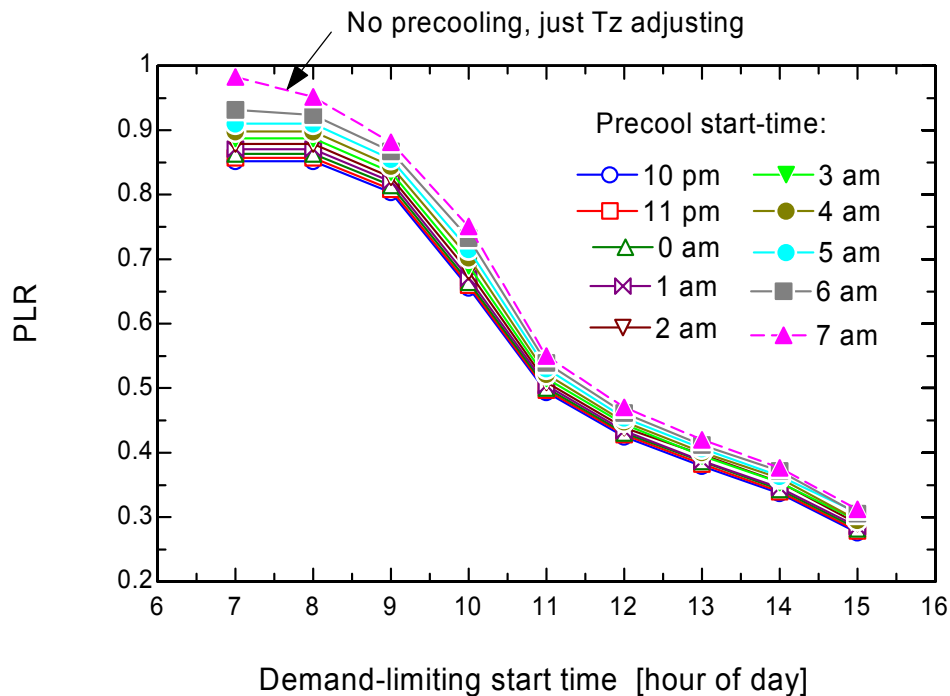


Figure 5.5 Peak load ratio for east test rooms

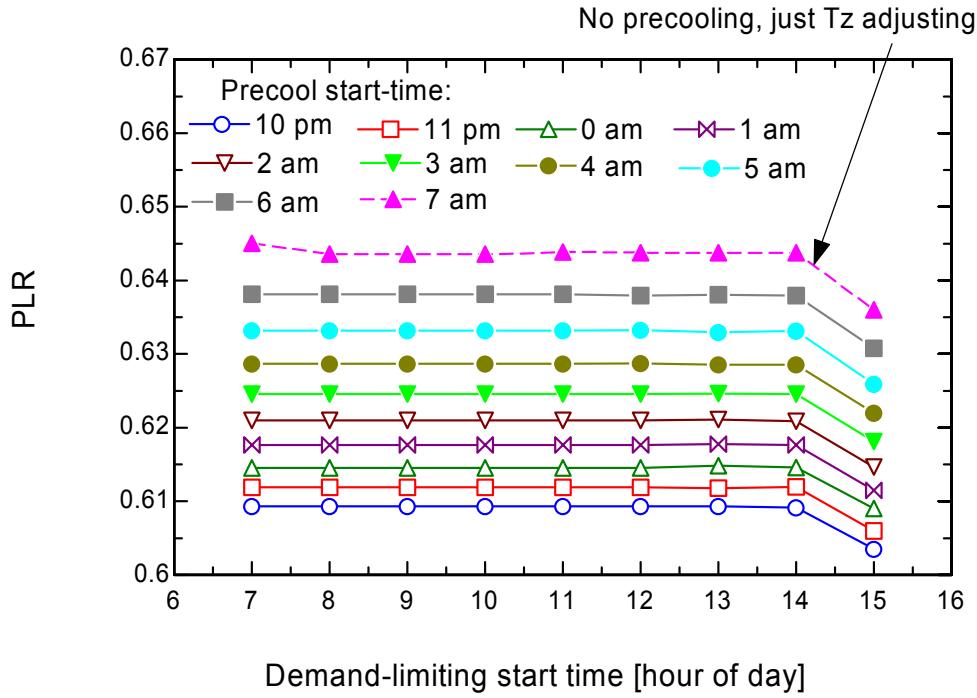


Figure 5.6 Peak load ratio for west test rooms

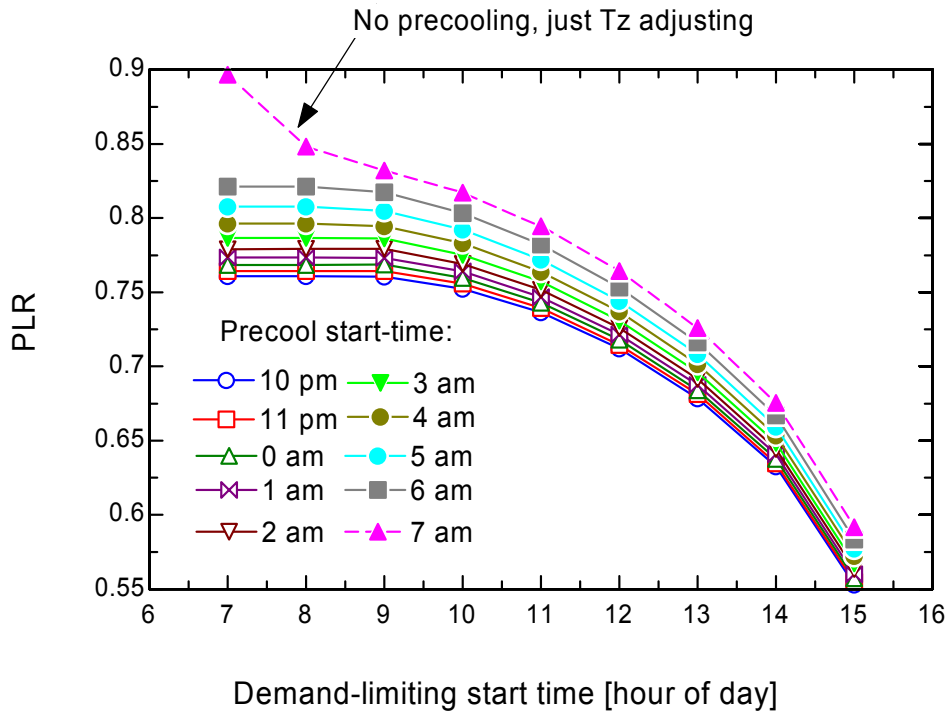


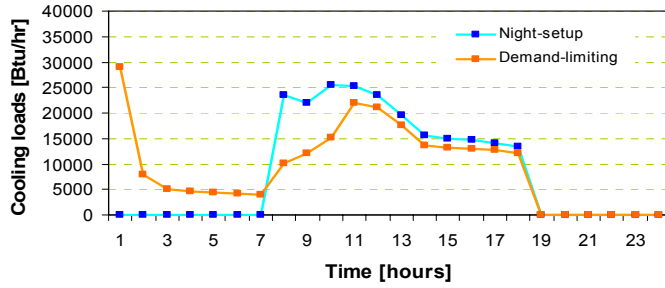
Figure 5.7 Peak load ratio for combined test rooms

Figures 5.8 to 5.16 show selected results that compare hourly cooling loads and zone temperatures for the NS and DL strategies. Figures 5.8 to 5.10 are for the east rooms, Figures 5.11 to 5.13 for the west rooms and Figures 5.14 to 5.16 for the combined zones. Three cases were considered for the three zones: (i) start-time of 67°F precooling at midnight and start-time of demand-limiting at 7 am, (ii) start time of precooling at midnight and start time of demand-limiting at 1 pm, and (iii) without precooling and start-time of demand-limiting at 1 pm.

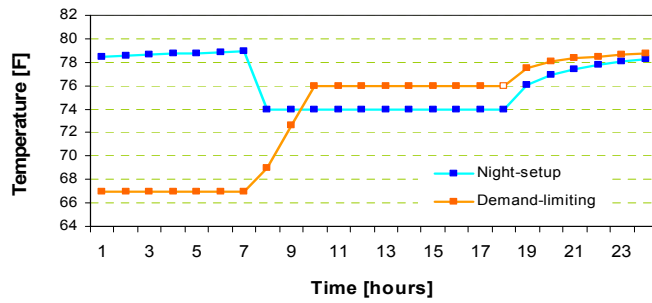
In Figure 5.8, the building was precooled from midnight to 7 am and demand-limiting began at 7 am. The peak load under night-setup occurred around 9 or 10 am in the morning, whereas for the demand-limiting strategy the peak occurred near noon. With demand limiting, the zone temperature setpoint was raised to 76 °F during a relatively short period in the morning in order to limit the peak cooling load. However, there wasn't sufficient energy storage to reduce the load in the early afternoon hours. Even though the peak load reduction was relatively small for this case, there was significant load shifting from the occupied to the unoccupied period.

For the results of Figure 5.9, the start-time for demand-limiting was delayed to 1 pm. Until 1 pm, the zone setpoint was maintained at 69 °F and after 1 pm the setpoint increased until it reached at 76 °F at the end of the on-peak period. Except at the start of the occupied period, the load closely follows the night setup load until 1 pm when demand-limiting begins. Then the load for the demand-limiting strategy is significantly lower than for night setup control.

Figure 5.10 is for the case of no-precooling and adjustment of the setpoints during an on-peak period starting at 1 pm. Zone setpoints were maintained 69°F until the on-peak period began at 1 pm. and after 1 pm the setpoint increased until it reached at 76 °F. It is found that there was a significant effect on peak load reduction during the on-peak period without nighttime precooling even though cooling loads were increased significantly in the morning.

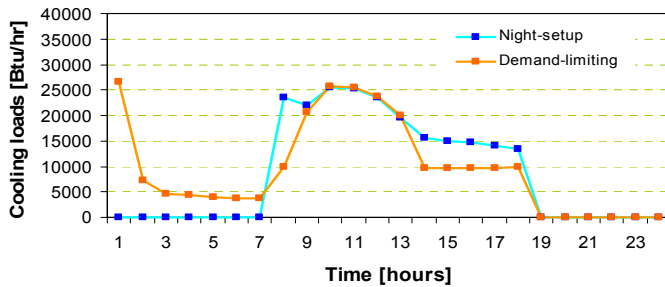


(a) Cooling loads

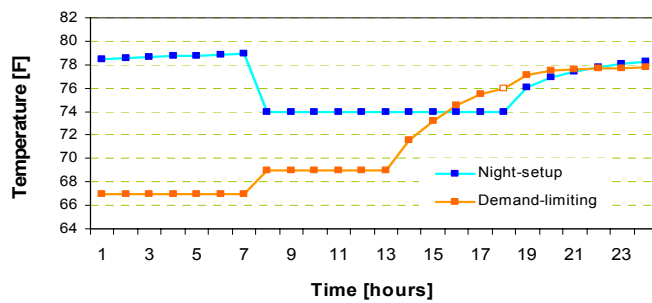


(b) Zone temperatures

Figure 5.8 Simulated night-setup and demand-limiting control for east test rooms (PC start-time of midnight and DL start-time of 7 am).

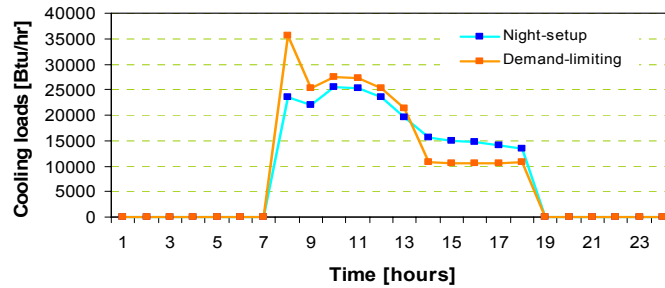


(a) Cooling loads

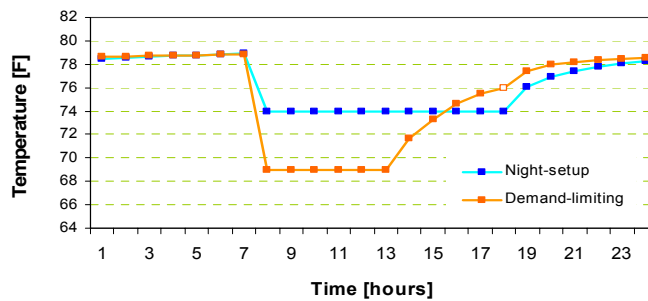


(b) Zone temperatures

Figure 5.9 Simulated night-setup and demand-limiting control for east test rooms (PC start-time of midnight and DL start-time of 1 pm).



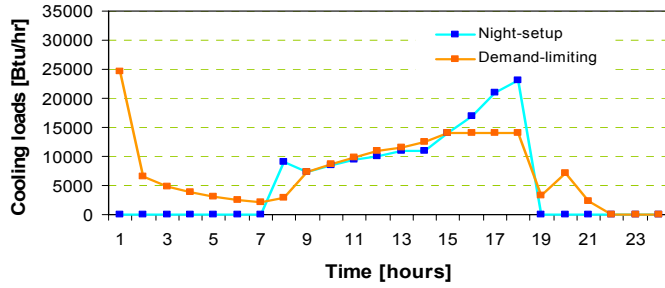
(a) Cooling loads



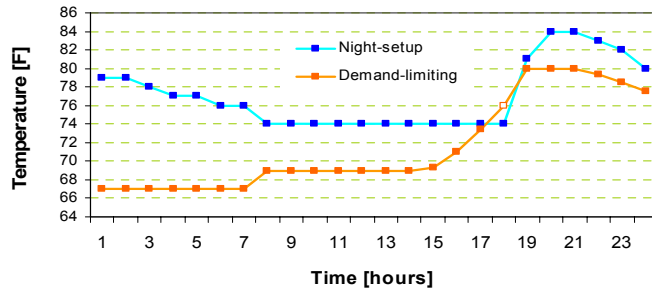
(b) Zone temperatures

Figure 5.10 Simulated night-setup and demand-limiting control for east test rooms (PC start-time of 7 am and DL start-time of 1 pm).

Figures 5.11 to 5.13 show results for the west rooms. The peak load under night-setup occurs in the afternoon around 6 pm. As a result, the demand-limiting strategy keeps the temperature at the lower comfort limit until the middle of the afternoon. For Figure 5.12, the on-peak period start was delayed and yet there was very little impact on the cooling load and zone temperature profile compared to Figure 5.11. Figure 5.13 is for the case of no-precooling with demand limiting during the on-peak period. Zone setpoints were maintained 69 °F during most of the on-peak which began at 7 am. The cooling loads were increased slightly in the morning, but the peak loads were reduced significantly in the afternoon.

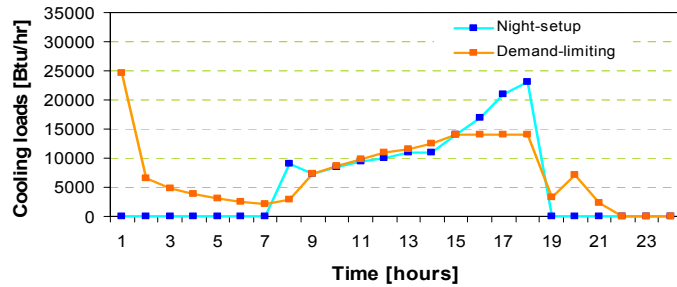


(a) Cooling loads

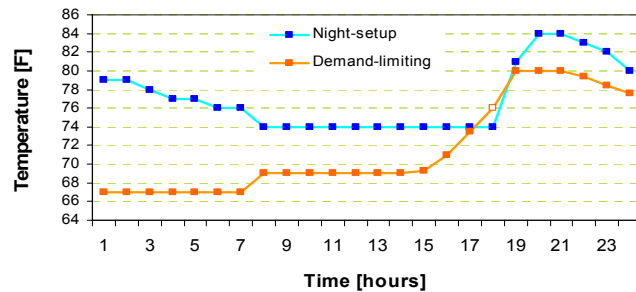


(b) Zone temperatures

Figure 5.11 Simulated night-setup and demand-limiting control for west test rooms (PC start-time of midnight and DL start-time of 7 am).

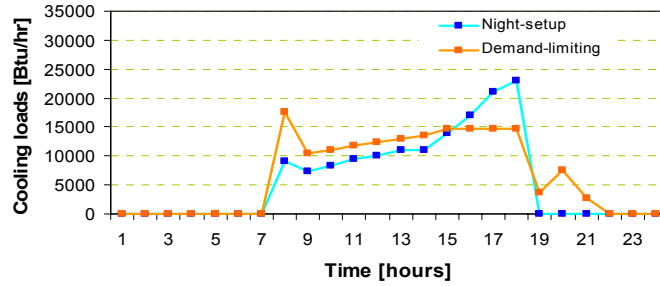


(a) Cooling loads

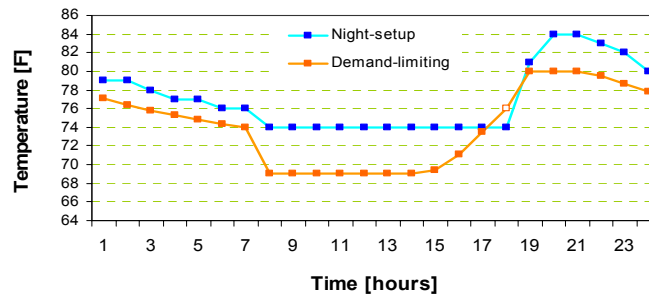


(b) Zone temperatures

Figure 5.12 Simulated night-setup and demand-limiting control for west test rooms (PC start-time of midnight and DL start-time of 1 pm).



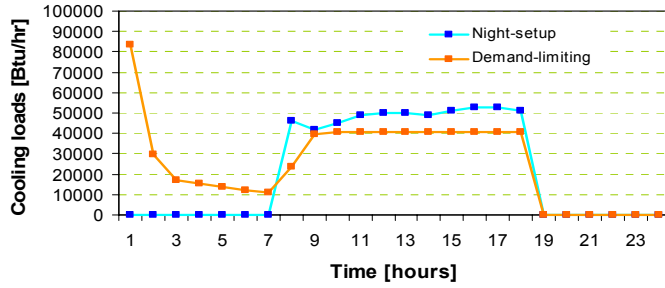
(a) Cooling loads



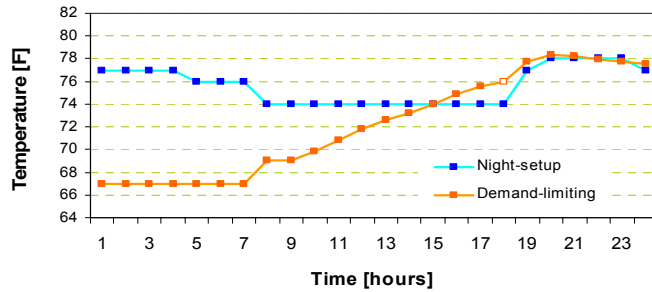
(b) Zone temperatures

Figure 5.13 Simulated night-setup and demand-limiting control for west test rooms (PC start-time of 7 am and DL start-time of 1 pm).

Figures 5.14 to 5.16 show hourly results for all the zones combined. For Figures 5.14 and 5.15, precooling resulted in a reduction in the morning spike and adjusting the zone temperatures leveled the cooling loads during the on-peak period. The zone temperature setpoints were adjusted over the entire on-peak period. A greater on-peak period load reduction occurred for the shorter on-peak period because the energy storage is more significant compared to the total load for a shorter period.

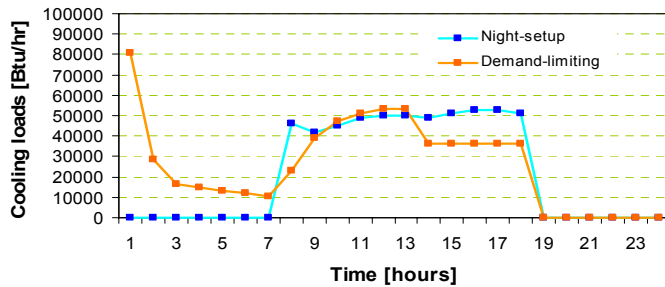


(a) Cooling loads

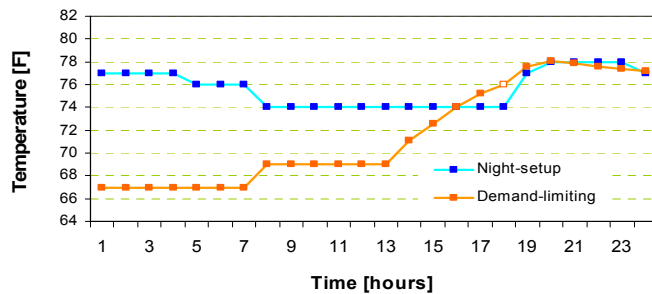


(b) Zone temperatures

Figure 5.14 Simulated night-setup and demand-limiting control for combined test rooms (PC start-time of midnight and DL start-time of 7 am).

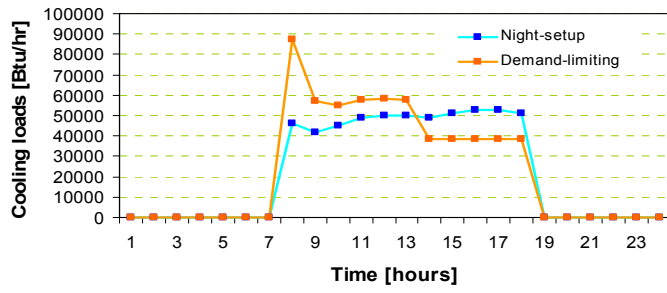


(a) Cooling loads

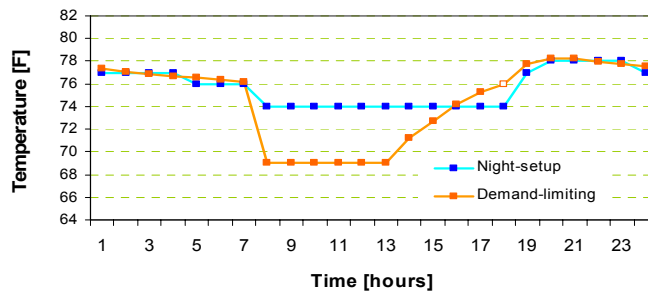


(b) Zone temperatures

Figure 5.15 Simulated night-setup and demand-limiting control for combined test rooms (PC start-time of midnight and DL start-time of 1 pm).



(a) Cooling loads



(b) Zone temperatures

Figure 5.16 Simulated night-setup and demand-limiting control for combined test rooms (PC start-time of 7 am and DL start-time of 1 pm).

Hourly simulated cooling load and zone temperature profiles for all of the precooling and demand-limiting start-times considered in this study are given in the Appendix C.

6. CONCLUSIONS

A simulation tool using an inverse model was developed and validated for the ERS building using simulated data from TRNSYS and measurements. The building model trained with measurements was then used to evaluate the potential for peak load reduction with a demand-limiting control strategy.

Evaluation of the inverse building model using simulated data showed that the model predicts cooling loads within about 3 % when trained with two or three weeks of data that utilizes a precooling strategy. More training data is necessary if night setup control is employed. Using measured data, the inverse model was able to predict cooling loads to within about 5 % when trained with 14 days of data that incorporated both precooling and night-setup control strategies.

The inverse model was used to study the potential for peak load reduction using a demand-limiting strategy. For all of the test zones of the ERS building combined, the peak demand during the on-peak period was reduced by about 25% to 45% with precooling with the savings depending on the start of the on-peak period. The percentage reduction increases as the start of the on-peak period is delayed because the energy storage of the building becomes a large fraction of the on-peak cooling requirements. However, the impact of the precooling is reduced as the on-peak period moves to later in the day. With no precooling, the peak load could be reduced by about 40% when the on-peak period began at 3 pm.

The facility considered in this study is relatively lightweight and is representative of many small commercial buildings. Greater potential should be possible for large commercial buildings because of a smaller ratio of external area to thermal mass, the use of heavier weight materials, and the availability of more favorable electrical rate structures. However, small commercial buildings are an excellent application for use of building thermal mass because the savings are significant and it is easier to develop an intelligent controller for small commercial buildings because they typically use packaged air conditioners with a single thermostat controlling a single unit for individual zones. In large commercial buildings, the equipment tends to be centralized and serves many zones. The systems tend to be complex and one of a kind with specialized control software.

One of the next steps should be to implement a demand-limiting control strategy at the ERS in order to fully demonstrate and validate the savings potential. Then, an intelligent control algorithm should be developed that can be incorporated within a “smart” thermostat for packaged air conditioners.

7. REFERENCES

1. Aird, T., Rice, J., “Systematic Search in High Dimensional Sets”, SIAM Journal on Numerical Analysis”, Vol.14, No.2, pp.216-312, 1977.
2. Braun, J.E., Lawrence, T.M., Klaassen, C.J., and House, J.M., “Demonstration of Load Shifting and Peak Load Reduction with Control of Building Thermal Mass”, Proceeding of the 2002 ACEEE Conference on Energy Efficiency in Buildings, Monterey, CA, 2002.
3. Braun, J.E. and Lawrence, T.M., “Testing at the Iowa Energy Center”, HL-2002-7, Report #5752-1, Ray W. Herrick Laboratories, Purdue University, 2002.
4. Braun, J.E. and Chaturvedi, N., “ Analytical tools for dynamic building control”, HL 2000-15, Report #5031-1, Ray W. Herrick Laboratories, W.Lafayette, IN, 2000.
5. Chaturvedi, N. and Braun, J.E., “An Inverse Grey-Box Model for Transient Building Load Prediction”, International Journal of Heating, Ventilating, Air-Conditioning and Refrigerating Research, Vol.8, No.1, pp.73-100, 2002.
6. Duffie, J.A. and Beckman, W.A., “Solar Engineering of Thermal Processes”, John Wiley & Sons, Second Edition, 1991.
7. Klein, S., et al., “TRNSYS – A Transient System Simulation Program, Reference Manual 1”, Solar Energy Laboratory, University of Wisconsin at Madison, 1994.
8. Montgomery, K., “Development of Analysis Tools for the Evaluation of Thermal Mass Control Strategies”, Masters Thesis, Report no 2464-2, HL 98-17, Herrick laboratories, West Lafayette, Indiana, 1998.
9. Price, B.A. and Smith, T.F., “Description of the Iowa Energy Center Energy Resource Station: Facility Update III”, Technical Report ME-TFS-00-001, The University of Iowa, March 2000.
10. Seem, J.E., Klein, S.A., Beckman, W.A. and Mitchell, J.W., “Transfer Functions for efficient calculations of multi dimensional heat transfer”, Journal of Heat Transfer – Transactions of the ASME, Vol.111, No.1, pp.5-12, 1989.
11. Thomas, H.R., Rees, S.W., “The Thermal Performance of Ground Floor Slabs – A Full Scale In-Situ Experiment”, Building and Environment, Vol.34, pp.139-164, 1999.
12. Travesi, J., Maxwell, G., Klaassen, C.J., and Holtz, M., “Empirical Validation of Iowa Energy Resource Station Building Energy Analysis Simulation Models’, A report of Task 22, subtask A, Building energy analysis tools, IEA, June 2001.

13. Zhou, Z., Rees, S.W., Thomas, H.R., “A Numerical and experimental investigation of ground heat transfer including edge insulation effects”, *Building and Environmental*, Vol.37, pp.67-78, 2002.

APPENDIX A:

Information on ERS Building Construction

1. Construction Information Based on Travesi's report [Travesi, 2001]

1.1 Properties of Construction Layers

Name	Description	t	k	ρ	Cp	R
2concrete*	2 in heavy weight concrete	0.05080	4.71985	2242.6320	0.83736	0.01076
4concrete*	4 in heavy weight concrete	0.10160	4.71985	2242.6320	0.83736	0.02152
4air	4 in horizontal air space	0.10160	-	-	-	0.04256
38air	3/8 in vertical air space	0.00965	-	-	-	0.04403
475air	4.75 in vertical air space	0.12065	-	-	-	0.04501
34air	¾ in vertical air space	0.01905	-	-	-	0.04403
138air	1 3/8 in vertical air space	0.03505	-	-	-	0.04354
4insulation**	4 in insulation	0.10160	0.08286	24.02820	1.59098	1.22594
1rigid insul**	1 in rigid insulation with foil face	0.02540	0.08286	24.02820	1.59098	0.30624
15rigid insul**	1.5 in rigid insulation with foil face	0.03810	0.08286	24.02820	1.59098	0.45936
single memb	Single-ply membrane	-	-	1121.3160	1.46538	0.02152
vapor	Vapor barrier	-	-	-	-	0.00294
washed rock	Washed river rock	0.02540	5.19582	881.03400	1.67472	0.00489
22steel deck	22 gage steel deck	0.00086	161.98	7689.0240	0.41868	-
58gypsum***	5/8 in gypsum board	0.01600	0.57690	800.94000	0.83736	0.02740
34gypsum***	¾ in gypsum board	0.01905	0.57690	800.94000	0.83736	0.03278
4pre concrete+	4 in pre-cast concrete	0.10160	4.71985	2242.6320	0.83736	0.02152
6pre concrete+	6 in pre-cast concrete	0.15240	4.71985	2242.6320	0.83736	0.03229
metal stud 1	Metal stud framing with R13 batt insulation with foil face	0.08890	0.15575	9.61128	0.83736	0.63400
metal stud 2	Metal stud framing with fiberglass fill, insulation, t=3.5"	0.08890	0.14018	48.05640	1.38164	0.63400
metal stud3	Metal stud framing with fiberglass fill, insulation, t=2.37"	0.06020	0.14018	48.05640	1.38164	0.63400
1in glass	1 in spandrel glass	0.02540	-	-	-	0.10175
door	1/8 in glass with steel frame	0.00318	4.96531	2210.5944	0.75362	0.00064
ceiling	Door	0.04445	-	-	-	0.20351
carpet	Ceiling	0.01905	0.20559	288.33840	1.33978	0.09246
perimeter	Carpet	0.10160	4.71985	2242.6320	0.83736	0.02152
	Perimeter insulation with a 2 inch wide	-	-	-	-	0.24460

*: layer name is CONCRETE, **: layer name is INSULATION

***: layer name is GYPSUM, +: layer name is PRECONCRET

Units are :

t:thickness, in m

k: conductivity, in kJ/hr-m-K

ρ : density, in kg/m²

Cp: specific heat, in kJ/kg-K

R:resistance, in hr-m²-K/kJ

1.2. Combination of Layers at the Walls

Walls are described from inside to outside.

Wall type	Layer name
Wall-R1	2concrete 4air space 2concrete vapor 4insulation single memb washed rock

Wall type	Layer name
Wall-R2	22 steel deck 4 insulation single memb washed rock

Wall type	Layer name
Wall-W1	58gypsum vapor 38air space 15rigid insul 4pre concrete

Wall type	Layer name
Wall-W2	58gypsum 38air space 1rigid insul 6pre concrete

Wall type	Layer name
Wall-W3	58gypsum vapor metal stud1 1rigid insul 475air space 1in glass

Wall type	Layer name
Wall-W4	metal stud1 34air space 1rigid insul 6pre concrete

Wall type	Layer name
Wall-W5	34gypsum vapor metal stud1 138air space 1rigid insul 6pre concrete

Wall type	Layer name
Wall-W6	58gypsum vapor metal stud1 34air space 1rigid insul 4pre concrete

Wall type	Layer name
Wall-W7	58gypsum metal stud1 34air space 1rigid insul 6pre concrete

Wall type	Layer name
Wall-P1	58gypsum metal stud2 58gypsum

Wall type	Layer name
Wall-P2	58gypsum metal stud3 58gypsum

Wall type	Layer name
Wall-P3	18in glass

Wall type	Layer name
Wall-P4	door

Wall type	Layer name
Wall-C1	ceiling

Wall type	Layer name
Wall-F1	carpet 4concrete perimeter

1.3 Window type

H:height in m, W: width in m, P:number of panes, S:shading coefficient,
C: heat conduction of the total window in BTU/hr-ft²-F

Type	Location	H	W	A (m ²)	P	S	C
Win-TR	Test rooms	4.268	1.524	6.5044	2	0.85	11.2429
Win-TYP1	Office(E)	3.5973	1.524	5.4823	2	0.31	6.1325
Win-TYP2	Office(S)	4.6643	1.524	7.1084	2	0.31	6.1325
Win-TYP3	Computer room(S)	4.6643	1.524	7.1084	2	0.31	6.1325
Win-TYP4	Computer room(W)	7.3166	1.524	11.1505	2	0.31	6.1325
Win-TYP5	Classroom(S)	1.067	1.524	1.6261	2	0.31	6.1325
Win-TYP6	Classroom(W)	2.134	1.524	3.2522	2	0.31	6.1325
Win-TYP7	Classroom(N)	1.067	1.524	1.6261	2	0.31	6.1325
Win-TYP8	Reception room(E)	2.4084	1.524	3.6704	2	0.31	6.1325
Win-TYP9	Door in vest	0.9146	2.1336	1.9514	2	0.31	6.1325
Win-SKY	Roof of media center	3.0486	3.048	9.2921	1	0.35	4.906

1.4 Identification of zone space

Zone name	Description
P-EAST	Plenum in the test room east
P-SOUTH	Plenum in the test room south
P-WEST	Plenum in the test room west
P-INTE	Plenum in the test room interior
EASTROOM	Conditioned space in the test room east
SOUTHROOM	Conditioned space in the test room south
WESTROOM	Conditioned space in the test room west
INTEROOM	Conditioned space in the test room interior

1.5 Description of the zone space and details of its six surfaces

C:Ceiling, E:Wall east, F:Floor, N:Wall north, R:Roof, S:Wall south, W:Wall west
Width, height in ft

A. Plenum zone

Plenum of East room A

Zone	Orientation	Width(ft)	Height(ft)	Wall	Window	Door
P-EASTA	R	17.74	15.50	Wall-R1	-	-
	C	17.74	15.50	Wall-C1	-	-
	N	17.74	5.50	Wall-P2	-	-
	E	15.50	5.50	Wall-W2	-	-
	S	17.74	5.50	Wall-P2	-	-
	W	15.50	5.50	Wall-P1	-	-

m²

SI Units:

Orientation	Width(m)	Height(m)	Area(m ²)	Zone volume (m ³)
R	5.4072	4.7245	25.5462	42.8261
C	5.4072	4.7245	25.5462	
N	5.4072	1.6764	9.0648	
E	4.7245	1.6764	7.9202	
S	5.4072	1.6764	9.0648	
W	4.7245	1.6764	7.9202	

Plenum of South room A

Zone	Orientation	Width(ft)	Height(ft)	Wall	Window	Door
P-SOUTH A	R	15.50	17.74	Wall-R1	-	-
	C	15.50	17.74	Wall-C1	-	-
	N	15.50	5.50	Wall-P2	-	-
	E	17.74	5.50	Wall-P2	-	-
	S	15.50	5.50	Wall-W2	-	-
	W	17.74	5.50	Wall-P1	-	-

SI Units:

Orientation	Width(m)	Height(m)	Area(m ²)	Zone volume (m ³)
R	4.7245	5.4072	25.5462	42.8261
C	4.7245	5.4072	25.5462	
N	4.7245	1.6764	7.9202	
E	5.4072	1.6764	9.0648	
S	4.7245	1.6764	7.9202	
W	5.4072	1.6764	9.0648	

Plenum of West room A

Zone	Orientation	Width(ft)	Height(ft)	Wall	Window	Door
P-WESTA	R	17.74	15.50	Wall-R1	-	-
	C	17.74	15.50	Wall-C1	-	-
	N	17.74	5.50	Wall-P2	-	-
	E	15.50	5.50	Wall-P1	-	-
	S	17.74	5.50	Wall-P2	-	-
	W	15.50	5.50	Wall-W2	-	-

SI Units:

Orientation	Width(m)	Height(m)	Area(m ²)	Zone volume (m ³)
R	5.4072	4.7245	25.5462	42.8261
C	5.4072	4.7245	25.5462	
N	5.4072	1.6764	9.0648	
E	4.7245	1.6764	7.9202	
S	5.4072	1.6764	9.0648	
W	4.7245	1.6764	7.9202	

Plenum of Interior room A

Zone	Orientation	Width(ft)	Height(ft)	Wall	Window	Door
P-INTEA	R	15.50	17.74	Wall-R1	-	-
	C	15.50	17.74	Wall-C1	-	-
	N	15.50	5.50	Wall-P2	-	-
	E	17.74	5.50	Wall-P2	-	-
	S	15.50	5.50	Wall-P2	-	-
	W	17.74	5.50	Wall-P1	-	-

SI Units:

Orientation	Width(m)	Height(m)	Area(m ²)	Zone volume (m ³)
R	4.7245	5.4072	25.5462	42.8261
C	4.7245	5.4072	25.5462	
N	4.7245	1.6764	7.9202	
E	5.4072	1.6764	9.0648	
S	4.7245	1.6764	7.9202	
W	5.4072	1.6764	9.0648	

B. Conditioned zone

East rooms A

Zone	Orientation	Width(ft)	Height(ft)	Wall	Window	Door
EAST ROOMA	C	17.74	15.50	Wall-C1	-	-
	F	17.74	15.50	Wall-F1	-	-
	N	17.74	8.50	Wall-P2	-	-
	E	15.50	8.50	Wall-W1	Win-TR	-
	S	17.74	8.50	Wall-P2	-	-
	W	15.50	8.50	Wall-P3	-	Wall-P4

SI Units:

Orientation	Width(m)	Height(m)	Area(m ²)	Zone volume (m ³)
C	5.4072	4.7245	25.5462	66.1858
F	5.4072	4.7245	25.5462	
N	5.4072	2.5908	14.0092	
E	4.7245	2.5908	12.2403	
S	5.4072	2.5908	14.0092	
W	4.7245	2.5908	12.2403	

South rooms A

Zone	Orientation	Width(ft)	Height(ft)	Wall	Window	Door
SOUTH ROOMA	C	15.50	17.74	Wall-C1	-	-
	F	15.50	17.74	Wall-F1	-	-
	N	15.50	8.50	Wall-P3	-	Wall-P4
	E	17.74	8.50	Wall-P2	-	-
	S	15.50	8.50	Wall-W1	Win-TR	-
	W	17.74	8.50	Wall-P1	-	-

SI Units:

Orientation	Width(m)	Height(m)	Area(m ²)	Zone volume (m ³)
C	4.7245	5.4072	25.5462	66.1858
F	4.7245	5.4072	25.5462	
N	4.7245	2.5908	12.2403	
E	5.4072	2.5908	14.0092	
S	4.7245	2.5908	12.2403	
W	5.4072	2.5908	14.0092	

West room A

Zone	Orientation	Width(ft)	Height(ft)	Wall	Window	Door
WEST ROOMA	C	17.74	15.50	Wall-C1	-	-
	F	17.74	15.50	Wall-F1	-	-
	N	17.74	8.50	Wall-P2	-	-
	E	15.50	8.50	Wall-P3	-	Wall-P4
	S	17.74	8.50	Wall-P2	-	-
	W	15.50	8.50	Wall-W1	Win-TR	-

SI Units:

Orientation	Width(m)	Height(m)	Area(m ²)	Zone volume (m ³)
C	5.4072	4.7245	25.5462	66.1858
F	5.4072	4.7245	25.5462	
N	5.4072	2.5908	14.0092	
E	4.7245	2.5908	12.2403	
S	5.4072	2.5908	14.0092	
W	4.7245	2.5908	12.2403	

Interior room A

zone	Orientation	Width(ft)	Height(ft)	Wall	Window	Door
INTER ROOMA	C	15.50	17.74	Wall-C1	-	-
	F	15.50	17.74	Wall-F1	-	-
	N	15.50	8.50	Wall-P2	-	-
	E	17.74	8.50	Wall-P2	-	-
	S	15.50	8.50	Wall-P3	-	Wall-P4
	W	17.74	8.50	Wall-P1	-	-

SI Units:

Orientation	Width(m)	Height(m)	Area(m ²)	Zone volume (m ³)
C	4.7245	5.4072	25.5462	66.1858
F	4.7245	5.4072	25.5462	
N	4.7245	2.5908	12.2403	
E	5.4072	2.5908	14.0092	
S	4.7245	2.5908	12.2403	
W	5.4072	2.5908	14.0092	

2. Construction information based on Price's report [Price, 2000]

2.1 Layers

Table 1 Thermal properties of wall and roof construction layers

Material	Description	t (m)	ρ (kg/m ³)	Cp (kJ/kg K)	k (kJ/hmK)	R (Km ² h/kJ)
GYPSUM	gypsum board, 5/8 in.	0.016	1249.439	1.089	0.579	0.027
RGDINSUL	rigid insulation, 1 in.	0.025	91.781	0.837	0.156	0.163
	rigid insulation, 1.5 in.	0.038	91.781	0.837	0.156	0.245
POLINSUL	polyisocyanurate insulation, 4 in.	0.102	32.204	1.047	0.087	1.165
HOLCONCR	hollow cored concrete panel, 4in.	0.203	1017.639	1.005	1.782	0.114
PRECONCR	pre-cast concrete panel, 4 in.	0.102	2318.671	0.670	6.230	0.016
	pre-cast concrete panel, 6 in.	0.152	2318.671	0.670	6.230	0.024
METLSTUD	metal studs, 3 5/8 in.	0.092	7873.819	0.502	2.741	0.034
	metal studs, 6 in.	0.152	7873.819	0.502	2.741	0.056
METLDECK	metal roof decking	0.000	7728.902	0.419	161.980	0.000
BATINSUL	batt insulation, 3 5/8 in.	0.092	6.441	0.754	0.143	0.294
GRAVEL	gravel ballast.(ASHRAE, 1997)	0.025	885.603	1.675	5.171	0.002
AIRFILMI	interior air film	-	-	-	-	0.033
AIRFLIME	exterior air film	-	-	-	-	0.012
AIRSPACE	air space, 6 in.	0.152	-	-	-	0.045
	air space, 3/4 in.	0.019	-	-	-	0.041
CEILING	ceiling	0.019	289.834	1.340	0.206	0.092
CARPET	carpet	-	-	-	2.118	0.060
HEVCONCR	4 in. heavy weight concrete	0.102	2254.263	0.837	4.720	0.022
PERINSUL	perimeter insulation with a 2 in. wide	-	-	-	-	0.245
14GLASS	1/4 in. clear insulating glass	-	-	-	-	0.001

2.2 Walls

Table 2 Test room wall bottom side sections (WBOTSIDE)

Layer	Description	T(m)	R(summer)
AIRFILMI	interior air film	-	0.033
GYP SUM	5/8 in. gypsum	0.016	0.027
AIRSPACE	6 in. air space	0.152	0.045
BATINSUL	3 5/8 in. batt insulation	0.092	0.294
RGDINSUL	1 in. rigid insulation	0.025	0.163
PRECONCR	4 in. pre-cast concrete panel	0.102	0.016
AIRFILME	exterior air film	-	0.012
Total thickness :		0.387	

Table 3 Test room wall bottom center section (WBOTCNTR)

Layer	Description	t(m)	R(summer)
AIRFILMI	interior air film	-	0.033
GYP SUM	5/8 in. gypsum	0.016	0.027
GRDINSUL	1.5 in. rigid insulation	0.038	0.245
PRECONCR	4 in. pre-cast concrete panel	0.102	0.016
AIRFILME	exterior air film	-	0.012
Total thickness :		0.156	

Table 4 Test room wall top section (WTOP)

Layer	Description	t(m)	R(summer)
AIRFILMI	interior air film	-	0.033
GYP SUM	5/8 in. gypsum	0.016	0.027
BATINSUL	3 5/8 in. batt insulation	0.092	0.294
AIRSPACE	3/4 in. air space	0.019	0.041
RGDINSUL	1 in. rigid insulation	0.025	0.163
PRECONCR	6 in. pre-cast concrete panel	0.152	0.024
AIRFILME	exterior air film	-	0.012
Total thickness :		0.305	

Table 5 Test room interior wall (WINTSOME)

Layer	Description	t(m)	R(summer)
GYP SUM	5/8 in. gypsum	0.016	0.027
METLSTUD	6 in. metal stud	0.152	0.056
GYP SUM	5/8 in. gypsum	0.016	0.027
Total thickness :		0.184	

Table 6 Test room interior wall (WINTREST)

Layer	Description	t(m)	R(summer)
GYP SUM	5/8 in. gypsum	0.016	0.027
METLSTUD	3 5/8 in. metal stud	0.092	0.034
GYP SUM	5/8 in. gypsum	0.016	0.027
Total thickness :		0.124	

Table 7 Roof (WROOF)

Layer	Description	t(m)	R(summer)
AIRFILMI	interior air film	-	0.045
HOLCONCR	8 in. pre-cast cored-concrete panel	0.203	0.114
POLINSUL	4 in. polyisocyanurate insulation	0.102	1.165
GRAVEL	gravel ballast	0.025	0.002
AIRFILME	exterior air film	-	0.012
Total thickness :		0.330	

Table 8 Ceiling(WALLC)

Layer	Description	t(m)	R(summer)
CEILING	ceiling	0.019	0.092

Table 9 Floor(WALLF)

Layer	Description	t(m)	R(summer)
CARPET	carpet	-	0.060
HEVCONCR	4 in. heavy weight concrete	0.102	0.022
PERINSUL	perimeter insulation with 2 in. wide	-	0.245

Table 10 Door(WDOOR)

Layer	Description	t(m)	R(summer)
DOOR	door	0.044	0.204

Table 11 Test room interior wall(WALLGLASS)

Layer	Description	t(m)	R(summer)
DOOR	1/4 in. clear insulating glass	0.006	0.001

2.3 Windows

Table 12 Window identification and its size

Type	Location	Width(m)	Height(m)	Area(m ²)	Panes
WNDWTRI	Interior wall in test rooms	1.829	2.134	3.902	1.000
WNDWTRE	Exterior wall in test rooms	2.591	1.524	3.948	2.000
WNDWTRE2	Exterior wall for center	1.920	1.524	2.926	2.000

2.4 Zones

West room A

Zone	Orientation	Width(m)	Height(m)	Area(m ²)	Wall	Window	Door	
WESTA	C	5.407	4.724	25.546	WALLC	-	-	
	F	5.407	4.724	25.546	WALLF	-	-	
	N	5.407	2.591	14.009	WINTREST	-	-	
	E		2.896	2.134	6.178	WINTREST	WNDWTRI	door
			4.724	0.457	2.160	WINTREST	WINTREST	-
			1.829	2.134	3.902	WNDWTRI	WNDWTRI	-
	S	5.407	2.591	14.009	WINTREST	-	-	
	W		2.804	2.591	7.265	WBOTSIDE	WNDWTRE	-
		1.920	2.591	4.975	WBOTCNTR	WNDWTRE2	-	

Zone volume : 66.183(m³)

Plenum of west room A

Zone	Orientation	Width(m)	Height(m)	Area(m ²)	Wall	Window	Door
PWESTA	R	5.407	4.724	25.546	WROOF	-	-
	C	5.407	4.724	25.546	WALLC	-	-
	N	5.407	1.676	9.065	WINTREST	-	-
	E	4.724	1.676	7.920	WINTREST	-	-
	S	5.407	1.676	9.065	WINTREST	-	-
	W	4.724	1.676	7.920	WTOP	-	-

Zone volume : 42.825(m³)

References for Appendix A

1. Price, B.A. and Smith, T.F., "Description of the Iowa Energy Center Energy Resource Station: Facility Update III", Technical Report ME-TFS-00-001, The University of Iowa, March 2000.
2. Travesi, J., Maxwell, G., Klaassen, C.J., and Holtz, M., "Empirical Validation of Iowa Energy Resource Station Building Energy Analysis Simulation Models", A report of Task 22, subtask A, Building energy analysis tools, IEA, June 2001.

APPENDIX B:

Building Parameters for the ERS whole combined zones

ERS building parameters, which were obtained by training using all data from Phase 1 and Phase 2 testing, are shown below.

Parameter	Value
C_{e1}	23883.59
C_{i1}	1630.68
C_{r1}	114945.54
C_{f1}	14710.39
R_{e1}	0.000398
R_{e2}	0.004329
R_{i1}	0.000018
R_{i2}	73.85
R_{r1}	0.000041
R_{r2}	0.000181
R_{f1}	0.002081
R_{f2}	0.001180
C_{e2}	2854.82
C_{i2}	6004.41
C_{r2}	499527.89
C_{f2}	625.91
R_{e3}	0.008449
R_{i3}	0.000702
R_{r3}	0.003271
R_{f3}	0.001464
R_{win}	0.003475
τ_{eff}	0.697443
C_z	5993.48

APPENDIX C:

All Results for Demand-Limiting Simulations

Simulation results for the following cases of

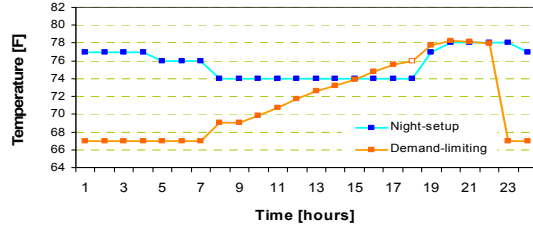
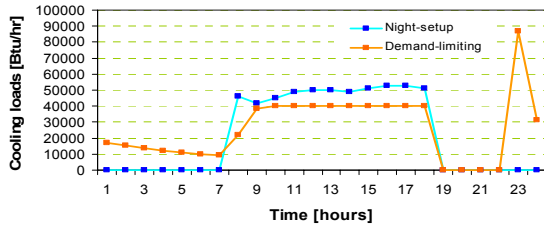
1. Cases for PC start-time: 10 cases (from 10 pm to 7 am) and
2. Cases for DL start-time: 9 cases (from 7 am to 3 pm)

are shown for each test zones of

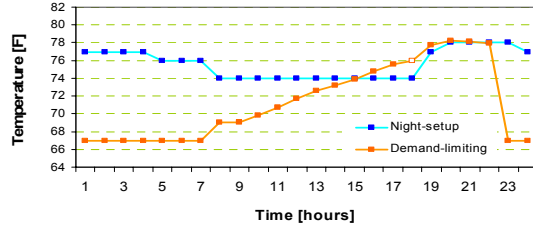
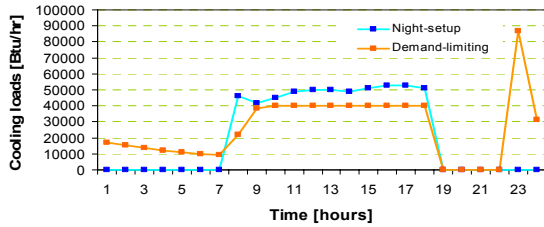
1. Combined zones
2. East zones
3. West zones.

1. Combined zones

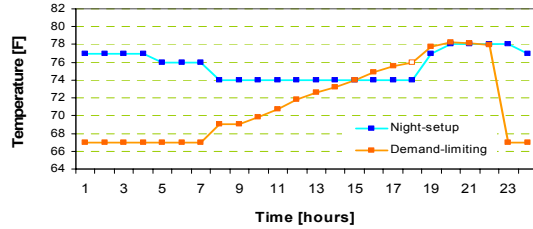
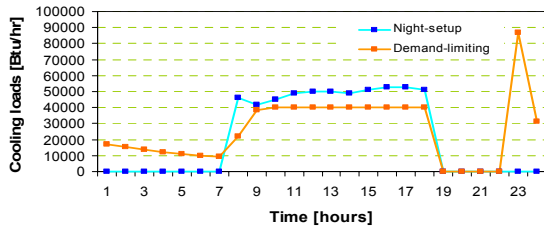
-Test zones: Combined zones
 -67°F PC start-time: 10 pm



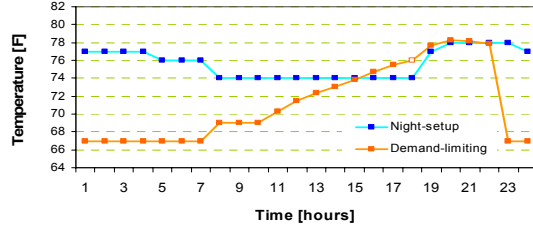
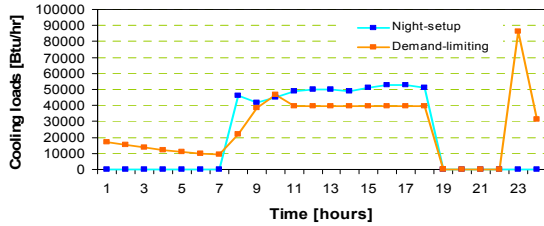
(a) DL start-time: 7am



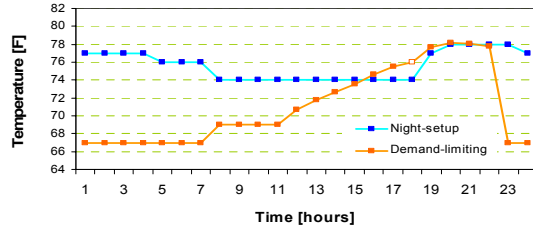
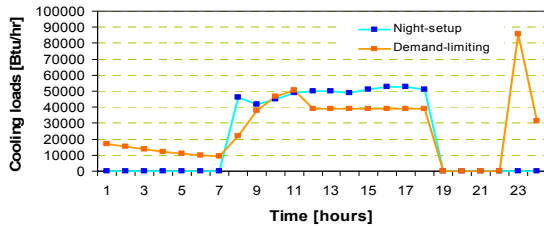
(b) DL start-time: 8am



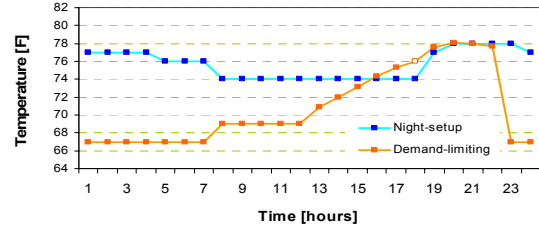
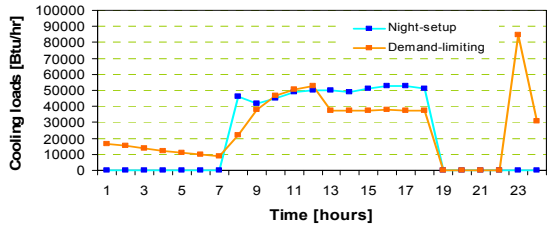
(c) DL start-time: 9am



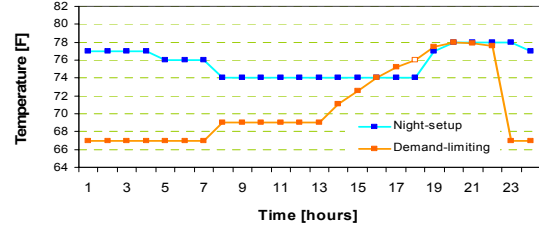
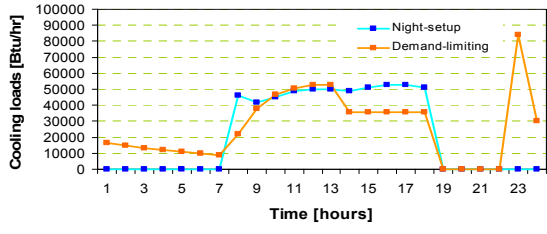
(d) DL start-time: 10am



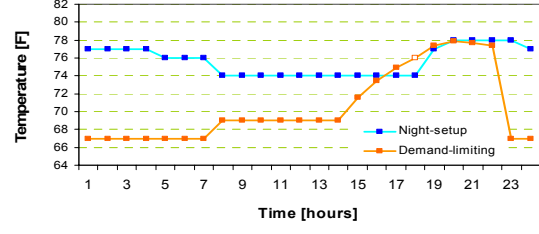
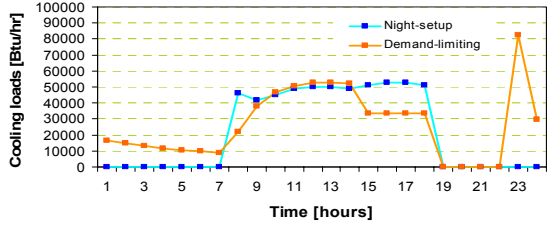
(e) DL start-time: 11am



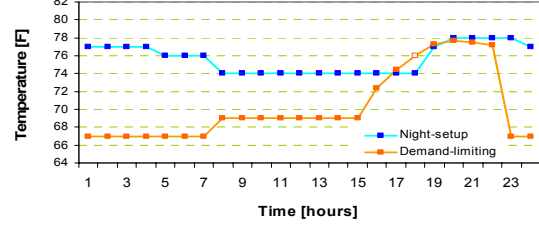
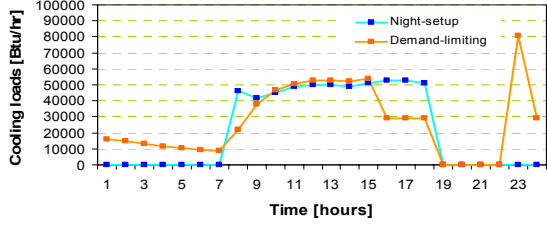
(f) DL start-time: noon



(g) DL start-time: 1pm

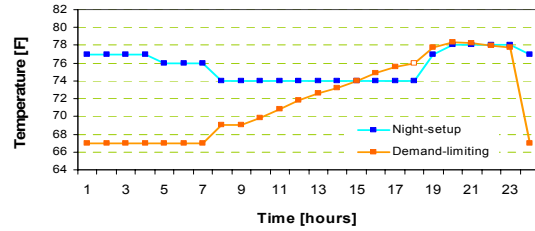
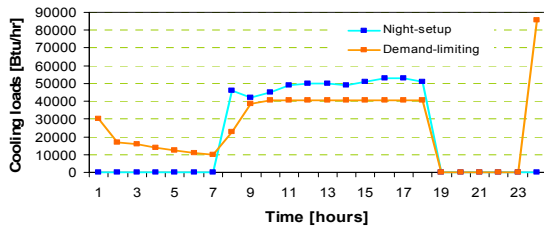


(h) DL start-time: 2pm

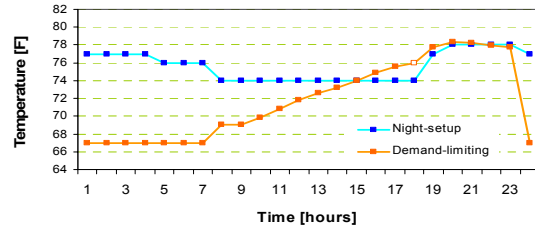
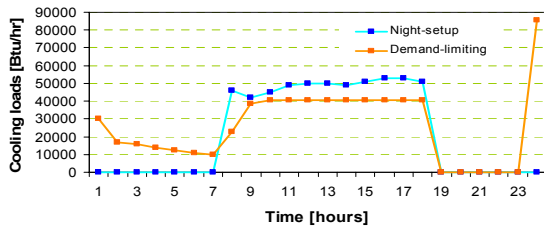


(i) DL start-time: 3pm

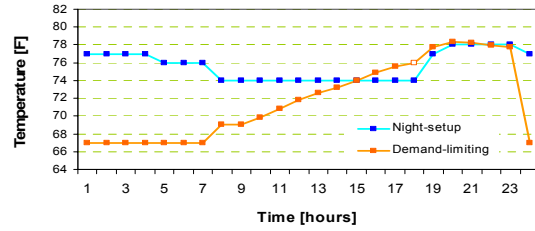
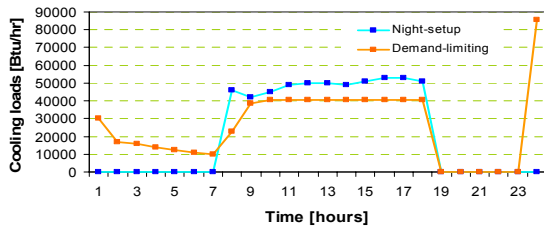
-Test zones: Combined zones
 -67°F PC start-time: 11 pm



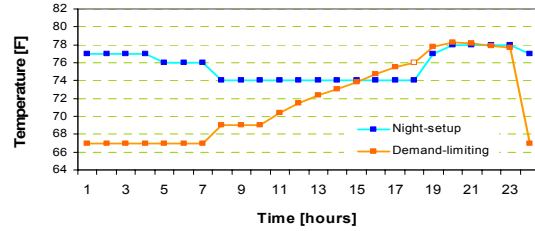
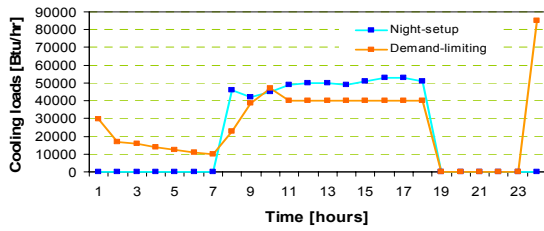
(a) DL start-time: 7am



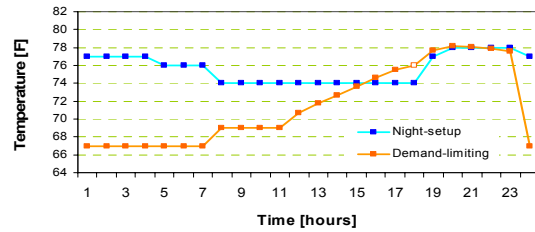
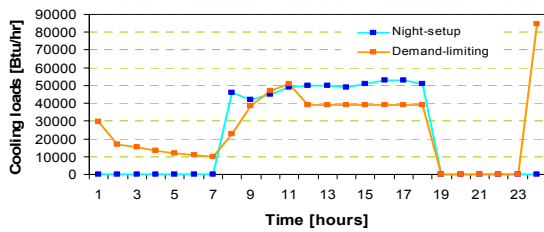
(b) DL start-time: 8am



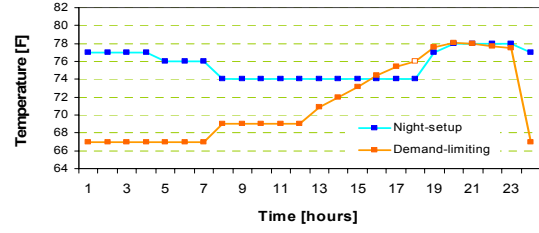
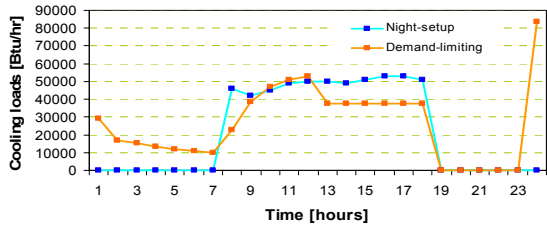
(c) DL start-time: 9am



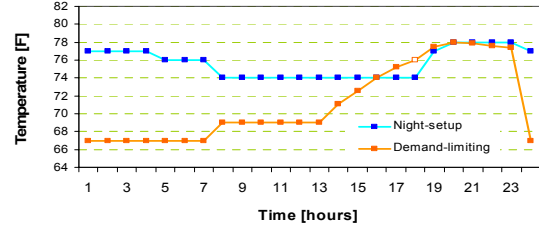
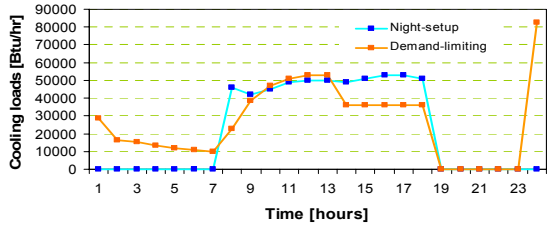
(d) DL start-time: 10am



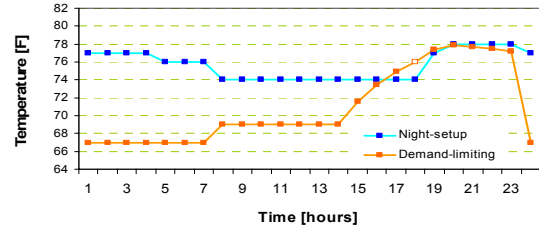
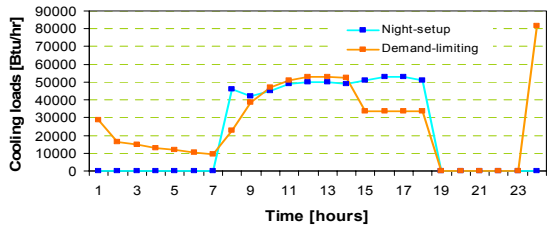
(e) DL start-time: 11am



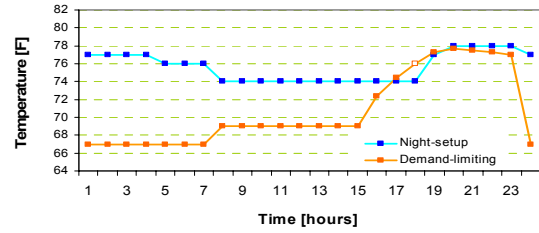
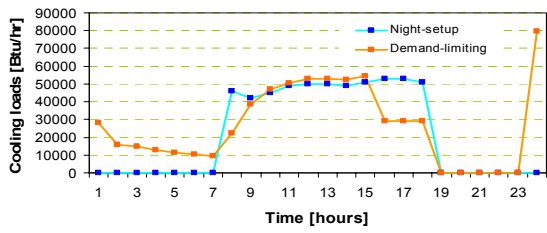
(f) DL start-time: noon



(g) DL start-time: 1pm

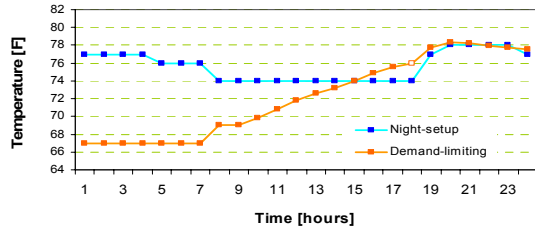
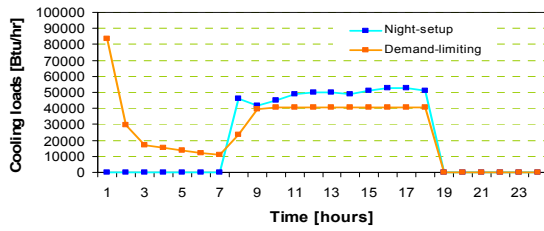


(h) DL start-time: 2pm

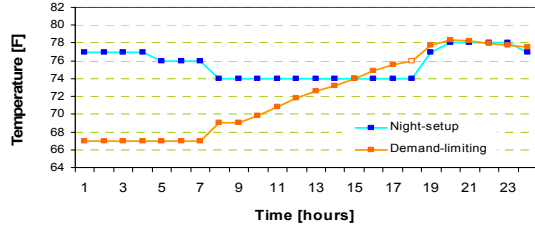
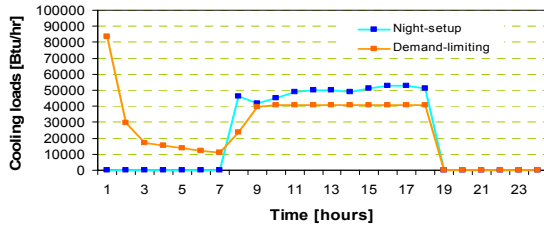


(i) DL start-time: 3pm

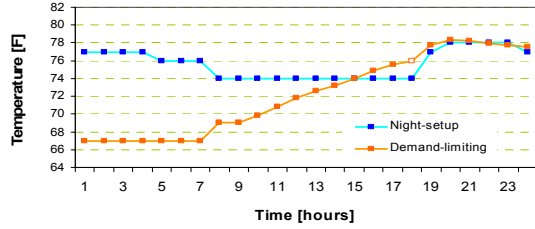
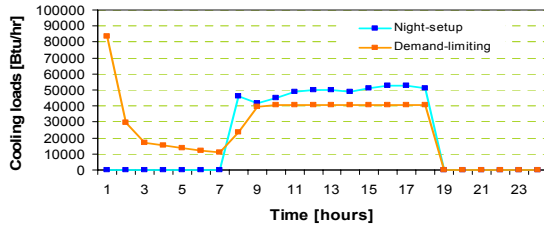
-Test zones: Combined zones
 -67°F PC start-time: midnight



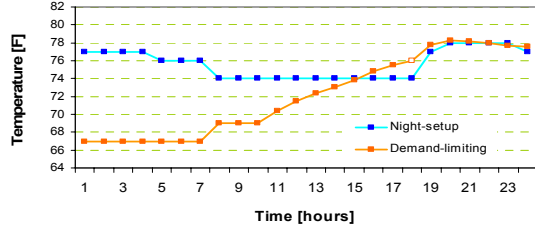
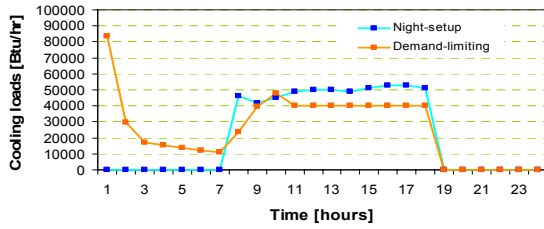
(a) DL start-time: 7am



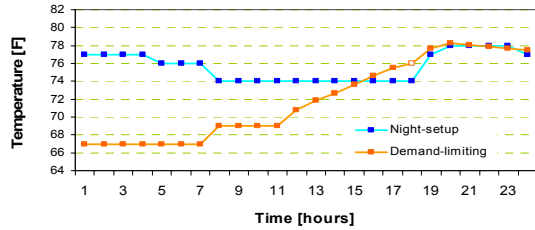
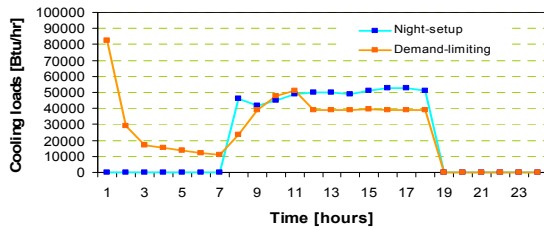
(b) DL start-time: 8am



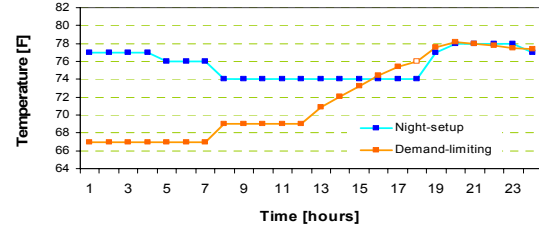
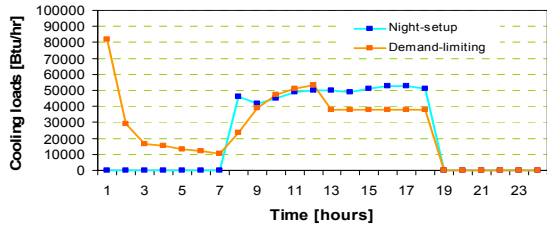
(c) DL start-time: 9am



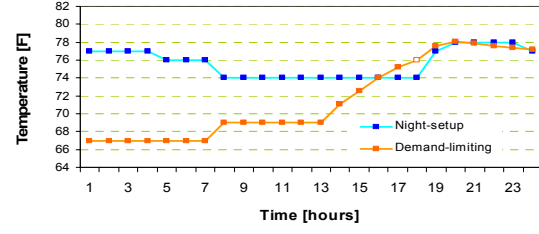
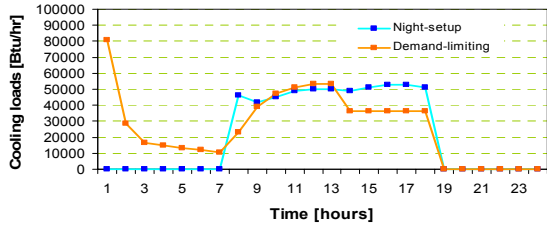
(d) DL start-time: 10am



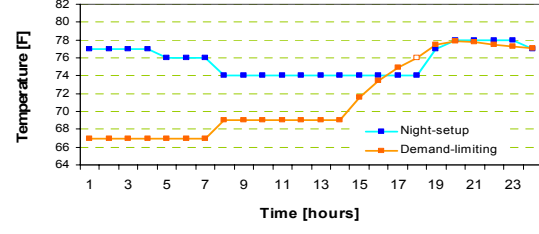
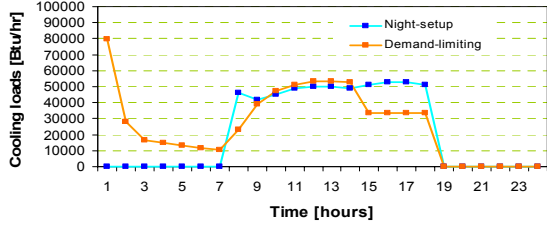
(e) DL start-time: 11am



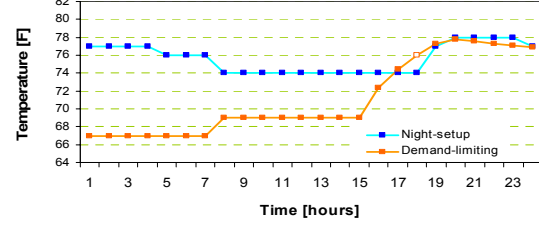
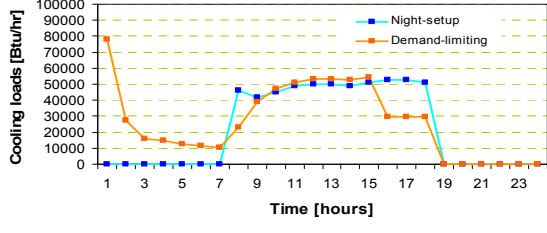
(f) DL start-time: noon



(g) DL start-time: 1pm

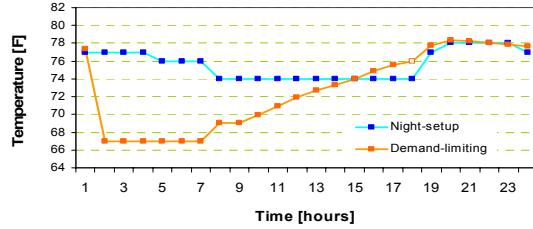
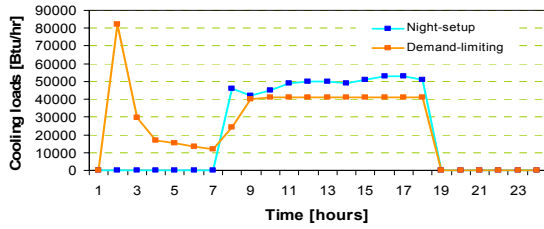


(h) DL start-time: 2pm

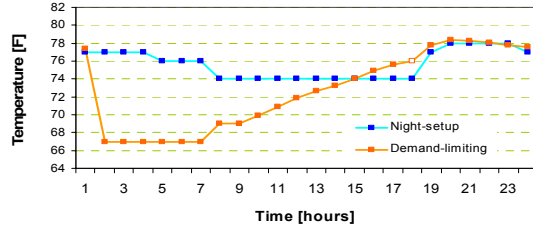
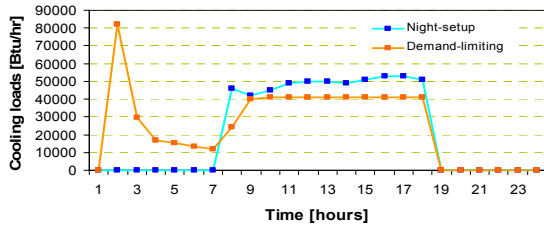


(i) DL start-time: 3pm

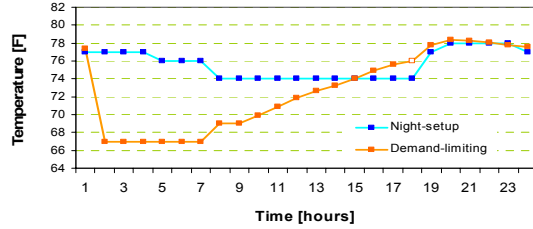
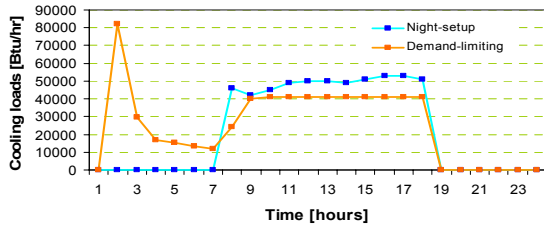
-Test zones: Combined zones
 -67°F PC start-time: 1 am



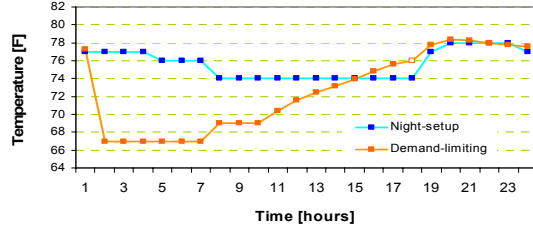
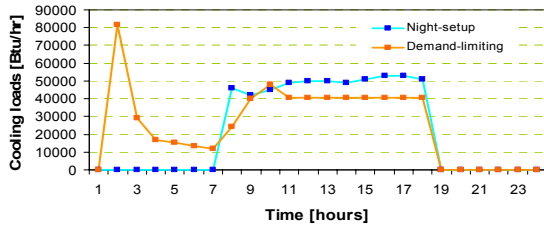
(a) DL start-time: 7am



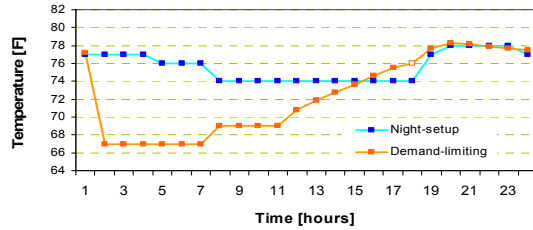
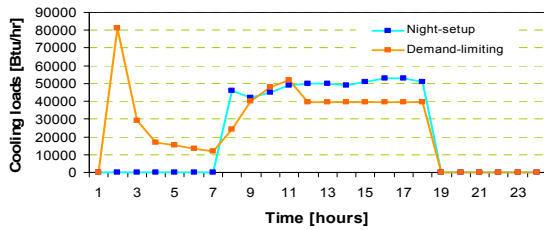
(b) DL start-time: 8am



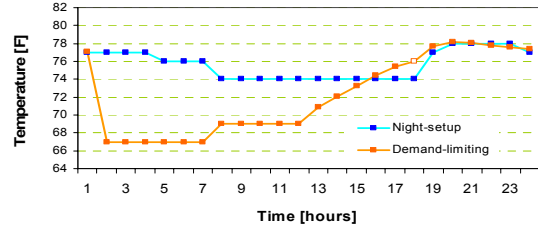
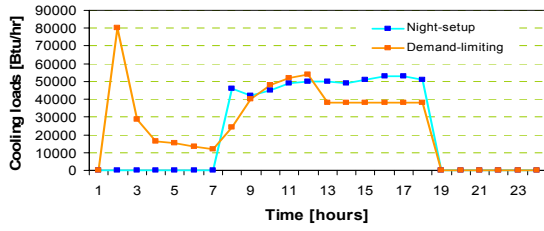
(c) DL start-time: 9am



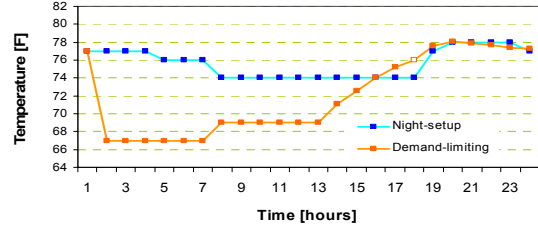
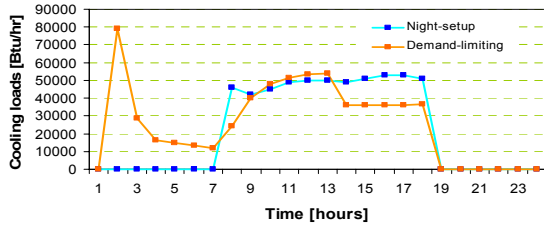
(d) DL start-time: 10am



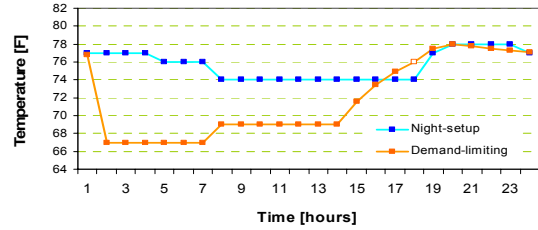
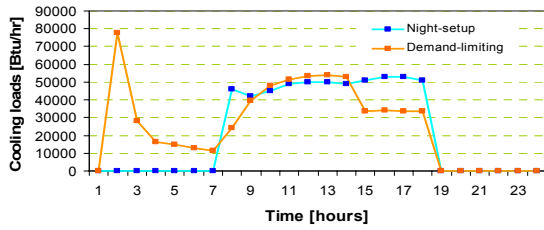
(e) DL start-time: 11am



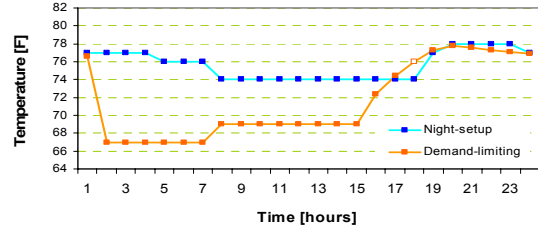
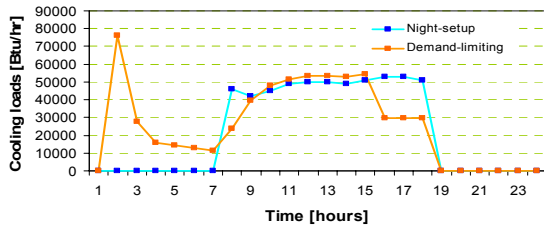
(f) DL start-time: noon



(g) DL start-time: 1pm

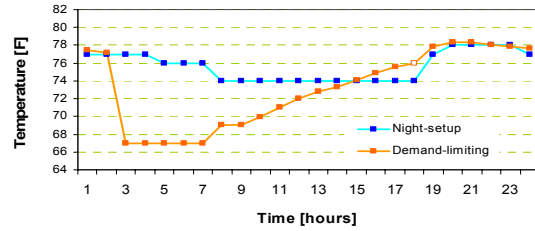
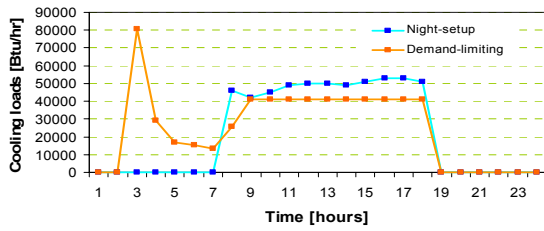


(h) DL start-time: 2pm

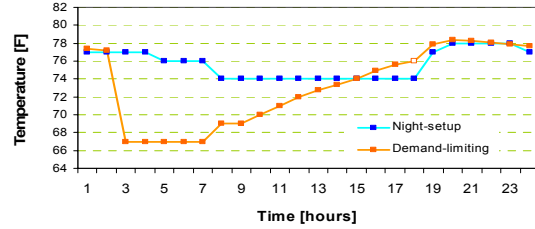
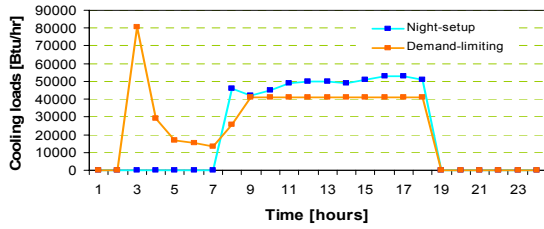


(i) DL start-time: 3pm

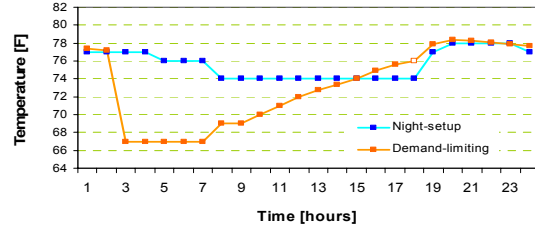
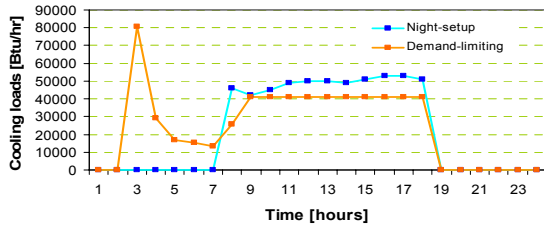
-Test zones: Combined zones
 -67°F PC start-time: 2 am



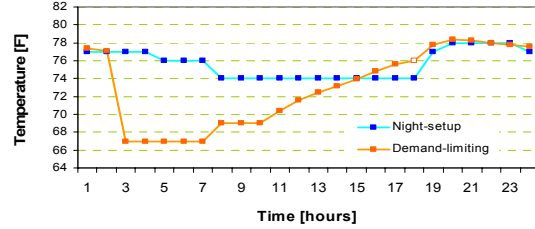
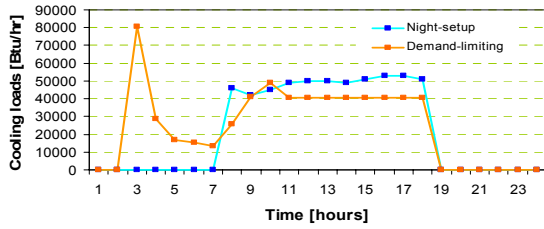
(a) DL start-time: 7am



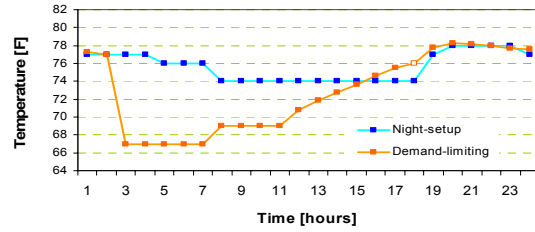
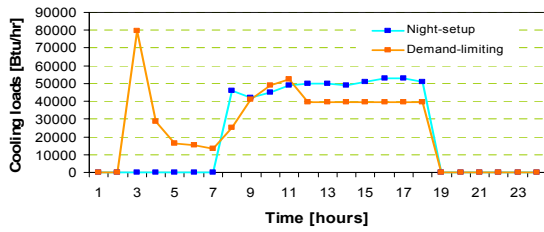
(b) DL start-time: 8am



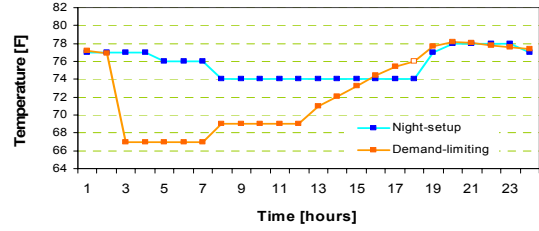
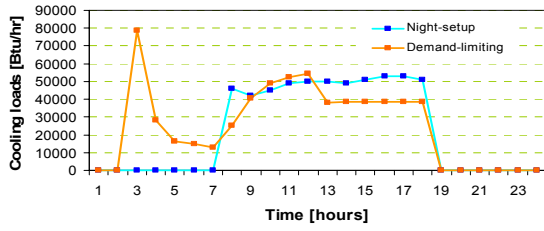
(c) DL start-time: 9am



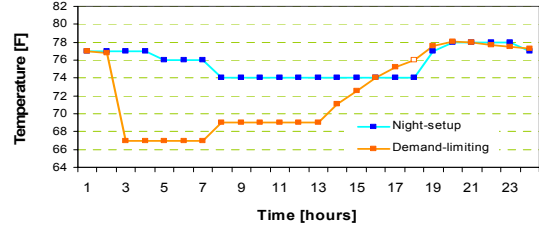
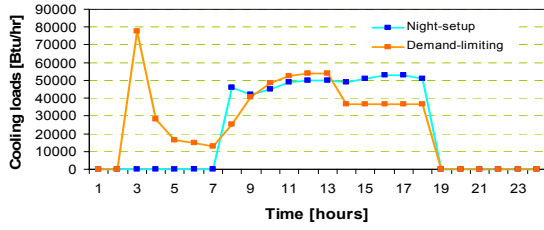
(d) DL start-time: 10am



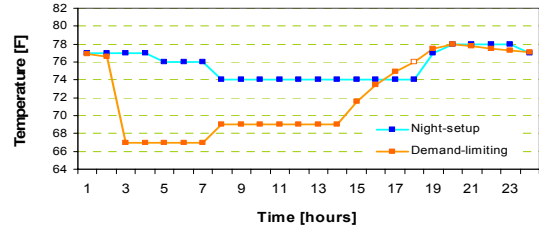
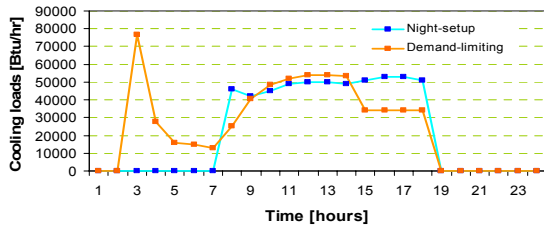
(e) DL start-time: 11am



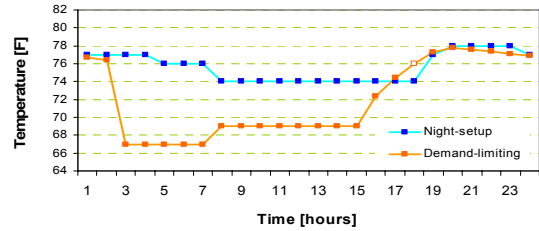
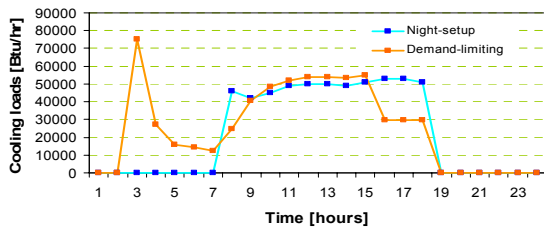
(f) DL start-time: noon



(g) DL start-time: 1pm

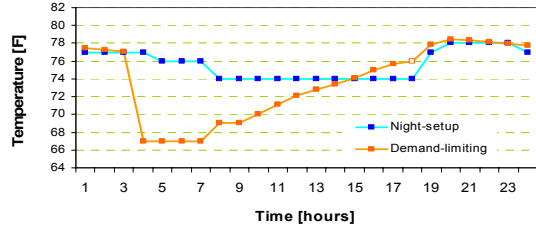
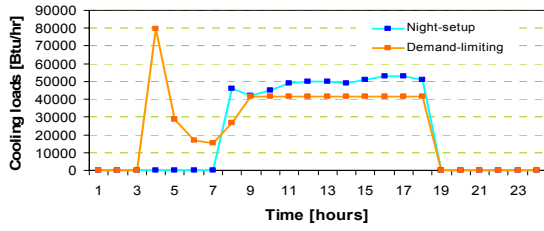


(h) DL start-time: 2pm

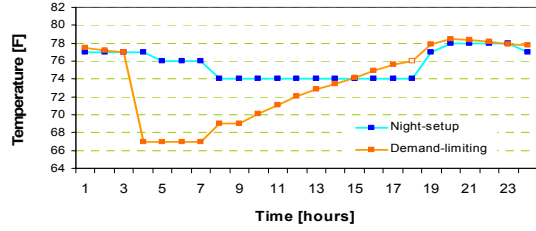
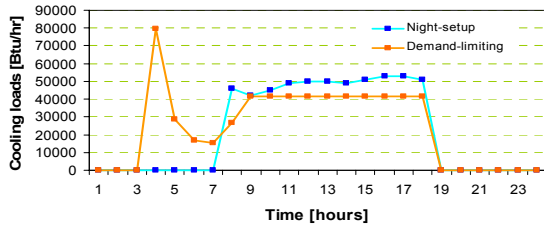


(i) DL start-time: 3pm

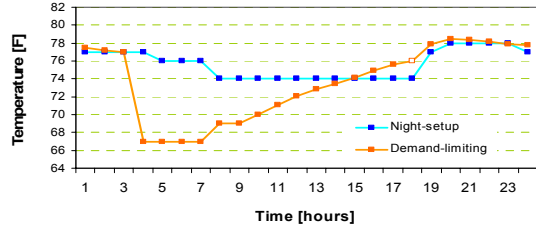
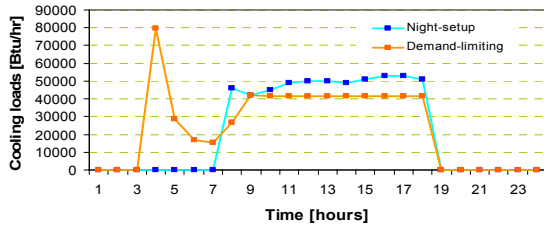
-Test zones: Combined zones
 -67°F PC start-time: 3 am



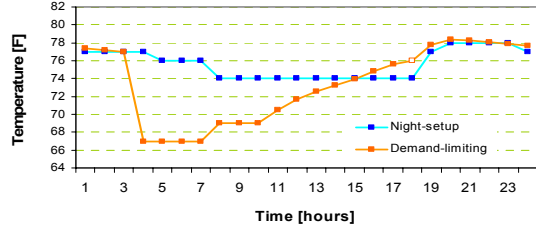
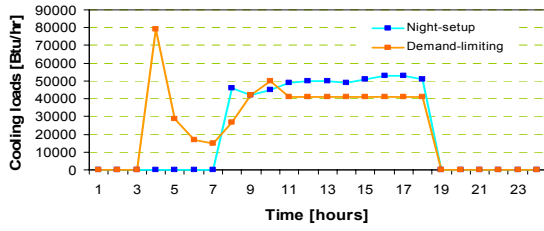
(a) DL start-time: 7am



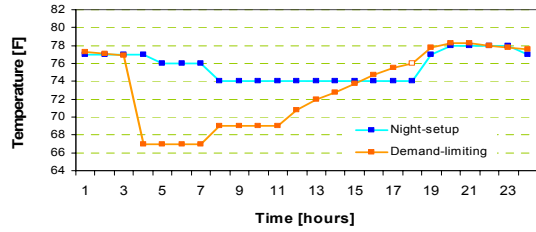
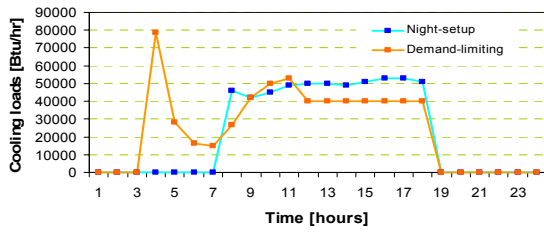
(b) DL start-time: 8am



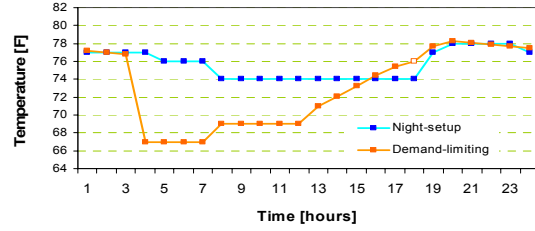
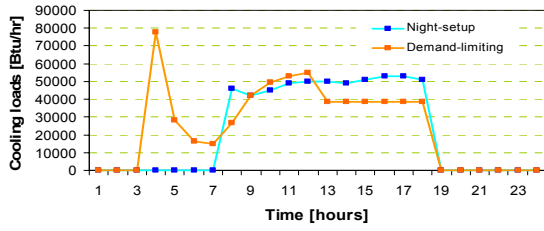
(c) DL start-time: 9am



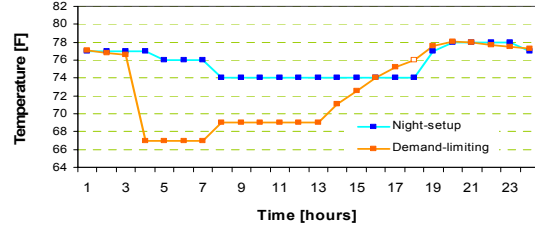
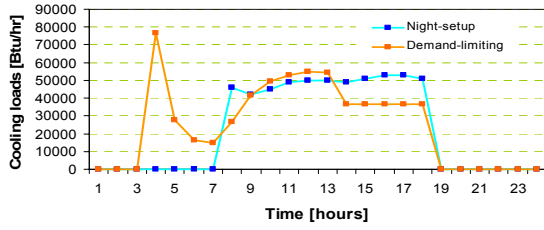
(d) DL start-time: 10am



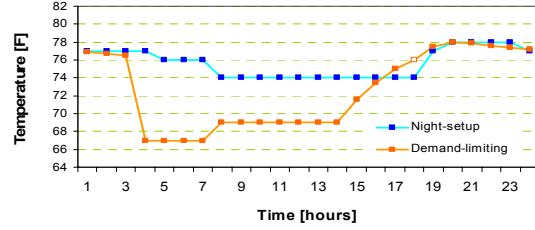
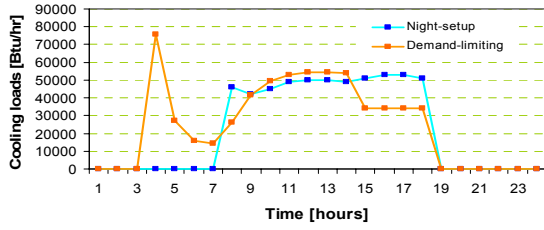
(e) DL start-time: 11am



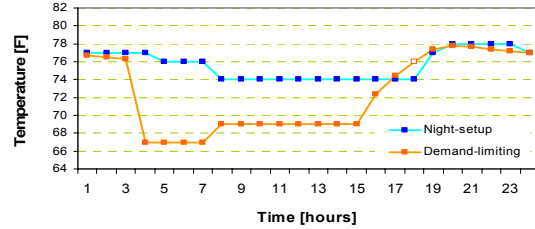
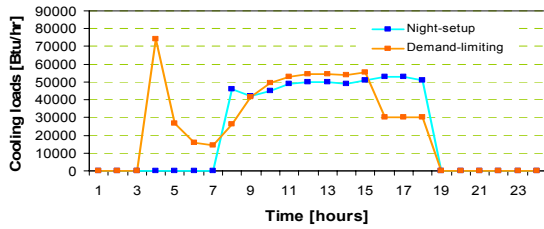
(f) DL start-time: noon



(g) DL start-time: 1pm

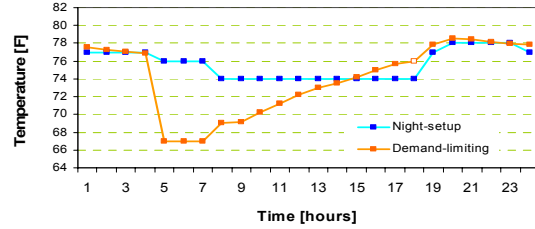
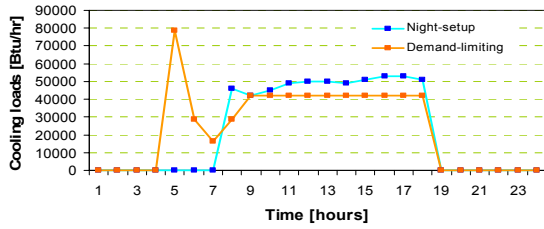


(h) DL start-time: 2pm

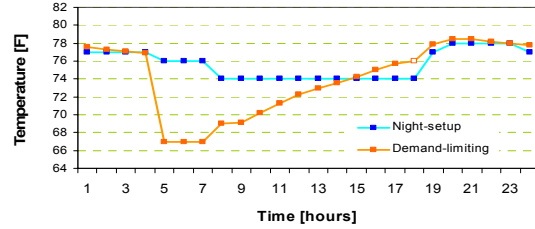
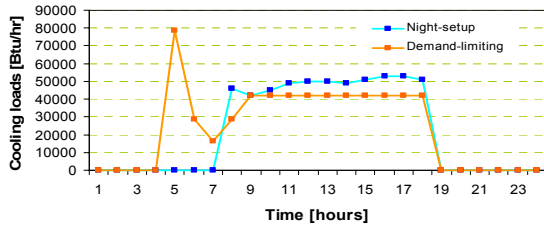


(i) DL start-time: 3pm

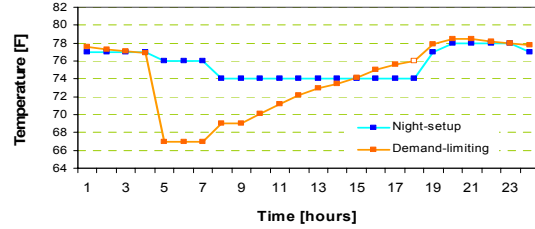
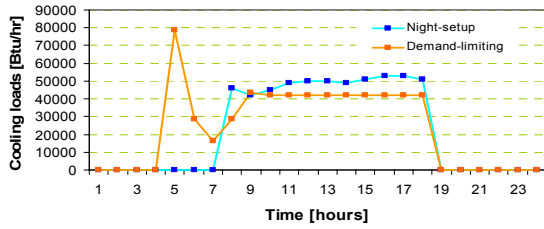
-Test zones: Combined zones
 -67°F PC start-time: 4 am



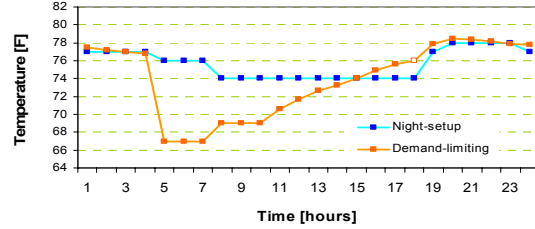
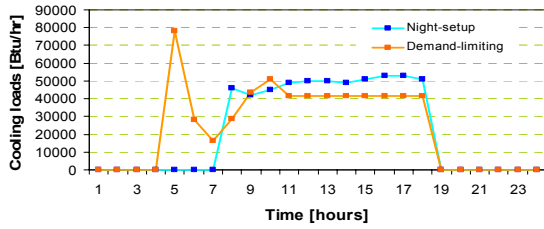
(a) DL start-time: 7am



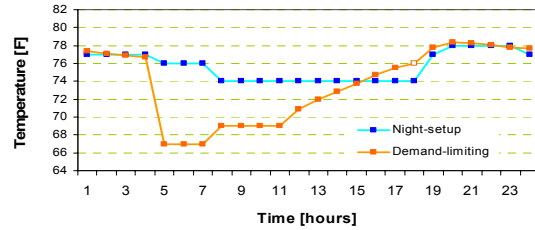
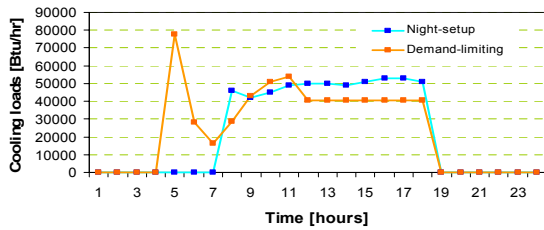
(b) DL start-time: 8am



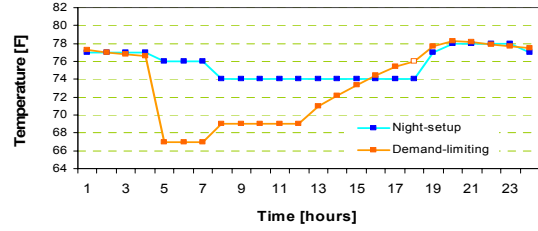
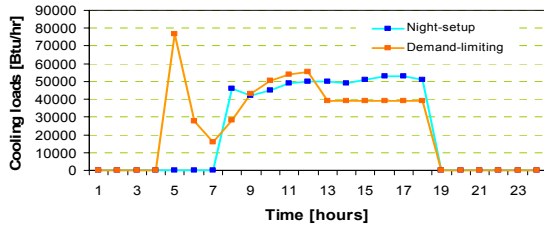
(c) DL start-time: 9am



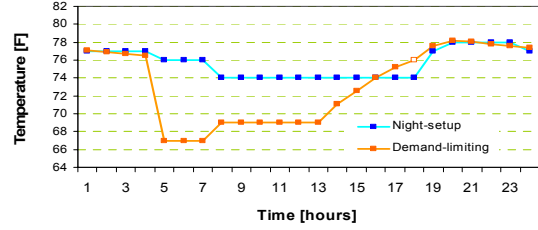
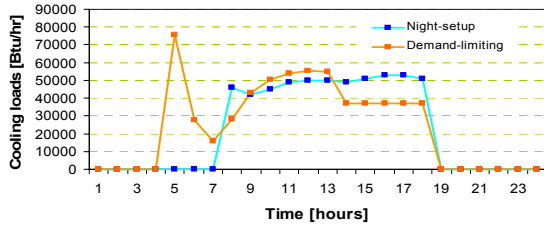
(d) DL start-time: 10am



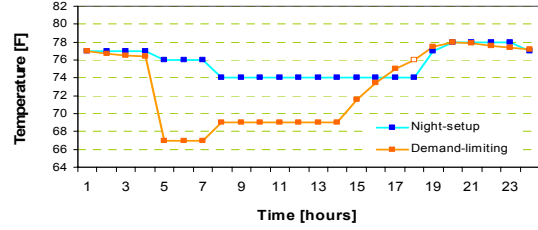
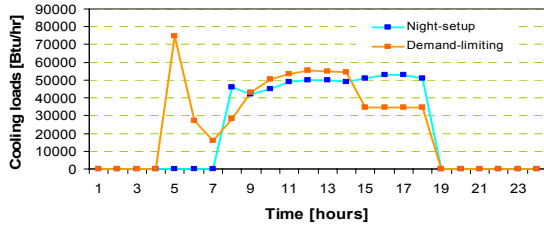
(e) DL start-time: 11am



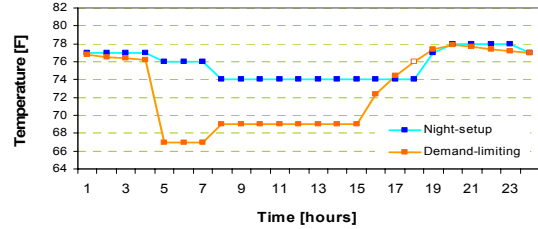
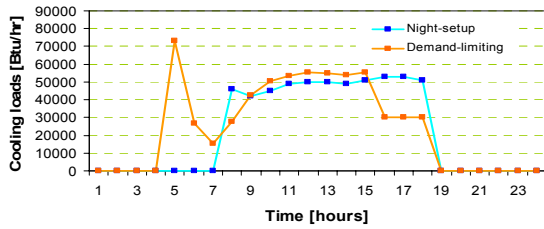
(f) DL start-time: noon



(g) DL start-time: 1pm

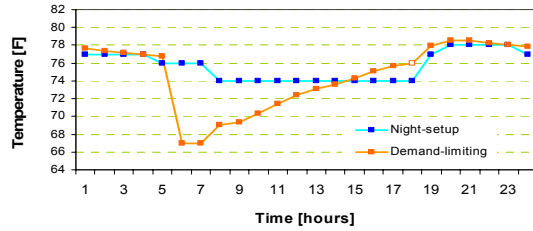
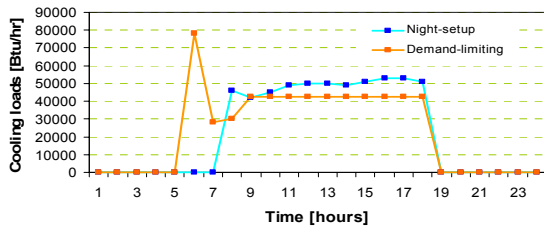


(h) DL start-time: 2pm

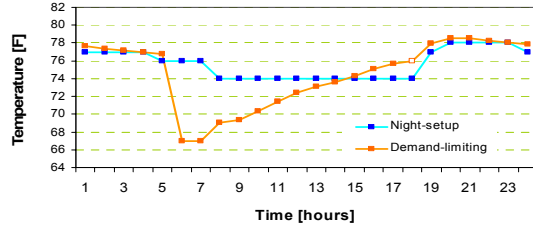
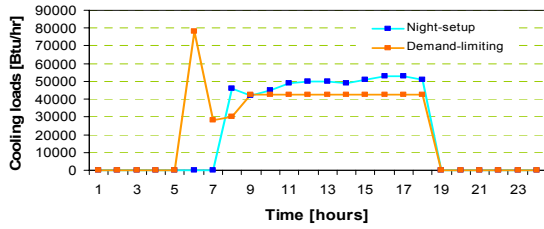


(i) DL start-time: 3pm

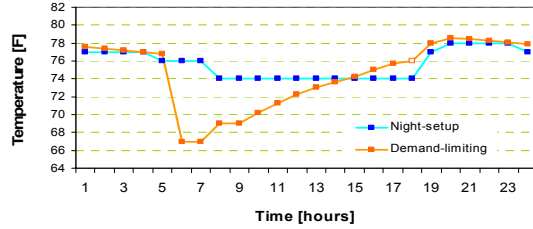
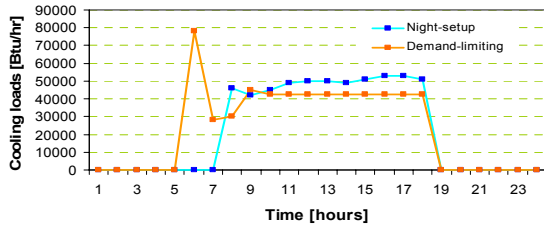
-Test zones: Combined zones
 -67°F PC start-time: 5 am



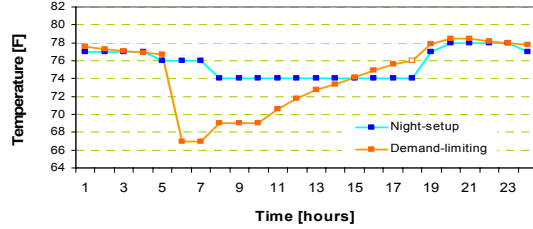
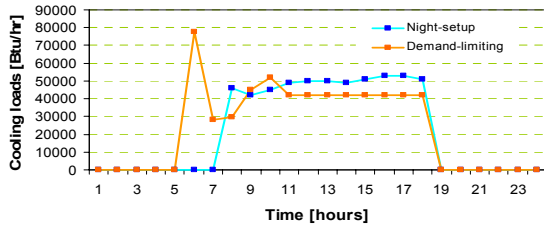
(a) DL start-time: 7am



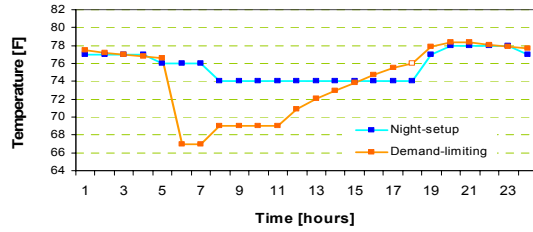
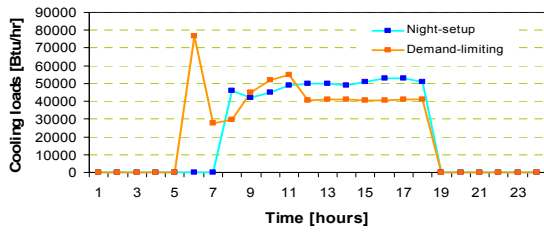
(b) DL start-time: 8am



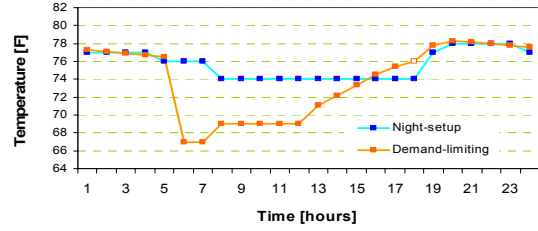
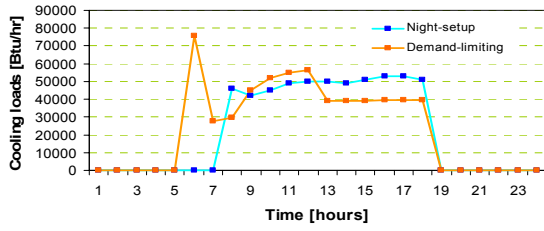
(c) DL start-time: 9am



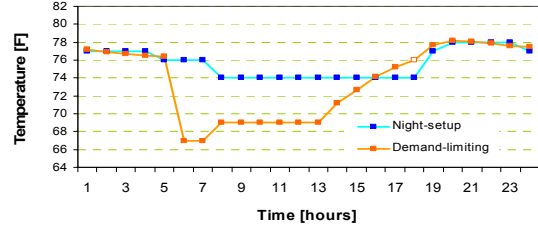
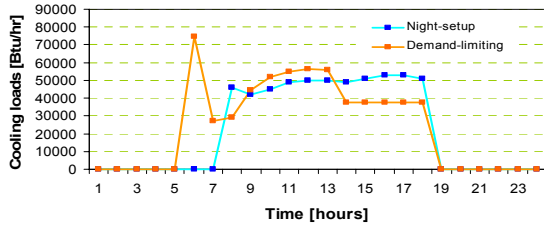
(d) DL start-time: 10am



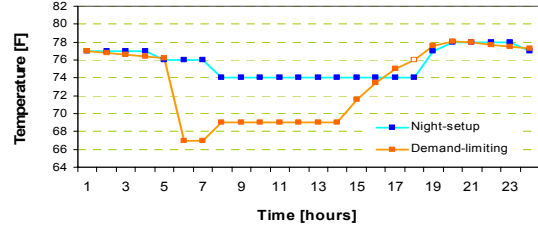
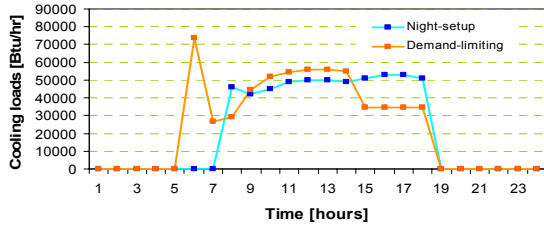
(e) DL start-time: 11am



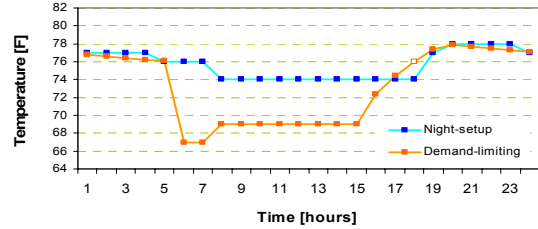
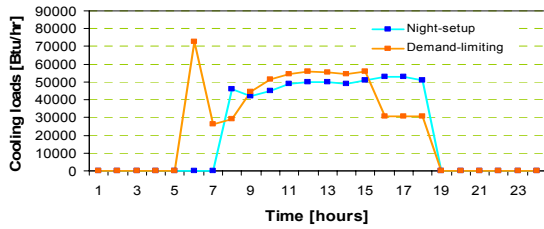
(f) DL start-time: noon



(g) DL start-time: 1pm

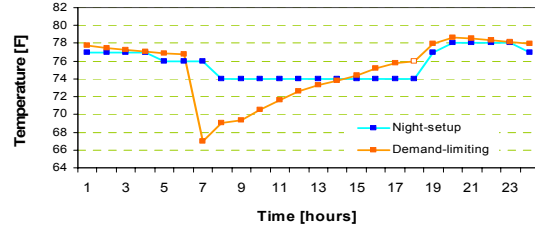
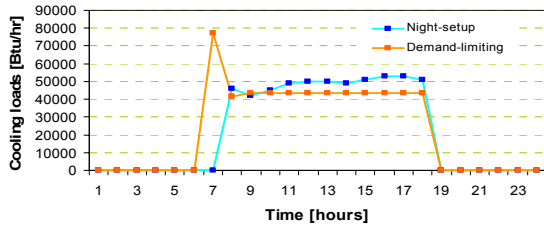


(h) DL start-time: 2pm

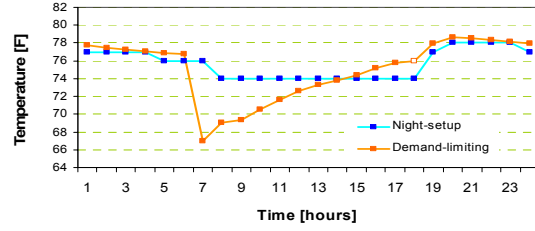
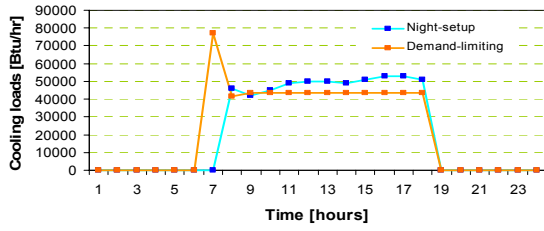


(i) DL start-time: 3pm

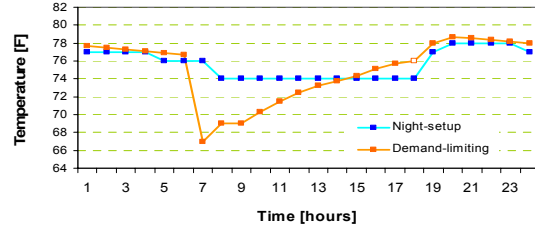
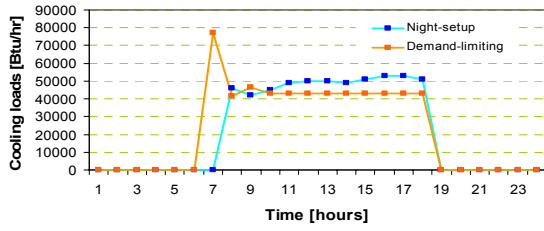
-Test zones: Combined zones
 -67°F PC start-time: 6 am



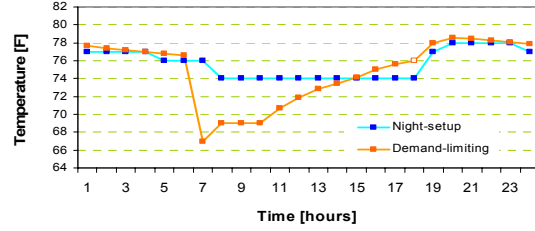
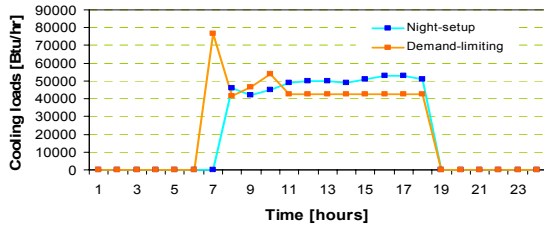
(a) DL start-time: 7am



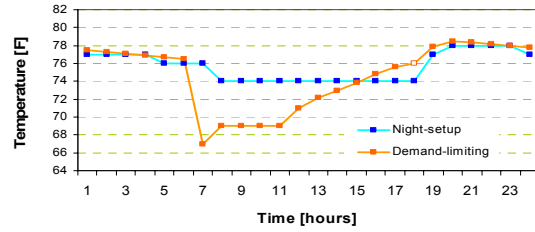
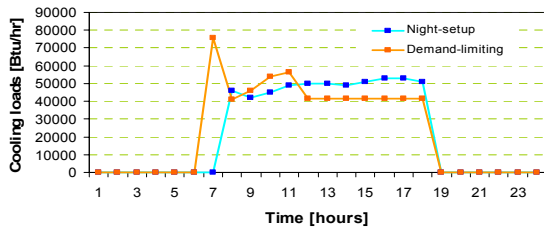
(b) DL start-time: 8am



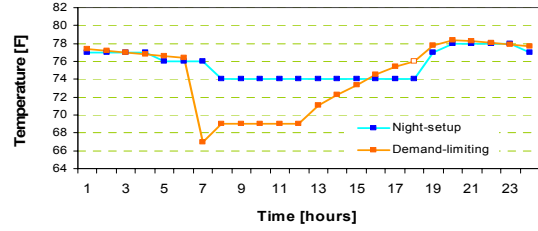
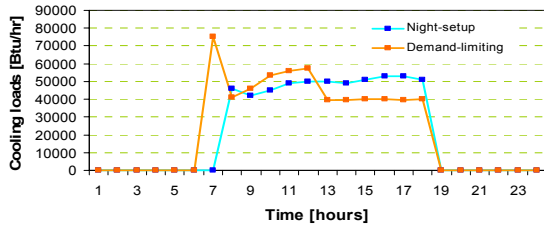
(c) DL start-time: 9am



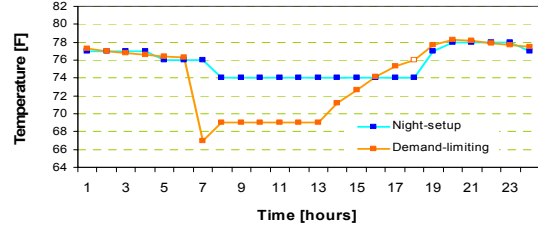
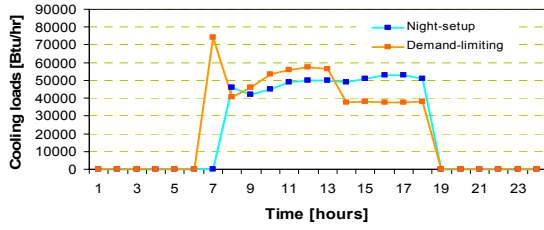
(d) DL start-time: 10am



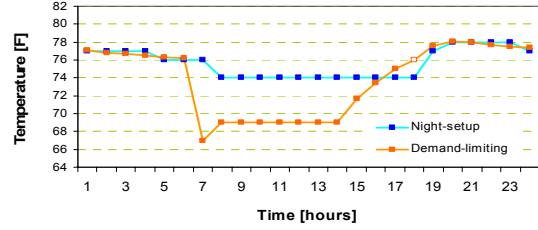
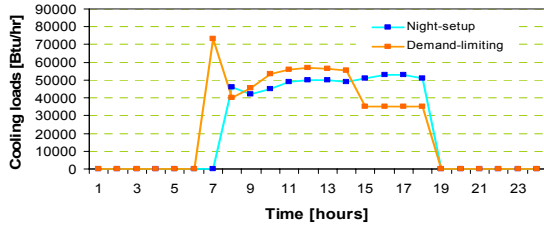
(e) DL start-time: 11am



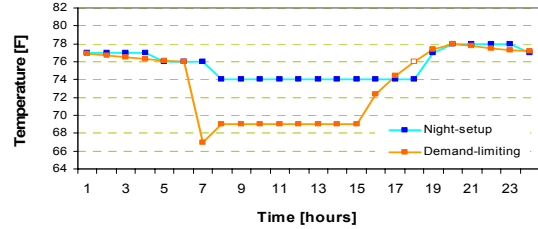
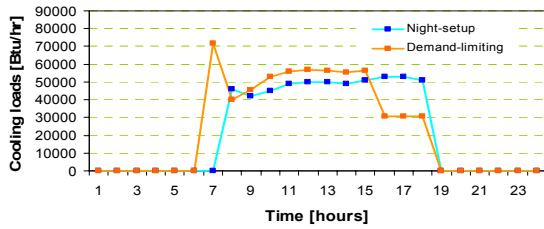
(f) DL start-time: noon



(g) DL start-time: 1pm

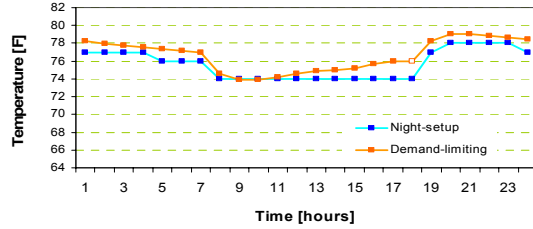
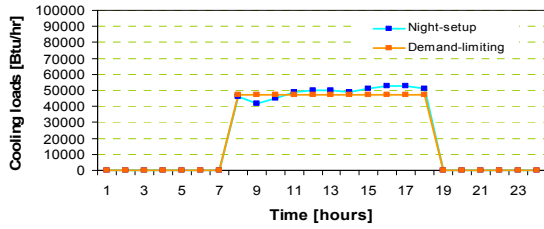


(h) DL start-time: 2pm

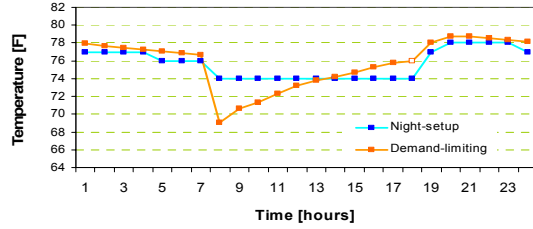
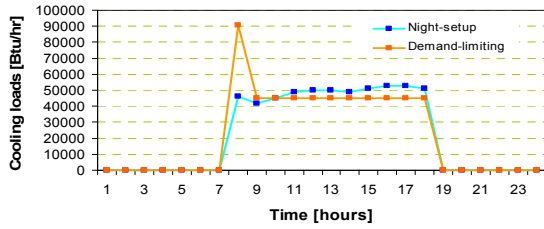


(i) DL start-time: 3pm

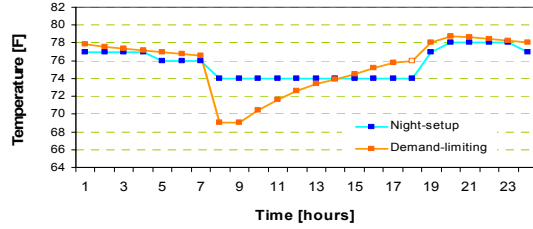
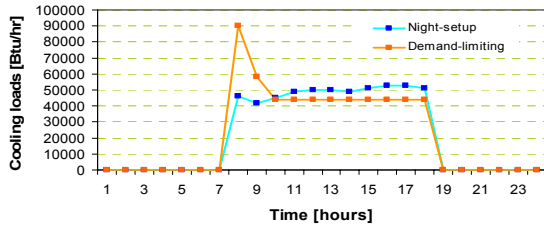
-Test zones: Combined zones
 -67°F PC start-time: 7 am



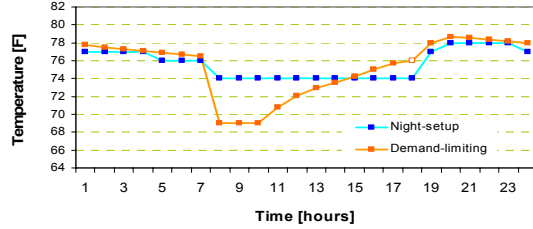
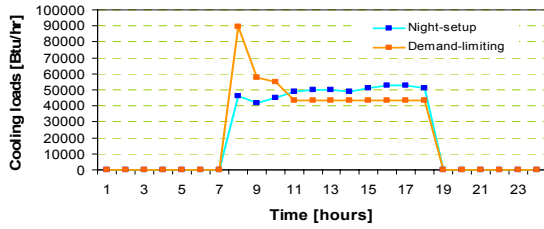
(a) DL start-time: 7am



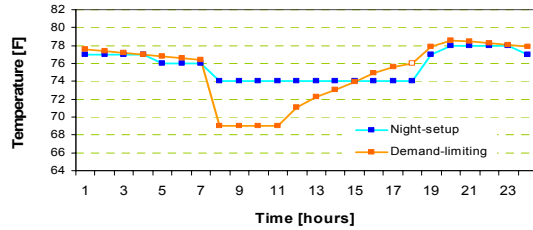
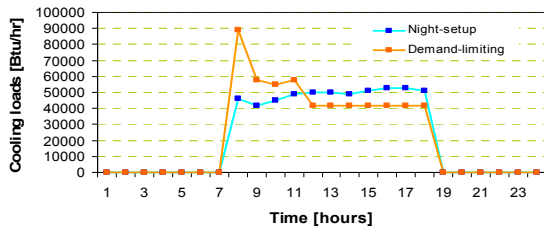
(b) DL start-time: 8am



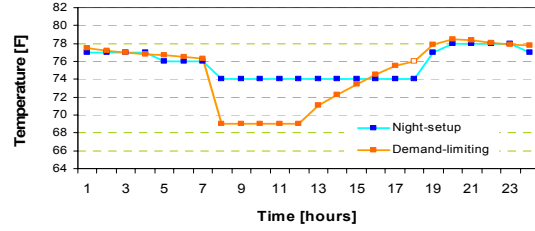
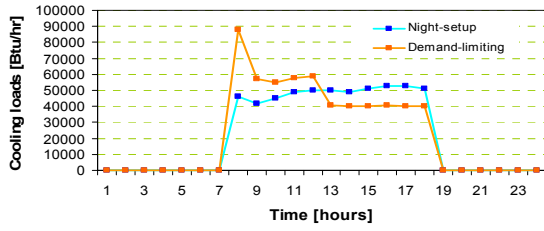
(c) DL start-time: 9am



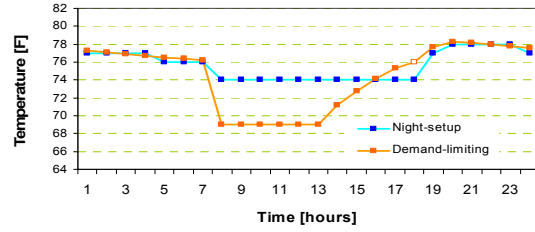
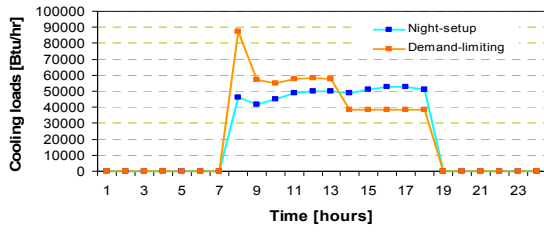
(d) DL start-time: 10am



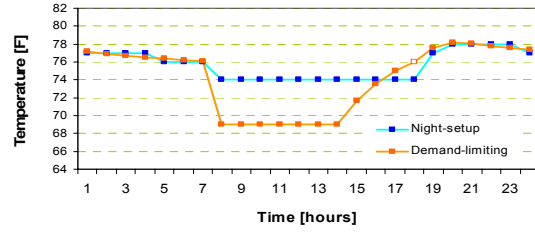
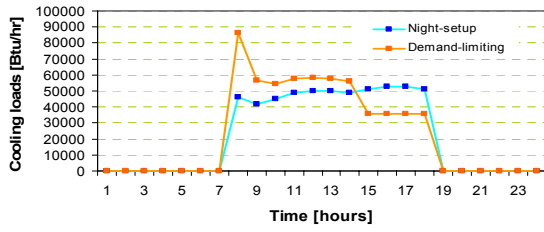
(e) DL start-time: 11am



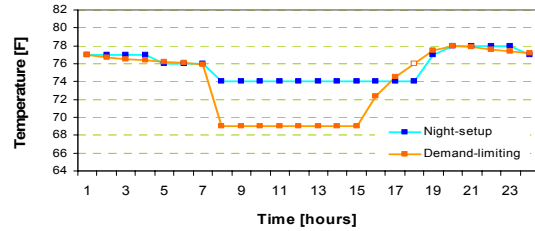
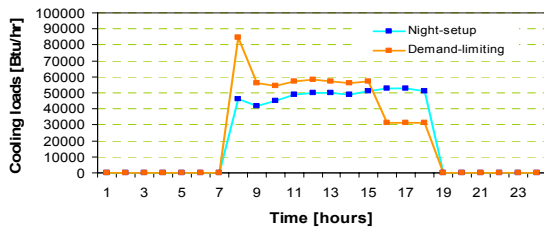
(f) DL start-time: noon



(g) DL start-time: 1pm



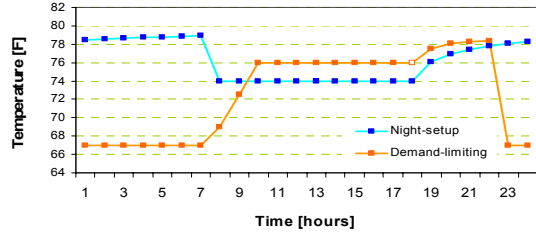
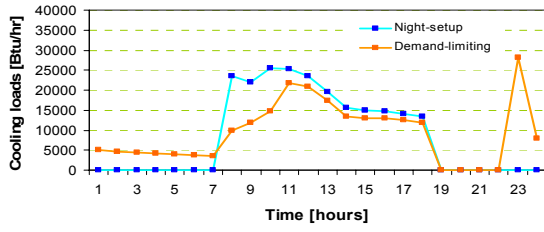
(h) DL start-time: 2pm



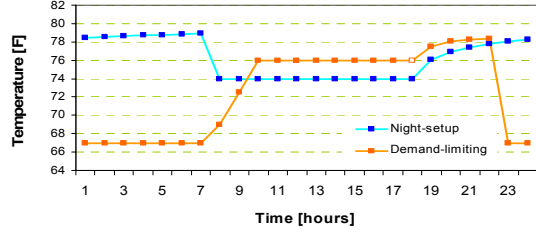
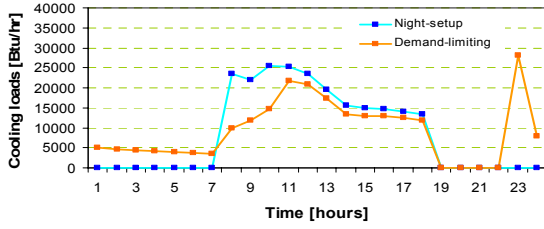
(i) DL start-time: 3pm

2. East zones

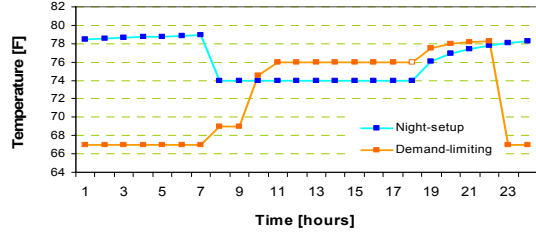
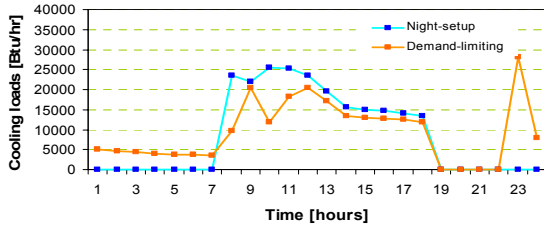
-Test zones: East zones
 -67°F PC start-time: 10 pm



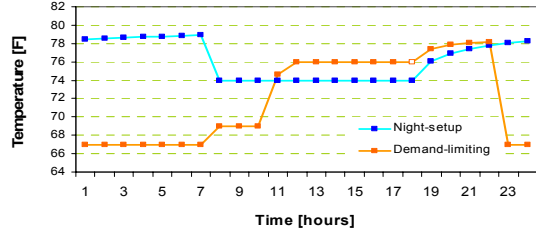
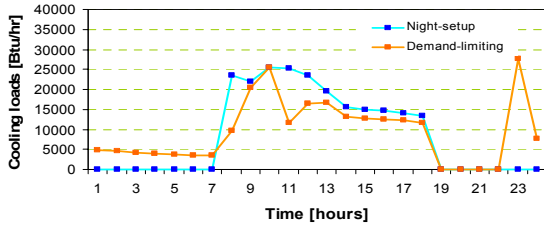
(a) DL start-time: 7am



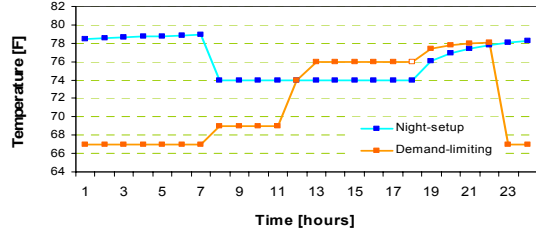
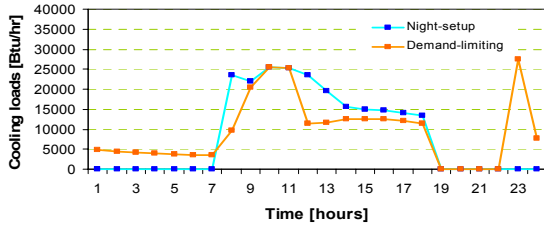
(b) DL start-time: 8am



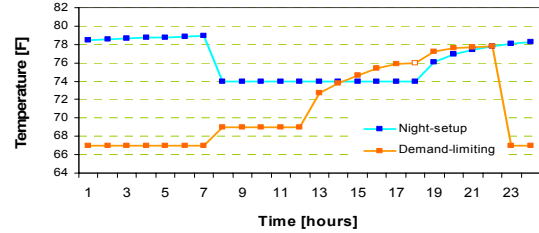
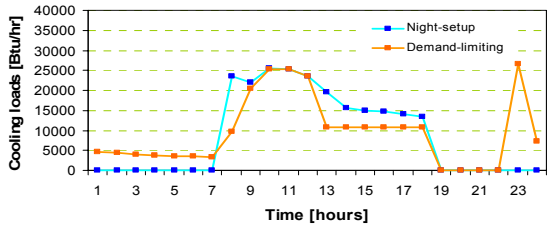
(c) DL start-time: 9am



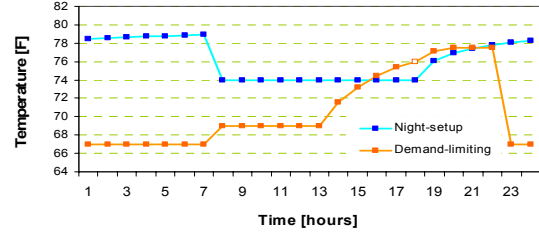
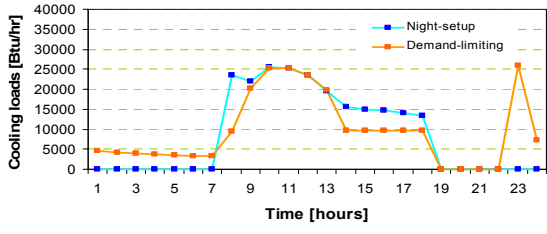
(d) DL start-time: 10am



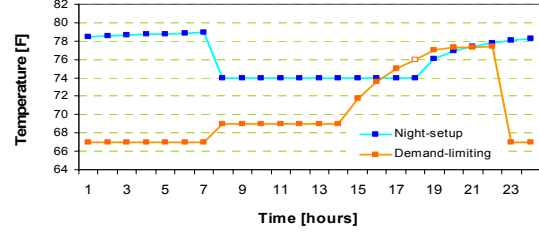
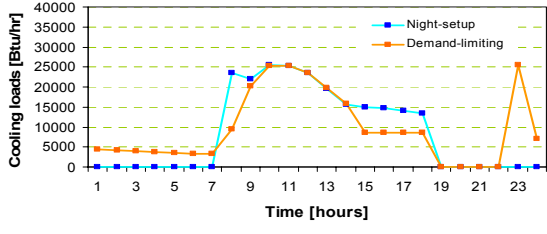
(e) DL start-time: 11am



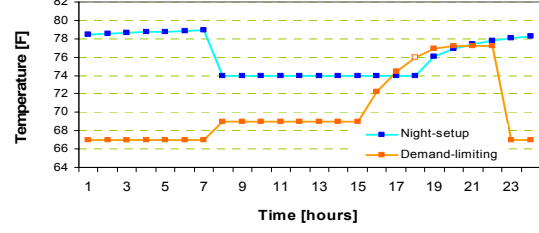
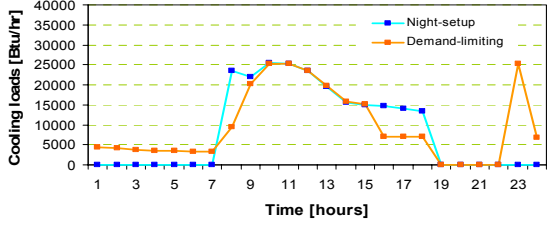
(f) DL start-time: noon



(g) DL start-time: 1pm

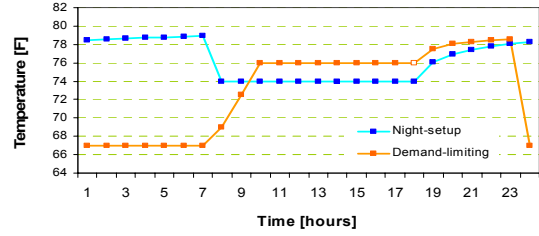
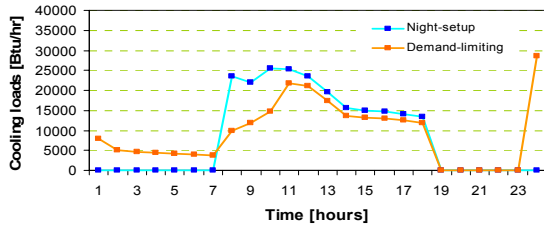


(h) DL start-time: 2pm

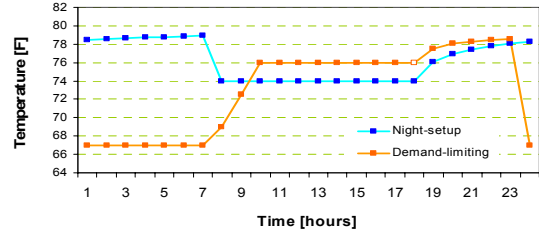
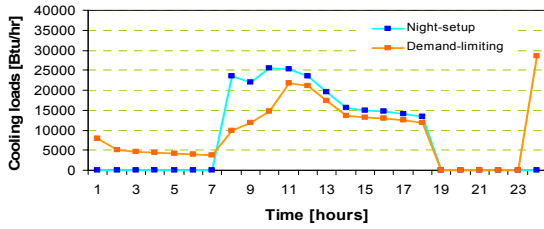


(i) DL start-time: 3pm

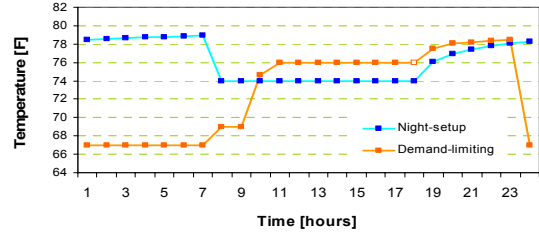
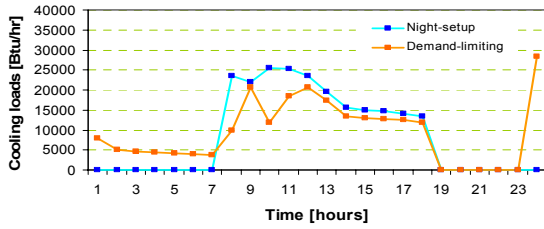
-Test zones: East zones
 -67°F PC start-time: 11 pm



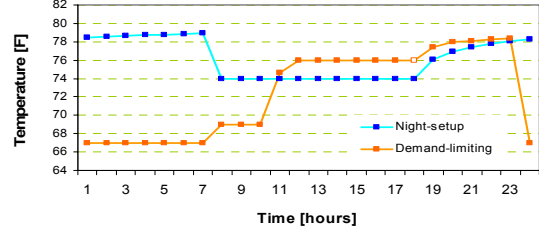
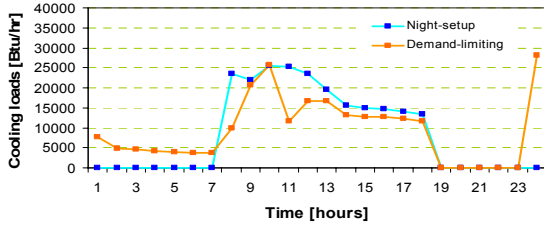
(a) DL start-time: 7am



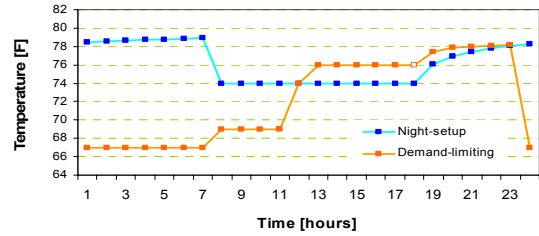
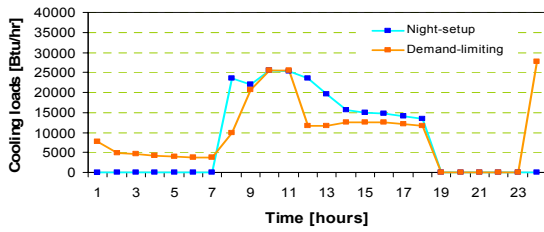
(b) DL start-time: 8am



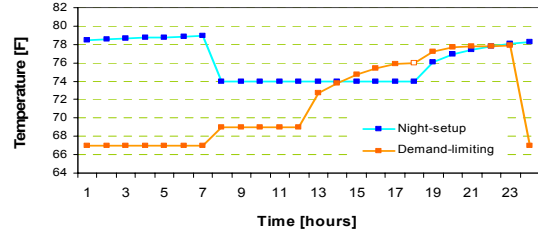
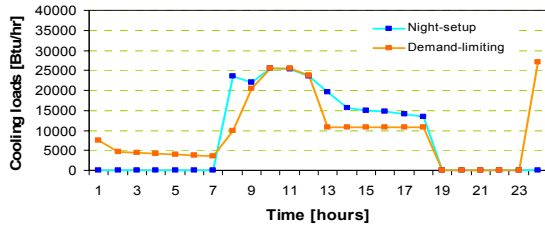
(c) DL start-time: 9am



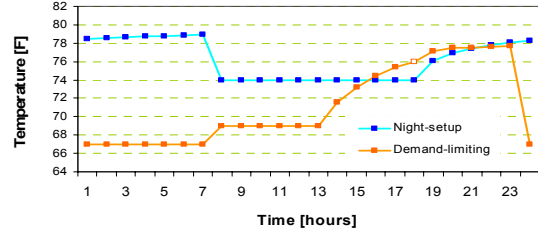
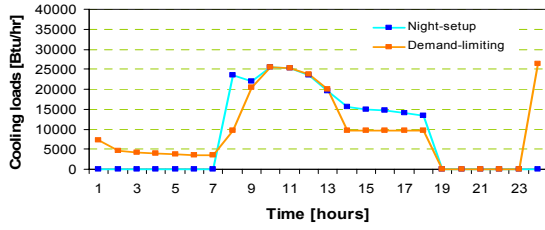
(d) DL start-time: 10am



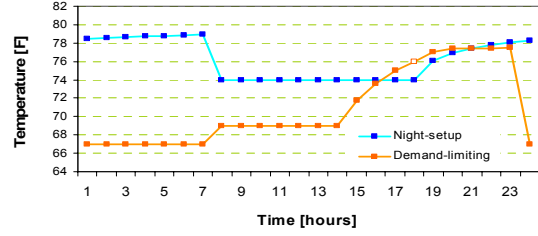
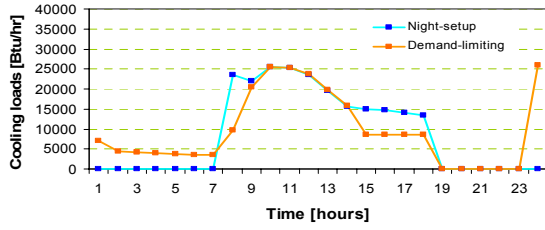
(e) DL start-time: 11am



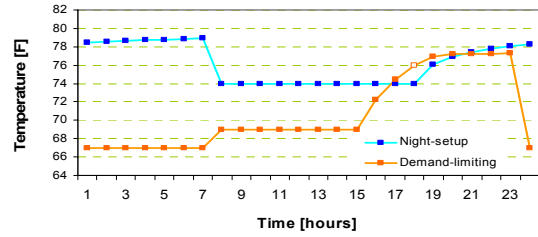
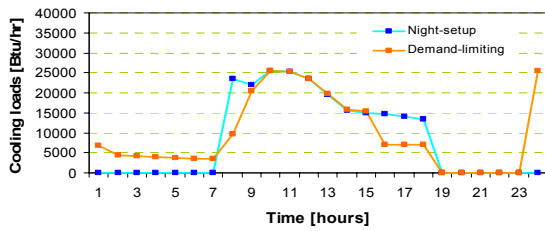
(f) DL start-time: noon



(g) DL start-time: 1pm

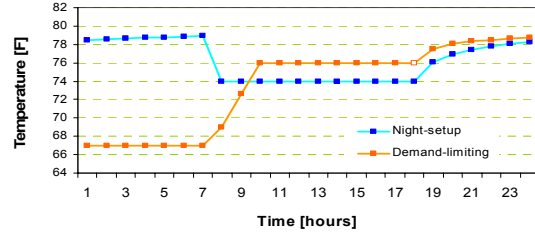
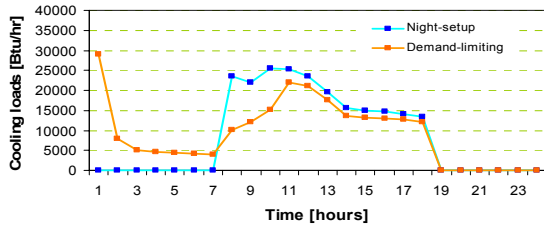


(h) DL start-time: 2pm

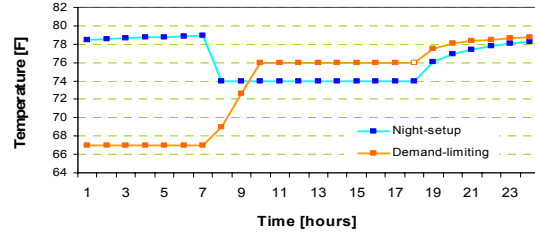
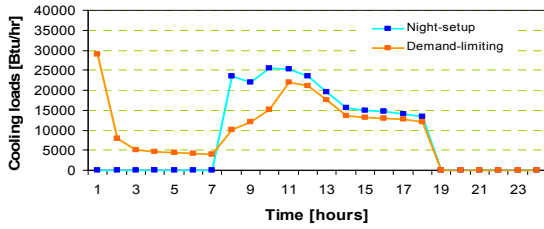


(i) DL start-time: 3pm

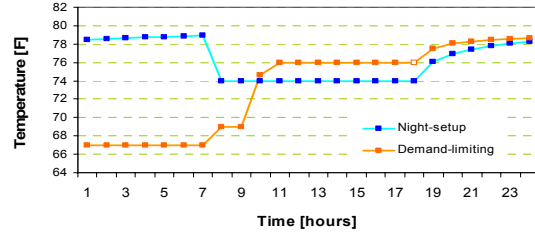
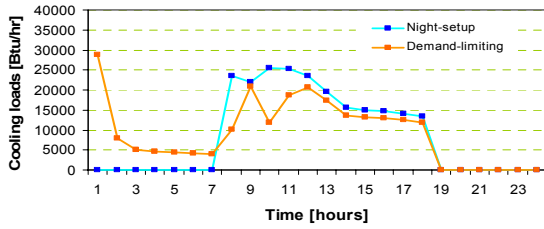
-Test zones: East zones
 -67°F PC start-time: midnight



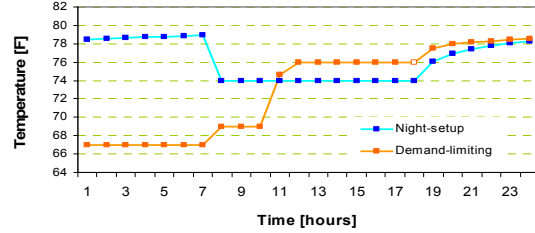
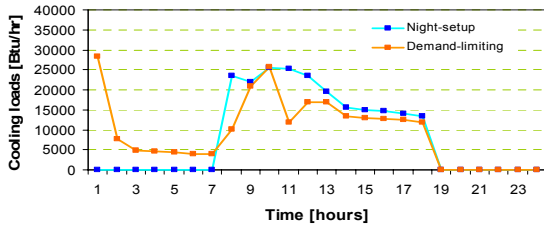
(a) DL start-time: 7am



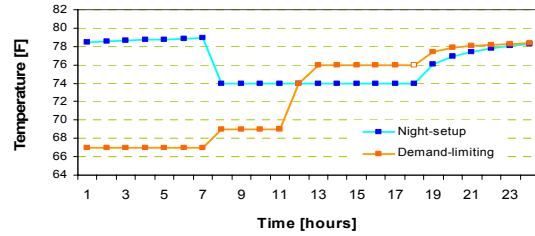
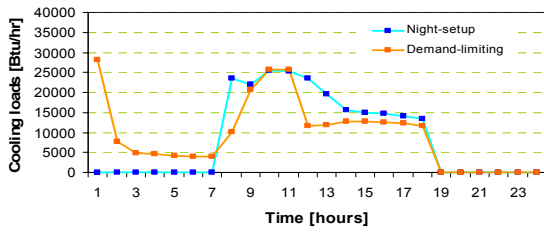
(b) DL start-time: 8am



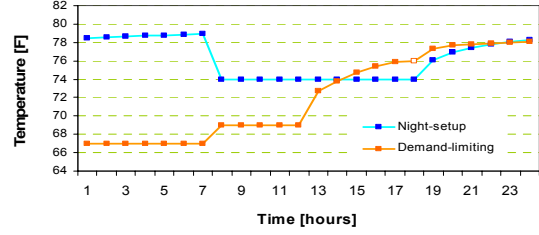
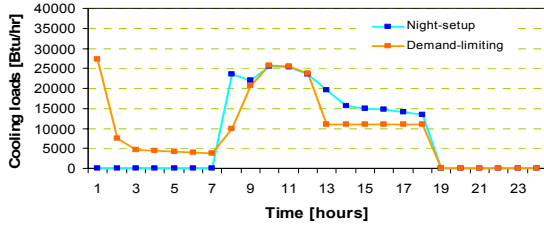
(c) DL start-time: 9am



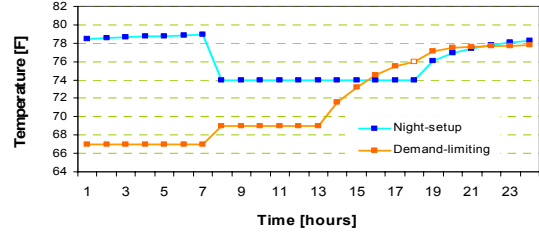
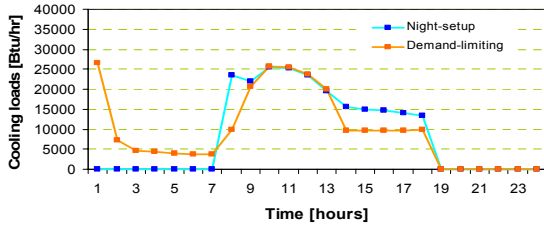
(d) DL start-time: 10am



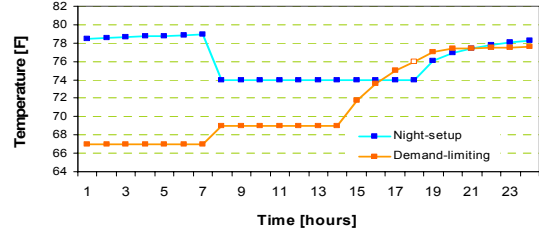
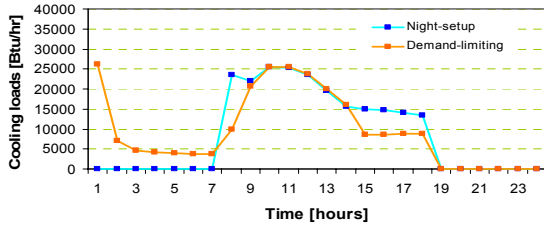
(e) DL start-time: 11am



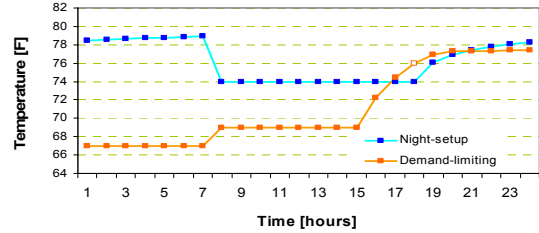
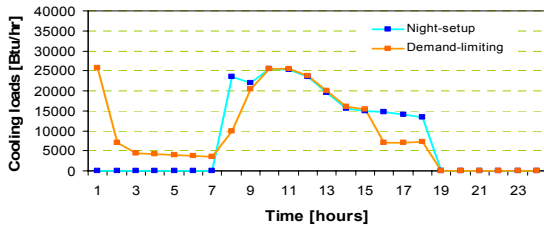
(f) DL start-time: noon



(g) DL start-time: 1pm

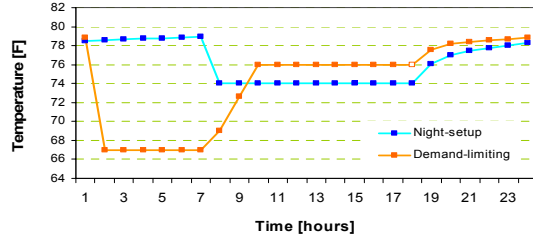
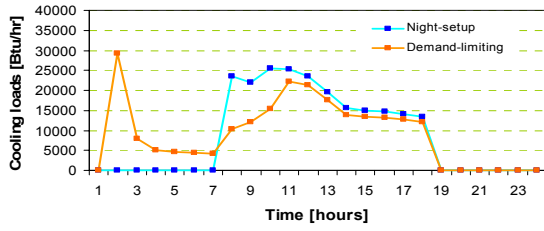


(h) DL start-time: 2pm

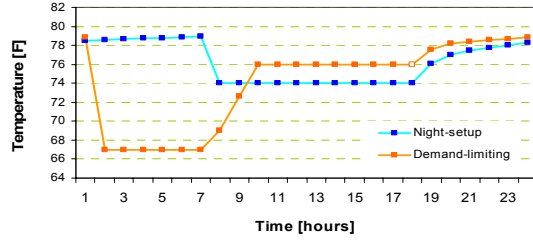
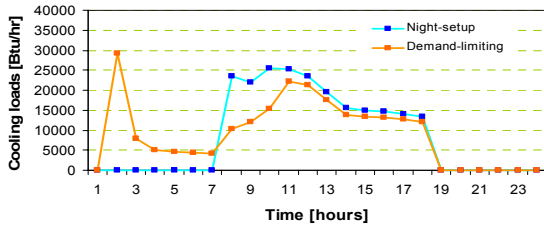


(i) DL start-time: 3pm

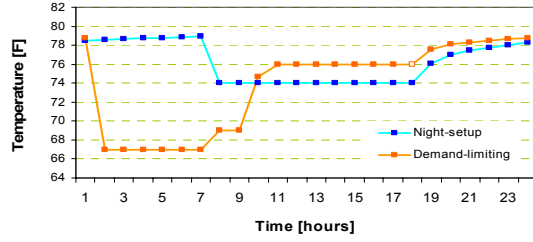
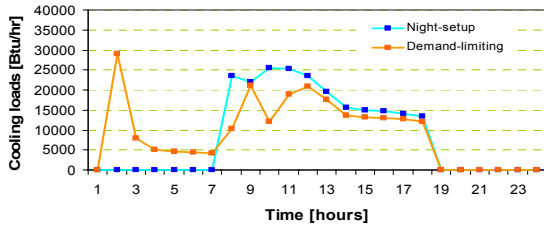
-Test zones: East zones
 -67°F PC start-time: 1 am



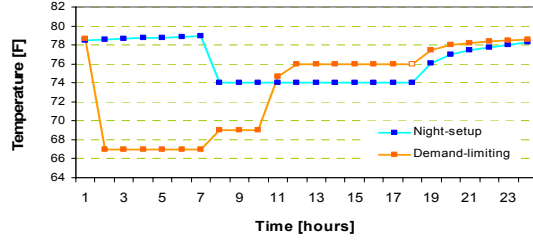
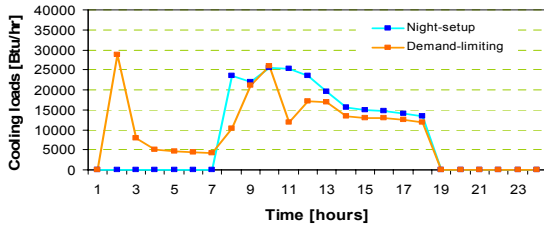
(a) DL start-time: 7am



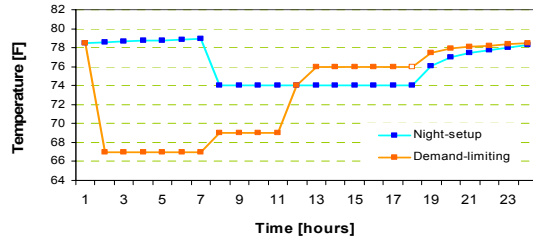
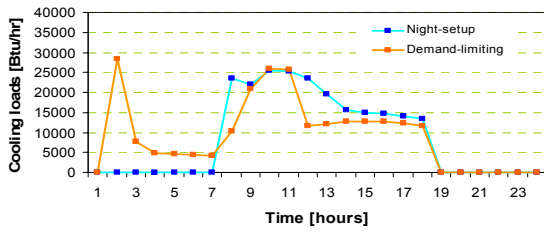
(b) DL start-time: 8am



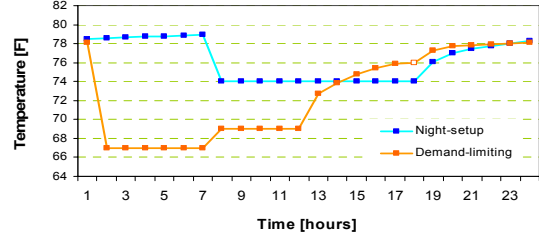
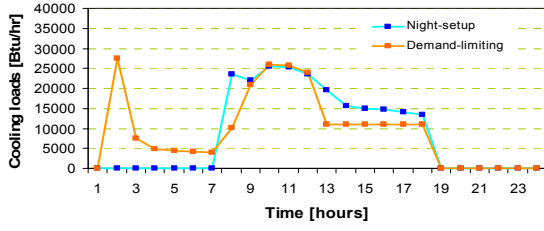
(c) DL start-time: 9am



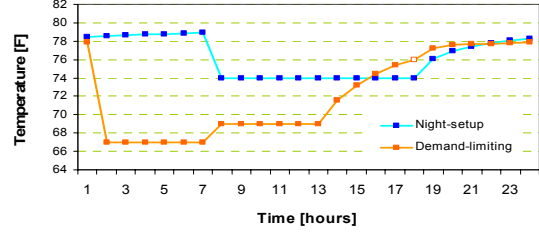
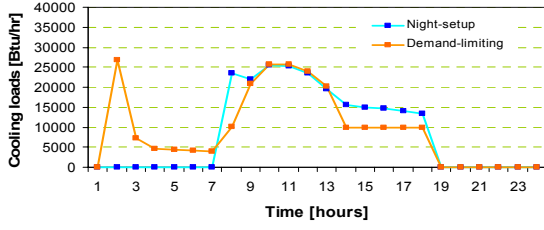
(d) DL start-time: 10am



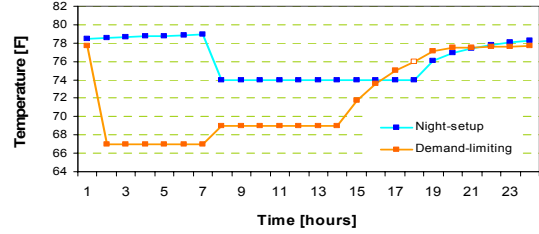
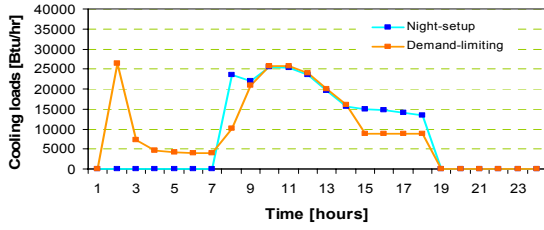
(e) DL start-time: 11am



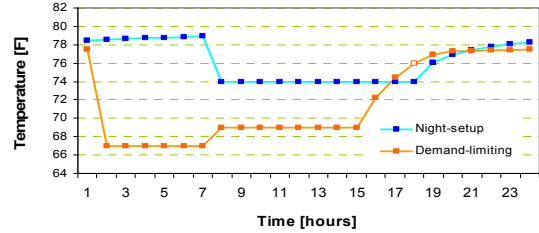
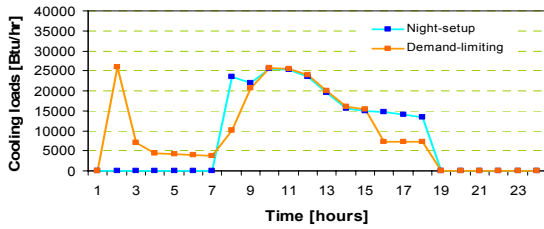
(f) DL start-time: noon



(g) DL start-time: 1pm

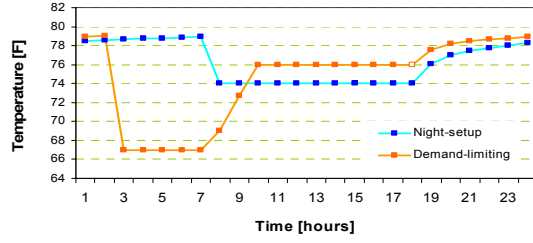
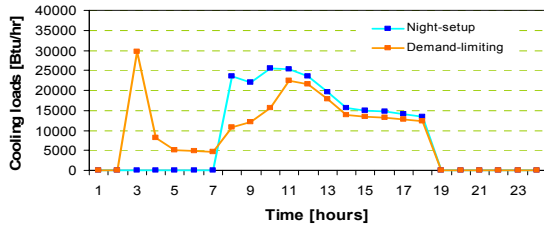


(h) DL start-time: 2pm

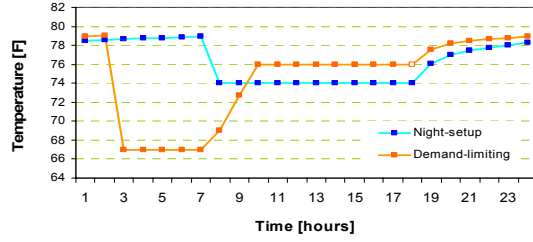
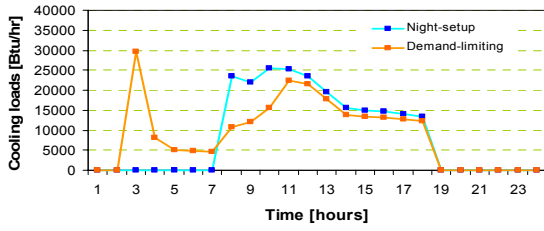


(i) DL start-time: 3pm

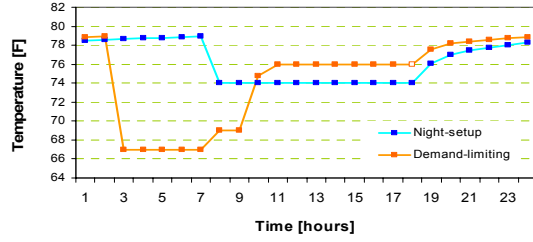
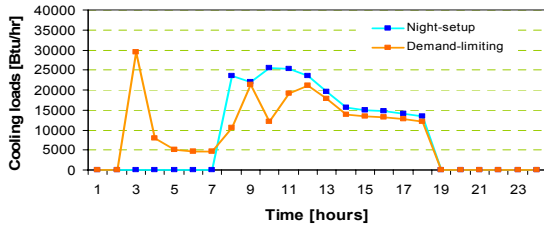
-Test zones: East zones
 -67°F PC start-time: 2 am



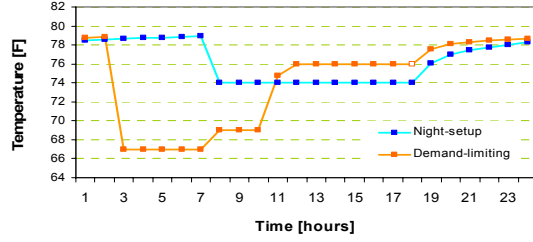
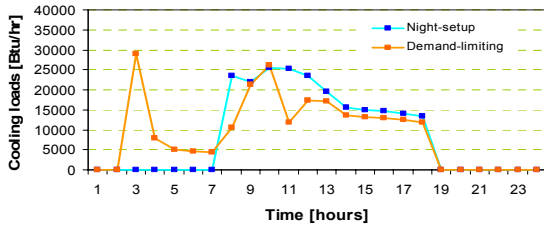
(a) DL start-time: 7am



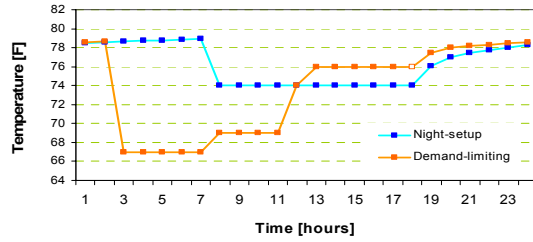
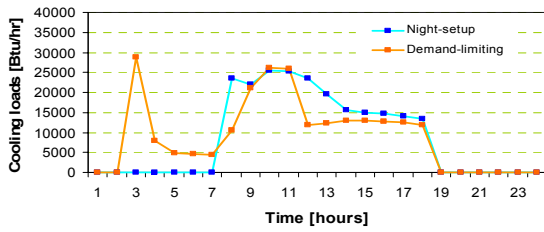
(b) DL start-time: 8am



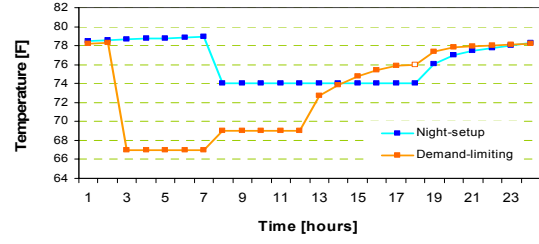
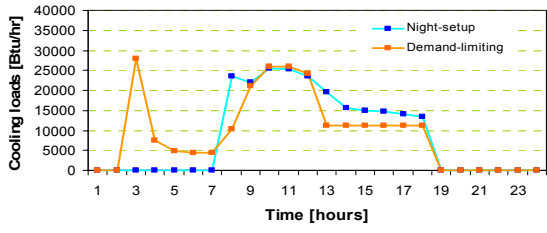
(c) DL start-time: 9am



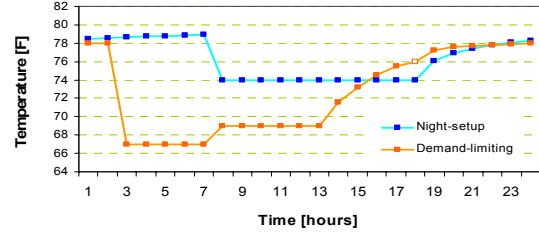
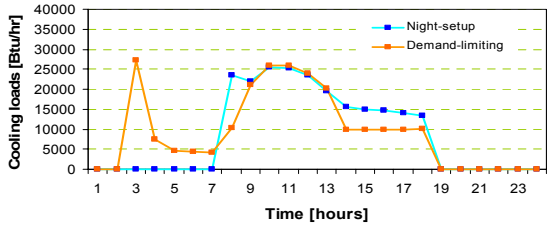
(d) DL start-time: 10am



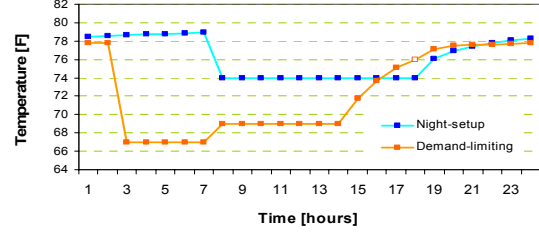
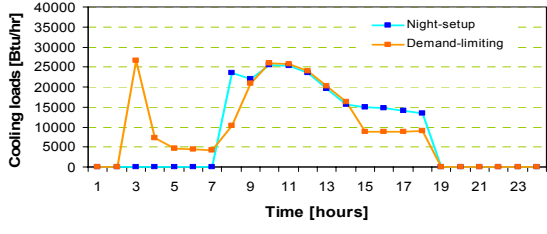
(e) DL start-time: 11am



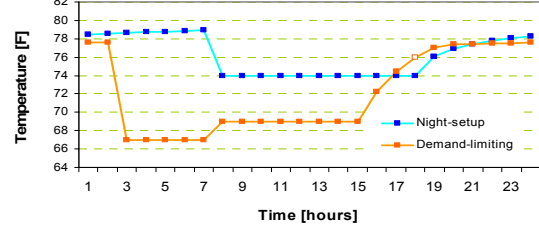
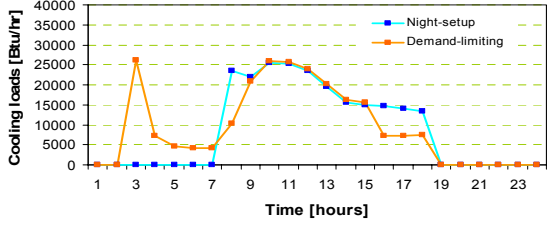
(f) DL start-time: noon



(g) DL start-time: 1pm

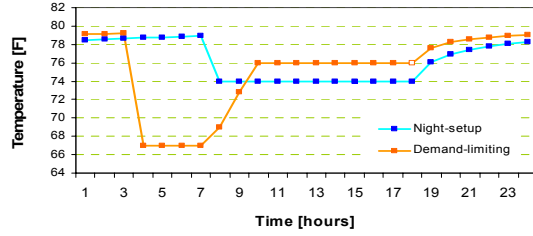
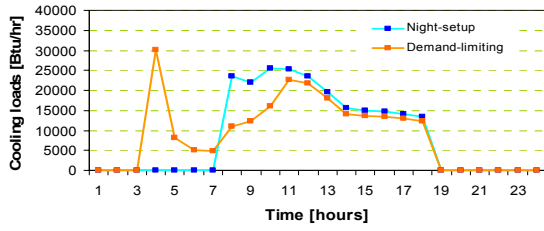


(h) DL start-time: 2pm

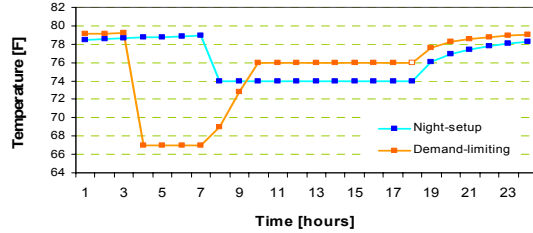
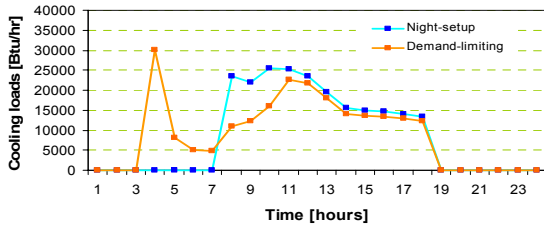


(i) DL start-time: 3pm

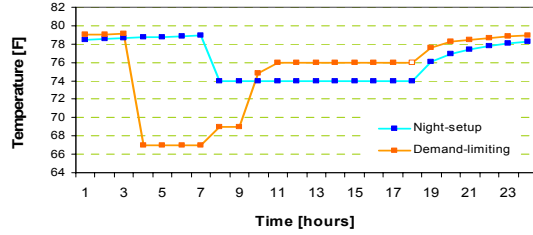
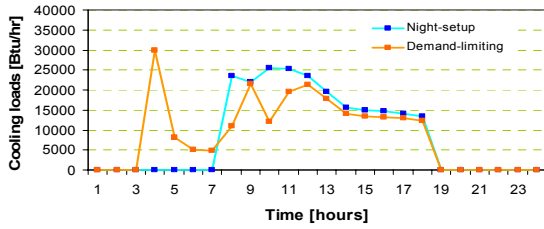
-Test zones: East zones
 -67°F PC start-time: 3 am



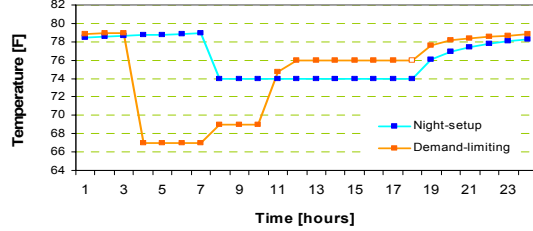
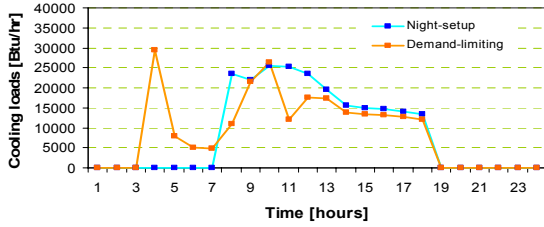
(a) DL start-time: 7am



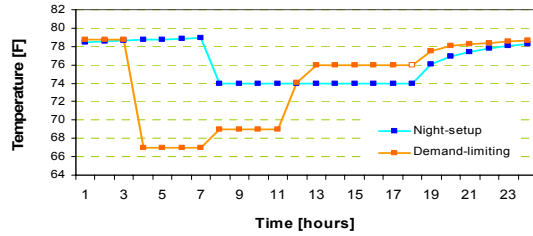
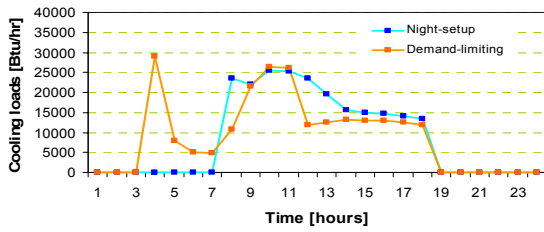
(b) DL start-time: 8am



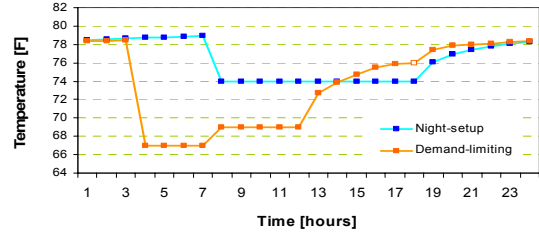
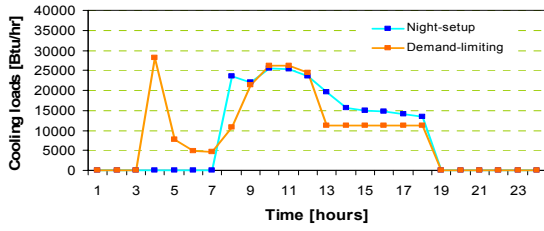
(c) DL start-time: 9am



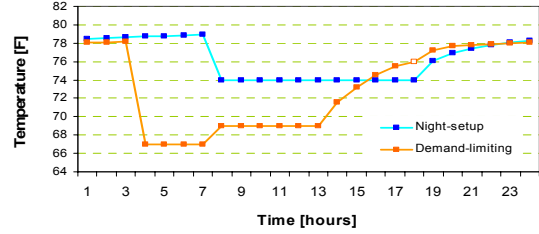
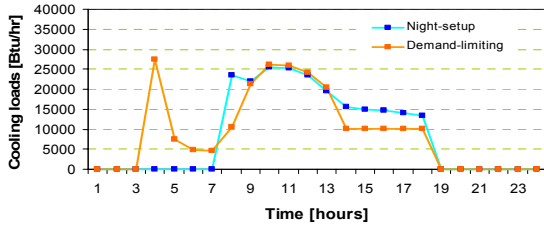
(d) DL start-time: 10am



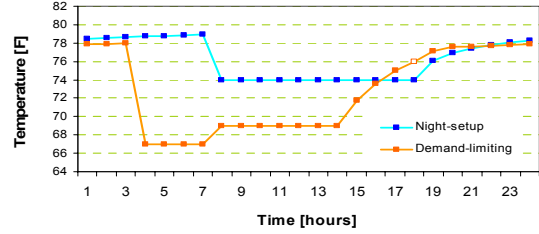
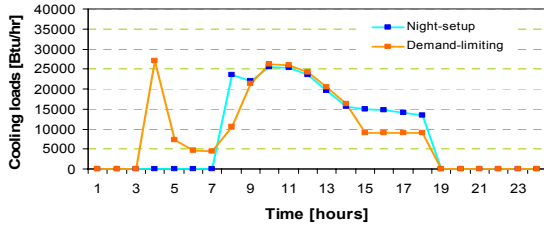
(e) DL start-time: 11am



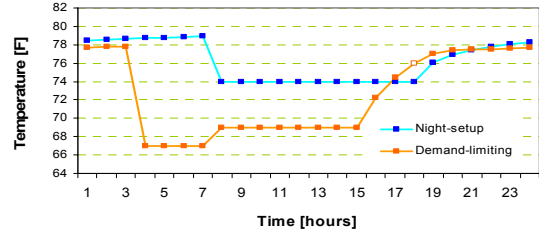
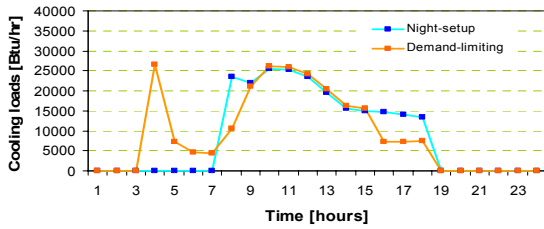
(f) DL start-time: noon



(g) DL start-time: 1pm

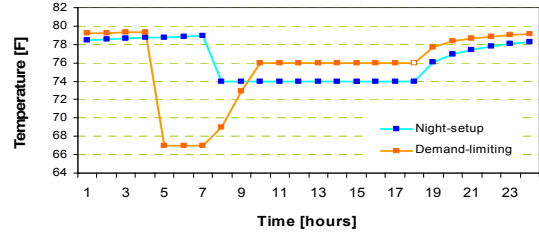
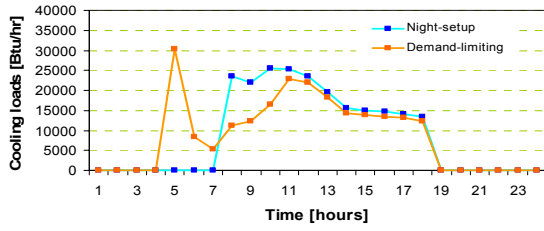


(h) DL start-time: 2pm

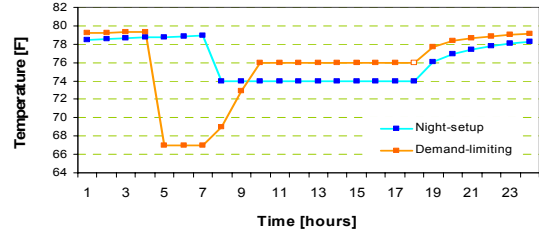
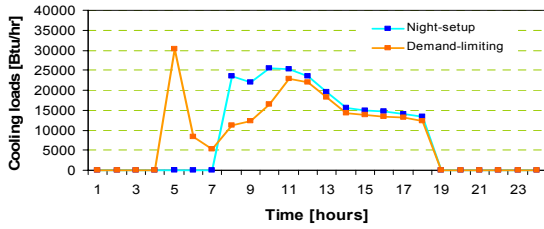


(i) DL start-time: 3pm

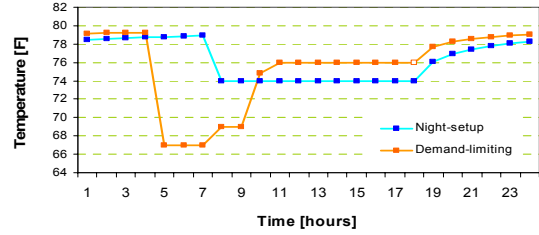
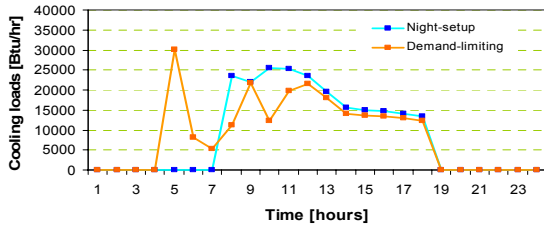
-Test zones: East zones
 -67°F PC start-time: 4 am



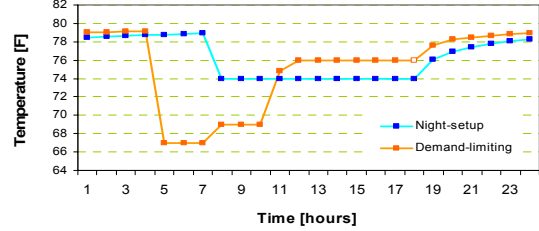
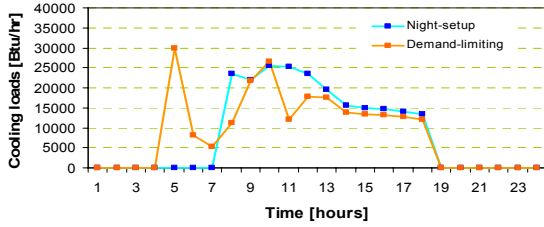
(a) DL start-time: 7am



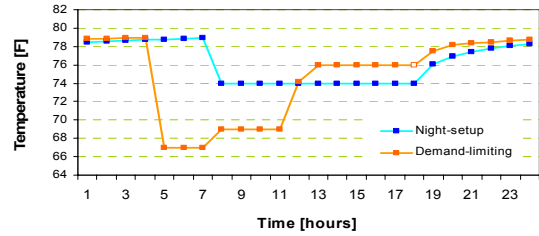
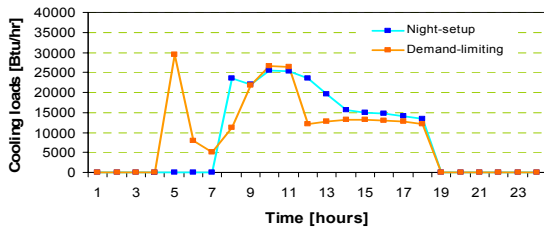
(b) DL start-time: 8am



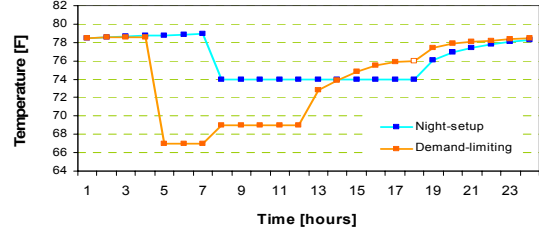
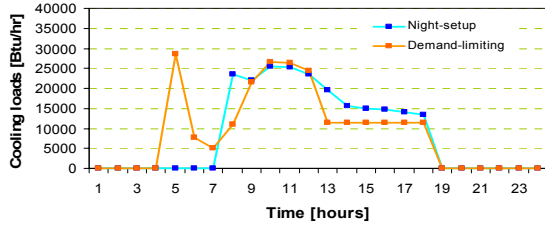
(c) DL start-time: 9am



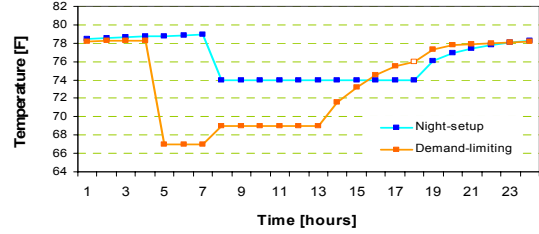
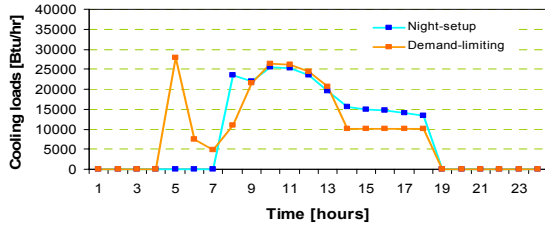
(d) DL start-time: 10am



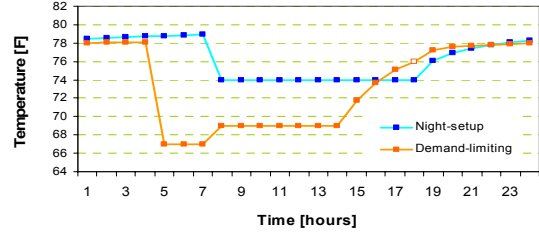
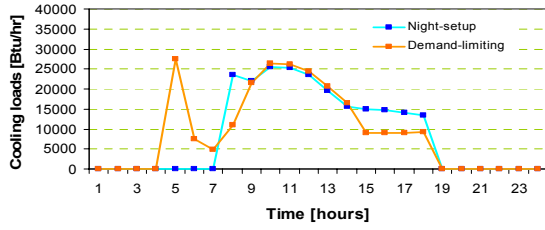
(e) DL start-time: 11am



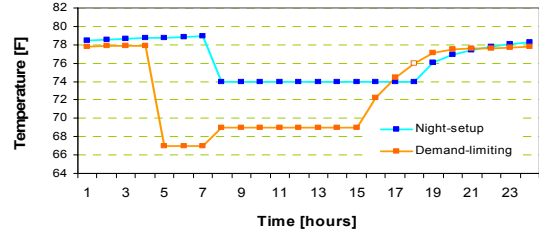
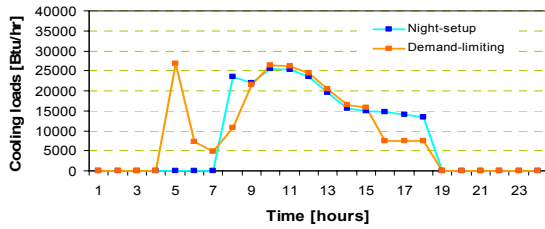
(f) DL start-time: noon



(g) DL start-time: 1pm

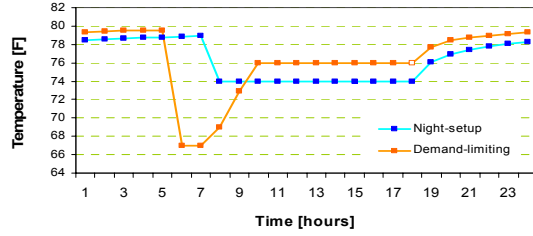
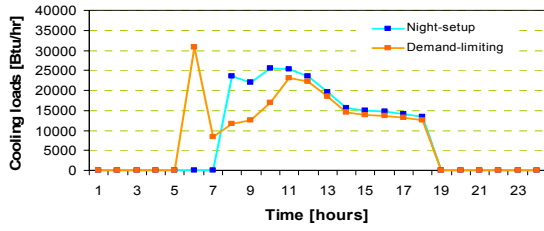


(h) DL start-time: 2pm

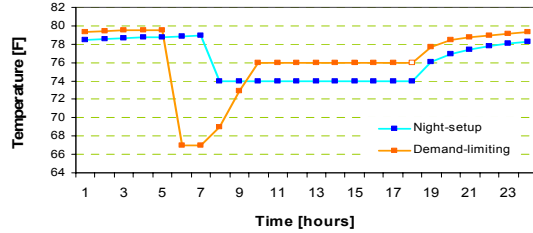
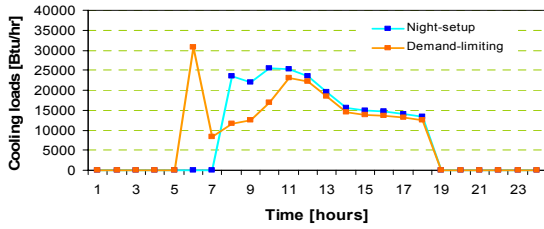


(i) DL start-time: 3pm

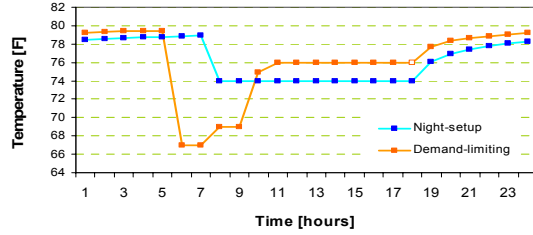
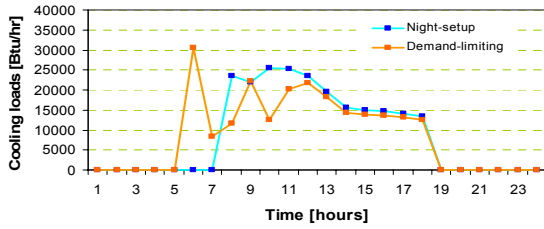
-Test zones: East zones
 -67°F PC start-time: 5 am



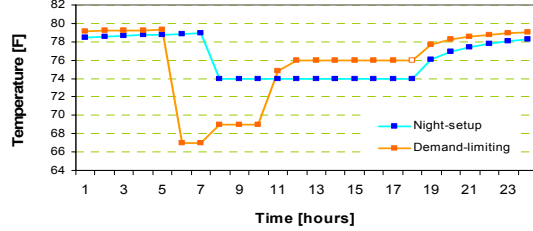
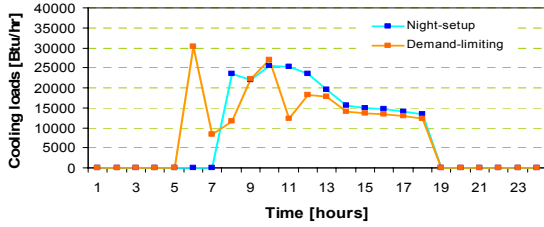
(a) DL start-time: 7am



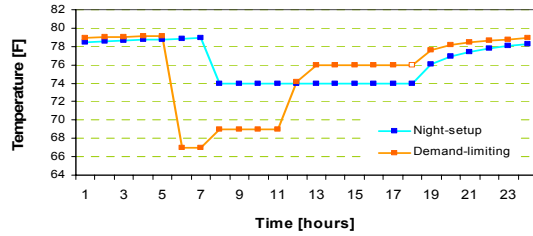
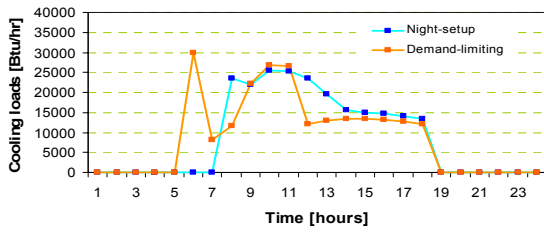
(b) DL start-time: 8am



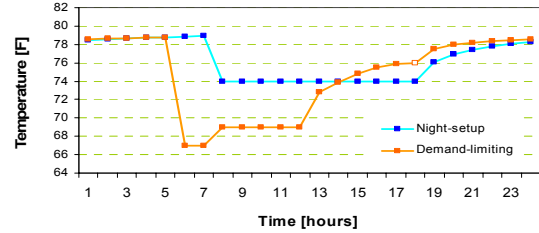
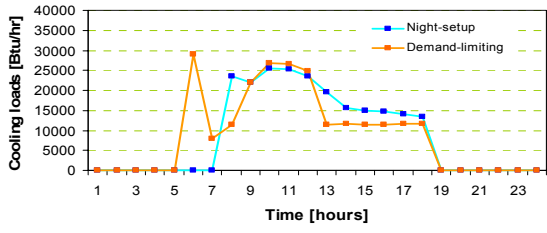
(c) DL start-time: 9am



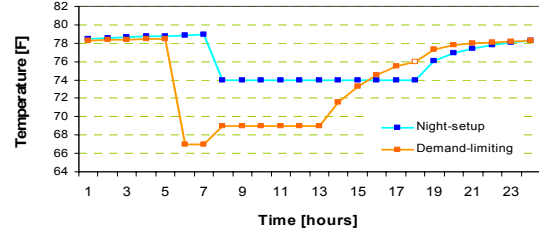
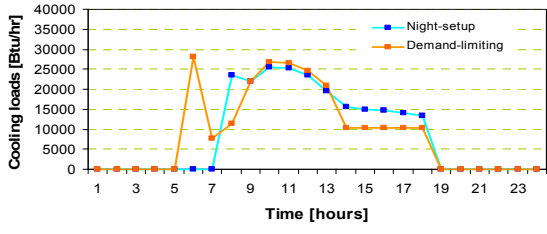
(d) DL start-time: 10am



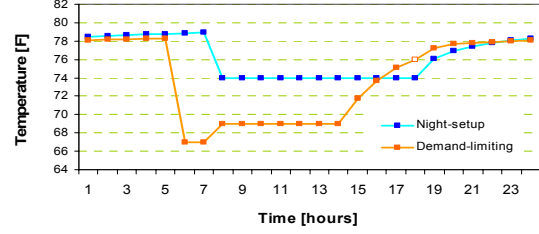
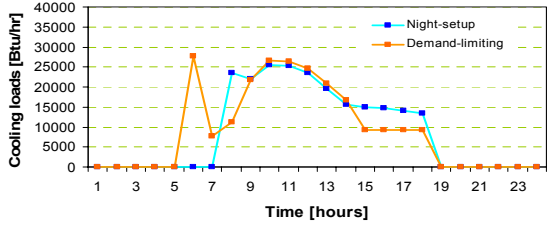
(e) DL start-time: 11am



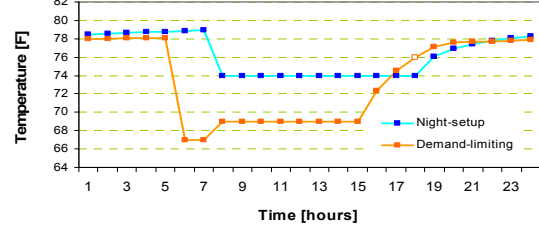
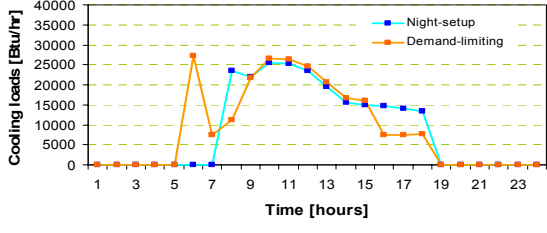
(f) DL start-time: noon



(g) DL start-time: 1pm

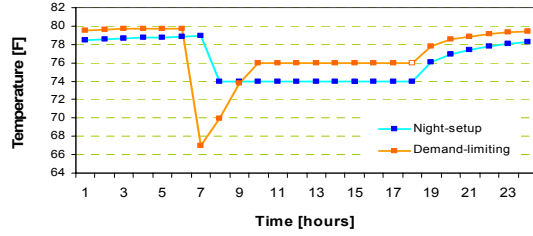
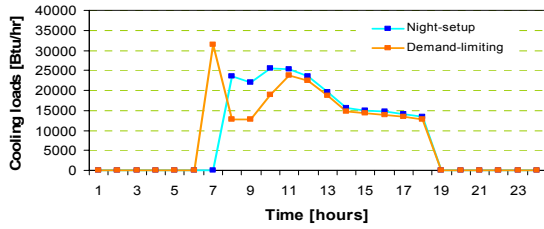


(h) DL start-time: 2pm

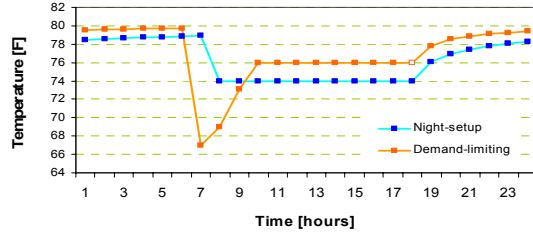
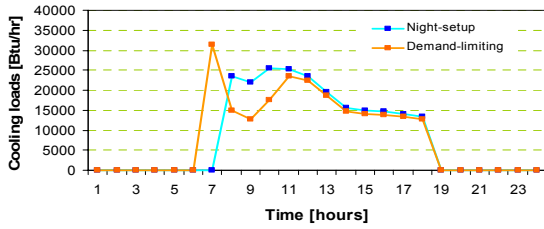


(i) DL start-time: 3pm

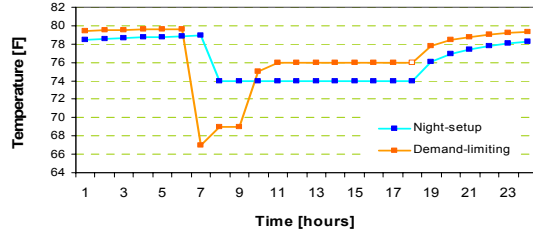
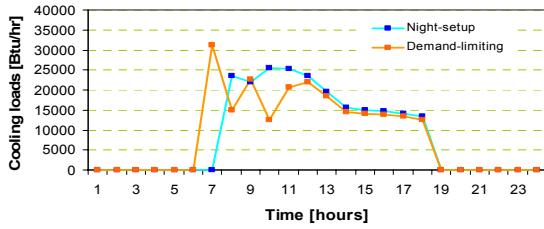
-Test zones: East zones
 -67°F PC start-time: 6 am



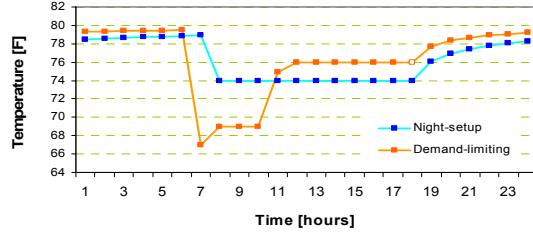
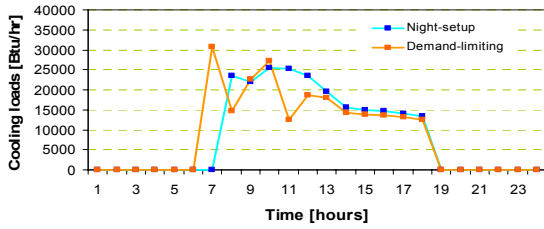
(a) DL start-time: 7am



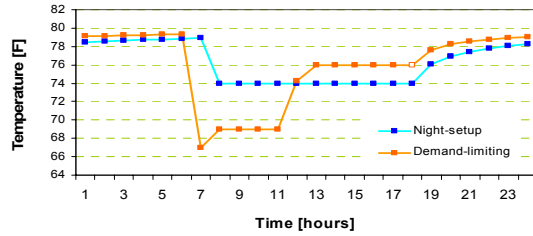
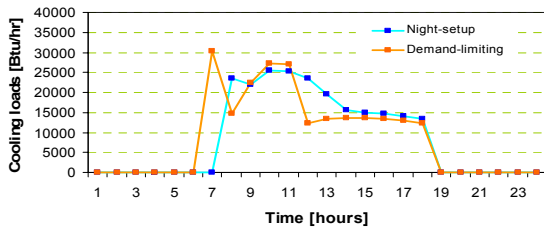
(b) DL start-time: 8am



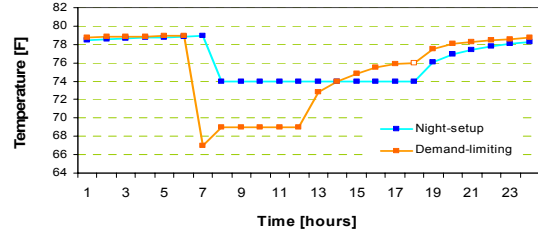
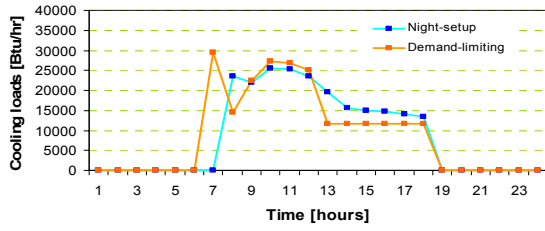
(c) DL start-time: 9am



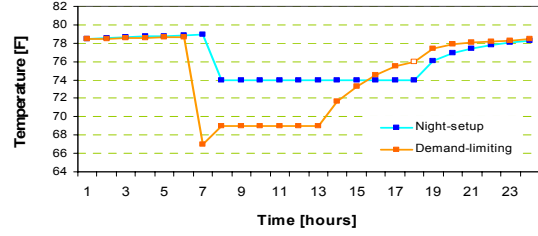
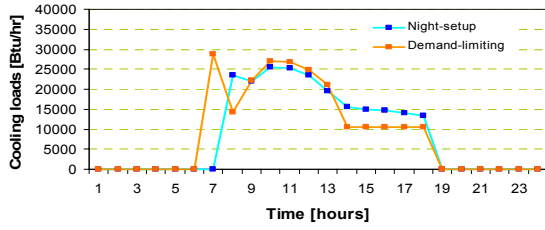
(d) DL start-time: 10am



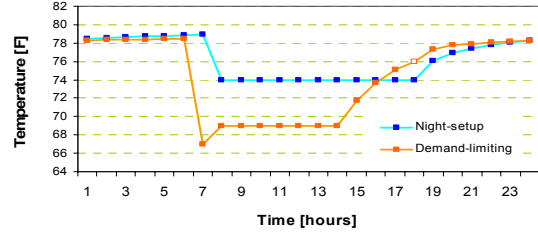
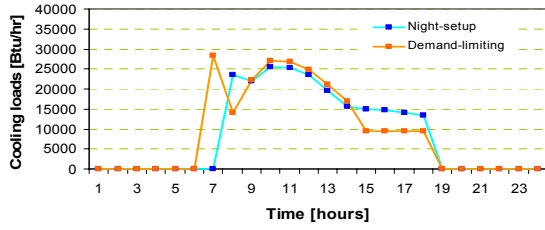
(e) DL start-time: 11am



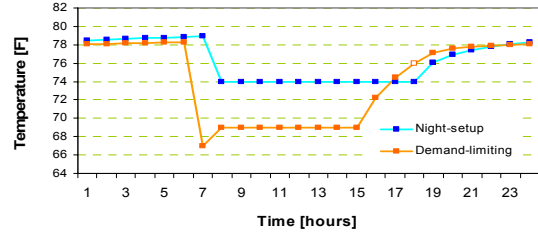
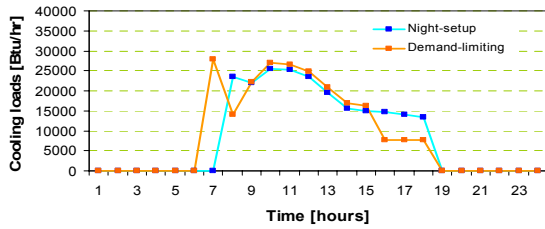
(f) DL start-time: noon



(g) DL start-time: 1pm

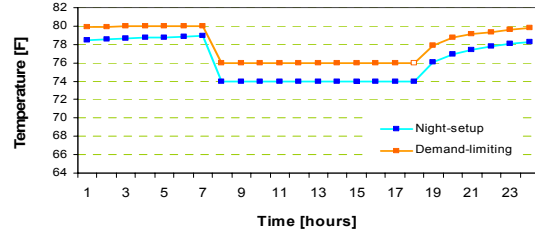
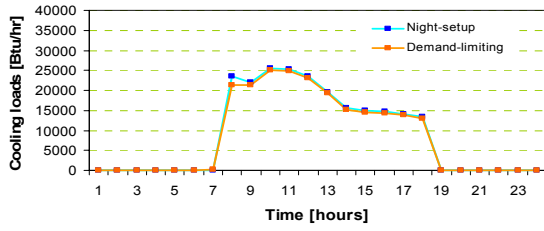


(h) DL start-time: 2pm

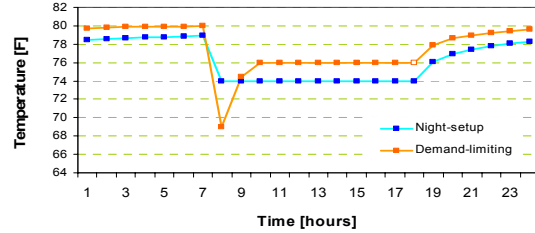
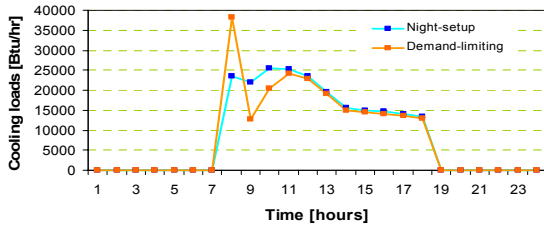


(i) DL start-time: 3pm

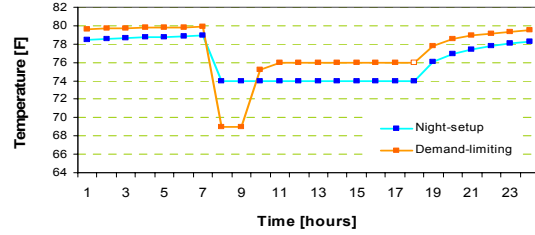
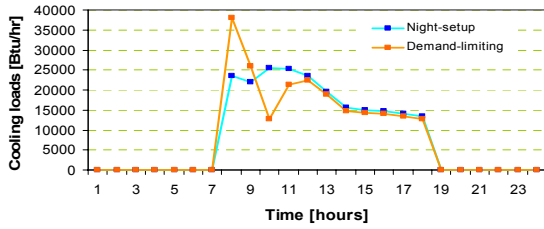
-Test zones: East zones
 -67°F PC start-time: 7 am



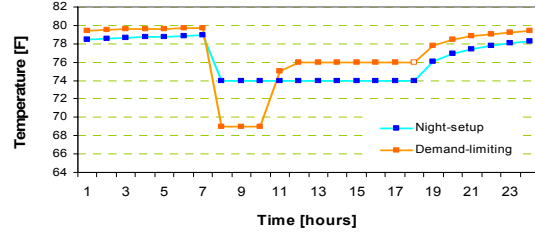
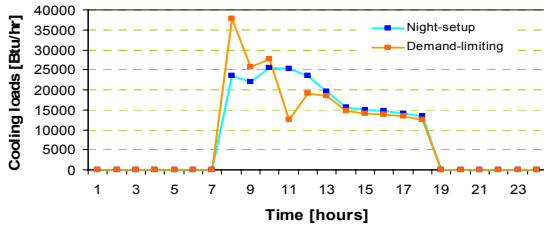
(a) DL start-time: 7am



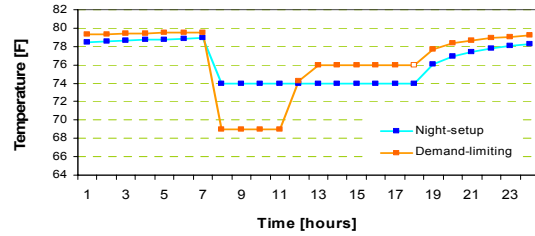
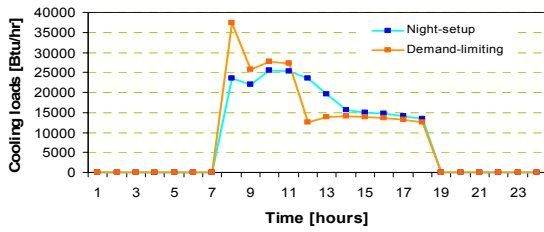
(b) DL start-time: 8am



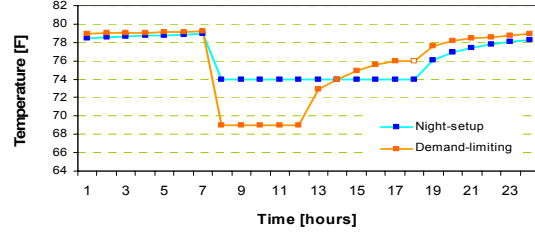
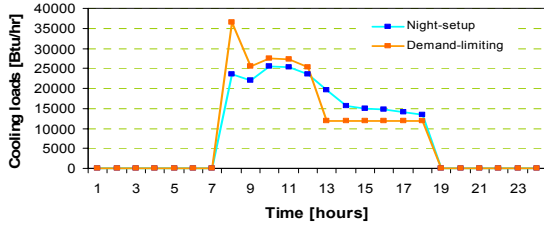
(c) DL start-time: 9am



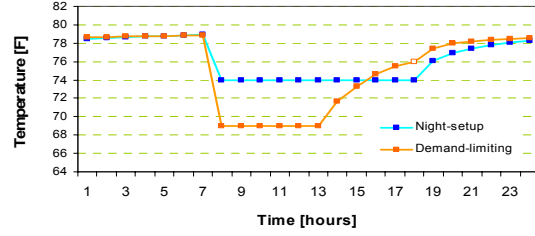
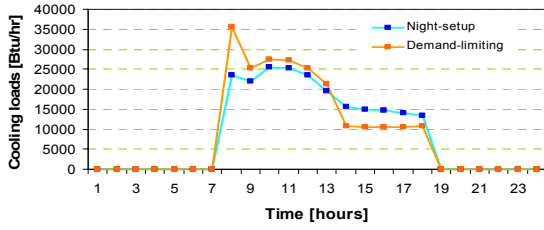
(d) DL start-time: 10am



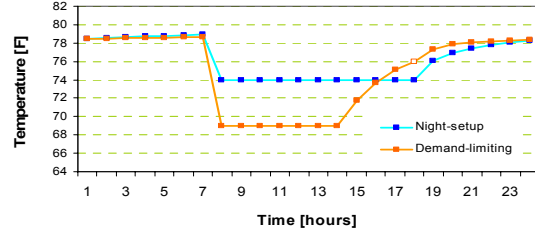
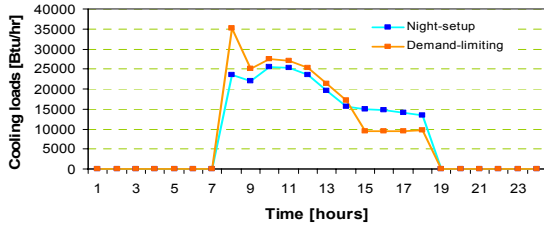
(e) DL start-time: 11am



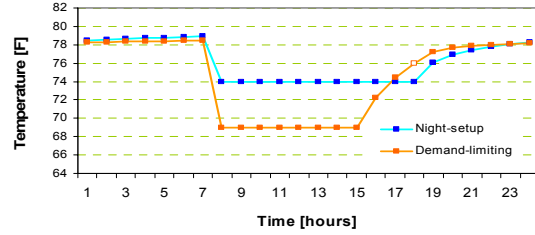
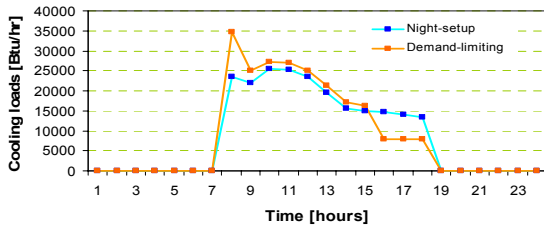
(f) DL start-time: noon



(g) DL start-time: 1pm



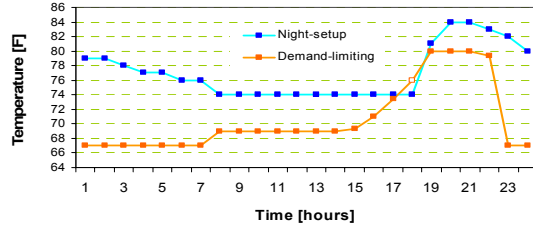
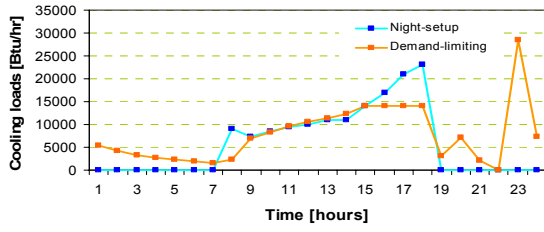
(h) DL start-time: 2pm



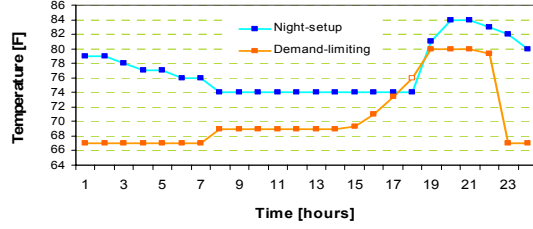
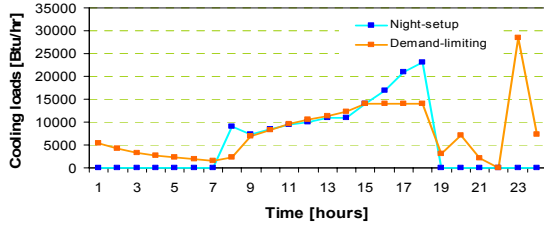
(i) DL start-time: 3pm

3. West zones

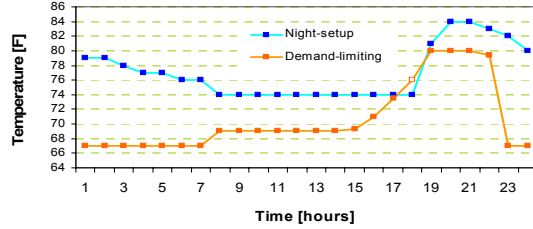
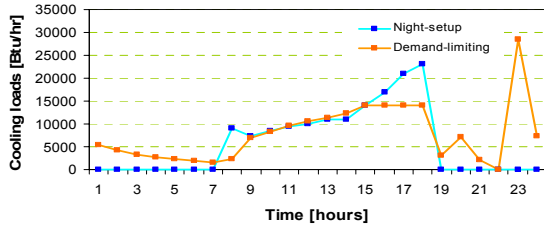
-Test zones: Weast zones
 -67°F PC start-time: 10 pm



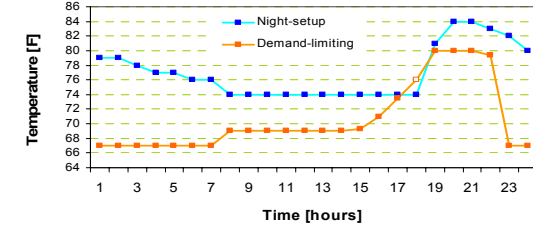
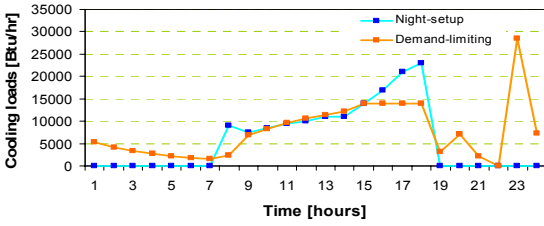
(a) DL start-time: 7am



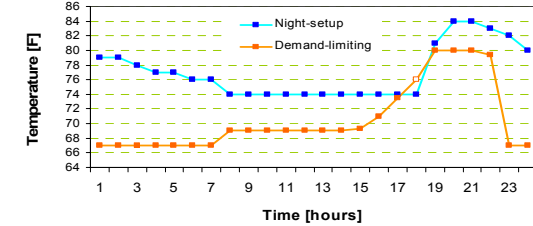
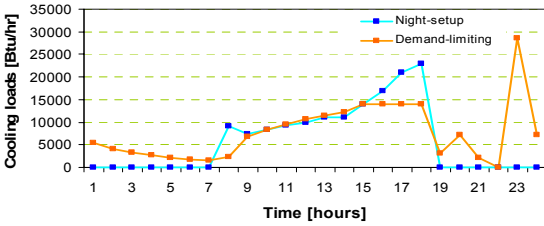
(b) DL start-time: 8am



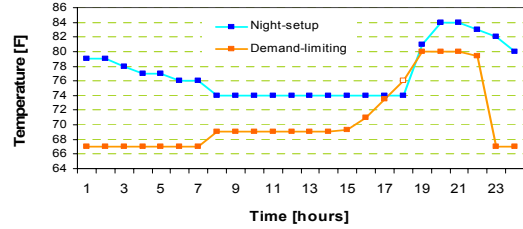
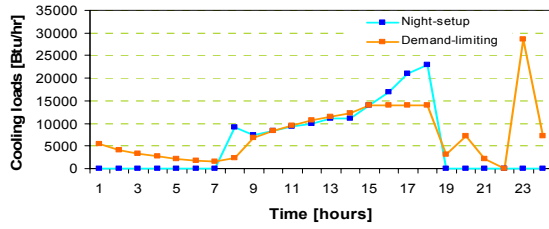
(c) DL start-time: 9am



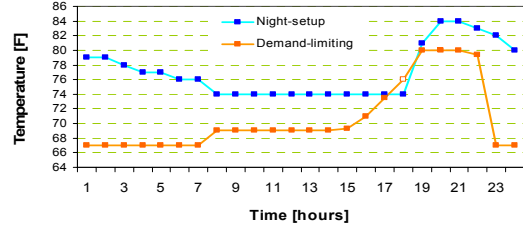
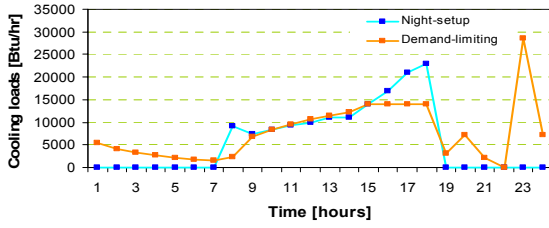
(d) DL start-time: 10am



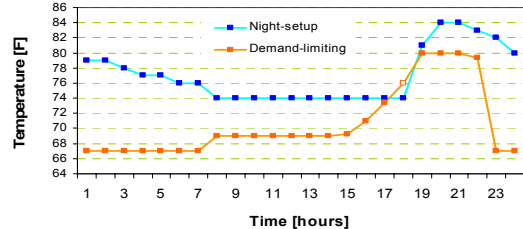
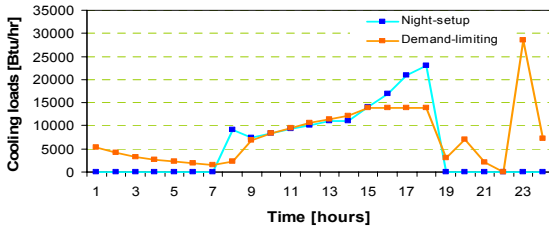
(e) DL start-time: 11am



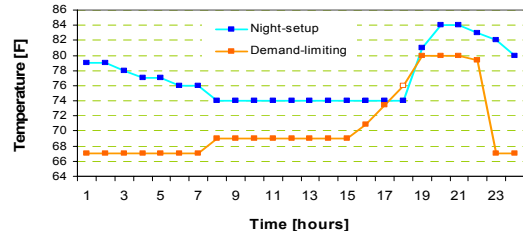
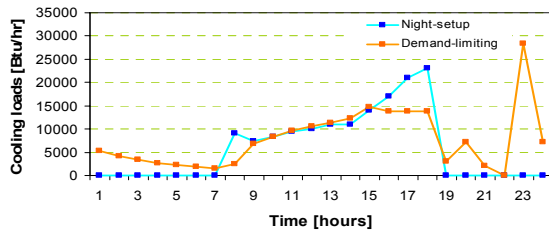
(f) DL start-time: noon



(g) DL start-time: 1pm

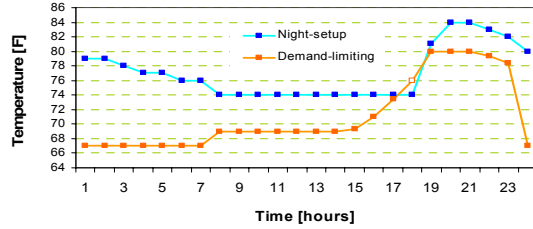
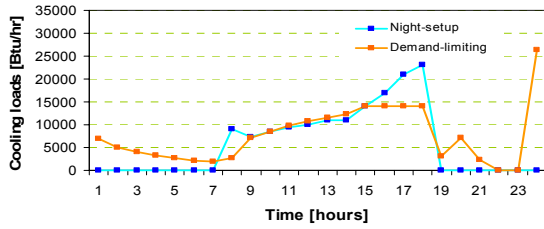


(h) DL start-time: 2pm

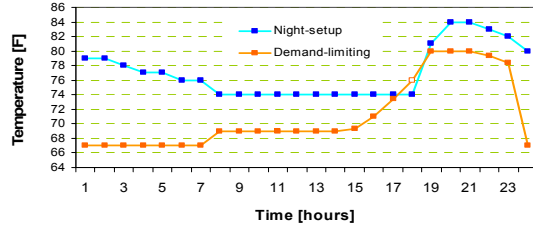
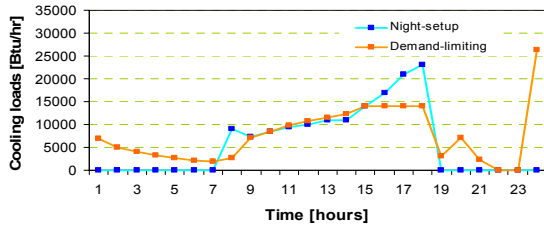


(i) DL start-time: 3pm

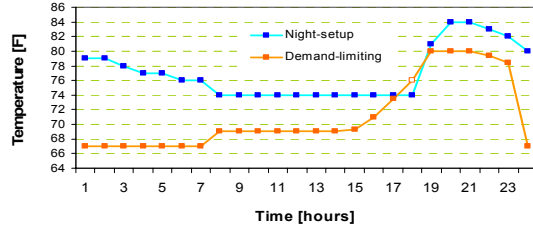
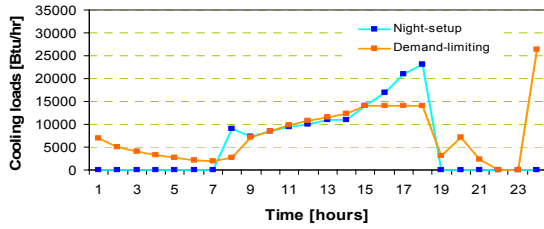
-Test zones: West zones
 -67°F PC start-time: 11 pm



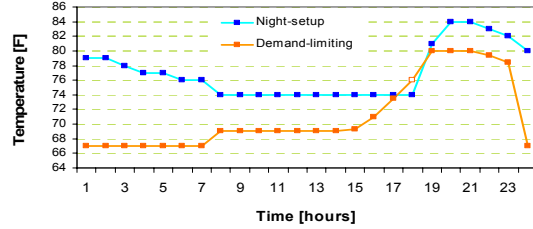
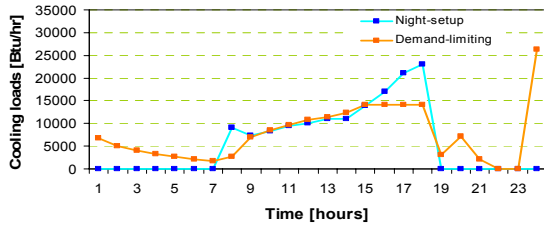
(a) DL start-time: 7am



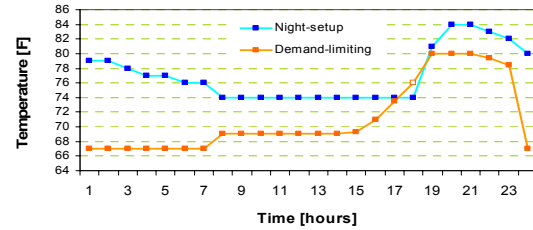
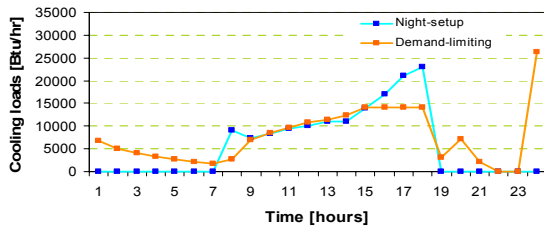
(b) DL start-time: 8am



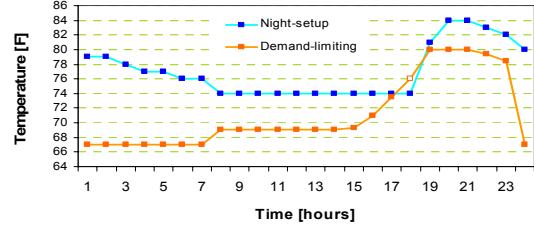
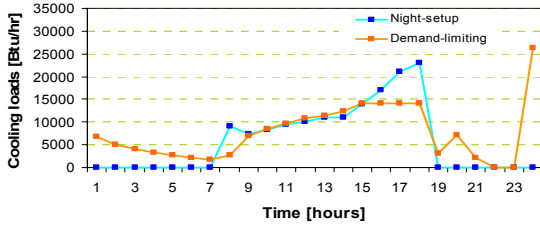
(c) DL start-time: 9am



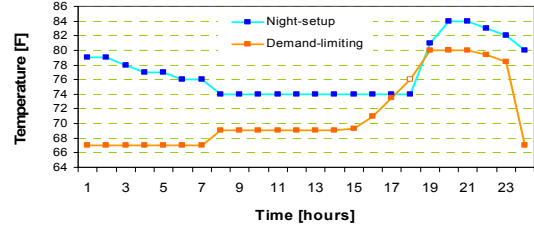
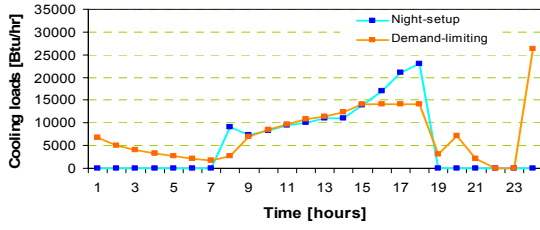
(d) DL start-time: 10am



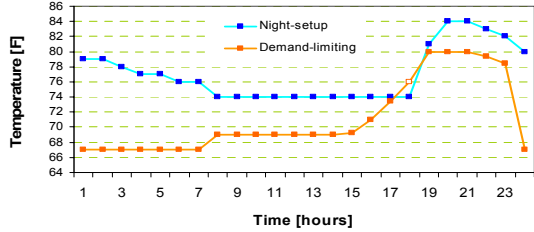
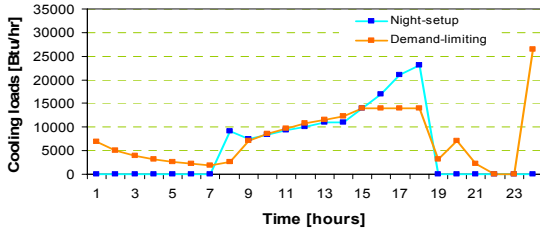
(e) DL start-time: 11am



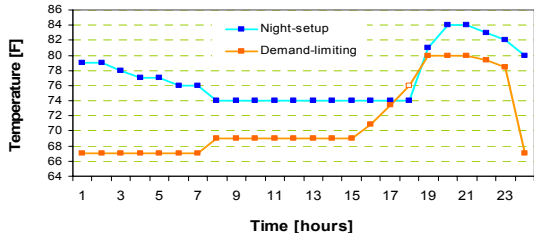
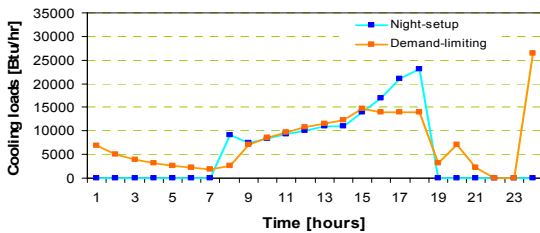
(f) DL start-time: noon



(g) DL start-time: 1pm

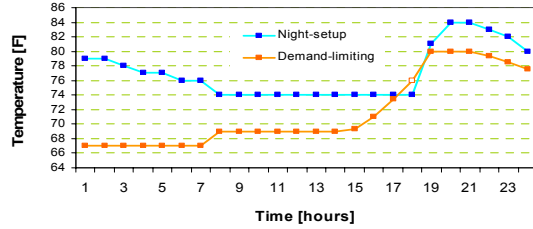
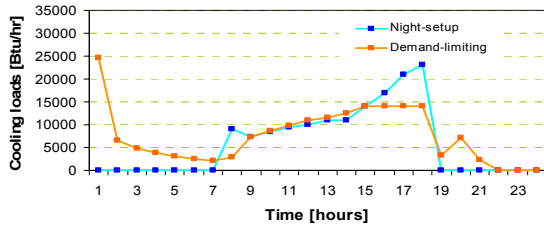


(h) DL start-time: 2pm

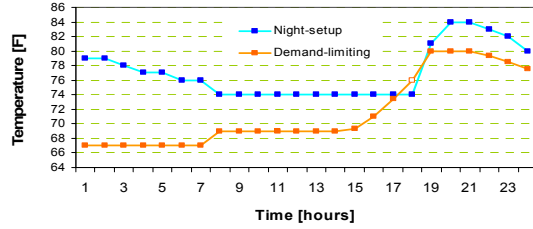
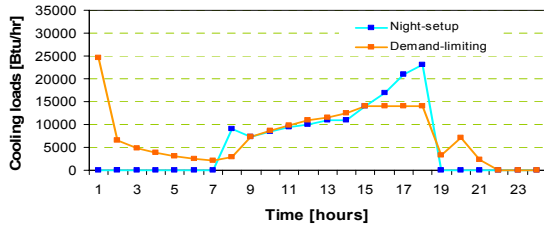


(i) DL start-time: 3pm

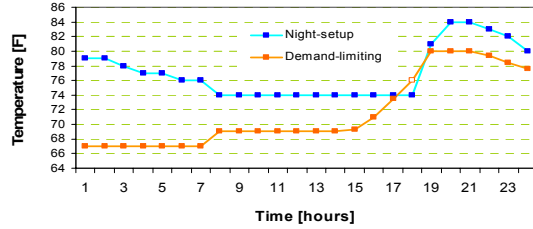
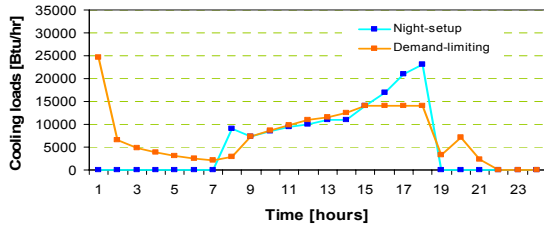
-Test zones: West zones
 -67°F PC start-time: midnight



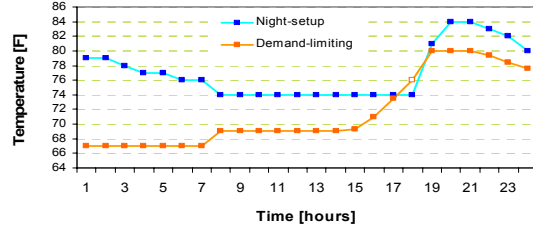
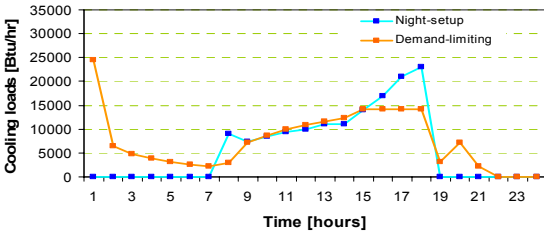
(a) DL start-time: 7am



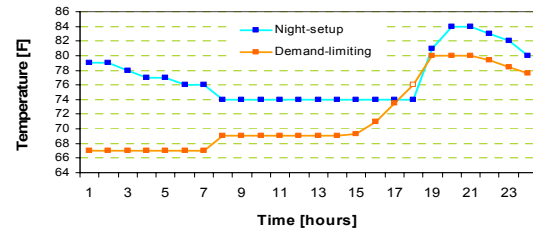
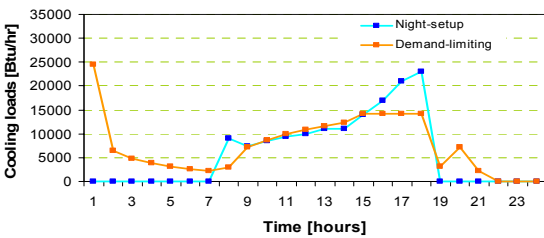
(b) DL start-time: 8am



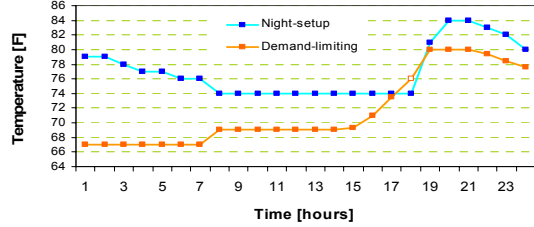
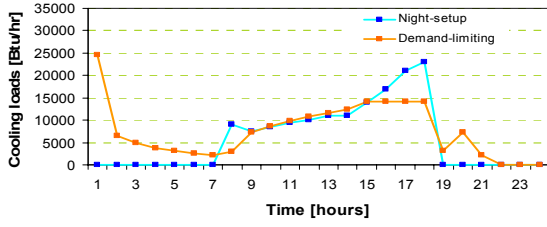
(c) DL start-time: 9am



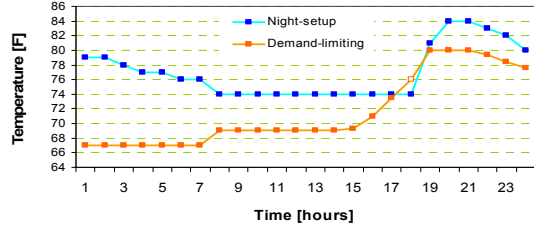
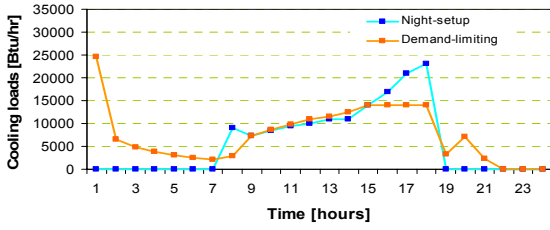
(d) DL start-time: 10am



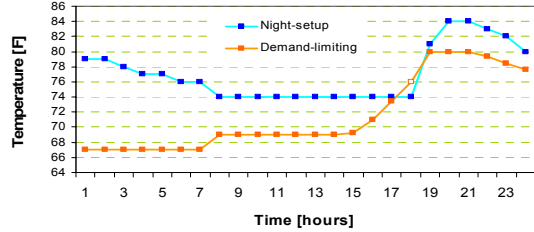
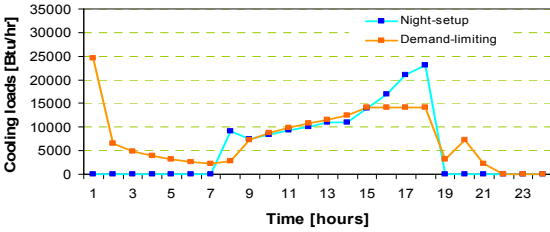
(e) DL start-time: 11am



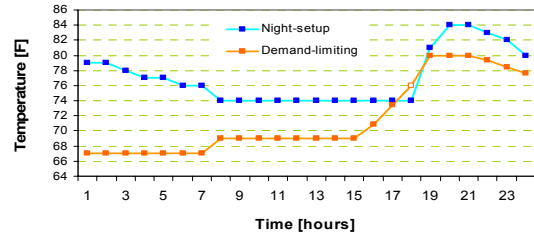
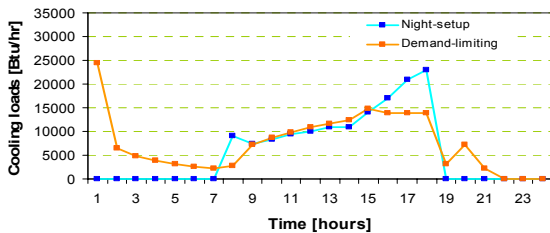
(f) DL start-time: noon



(g) DL start-time: 1pm

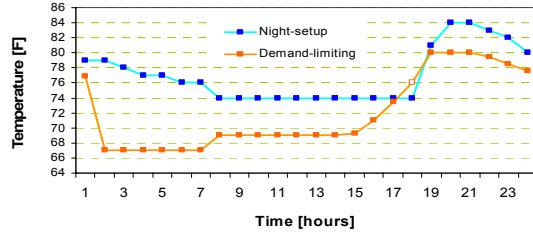
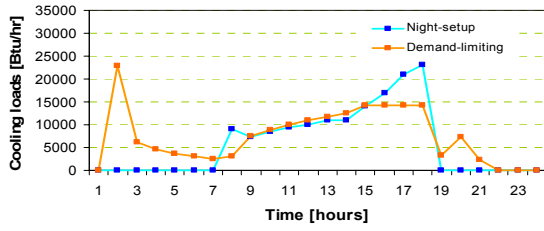


(h) DL start-time: 2pm

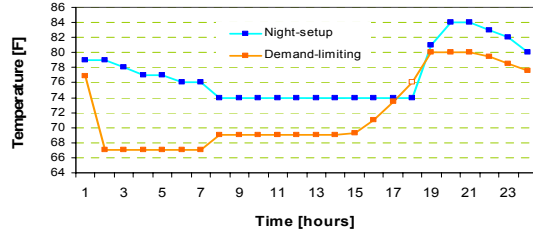
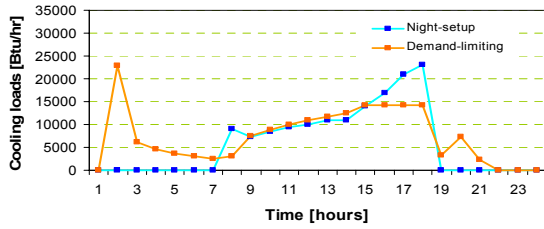


(i) DL start-time: 3pm

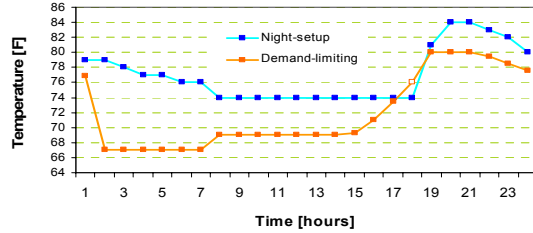
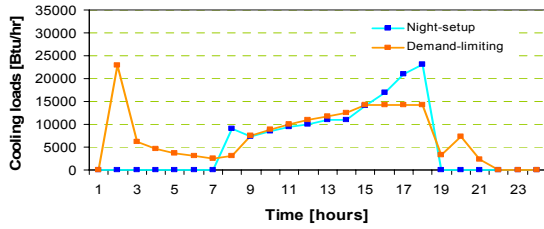
-Test zones: Weast zones
 -67°F PC start-time: 1 am



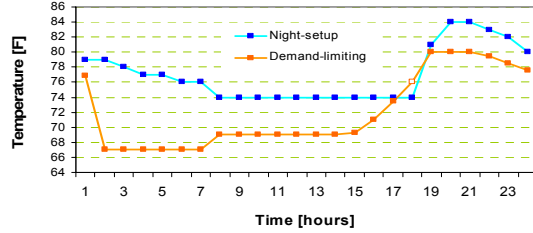
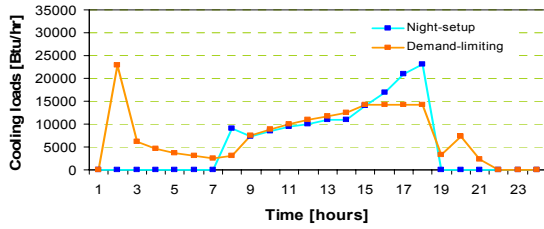
(a) DL start-time: 7am



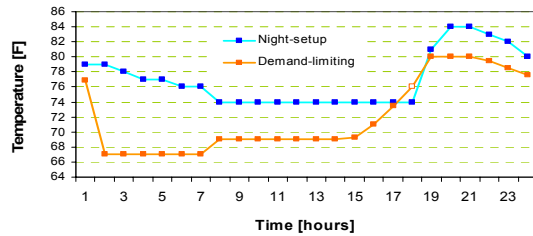
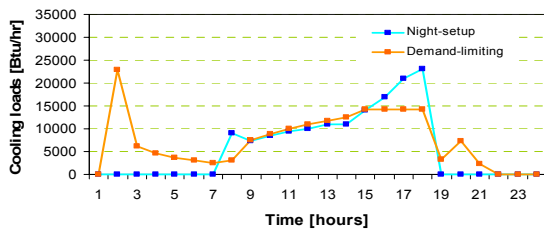
(b) DL start-time: 8am



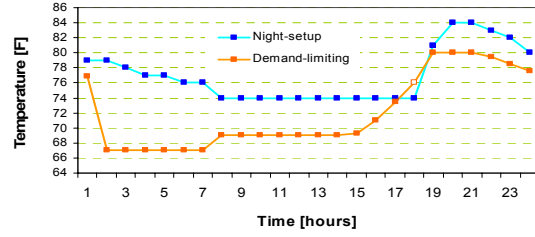
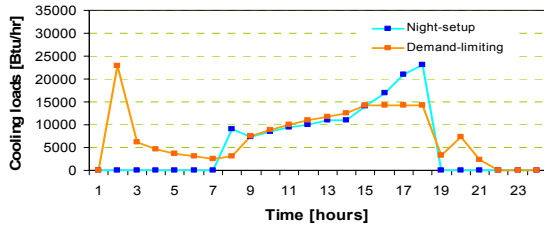
(c) DL start-time: 9am



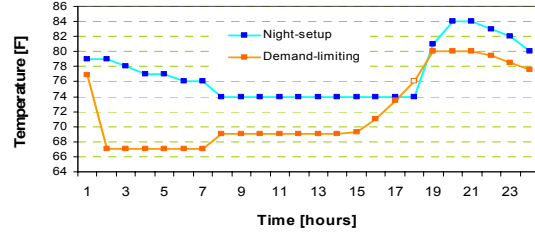
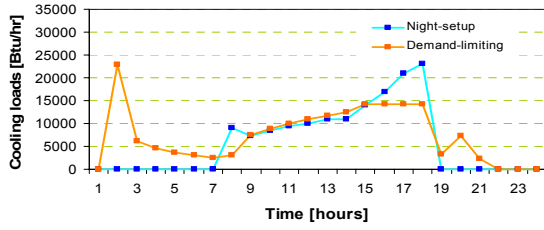
(d) DL start-time: 10am



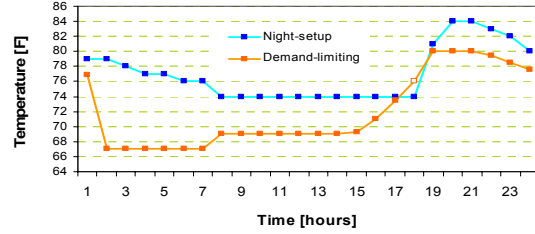
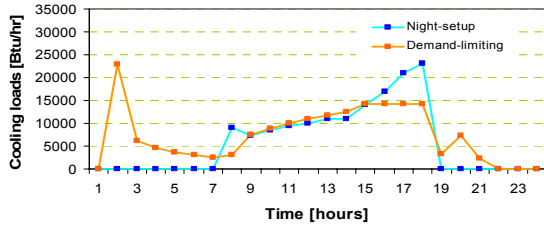
(e) DL start-time: 11am



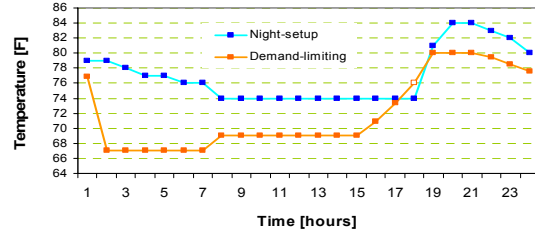
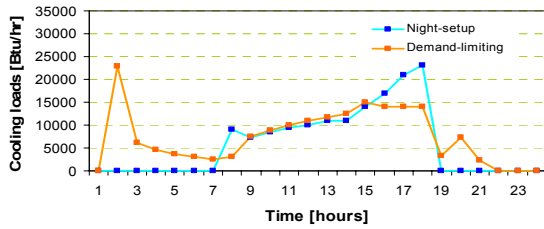
(f) DL start-time: noon



(g) DL start-time: 1pm

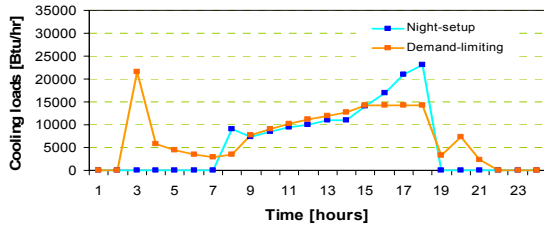


(h) DL start-time: 2pm

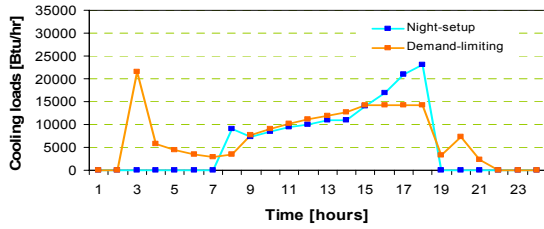
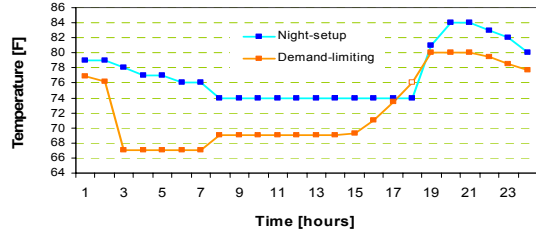


(i) DL start-time: 3pm

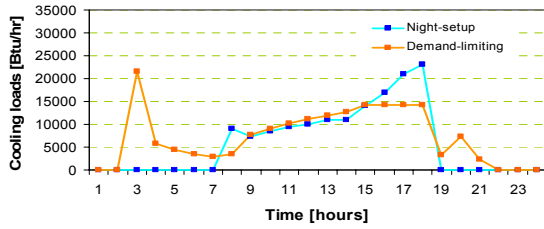
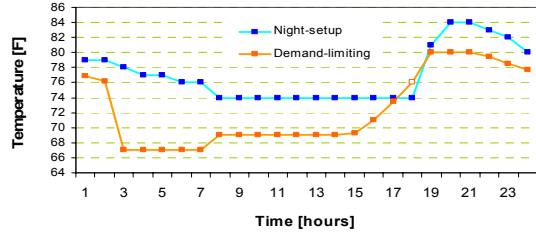
-Test zones: Weast zones
 -67°F PC start-time: 2 am



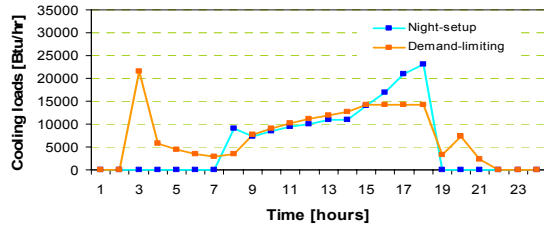
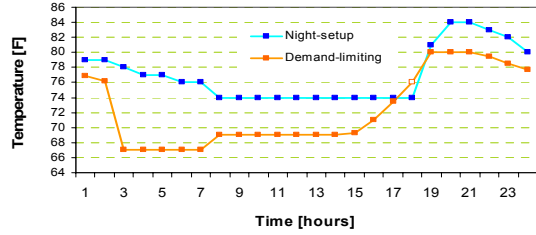
(a) DL start-time: 7am



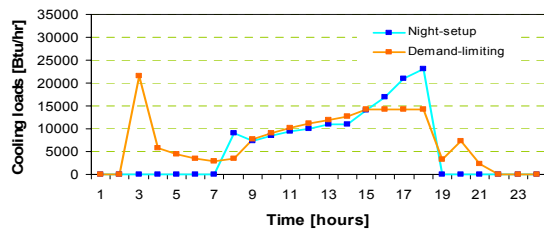
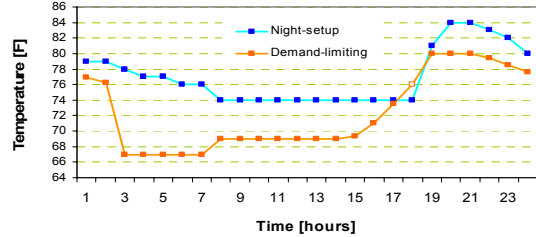
(b) DL start-time: 8am



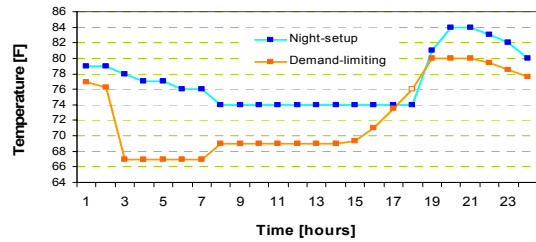
(c) DL start-time: 9am

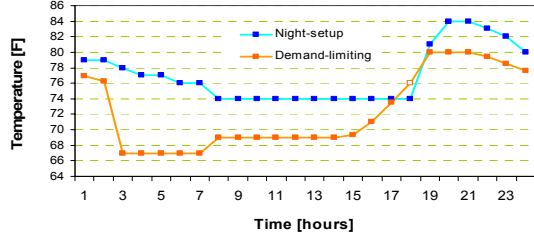
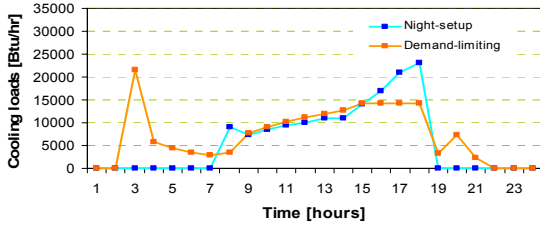


(d) DL start-time: 10am

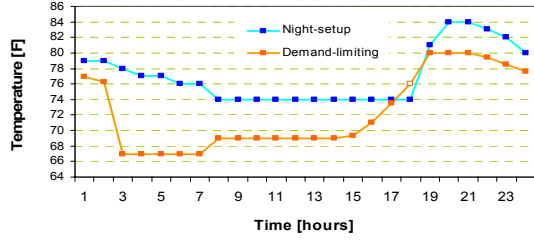
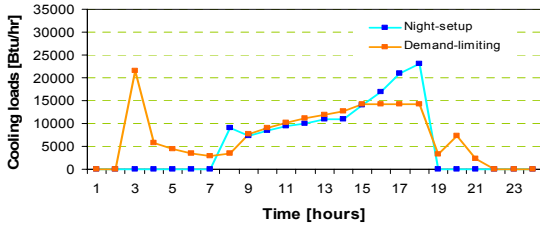


(e) DL start-time: 11am

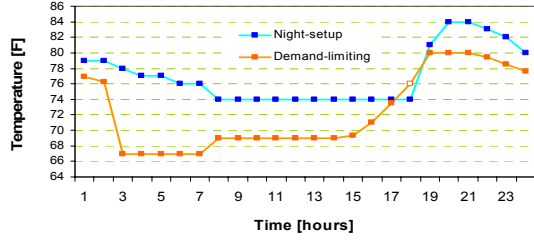
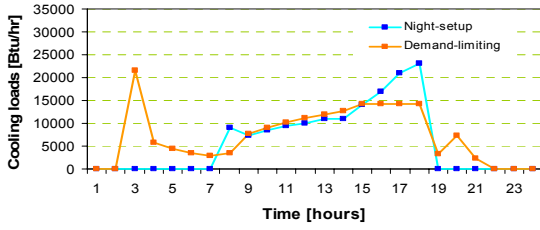




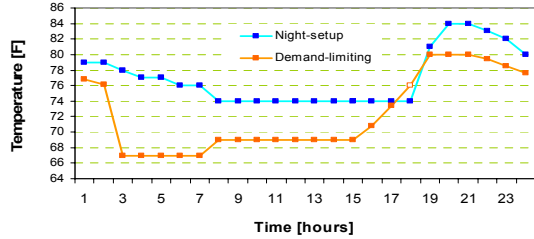
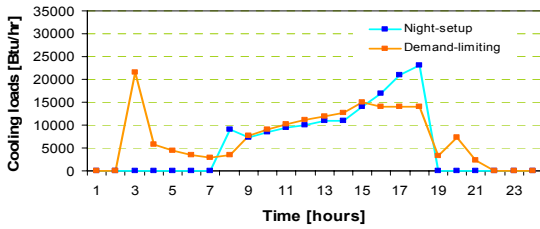
(f) DL start-time: noon



(g) DL start-time: 1pm

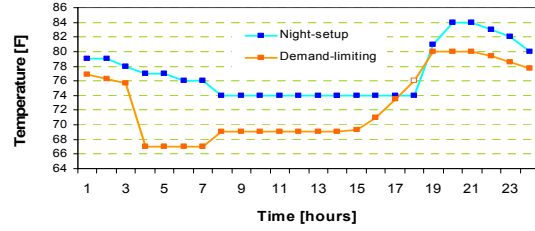
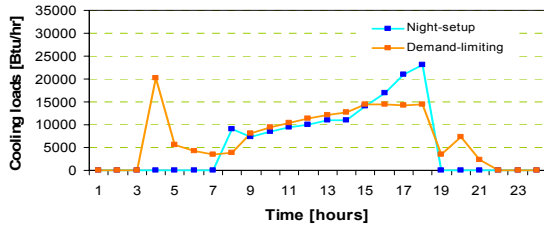


(h) DL start-time: 2pm

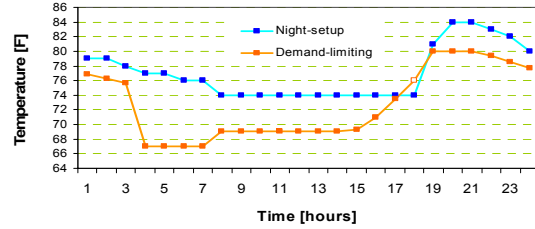
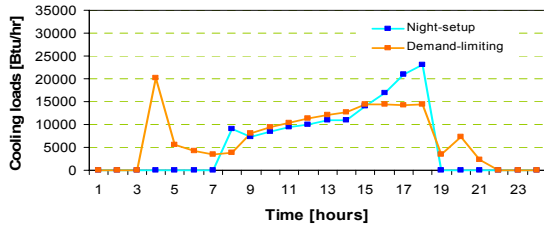


(i) DL start-time: 3pm

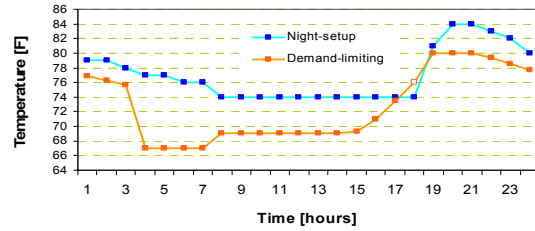
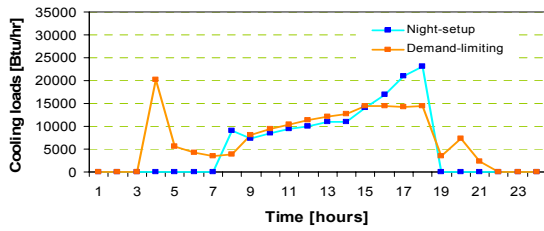
-Test zones: West zones
 -67°F PC start-time: 3 am



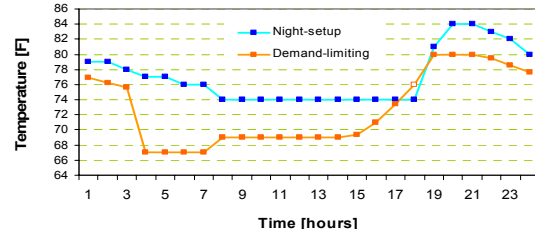
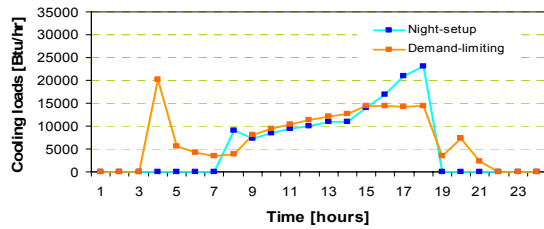
(a) DL start-time: 7am



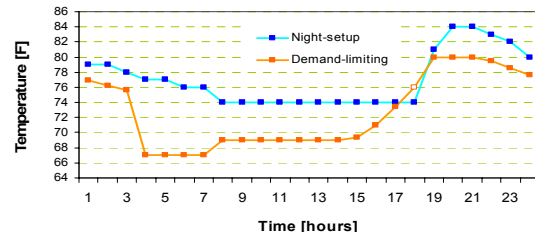
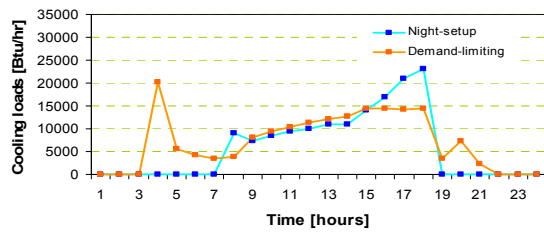
(b) DL start-time: 8am



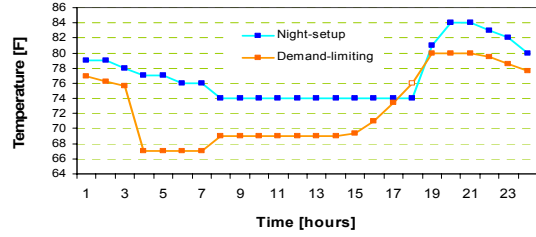
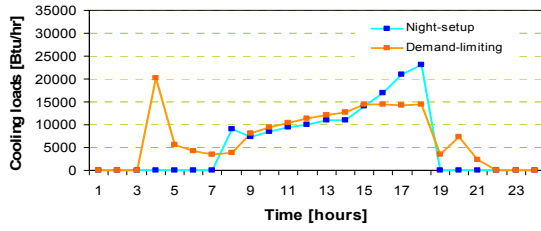
(c) DL start-time: 9am



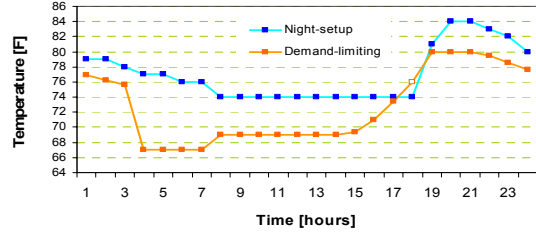
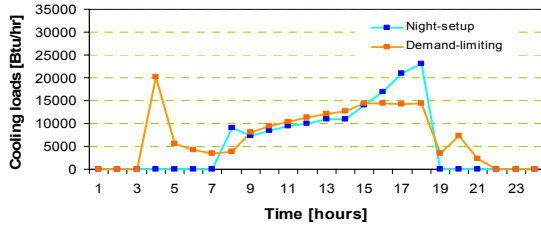
(d) DL start-time: 10am



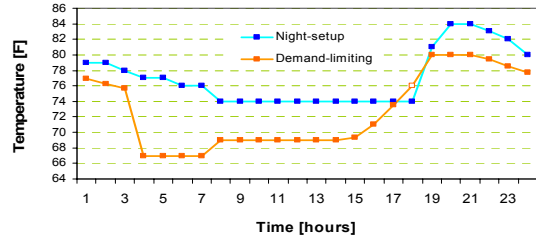
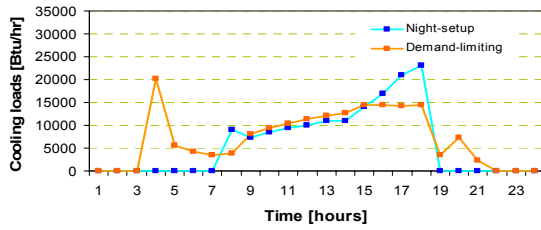
(e) DL start-time: 11am



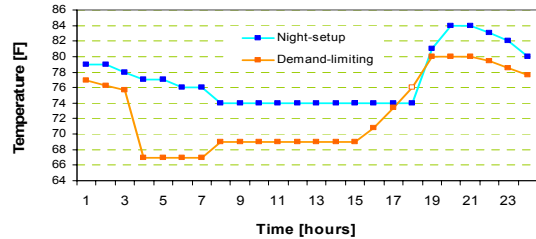
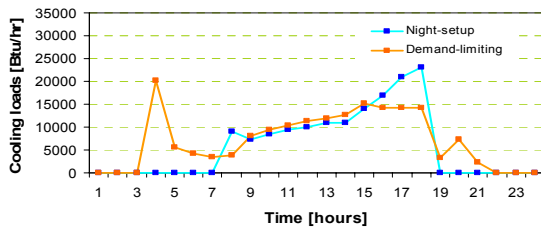
(f) DL start-time: noon



(g) DL start-time: 1pm

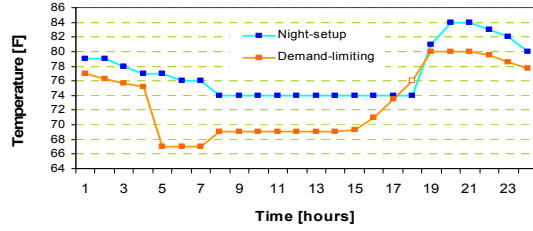
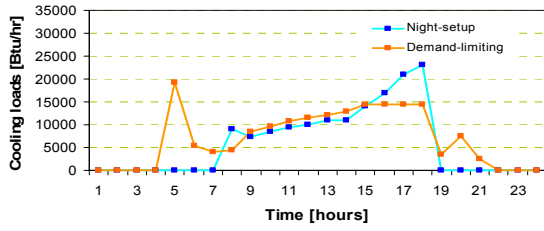


(h) DL start-time: 2pm

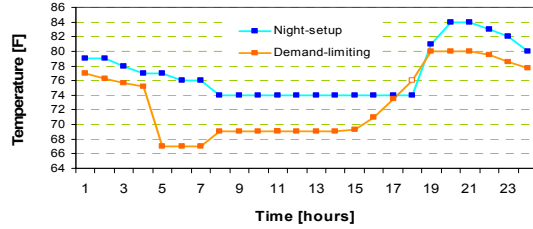
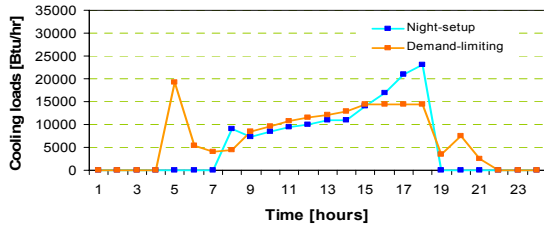


(i) DL start-time: 3pm

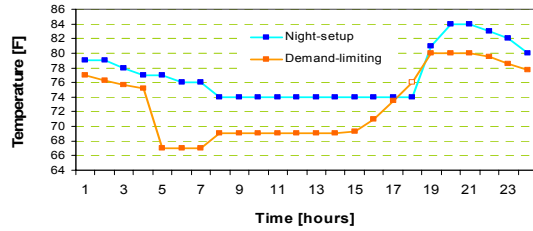
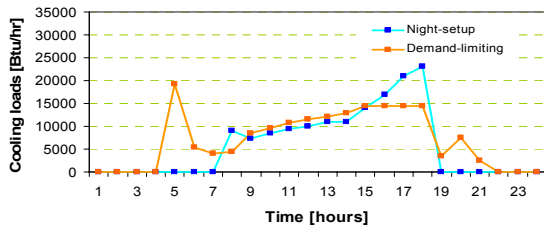
-Test zones: West zones
 -67°F PC start-time: 4 am



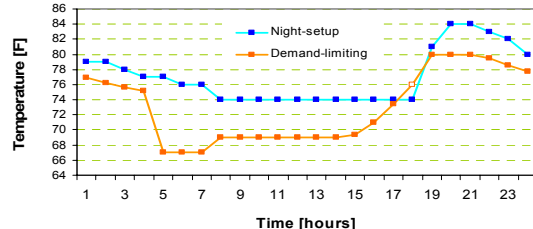
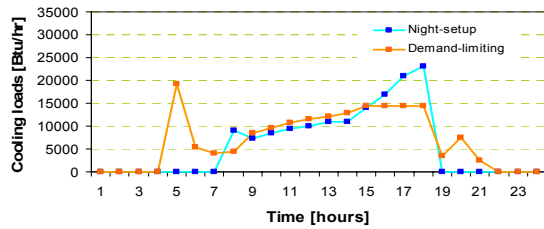
(a) DL start-time: 7am



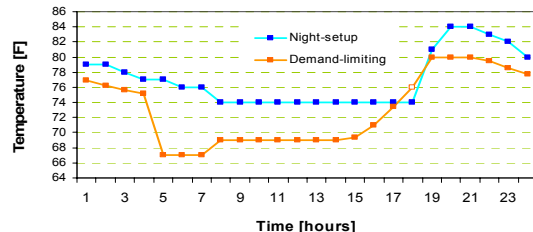
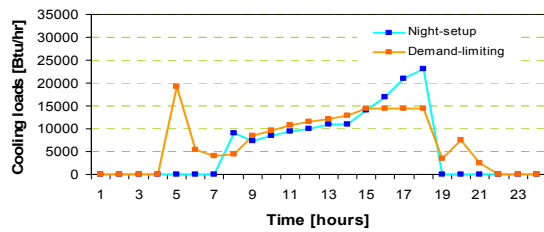
(b) DL start-time: 8am



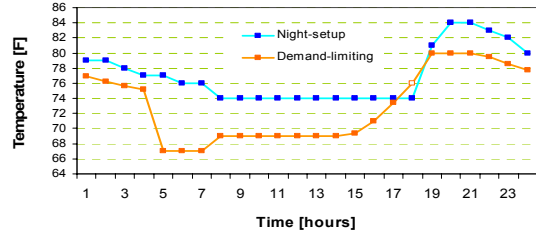
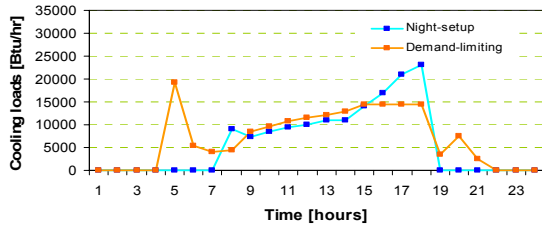
(c) DL start-time: 9am



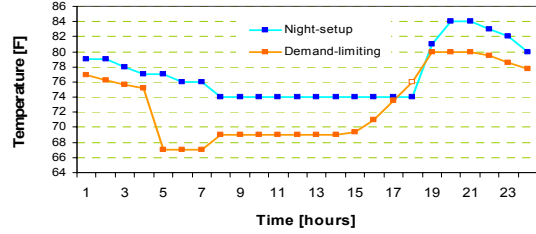
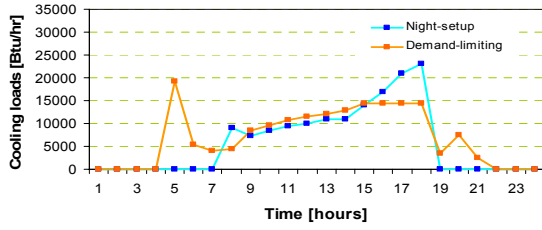
(d) DL start-time: 10am



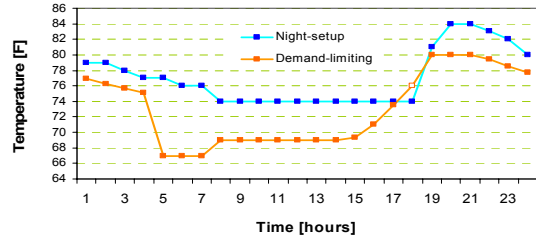
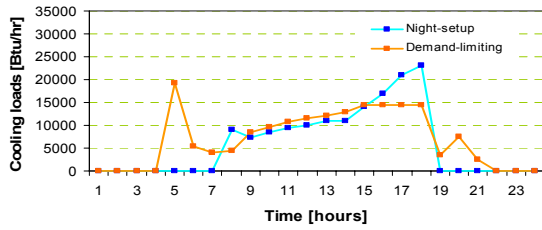
(e) DL start-time: 11am



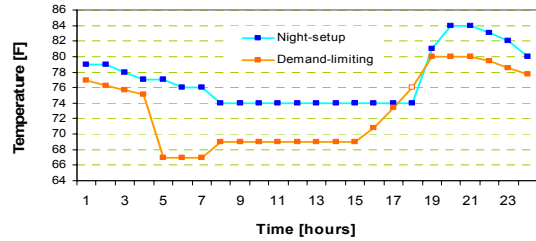
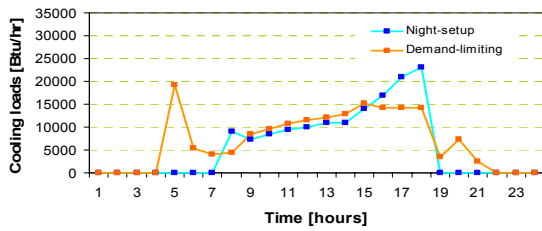
(f) DL start-time: noon



(g) DL start-time: 1pm

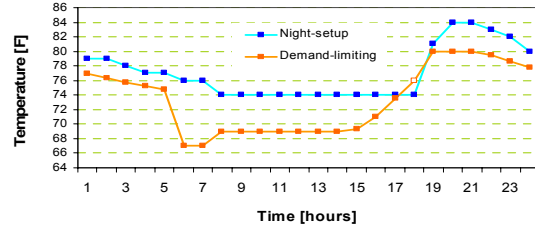
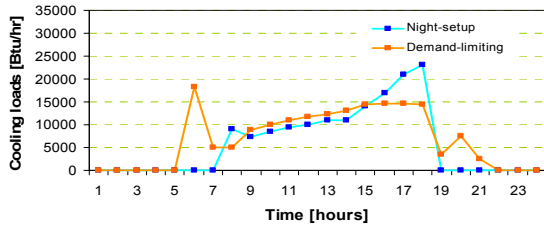


(h) DL start-time: 2pm

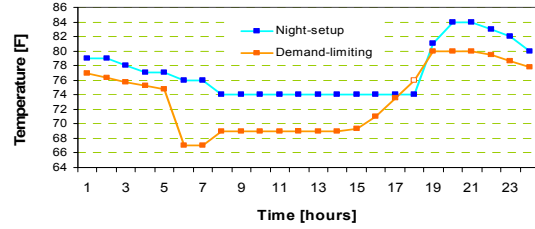
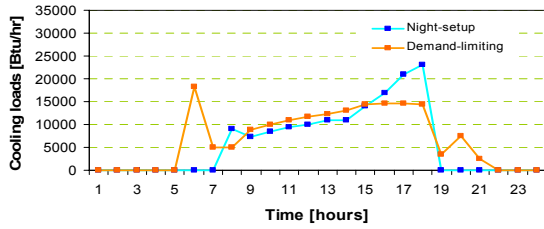


(i) DL start-time: 3pm

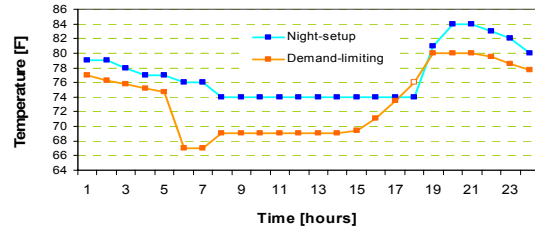
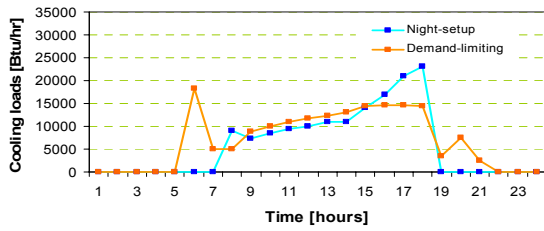
-Test zones: West zones
 -67°F PC start-time: 5 am



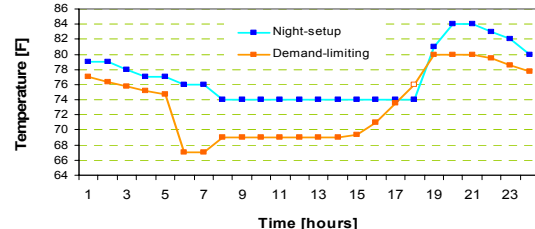
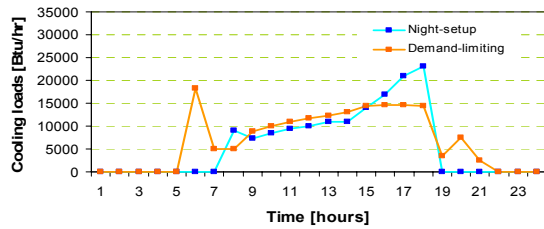
(a) DL start-time: 7am



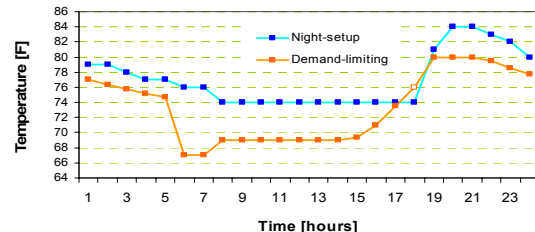
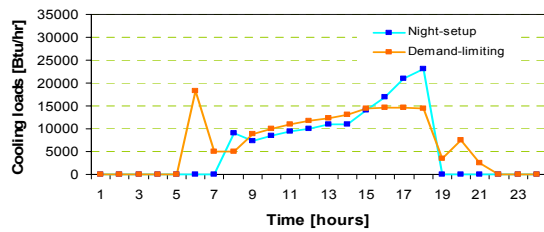
(b) DL start-time: 8am



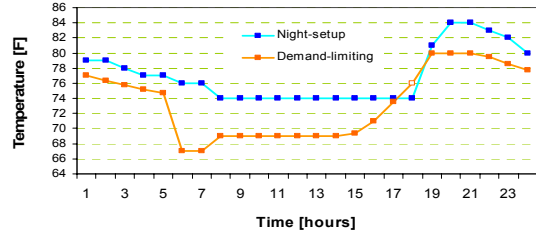
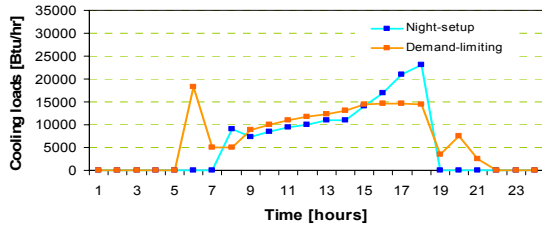
(c) DL start-time: 9am



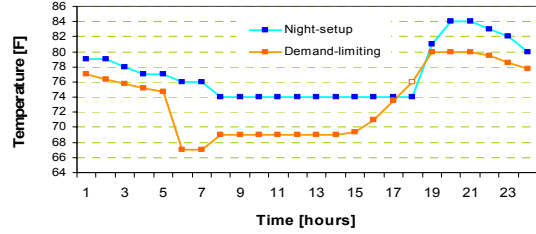
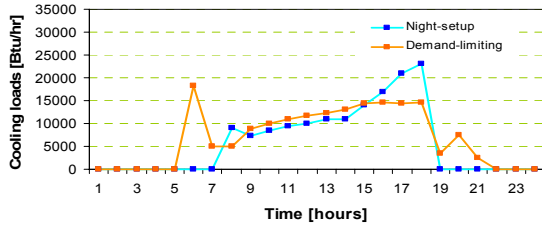
(d) DL start-time: 10am



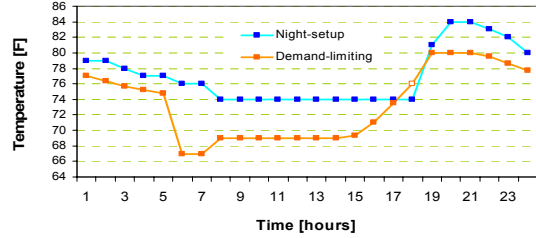
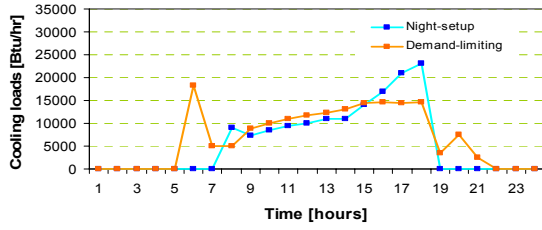
(e) DL start-time: 11am



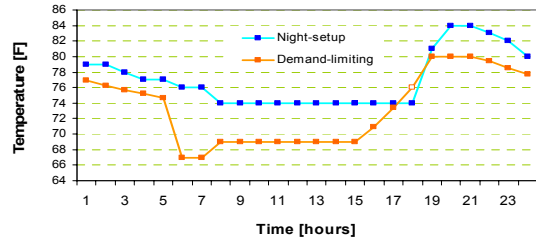
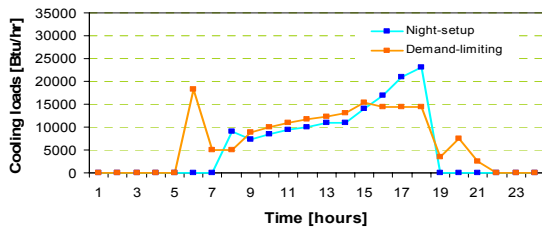
(f) DL start-time: noon



(g) DL start-time: 1pm

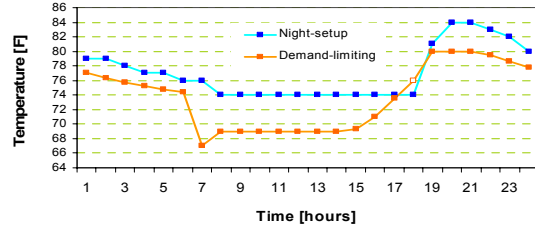
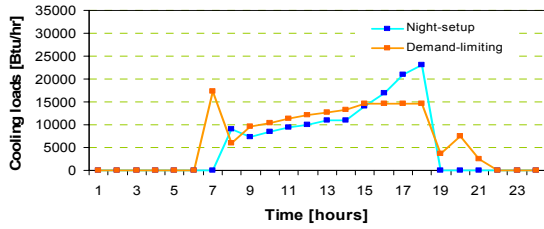


(h) DL start-time: 2pm

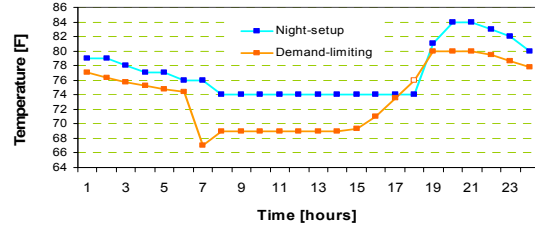
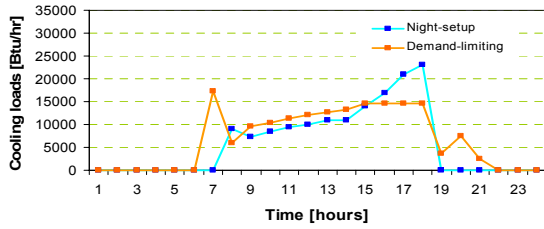


(i) DL start-time: 3pm

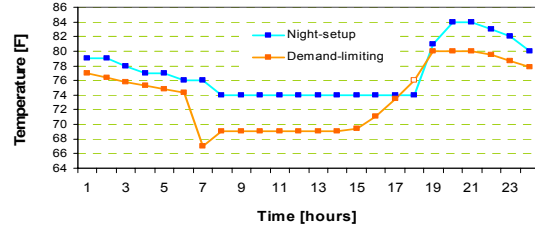
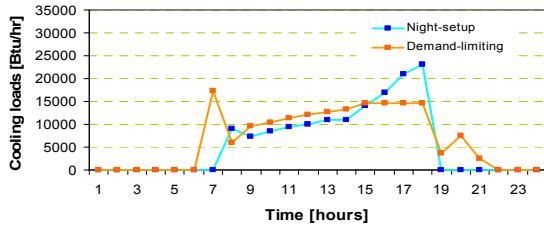
-Test zones: West zones
 -67°F PC start-time: 6 am



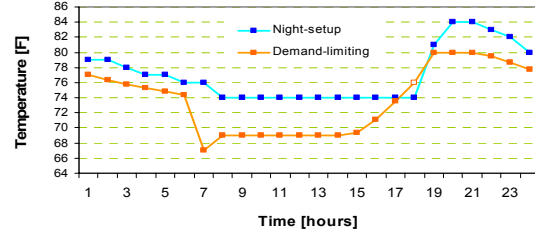
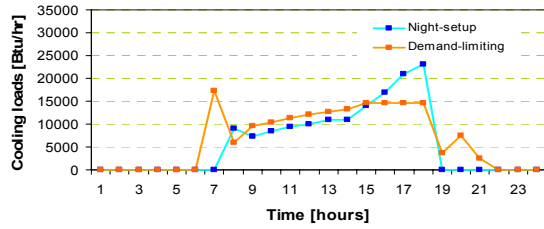
(a) DL start-time: 7am



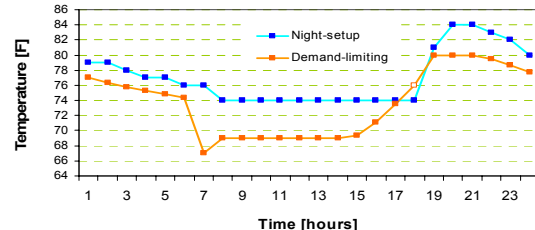
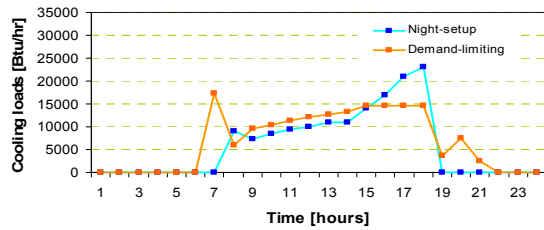
(b) DL start-time: 8am



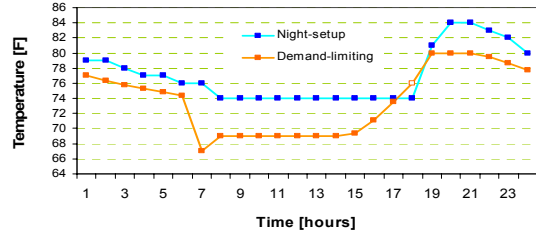
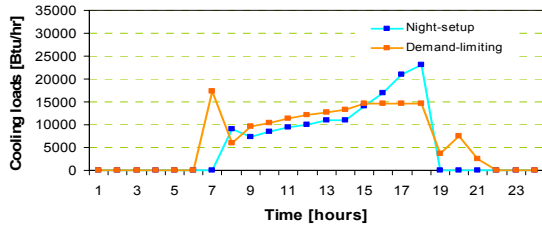
(c) DL start-time: 9am



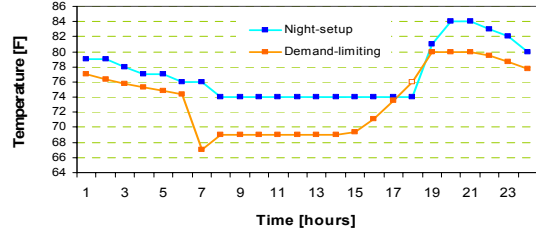
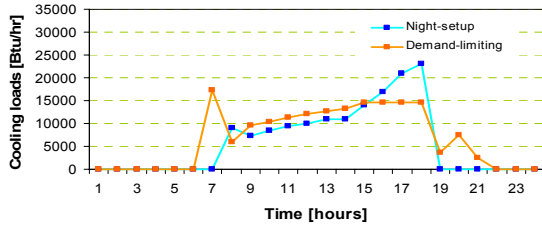
(d) DL start-time: 10am



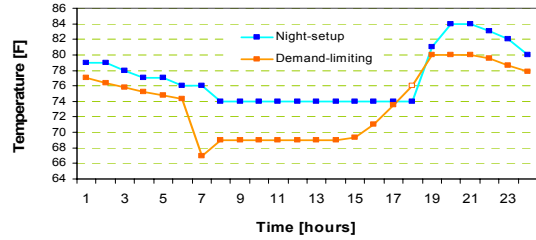
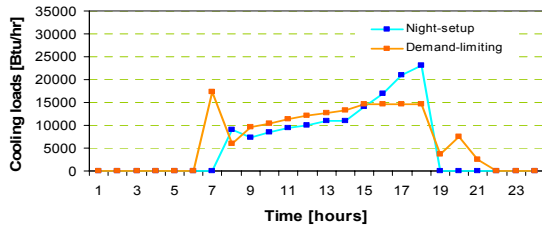
(e) DL start-time: 11am



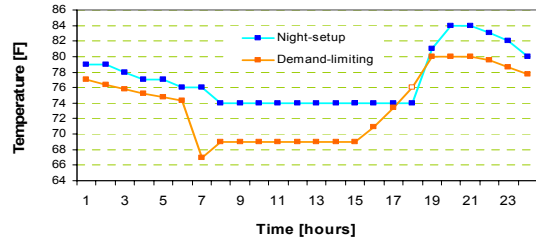
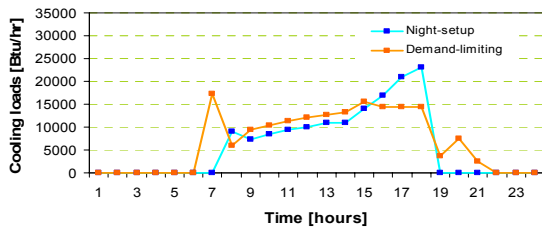
(f) DL start-time: noon



(g) DL start-time: 1pm

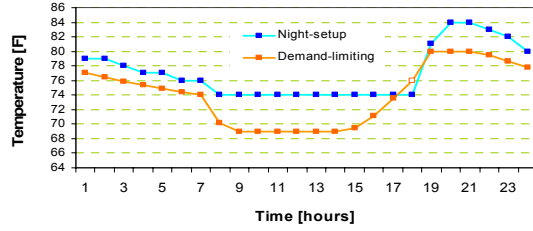
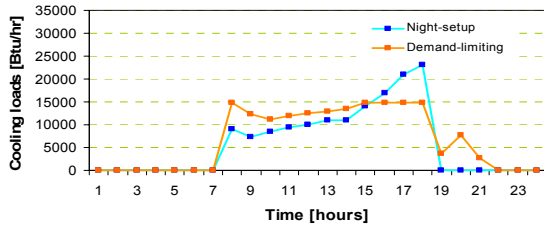


(h) DL start-time: 2pm

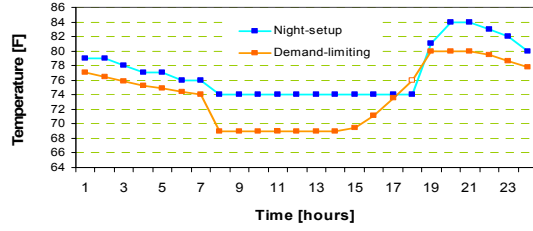
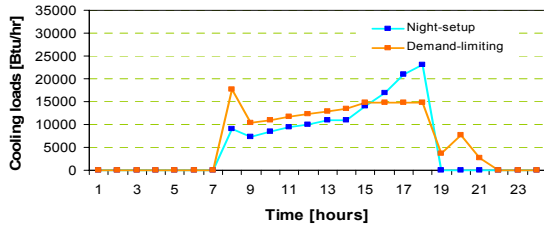


(i) DL start-time: 3pm

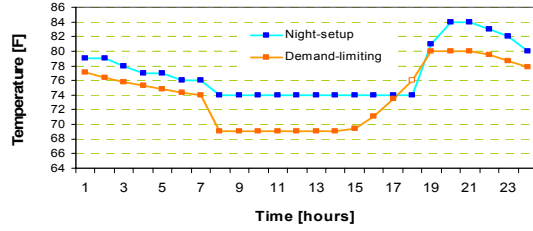
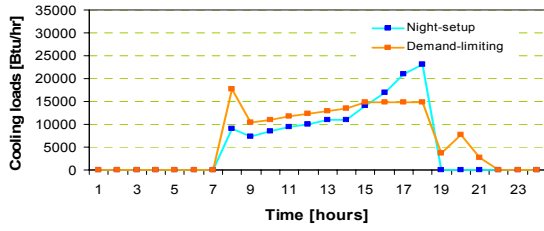
-Test zones: West zones
 -67°F PC start-time: 7 am



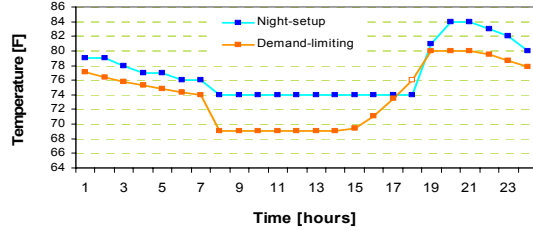
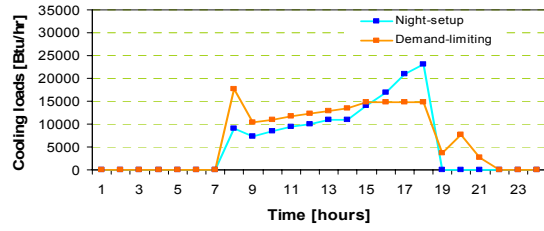
(a) DL start-time: 7am



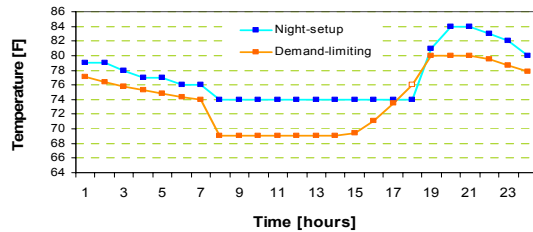
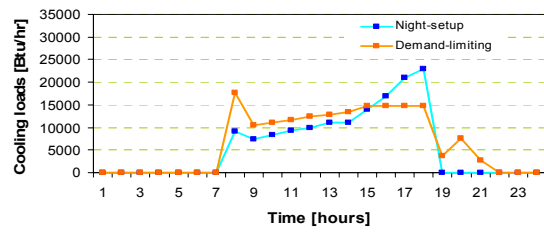
(b) DL start-time: 8am



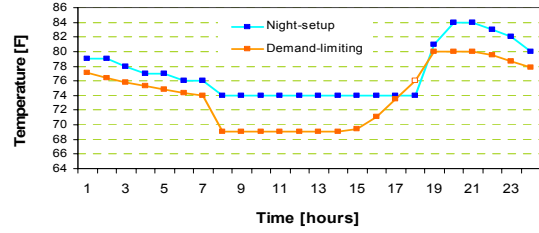
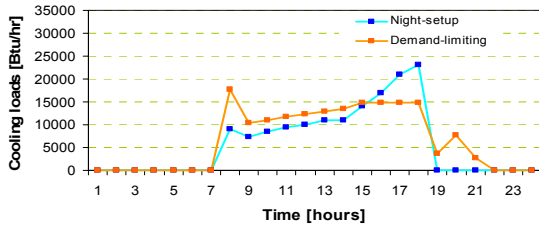
(c) DL start-time: 9am



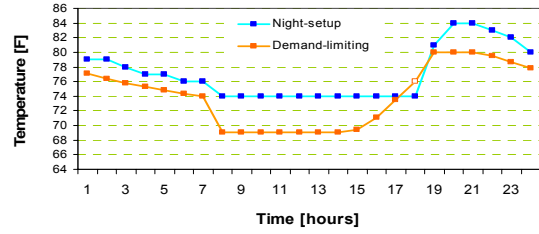
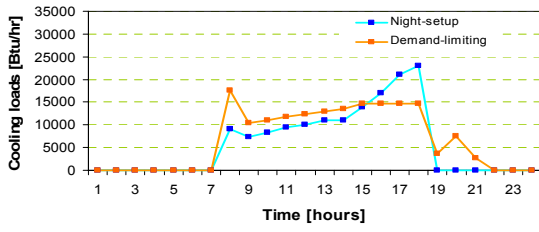
(d) DL start-time: 10am



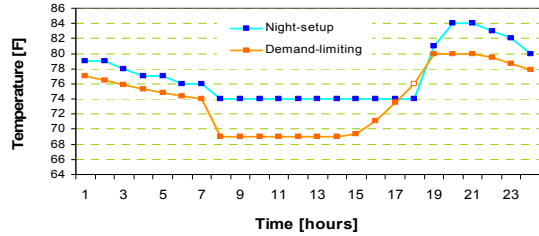
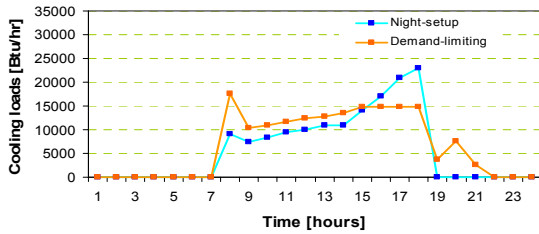
(e) DL start-time: 11am



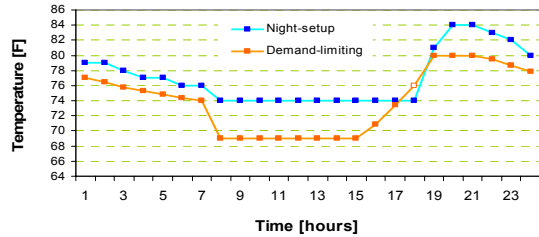
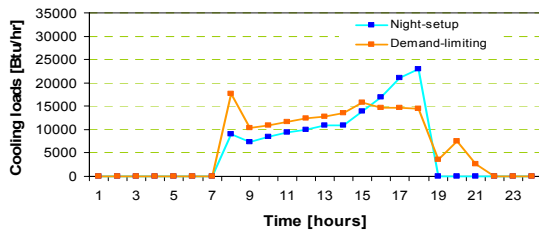
(f) DL start-time: noon



(g) DL start-time: 1pm



(h) DL start-time: 2pm



(i) DL start-time: 3pm